JULY, 1952

Journal of METALS

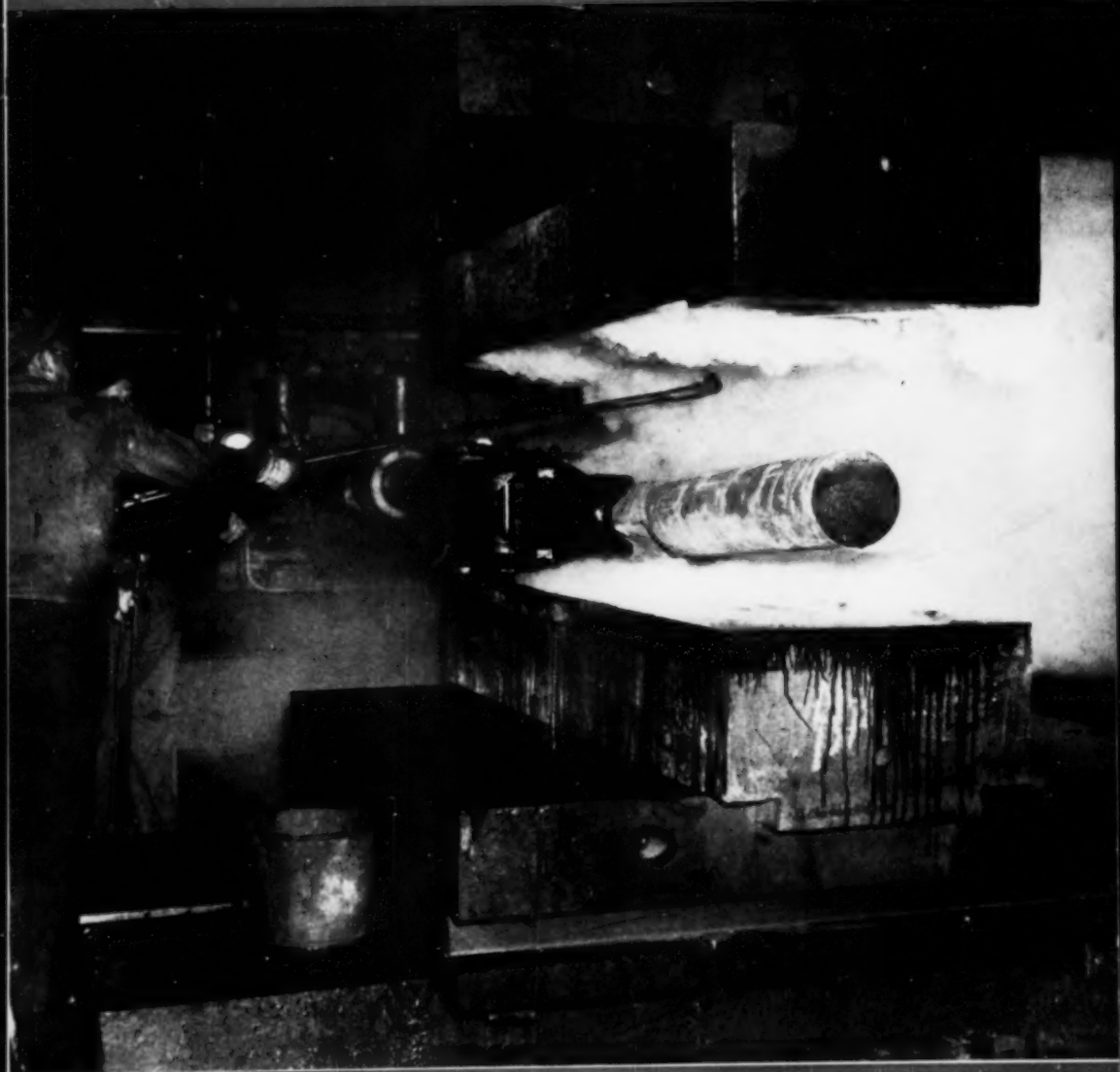

July JOURNAL OF METALS Highlights:

"Critical Jet Engine Materials" - p. 698
"Oxygen in Steelmaking" - p. 703
"Chlorination of Zirconium Oxide" - p. 733

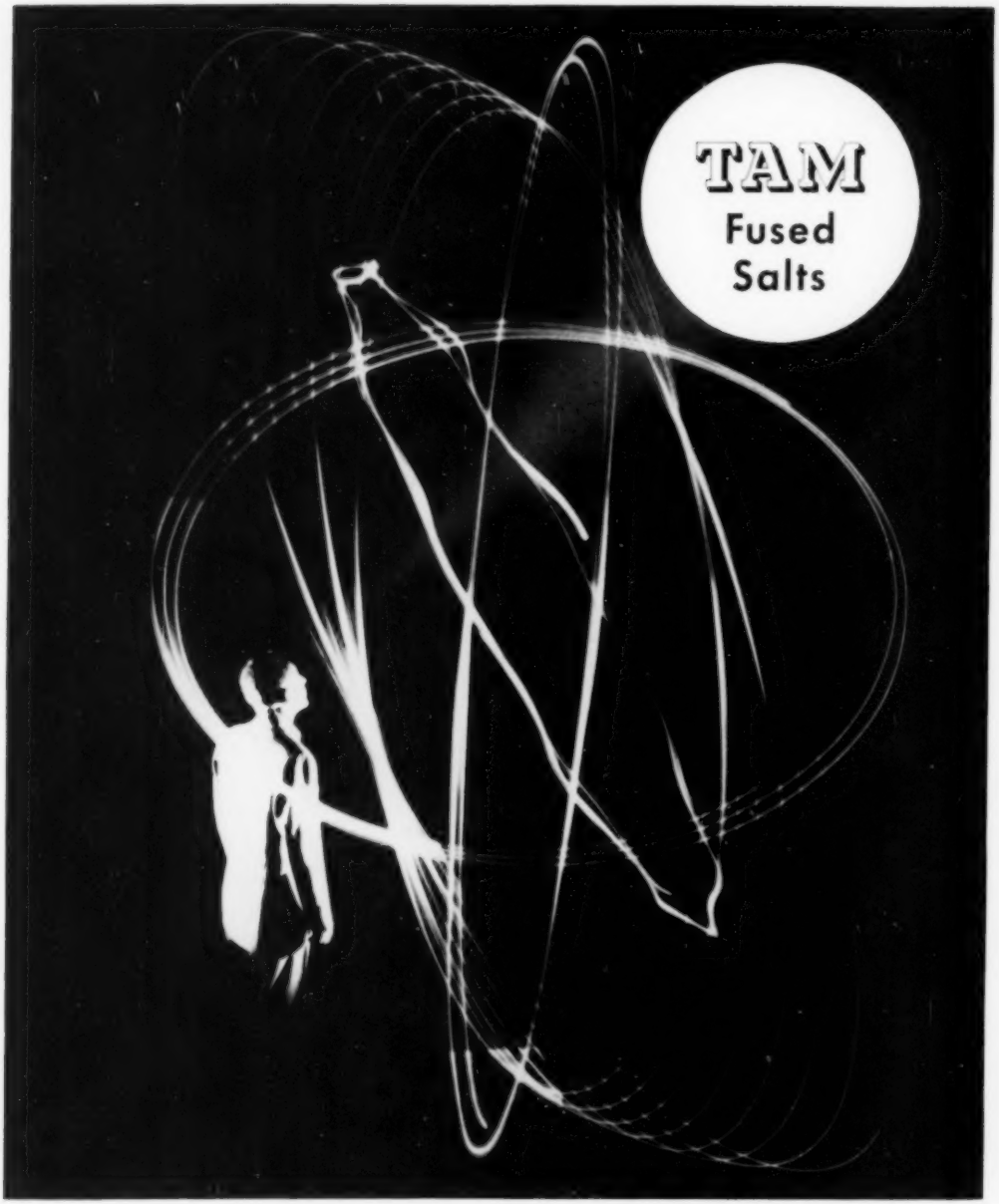

HAVE YOU INVESTIGATED THE ADVANTAGES OF TAM FUSED SALTS RECENTLY?

These TAM products are finding increasingly successful use as a source of zirconium for magnesium alloys. By refining grain size, they help improve strength in castings and eliminate problems in extruding bars. Ask our field engineers for details or write us at New York.

TAM is a registered trademark.

TAM PRODUCTS

TITANIUM ALLOY MFG. DIVISION
NATIONAL LEAD COMPANY

Executive and Sales Offices: 111 BROADWAY, NEW YORK CITY
General Offices, Works and Research Laboratories: NIAGARA FALLS, N. Y.

Journal of **METALS**

Published to provide a continuing, authoritative, and up-to-date record of technological, engineering, and economic progress in all branches of the metals industry by the Metals Branch American Institute of Mining and Metallurgical Engineers, Inc. 29 West 39th Street, New York 18

• • •

JOHN V. BEALL
Manager of Publications

A. J. CROMPTON — Associate Editor

• • •

E. C. BARRETT — M. MATZKIN
G. M. ZIEL
Assistant Editors

GRACE PRESLEY — Production Manager

W. E. SEWARD — Asst. Prod. Mgr.

• • •

METALS BRANCH COUNCIL

R. M. Brick — Chairman
E. O. Kirkendall — Secretary
W. A. Tiller — IMD Chairman
K. C. McCutcheon — ISD Chairman
T. D. Jones — EMD Chairman
T. L. Joseph — D. C. Ralston
W. E. Perry — D. S. Eppelsheimer

EDITORIAL ADVISORY COMMITTEE

H. K. Work — Chairman
L. F. Bement — J. S. Smart, Jr.
W. A. Dean — J. C. Kinnear, Jr.
W. D. Bradford — Ex-officio

TECHNICAL PUBLICATIONS COMMITTEES

J. T. Lundenwick — AIME Chairman
M. Gensamer — IMD Chairman
A. G. Forrest — ISD Chairman
J. Glover — EMD Chairman
E. T. Kennedy, Jr. — Secretary

• • •

JAMES A. STANGARONE
Advertising Manager

B. C. SNELL
Regional Manager, Pittsburgh
1110 McDonald Place, Sewickley, Pa.

• • •

The AIME Publishes
Journal of Metals
Mining Engineering
Journal of Petroleum Technology

VOL. 4, NO. 7 — JULY, 1952

COVER

A large aluminum ingot is shown being placed in the 15,000 metric ton forging press leased by Alcoa from the Air Force, and now in operation in Cleveland. Schloemann Co., Dusseldorf, Germany, built the press which operated in Germany from 1940 until seized by the Air Force after VE Day. See p. 690

NEWS

Journal of Metals Reporter	697	Employment Service	682
Trends	692	Books for Engineers	690
Drift of Things	695	Nominations for Officers	781
Industrial Notes	688	Pacific Northwest Meeting	783
New Products	686	Coming Events	786
Meet the Authors	678	Personals	787

TECHNICAL FEATURES

Conservation of and/or Substitution for Critical Jet Engine Materials — 698

Oxygen in Steelmaking — 703

TRANSACTIONS

Physical Conditions in the Combustion and Smelting Zones of a Blast Furnace — 709

Distribution of Manganese and Oxygen Between Molten Iron and FeO MnO SiO Slags — 718

Thermodynamics of Iron Silicate Slags; Slags Saturated with Solid Silica — 723

Deleading Zinc Concentrate at the Parral and Santa Barbara Mills — 729

Chlorination of Zirconium Oxide — 733

Observations on Nodular Graphite — 738

Observations on the Tension Texture of Aluminum — 743

Preferred Orientations in Vanadium — 745

Principles of Zone Melting — 747

A Study of Grain Shape in an Aluminum Alloy and Other Applications of Stereoscopic Microradiography — 755

Titanium-Copper Binary Phase Diagram — 766

Effect of Molybdenum and of Nickel on the Rate of Nucleation and the Rate of Growth of Pearlite — 771

TECHNICAL NOTES

Recrystallization Textures in Copper Wire — 753

Published the first day of each month by the American Institute of Mining and Metallurgical Engineers, Inc., 29 West 39th Street, New York 18, N. Y. Telephone: PEnnsylvania 6-9320. Subscription $8 per year for non-AIME members in United States and Nigeria, South and Central America; $9, foreign; $6 for AIME members, or $4 additional in combination with a subscription to "Mining Engineering" or "Journal of Petroleum Technology". Single copies, 75 cents; special issues, $1.50. The AIME is not responsible for any statement made or opinion expressed in its publications.
Copyright 1952 by the American Institute of Mining and Metallurgical Engineers, Inc.
Registered cable address, AIME New York. Indexed in Engineering Index, Industrial Arts Index and Chemical Abstracts. Entered as second-class matter Sept. 21, 1945, at the post office at New York, N. Y., under the Act of March 3, 1879. Additional entry established at Manchester, N. H.

MEET THE AUTHORS

N. E. PROMISEL

J. B. WAGSTAFF

N. E. Promisel (p. 696), graduate of Massachusetts Institute of Technology (B.S.) and Yale (M.S.), is now chief metallurgist and head of the materials branch, Navy Dept., Bureau of Aeronautics. From 1930 to 1940, Mr. Promisel was assistant director of research for the International Silver Co. He was a consulting engineer in metallurgy and chemistry for one year and in 1941 joined the Navy Dept. Now residing in Silver Spring, Md., he counts photography, oil painting, and chess as his hobbies. Mr. Promisel holds membership in the Electrochemical Society and American Electroplaters Society.

J. B. Wagstaff (p. 709) has been with the U. S. Steel Research Laboratory since 1949 and is presently engaged in fundamental work on blast furnace processes by the use of models. He was born in London and graduated from Sheffield University (B.Sc.) and Massachusetts Institute of Technology (M.S.). In 1937 Mr. Wagstaff joined Hadfield Ltd. as combustion engineer. He remained with this firm until 1944 when he became associated with the British Coal Utilization Research Assn. Prior to joining U. S. Steel, he was employed by Hydrocarbon Research, Inc. engaged in process design work on oxygen gasification of coal. Gardening and photography occupy his spare moments. He holds membership in the Iron and Steel Institute and Institute of Fuel.

R. A. BUCHANAN

H. M. WELD

R. A. Buchanan (p. 709), a graduate of the School of Modern Photography, New York City, is chief photographer for the U. S. Steel Research Laboratory, Kearny, N. J. Born in Portsmouth, England, Mr. Buchanan is a member of the Photographers Assn. of America, Industrial Photographers Assn. of N. J., and Society of Motion Picture & Television Engineers. Photography is his favorite hobby, along with fishing and camping.

H. M. Weld (p. 736) is an alumnus of McMaster University (B.Sc.). In 1939 Mr. Weld was associated with the magnesium development dept. of the National Research Council, Ottawa. He was made research officer for the Dominion Magnesium Co., Haley, Ont. in 1940. Presently he is physical metallurgist with the mines branch of the Dept. of Mines and Technical Surveys, Ottawa. A member of the American Society for Metals and Professional Institute of the Public Service of Canada, his hobbies are hunting, fishing, and gardening.

W. G. PFANN

J. P. HAMMOND

W. G. Pfann (p. 747) has been a member of the technical staff at the Bell Telephone Laboratories, Murray Hill, N. J. since 1935. He holds a B.Ch.E. from Cooper Union, New York. This AIME member has presented two papers before AIME: *Electropointing of Tungsten Wires* (1947) and *Microstructure of Silicon Ingots* (1949).

Joseph P. Hammond (p. 745), born in Owensboro, Ky., graduated from the University of Kentucky and received his D.E. in metallurgy from Yale University in 1949. In 1941 Dr. Hammond was a member of the metallurgy staff at the E. I. duPont deNemours Co., Wilmington. He joined the Frankford Arsenal, Philadelphia, in 1942 as metallurgist and materials engineer. He was associated with the Office of Ordnance as metallurgist for one year and then became research associate for Battelle Memorial Institute. Presently with the University of Kentucky he is associate professor of metallurgical engineering.

J. F. Elliott (p. 709) is now section head, research div., iron and steel section, Inland Steel Co., East Chicago, Ind. He was born in St. Paul and graduated from the University of Minnesota (B.Met.E.) and Massachusetts Institute of Technology (Sc.D.). During World War II, Dr. Elliott served with the Navy for four years. From 1946 to 1949 he attended MIT under a National Research Council predoctoral fellowship. Prior to joining Inland, he was at the research laboratory of the U. S. Steel Co., Kearny, N. J. A member of the AIME Chicago Section, he enjoys music and gardening in his spare time.

P. T. Carter (p. 718) has been lecturer in metallurgy at the Royal Technical College, Glasgow. Born in Middlesbrough, Yorkshire, he holds B.Sc. and Ph.D. degrees. In addition to being an AIME member, he holds membership in the British Iron and Steel Institute, West of Scotland Iron and Steel Institute, and the Faraday Society. Mountaineering and music are his avocations.

C. S. Smith (p. 755), director of the Institute for the Study of Metals at the University of Chicago, was born in Birmingham, England. He received his B.Sc. from the University of Birmingham and his D.Sc. from Massachusetts Institute of Technology. From 1927 to 1942, Dr. Smith was research metallurgist for the American Brass Co. He then joined the National Research Council as research supervisor and for three years was associate division leader for the Los Alamos Scientific Laboratory. Dr. Smith was appointed director of the Institute for the Study of Metals in 1946. The study of the history of metallurgy is of interest to this AIME member. A member of the American Physical Society, American Society for Metals, History of Science Society, and other societies both here and abroad, Dr. Smith has previously presented several papers.

F. W. BOSWELL

C. J. McHARGUE

F. W. Boswell (p. 738), physical metallurgist with the mines branch of the Dept. of Mines and Technical Surveys, Ottawa, was born in Hamilton, Ont. An alumnus of the University of Toronto, he holds a B.A., M.A., and Ph.D. in physics. A member of ASM and Electron Microscope Society of America, he enjoys photography in his spare time.

Carl J. McHargue (p. 745) was born at Corbin, Ky. He has been a research associate at the University of Kentucky, where he received his B.S. in metallurgical engineering in 1949. He is presently completing work for his doctorate. Tennis and photography are Mr. McHargue's hobbies.

Guido Bassi (p. 753) was born in Monfalcone, Italy. He was awarded the degree of Dipl. Ing. in Leoben, Austria. Now research engineer at AB Svenska Metallverken, Vasteras, Sweden, he enjoys chess and tennis.

C. L. Boeke (p. 729), born in Lena, Ill., was graduated from the Colorado School of Mines. A member of the AIME, Mr. Boeke has been associated with the American Smelting & Refining Co. in Mexico for many years.

R. L. CUNNINGHAM

W. M. WILLIAMS

R. L. Cunningham (p. 738) was born in North Sidney, Nova Scotia. Dr. Cunningham attended Dalhousi University, Halifax (B.Sc. and M.Sc.) and McGill University, Montreal (Ph.D.). He joined the Dept. of Mines and Technical Surveys in 1942 and is presently physical metallurgist in charge of the metal physics section, physical metallurgy research laboratories. He enjoys amateur radio and stamp collecting in his spare time. He also belongs to several professional societies.

W. M. Williams (p. 755), born in Tonypandy, Wales, graduated from the University of Bristol (B.Sc.) in July 1948. After graduation he worked on recrystallization of light alloys for the British Non-Ferrous Metals Research Assn., London. He is now in the United States on a two year ECA fellowship working with the research dept. of Revere Copper & Brass Co., Rome, N. Y. In his free time, Mr. Williams enjoys cycling.

E. J. Michal (p. 723) is presently employed at the research laboratory of the National Lead Co., South Amboy, N. J. A graduate of the University of Nevada, Mackay School of Mines (B.S.) and Massachusetts Institute of Technology (S.M., Sc.D.), he was employed as a physicist with the Navy Dept., San Francisco for one year. Prior to becoming an instructor at MIT, Dr. Michal served overseas with the Navy. A member of the New York Section, AIME, he presented a paper before the 1952 Annual Meeting. Camping, fishing, and mineralogy occupy his spare moments.

C. F. Floe (p. 766), a member of the Boston Section, AIME, is presently assistant provost at Massachusetts Institute of Technology. Born in Dawson, Yukon, Canada, he attended the State College of Washington and MIT. Dr. Floe was an instructor at the State College of Washington for four years and then joined the faculty of Notre Dame as an assistant professor. He held the same appointment at MIT from 1939 to 1942. He was appointed to associate professor in 1942 and became professor in 1950. He has been executive officer of the metallurgy dept. since 1943. Golfing is his hobby.

R. Wayne Parcel (p. 771), senior research metallurgist for Rem-Cru Titanium, Inc., Midland, Pa., was born in Madison, Wis. He received his B.S. in 1937 (University of Kansas), M.S. in 1939 (Massachusetts Institute of Technology), and Sc.D. in 1949 (Carnegie Institute of Technology). He joined the Denver, Rio Grande & Western Railroad Co. in 1939 as research metallurgist. In 1941 he became chief metallurgist. Dr. Parcel became associated with the Remington Arms Co. as research metallurgist and in 1950 joined Rem-Cru. The construction of high fidelity audio equipment occupies Dr. Parcel in his free time.

Wanted
HARD JOB
BLASTING
EXPERTS
Cut "DOWN TIME"
To MINIMUM
The BEST EQUIPPED organization
in the field for engineering
CONCRETE, SLAG or SALAMANDER REMOVAL
Our personnel are experts in the field of demolition.
CONSULT US ON YOUR NEXT REMOVAL PROBLEM
for the Fastest, Most Efficient Service--
24 Hours a Day, 7 Days a Week . . .
Anywhere on the face of the Globe

SERVING THE STEEL INDUSTRY FOR OVER 25 YEARS

CHICAGO
CONCRETE BREAKING CO.

Edward Gray, President

PITTSBURGH OFFICE
530 Wm. Penn Place
Atlantic 1-4674

GENERAL OFFICES
12233 Avenue O, Chicago 33, Ill.
Bayport 1-8400

"Lean Carilloy

At Commercial Shearing and Stamping Company, gears are machined directly from bar stock. Since the change from rich to lean alloy steel, the need for normalizing and straightening the metal before machining has been eliminated.

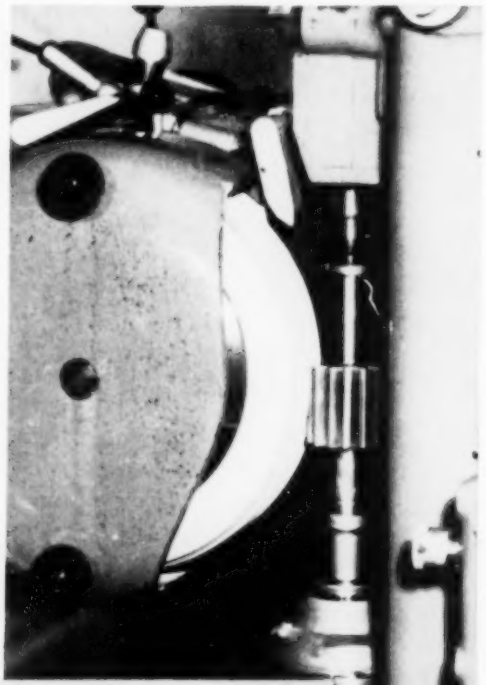

Gears are completed on precision grinders like the one shown here.

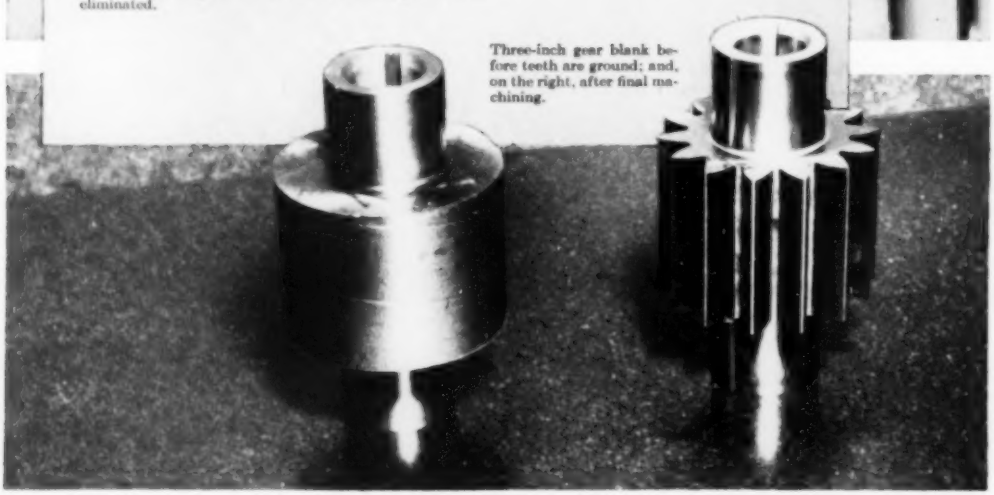

Three-inch gear blank before teeth are ground; and, on the right, after final machining.

alloy steel is saving us $40 a ton ...with no loss in performance."

—T. C. Kane, Chief Engineer

Commercial Shearing and Stamping Co.

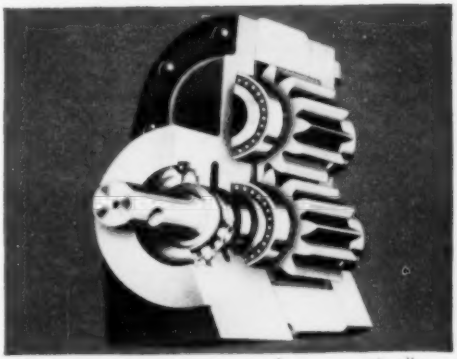

In gear-type rotary pumps, speeds are exceptionally high—up to 2000 rpm; and pumps operate at pressures as high as 1500 psi. At Commercial Shearing and Stamping Company, gears for this severe service are now made of straight-chrome instead of nickel-molybdenum steel.

LIKE MANY other manufacturers who, today, cannot get rich alloy steel, Commercial Shearing and Stamping Company of Youngstown, Ohio, has found that many parts that must operate in extremely tough service can be made of *lean* alloy steels with no loss in performance.

Commercial Shearing makes a wide variety of steel products, including stampings and forgings; but it is in their gear-type rotary hydraulic pumps that they must do without rich alloy steel. Choosing a satisfactory alternate steel for the precision gears in these pumps presented quite a problem.

Mr. T. C. Kane, Chief Engineer at Commercial, tells the story this way: "We used to make the gears for our heavy-duty hydraulic pumps out of Carilloy 4615 (a Ni-Mo steel, with 1.65-2.00% nickel). But when nickel started getting scarce, we had to find a steel in better supply that would stand up in this severe service.

"Our gear-type rotary pumps are used in heavy-duty hydraulically-operated mobile equipment and must deliver a constant supply of oil at the correct pressure. In these pumps, oil is trapped between the teeth of two meshing gears and forced through the pump as the gears rotate. To obtain the high efficiencies necessary, gear dimensions must be held within extremely close tolerances. And wear must be held down, because a loss of just 0.005 inch causes a substantial drop in pump efficiency. These pumps operate at pressures as high as 1500 psi and speeds up to 2000 rpm; so we have to be sure to use a tough, wear-resistant steel for the gears. The question was, how to get this in a lean alloy steel.

"One of United States Steel's service metallurgists helped us out. After analyzing our requirements, he suggested a straight-chrome alloy steel—Carilloy 5120. Now that we have lived with this steel for a while, we are frankly surprised at the excellent results we are getting. Not only are our pumps as good as ever, but this straight-chrome steel has important advantages for us over the richer alloy:

"First of all, Carilloy 5120 is easier to machine, so naturally our tools last longer.

"Our heat treating problems are easier, too. Carilloy 4615 had to be normalized and straightened before machining. This is no longer necessary since there is less distortion in carburizing operation.

"With reduced heat-treating costs and a lower grade extra, the change to lean alloy steel is saving us $40 on each ton of steel we buy."

★ ★ ★

The switch from rich to lean alloys is not always as easy as it was at Commercial Shearing and Stamping Company. You may require special heat treating, or simply more *careful* heat treating, to obtain desired mechanical properties. But whatever your steel problems, our metallurgists will be glad to help you with them. Just call the nearest District Sales Office or write to United States Steel, 525 William Penn Place, Pittsburgh 30, Pa.

U·S·S Carilloy Steels

USS

UNITED STATES STEEL COMPANY, PITTSBURGH • COLUMBIA GENEVA STEEL DIVISION, SAN FRANCISCO
TENNESSEE COAL & IRON DIVISION, FAIRFIELD, ALA. • UNITED STATES STEEL SUPPLY DIVISION, WAREHOUSE DISTRIBUTORS, COAST-TO-COAST
UNITED STATES STEEL EXPORT COMPANY, NEW YORK

3-1250

UNITED STATES STEEL

Metallurgist
(Mechanical)

organize and direct research projects of fundamental nature in the flow and fracture of metals to work in SYLVANIA'S Metallurgical Research & Development Laboratories located at Bayside, L. I.

Ph.D in metallurgy or mechanical engineering highly desirable. Creep testing experience desirable but not necessary. Send complete resume.

MANAGER OF PERSONNEL

SYLVANIA
Electric Products, Inc.
40-22 Lawrence St.
Flushing, New York

METALLIC SINGLE CRYSTALS

Single Crystals of the following high-purity metals and alloys are now available:

Copper	Aluminum
Zinc	Brasses
Lead	Bronzes
Cadmium	Nickel
Tin	Permalloy
Bismuth	Cobalt
Iron-Nickel Alloys	

Available in rod form ¼" to 1½" diameter up to 10" long.

Special shapes provided upon request.

We will be glad to answer your request for information on prices, specifications, and special problems in this field.

HORIZONS INCORPORATED
2891 E. 79th Street
CLEVELAND, OHIO

Personnel Service

The following employment items are made available to AIME members only as a service. Inquiries should be addressed directly to the Engineering Societies Personnel Service, Inc., operating in cooperation with the Four Founder Societies, Local offices of the Personnel Service are at 29 W. 39th St., New York 18; 345 Montgomery St., San Francisco; 84 E. Randolph St., Chicago 1; and Penobscot Bldg., Detroit.

POSITIONS OPEN

Metallurgists, with knowledge of milling processes for lead, copper, and concentrates. Good operating experience acceptable. Salary open. Location, midwest. Y7042.

Sales Manager with metallurgical experience, to take general charge of sale of tungsten carbide products. Salary, $10,000 a year plus bonus. Location, New Jersey. Y7067.

Production Manager, 35 to 45, with considerable experience on direct line production for metal forming, plant layout, scheduling, and costs. Salary, $10,000 to $12,000 a year. Location, southern New Jersey. Y6618.

Research Assistant, minimum requirement B.S. in metallurgy, chemistry or physics. Metallography, mechanical testing, statistical studies, interpretation of data, writing of technical reports and papers. Opportunity for tuition free advanced study and for publishing technical material. One month's vacation. Apply by letter giving qualifications and salary expected. Location, western Pennsylvania. Y7172.

Metallurgist, welding engineer, 32 to 40, experienced in plate metal fabrication or castings for machinery and equipment manufacturer. Salary, $4800 to $7200 a year. Location, northern New Jersey. Y7156.

Engineers. (b) Assistant mill metallurgist, graduate, to work in mill metallurgical laboratory consisting of flotation machines, microscopes, laboratory furnaces and all kinds of chemical apparatus for metallurgical processes. Should have at least a year's experience. (c) Assistant foundry foreman, experienced in modern molding practice. Production averages over 1100 tons a month of castings made up of iron, steels and nonferrous metals. (e) Mill metallurgist to work directly under the assistant superintendent and to take full charge of all testing and research. Graduate required with experience in operation of milling plants using crushing, grinding and froth flotation, etc. Three year contracts with transportation paid. Salaries open. Location, Chile, S.A. Y7154.

Metallurgical Engineers, experienced, to assist a small management group responsible for development and control work in nonferrous process metallurgy of special alloys. Must

CHIEF MATERIALS AND PROCESS ENGINEER

Opening for experienced man to supervise Materials and Process Department. Work is in the fields of chemistry, metallurgy and mechanical processing, plastics, adhesives and sealers. Must be engineering graduate and have had supervisory and a minimum of five years' aircraft experience.

Send complete resume to Technical Placement Supervisor

MCDONNELL AIRCRAFT CORPORATION
St. Louis 3, Missouri

METALLURGISTS
Wanted at Once
for
Production Manufacturing Department
or
Research

Openings consist of fundamental metallurgical research and development as applied to diesel engines, tractors, and earthmoving equipment.

Graduate Metallurgical Engineers with industrial experience in ferrous metallurgy preferred.

Please forward complete information to:

J. J. Sheehan, Personnel Director
CATERPILLAR TRACTOR CO.
Peoria, Illinois

STEEL METALLURGIST

Minimum four years' experience steel plant operation. Must be graduate B.S. in metallurgy. Write

Box F-13 JOURNAL OF METALS

METALLOGRAPHIST

B. S. metallurgy. Some previous experience in steel plant operations desirable but not essential. Write

Box F-14 JOURNAL OF METALS

have had experience in metal casting, rolling, heat treatment and associated operations as required. Salary, $8000 a year. Location, metropolitan New York area. Y7147.

Quality Control Dept. Manager with 2 to 5 years' shop experience in inspection, test methods and statistical quality control in metalworking, instrument or apparatus fields, to be responsible for the specifications of all departments, divisions and subsidiaries, to maintain quality of all items and establish all necessary controls, inspection and test reports, customer complaint reports, etc. Salary, $5000 to $5600 a year. Location, New York metropolitan area. Y7126(a).

Production Manager, 35 to 50, mechanical graduate, with at least 5 years' aircraft aluminum or other light metal fabricating experience, to supervise production and liaison engineering covering frame sections and accessories. Salary, $8000 to $10,000 a year plus bonus. Location, Connecticut. Y7102.

Metallurgist, graduate, with 5 years' or more experience in nonferrous metallurgical work. Knowledge of electrical equipment helpful. Will do research and administrative work on copper base and aluminum alloys used for electrical equipment. Salary, $7000 to $8000 a year. Company may pay or negotiate placement fee. Location, Alabama. Y6835.

Lead Smelter Engineer familiar with the blast furnace operations and subsequent refining and alloying processes, for a lead smelter operation based on the melting of battery lead scrap. Location, New York City. Y6778.

Assistant Mill Superintendent, graduate metallurgist preferred, with considerable experience in base metals. Should be first class maintenance man to supervise repairs in mill. Salary, $6000 a year. Location, northeast of continental U. S. Y6530(c).

Metallurgists, Project leader with M.S. degree and several assistants, graduates, for fatigue studies. Work will involve studies of grain size effect on high temperature fatigue, notch effects, fatigue gage for metals and related work. Salary, $4680 to $6240 a year. Location, western New York state. Y6297.

Assistant Mill Superintendent at property using magnetic, gravity, and flotation processes. Sound metallurgical and operating background required. Large progressive organization. Salary open. Location, upstate New York. Y6200.

Mechanical Engineers for the design of laboratory equipment and pilot plants, for the operation of a metallurgical research laboratory. Salary open. Location, Pacific Northwest. Y6441(b).

MEN AVAILABLE

Engineer, 28, family. Seeking Latin American opportunity. B.S. metallurgy. Graduate American Institute for Foreign Trade. Knowledge Spanish. Aviator. Two years' experience selling copper-base alloys for mechanical and corrosion applications. Resourceful record. One and one half years' factory experience fabricating concerns. Presently located Chicago. M-686.

Sales Engineer, B.S. mining engineering, some metallurgical engineering, age 33. Four and one half years' steel mill experience, 5½ years' sales experience. Desires sales position in company serving the metal producing industry. M-688-Chicago.

POSITION WANTED

METALLURGIST, research, age 40. Recovery of nonferrous metals from ores, residues, scrap, applying furnace, electrolytic, and leaching methods. Experience with copper, silver, zinc, cadmium, selenium, tin, lead, and others. Also metal powders. Box E-12 JOURNAL OF METALS

PHYSICIST
METALLURGY

SYLVANIA needs for its new metallurgy laboratory, now being completed at Bayside, L. I., an applied physicist to operate radio-activity laboratory. Work involves making radio-activity measurements in connection with metallurgical and chemical research problems. Supervision over small group of technicians. B.S. in applied Physics or Metallurgy and laboratory experience in handling Radio Isotopes essential. Some experience in selection and operation of radio-activity measuring instruments highly desirable. Unusual opportunity to head up and develop well-equipped radio-activity laboratory, working on a wide variety of research programs. Send complete resume:

MANAGER OF PERSONNEL

SYLVANIA
Electric Products, Inc.

40-22 Lawrence St., Flushing, N. Y.

Greater Size and Speed in Aircraft have created engineering problems, the solution of which has required larger and larger forgings of high-strength aluminum alloy. Examples shown above are forged structural members used in a modern military bomber, the largest more than seven feet over all. These are forged on an 18,000-ton press, the biggest ever built in this country.

Wyman-Gordon Experience—the most extensive in the industry—is keeping abreast of new forging demands involving the use of Steel, Aluminum, Magnesium, High Density Alloys and Titanium.

• • •

Standard of the Industry for More than Sixty-five Years

WYMAN-GORDON

FORGINGS OF ALUMINUM • MAGNESIUM • STEEL

WORCESTER, MASSACHUSETTS

HARVEY, ILLINOIS DETROIT, MICHIGAN

In Furnace and Foundry...

These SMALL PARTS do a BIG JOB

● High temperature applications of "National" Carbon and Graphite are not limited to big-tonnage items. A part of National Carbon's service is to develop *any* application, however small, where the unique properties of carbon and graphite assure a convenience and economy to the user. In the following two instances, a few *pounds* of graphite serve literally *tons* of metal . . . efficiently and at a saving.

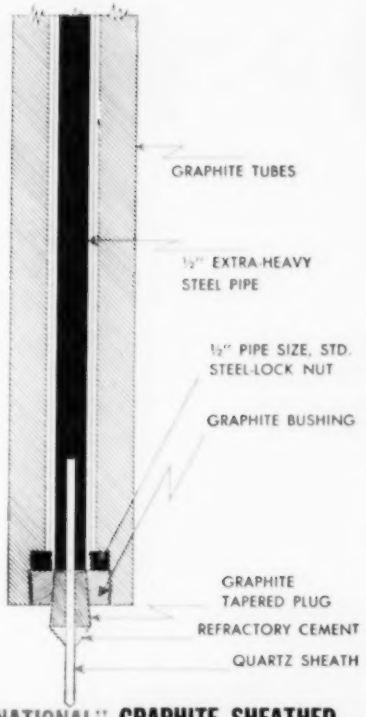

"NATIONAL" [illegible] TUBES

Can't be equalled by any other ma[illegible]duction of purifying gases into molten metal. Graph[illegible] melt in the bath, can't contaminate the metal. Its low coefficient of expansion prevents cracking and spalling. Metal and dross do not adhere tightly to it. And whatever gases are used, graphite will not corrode.

"NATIONAL" GRAPHITE-SHEATHED THERMOCOUPLE ASSEMBLY (Typical)

Only graphite could provide the degree of low-cost, trouble-free protection required by thermocouple assemblies of this type for the immersion method of measuring open hearth and electric furnace bath temperatures. Reclamation and maintenance for re-use are simple, quick, and economical. Molten metal won't stick to the graphite parts and they're immune to thermal shock.

HERE'S HOW TO LICK MY HEET

National Carbon Company
30 E. 42nd Street
New York, N. Y.

PLEASE SEND INFORMATION ON:

☐ Thermocouple Sheath Parts ☐ Fluxing Tubes

NAME_____

COMPANY_____

ADDRESS_____

The terms "National" and "Eveready" are registered trade-marks of Union Carbide and Carbon Corporation

NATIONAL CARBON COMPANY
A Division of Union Carbide and Carbon Corporation
30 East 42nd Street, New York 17, New York
District Sales Offices: Atlanta, Chicago, Dallas, Kansas City, New York, Pittsburgh, San Francisco
IN CANADA: National Carbon Limited
Montreal, Toronto, Winnipeg

LOW LIGHT BILLS . . .

. . . mark phenomenal acceptance of "EVEREADY" No. 1050 Industrial Flashlight Batteries by a broad cross-section of industry. Delivering twice the usable light of any battery we've ever made before, it will not swell, stick or jam in the flashlight . . . has no metal can to leak or corrode.

BLAST FURNACE LININGS • BRICK • CINDER NOTCH LINERS • CINDER NOTCH PLUGS • SKIMMER BLOCKS • SPLASH PLATES • RUNOUT TROUGH LINERS • MOLD PLUGS • TANK HEATERS

New Products

New Products | New Literature | New Services

For Further Information on Literature on any Product, Fill in the Coupon and Send to JOURNAL OF METALS
Students are Requested to Apply Directly to Manufacturers for Bulletins and Information

1—ROLLER BEARING END ROLL: A new roller bearing end roll with features designed for flexibility, ease of adjustment, and a minimum amount of maintenance work has been announced by the *Birdsboro Steel Foundry & Machine Co.* A totally enclosed bearing housing is locked to the end of the roll but may be changed from one roll to another in a few minutes. Vertical adjustment can be made without disturbing the axial adjustment, which is obtained through heavy adjusting nuts, graduated to 0.001 in.

2—AIRLESS ROTOBLAST BARREL: Available in 6 and 12 cu ft capacity, this new airless rotoblast barrel is a product of *Pangborn Corp.* Drive motor for the unit is

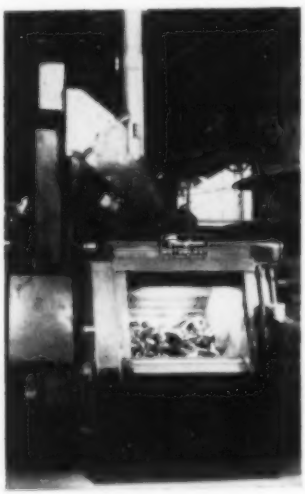

1½ hp. Drive is by means of V-belts to a spur gear reducer mounted directly on the work conveyor shaft. The newly designed work conveyor is driven by a hardened steel chain and uses cast ductile iron slats.

3—TUBE BENDER: An operating circuit that permits individual control of all functions at any time during the cycle, is one of the new features of the aircraft tube benders built by *Pines Engineering Co.* Bending arm speed is 25 rpm. The bender will handle stainless steel tubing 1 in. 16 gage, ips extra heavy pipe up to ¾, and nonferrous metals 1¼ in. 0.134 wall, as well as extruded shapes within its capacity range.

4—TRANSFORMER BUSHING: High voltage transformer bushing, with simplified construction for minimizing porcelain breaking, has been developed by *General Electric Co.* The bushing will decrease the height of power transformers from 1 to 5 in. and is liquid filled and completely sealed to prevent internal corona discharges under high stress.

5—WAX LUBRICANT: A stick type wax lubricant for use in machining, sanding, grinding, polishing, and forming operations is available from the *DeAtt Co.* It is supplied in a dispenser tube 11 in. long and 2 in. diam.

6—VISE AND ANGLE PLATE: *Kearsarge Tool & Mfg. Co.* announces the development of a combination vise and angle plate with two independent clamping jaws. The jaws can be adjusted to a number of positions, permitting clamping pressure to be put on the right spot to hold the workpiece securely against the squaring face. It will hold regular, conical, hexagonal, spherical, and irregular shapes.

7—ROTARY DRYER: A rotary dryer of the direct heat parallel current type, measuring 8 ft diam, 60 ft long, has been built by *Standard Steel Corp.*

8—METAL FORMING MACHINE: Machines using a flexible pressurized die member have been announced by the *Cincinnati Milling Machine Co.* In operation, the flexible die member is lowered and locked, initial pressure is released, and the punch member moves upward into the flexible die member. Machines are available in 12 and 16-in. sizes.

9—HYDRAULIC DRIVE: A new hydraulic drive for powering ram type hand turret lathes is announced by *Viking Industries.* The attachment is designed for turret lathes with 6 station turrets and is adaptable to lathes with bar stock capacity up to 2½ in.

10—LUBE OIL: *Shell Oil Co.* is now offering a new lube oil that cuts down engine wear from corrosion and fouling, with consequent reduction in oil consumption. Shell Rimula Oil combats sludge and lacquer deposits and extends service life of engines by reducing cylinder, ring, piston, and bearing wear.

11—CREEP TESTING MACHINE: Lever-arm creep testing machine of 12,000 lb capacity has been developed by *Heppenstall Co.* It was designed primarily for testing special alloy steels used in high temperature applications, such as jet engines

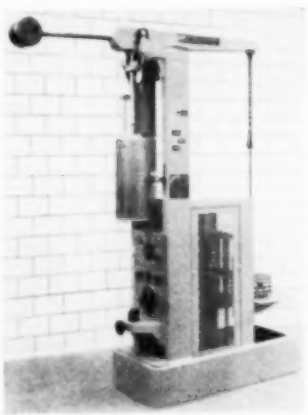

and gas turbines. During testing, the lifting platform automatically positions itself about ½ in. below the weight pan so that the shock of dropping weights is minimized when the specimen breaks in stress-rupture tests.

12—CHIP REMOVER: A new device for prolonging tool life on steel milling operations has been announced by *Detroit Milling Cutter Co.* A rotating wire brush on a magnetic base is placed in contact with the revolving teeth or blades of the milling cutter and pushes off adhering chips.

13—MAGNETIC HANDLER: A magnetic remote handler has been developed by *Tracerlab, Inc.* to make possible easy positioning and manipulation of radioactive sources, encased in ferromagnetic materials, with increased safety for radiographers.

14—PRECISION LATHE: Lap-winding 4000 turns on a minute armature only 1/8 in. long and 3/16 in. diam is one delicate task assigned to this highly precisioned lathe. The arma-

ture is the heart of a vibration pickup coil used in an instrument that balances dollar sized air turbine wheels within 0.0005 in. *AiResearch Mfg. Co.*

15—FORGING FURNACE: A forging furnace able to heat high speed and alloy chisels for both forging and hardening and provide true cold shank heating, has been announced by the *Delaware Tool Steel Corp.* A new principle prevents loss of temper in the shank during tool redressing.

16—VACUUM FURNACES: Complete line of vacuum furnaces for metal processing are electrically heated and built for one of three purposes: Resistance heating, induction heating, or arc melting. *F. J. Stokes Machine Co.*

Free Literature

20—BASIC REFRACTORIES: Booklet issued by *Basic Refractories, Inc.* explains in nontechnical language basic refractories and basic steel process.

21—SCALES: Condensed scale catalog released by *Howe Scale Co.* is a handy 28-page reference featuring standard Howe scales weighing from 1/64 oz to 400 tons.

22—ZINC: Data on spinning and drawing of zinc is contained in folders obtainable from *American Zinc Institute.*

23—SEAMLESS TUBING: Advantages of using seamless cold drawing carbon steel mechanical tubing are given in data card published by *Babcock & Wilcox Tube Co.* Tables of tolerances and mechanical properties are included.

24—AUSTENITIC CR-NI STAINLESS: Booklet issued by *International Nickel Co., Inc.* shows the results of tests on numerous austenitic stainless steels in various solutions. Nickel in combination with chromium increases corrosion resistance in both oxidizing and reduction solutions.

25—AIR HANDLING: A 60-page catalog on air handling, cleaning, and conditioning is available from *Westinghouse Electric Corp.* The catalog contains an equipment section, application section, and an engineering data section.

26—SPECIMEN POLISHING: Advantages of diamond abrasives for polishing metallurgical specimens are described in folder from *Buehler, Ltd.* Diamet-Hyprez is offered in 3 different particle sizes, in 5 and 18 g gun applicators.

27—PIT COVERS: Between open hearth and rolling mill, billets stop for a reheating in the soaking pits. A weak spot in the roofs of these pits is troublesome. Bulletin 352 offered by *Geo. P. Reintjes Co.* describes features of Reintjes pit covers.

28—FLOW METER: Variable area flow meters with newly developed, tapered metal metering tubes are described in catalog 40 issued by *Fischer & Porter Co.* Armored Flowrator meters designed for both high temperatures and high pressure are discussed.

29—TEMPERATURE CONTROLLER: A new temperature control unit that automatically monitors up to 20 individual temperature points a minute is illustrated in bulletin released by *Illinois Testing Laboratories, Inc.*

30—DIE BLOCKS: Handbook on die blocks has been published by *Hepenstall Co.* Types of die steels are described and recommended applications are listed. Detailed instructions for heat treatment of the annealed steels are given.

31—HEAT TREAT FURNACES: Bulletin on direct fuel fired furnaces for all types of heat treat processing has been released by *Surface Combustion Corp.* Practical applications of direct fuel fired batch and continuous furnace designs in the ferrous and nonferrous industries are shown.

32—GRAIN SIZE: Stressing the relation of grain size to the physical characteristics of an alloy, 4-page folder obtained from *Bridgeport Brass Co.*, illustrates by microphotographs how grain structure is affected by annealing and cold rolling.

33—ABRASIVE CUTOFF: Line of abrasive wheel cutting machines in foundry, general metalworking, and special applications is described in bulletin available from *Tabor Mfg. Co.* Units ranging from 3 to 20 hp are covered.

34—BRAZING ALLOYS: Bulletin 20 issued by *Handy & Harman* illustrates Easy-Flo and Sil-Fos low temperature silver alloy brazing. Brazing steps, applications, and specifications are included.

35—DIE CASTING LUBRICANTS: Four die casting lubricants are fully described in folder obtainable from *E. F. Houghton & Co.* Proper dilutions and application of these special heat resisting lubricants for various types of zinc and aluminum die casting operations are recommended.

36—METALLOGRAPHIC POLISHING: Two speed polishers are described in booklet available from *Buehler Ltd.* Units are available for flush or table mounting and in single, double, or triple unit tables.

37—ARC WELDING: Single phase, 60 cycle atomic hydrogen arc welding equipment is described in bulletin issued by *General Electric Co.*

38—KARBATE: Carbon and graphite and Karbate impervious carbon and graphite products are described in catalog section 5-5005, *National Carbon Co.* Chemical, metallurgical, mechanical, and electrical applications are given.

39—CAST ALLOY TOOLS: Data on cast alloy metal cutting tools is given in manual and catalog published by *Haynes Stellite Co.* Physical, mechanical, and chemical properties are given and a brief general description of chip formation and tool design is included. Catalog section is devoted to description of forms that are available: Solid and tipped tool bits, grooving tools, burnishing rollers, and cutoff tools.

Journal of Metals
29 West 39th St.
New York 18, N. Y.

July

Please send me { More Information ☐ / Free Literature ☐ / Price Data ☐ } on items indicated

1	2	3	4	5	6	7	8	9	10
11	12	13	14	15	16	17	18	19	20
21	22	23	24	25	26	27	28	29	30
31	32	33	34	35	36	37	38	39	40
41	42	43	44	45	46	47	48	49	50
51	52	53	54	55	56	57	58	59	60

Name _____ Title _____

Company _____

Street _____

City and Zone _____ State _____

For low cost

HARD ALLOY COMPACTS ...

Titanium and Zirconium Alloy Powders

. . . without the high cost and expensive equipment needed for sheet metal fabrication and bar stock for small metal and/or alloy parts, metallurgists now turn to

Titanium Metal Powder . . . Titanium Hydride
Zirconium Powder . . . Zirconium Hydride

Equal to the low cost advantage of pressing and sintering for small parts, (such as components requiring hardness, corrosion resistance, and high temperature service) are the considerations that *no waste* results when these powders or hydrides are employed. Particles are homogeneous alloys, thus insuring homogeneous products.

Available from Metal Hydrides Incorporated are powders of titanium and zirconium alloyed with Nickel; Chromium; Cobalt; Manganese; Thorium; Uranium; Tantalum; and Niobium (formerly Columbium)

Titanium hydride can be sintered under vacuum to produce Titanium metal.

Zirconium hydride can be likewise handled to produce Zirconium metal.

Save time, money, investment in equipment and machinery, and waste by using Metal Hydrides alloy powders.

METAL HYDRIDES INC.

12-24 CONGRESS STREET • BEVERLY • MASS.

Industrial Notes . .

• The National Production Authority announced that the U. S. is receiving about 17 million lb of nickel a month, or about 68.4 pct of the world's supply. Approximately 70 pct of the total goes into expanding military and atomic energy programs. The remaining 30 pct is being divided between supporting industries, power for example, and civilian use.

• *The valve div. of Minneapolis-Honeywell Regulator Co. has established a research center in Philadelphia in support of an extensive development program in industrial valves. Research and test equipment will evaluate present valve design and will also aid in development of new type valves. Also to be investigated will be substitutes for critical valve materials.*

• Penn-Ohio Steel Co., of Birdsboro, Pa., has acquired control of Buhl Mfg. Co., of Detroit. Control was effected through purchase of Buhl's cumulative preferred stock and a majority of the common stock. Buhl manufactures automotive and airline products and is one of the nation's largest makers of milk cans. Penn-Ohio plans to expand the Detroit plant through acquisition of other automotive products.

• Members of the aircraft industry and the National Production Authority held a recent meeting to settle details of a program for the testing of boron steel in more aircraft. Final specifications were tentatively reached for special heats to be used by individual aircraft manufacturers. Five heats, each type made within the ranges of high and low alloying content, will be tested in bar, tube, and sheet form.

• Armco Steel Corp. filed a suit for infringement of patent rights against U. S. Steel in Federal District Court, Pittsburgh. The court battle arose from application of metal coating to steel strip. Armco seeks an injunction against infringement of three patents and asks for an accounting of profits and damages resulting from the alleged infringement.

• Kaiser Aluminum & Chemical Co. expects to have its eighth potline in operation at its Mead reduction plant by the end of the summer. The new installation is part of the $12.8 million expansion program at Mead that will add another 40 million lb to the annual 300 million lb annual capacity.

About $4 million also will be spent upon fume control, a problem at the Mead plant.

• A crushing plant and conveying system will be installed at the government owned experimental alumina plant at Laramie, Wyo. The crushing plant will be used for experimental work in recovering alumina from low grade ores.

• **Westinghouse Electric Corp. plans to build a new plant for the manufacture of watt-hour electric meters at Raleigh, N.C. Part of a $296 million expansion program, the plant will occupy 500,000 sq ft and employ 2500 persons. The program is the second for Westinghouse since World War II. The first cost $130 million and increased production 50 pct. The new program is expected to boost production an additional 50 pct.**

• Bethlehem Steel has contracted to purchase part of the output of the manganese deposits at Macapa, Para, Brazil. The mine is expected to produce 300,000 tons during its first year of operation, with an eventual target of 500,000 tons. The Companhia Industrie e Comercia expects to have the mines in operation by the end of the year.

• General Electric plans to build a multi-million dollar transformer manufacturing plant at Rome, Ga. Construction is scheduled to begin in 1953 and full production is expected by 1955. Transformers producing the equivalent of 7 1/3 million hp will be built annually at the new plant. Transformer ratings to be manufactured will range from 300 kva to a maximum of 7500 kva, 69 kv and below.

• *Apex Smelting Co., makers of aluminum zinc base and magnesium alloys, is building a commercial plant in the Pacific Northwest. The plant will produce intermediate alloys containing aluminum and silicon from clay. The expansion is a step forward in the program started five years ago when Apex began experiments on clays that contain these materials.*

• Jones & Laughlin Steel Corp., has decided to abandon operation of its three Bessemer converters at the Pittsburgh south side works. The first of the three furnaces was built in 1885. The corporation's decision is said to stem from its modernization program and expansion of open hearth furnace capacity.

Specific Purpose Grinding Wheels

Electro's special composition wheels for the specific purpose of grinding any particular metal have repeatedly shown savings on abrasive cost at both vitrified and resin speeds, plus labor savings.

Requirements in grinding wheels become increasingly individual. If the wheel you need isn't made, we'll make it for you. Write, wire or phone for an Electro Sales Engineer to survey your needs without obligation; and send for Grinding Wheel Manual 645 and Speed Calculator. Both free and very useful.

Electro Refractories & Abrasives Corporation

344 Delaware Avenue, Buffalo 2, N. Y.

WEST COAST WAREHOUSE: LOS ANGELES 58. PLANTS IN BUFFALO, N.Y. AND P.Q., CANADA

Books for Engineers

Tungsten, by Colin J. Smithells. *Chapman & Hall, Ltd.* $10.50, 326 pp. 1952—The last edition of this book was published 15 years ago, but since then many developments have taken place and author and publisher felt a third edition was warranted. The author assumes the role of editor, with most of the chapters written by authorities in the field. Chapters deal with preparation, purification and reduction of tungsten oxide; manufacture of ductile tungsten; metallography of tungsten; effect of cold work and annealing on physical properties; properties of tungsten as a function of temperature; thermionic properties; tungsten iron alloys and tungsten steels; nonferrous alloys and industrial applications of tungsten; tungsten carbides and the hard tungsten alloys, and determination of impurities. The introduction traces the history of tungsten and gives an account of tungsten minerals.

Nomography and Empirical Equations, by Lee H. Johnson. *John Wiley & Sons, Inc.* $3.75, 150 pp. 1952—The purpose of the book is to explain the use of nomographs and empirical equations without going into too much detail. The approach to empirical equations requires a knowledge of logarithms and analytical geometry. The book is aimed not only at engineers but also physicists, chemists, doctors, and other scientific and professional people who may find the two methods for recording discovery of new knowledge useful.

A History of Phelps Dodge 1834-1950, by Robert Glass Cleland. *Alfred A. Knopf.* $4.00—The book traces the growth of Phelps Dodge from the day Anson Greene Phelps opened a small saddle shop in Hartford, Conn., to the present. As the country grew, so did Phelps Dodge. The company took part in large affairs from its very beginning. It bought and sold, exported and imported, built factories and railroads, and widened its scope of operations economically and geographically. The author traces the entrance of Phelps Dodge into the copper field and the gradual giving way of other interests in favor of the new venture.

Elementary Metallurgy, by W. T. Frier. *McGraw-Hill.* $4.50, 258 pp.—The second edition of this popular text is a practical easily understood analysis of elementary metallurgy. It is designed to give the reader a better understanding of the metals with which he is specifically concerned. The chapter on the blast furnace reactions has been enlarged. Greater stress has been placed on the origin of steel and the influence of carbon. The chapter arrangement takes into account the interrelation of materials so that the first chapter deals with pig iron while the second chapter is concerned with steel production. Greater detail is included on the open hearth process. The chapter on wrought iron contains a description of the Aston process. Other changes have been made in the book in line with recent metallurgical developments. A bibliography is included at the end of each chapter and a list of films added.

Design Manual for the Repair of Aluminum Alloy Structures, edited by Howard M. Jensen. *Johnson Research Corp.* $3.50, 208 pp. 1952—Almost every repair that might be required on an aluminum alloy structure is covered by the book. Skin repairs, extrusion and rolled section repairs, tubing repairs, and others. Each repair has been accurately designed and stress analyzed.

Bolt, Nut, and Rivet Standards. *Industrial Fasteners Institute.* $3.00, 256 pp. 1952—This revised issue replaces the first edition published in 1941. It contains all current standards for commercial fasteners. Among the new standards included in the book are those for round head bolts, plow bolts, track bolts, studs, slotted and recessed screws, socket head screws, small solid rivets, large rivets, unified screw threads, and the newly-adopted square and hexagonal bolts and nuts unified dimensionally with Britain and Canada. One section lists weights and stock production sizes.

Forging and Forming Metals, by S. E. Rusnoff. *American Technical Society.* $3.95, 279 pp.—The book was written with the idea of bringing knowledge in the field up to date. The author expresses the belief that earlier publications are worthless in view of modern technological progress. Impact forging, press forging, extrusion, heat treatment of forgings, cleaning and finishing, inspection, safety, metal quality, and the designing of forgings and tools and dies, are covered in the book.

Communication of Technical Information, by Robert M. Dederich. *Chemonomics, Inc.* $5.00, 116 pp. 1952—The book is designed as an aid in bridging the gap between the executive and his technical personnel. It is concerned with the fundamental principles of writing in language understandable to the laymen and the scientist. Stress is placed on the thinking and logic which must underly communication of technical information. The book deals not only with the written report but with inter-office memos, progress statements, and oral presentation at conferences.

ORDER YOUR BOOKS THROUGH AIME—Address Irene K. Sharp, Book Department. Ten per cent discount given whenever possible. Order Government publications direct from the agency concerned.

PROFESSIONAL SERVICES

Limited to AIME members, or to companies that have at least one AIME member on their staffs. Rates $40 per year per inch.

ENGINEERS
CONSULTANTS
METALLURGISTS
Small Jobs Welcomed
SAM TOUR & CO., INC.
Laboratories and offices
44 Trinity Place, New York 6, N. Y.
Testing—Certifying
American Standards
Testing Bureau, Inc.

LEWIS B. LINDEMUTH
Consulting Engineer
140 CEDAR STREET NEW YORK 6, N. Y.
STEEL PRODUCTION
DESIGN · OPERATION · CONSTRUCTION · METALLURGY

R. S. DEAN LABORATORIES, INC.
Consulting Research Development
Chemistry, Electrochemistry & Metallurgy. Laboratory Research on a Contract Basis
5810—47TH AVENUE AP 2821
RIVERDALE, MD.

MAX STERN
Consulting Engineer
150 Broadway New York 7, N. Y.

T. STARLING WINTERS
Consulting Engineer
100 East Palisade Ave. Englewood, N. J.

Advertisement

ELECTROMET Data Sheet

A Digest of the Production, Properties, and Uses of Steels and Other Metals

Published by Electro Metallurgical Company, a Division of Union Carbide and Carbon Corporation, 30 East 42nd Street, New York 17, N. Y. • In Canada: Electro Metallurgical Company of Canada, Limited, Welland, Ontario

VANADIUM...the metal that accentuates the effects of other alloying elements

Vanadium is usually added to steel or iron along with other alloying metals, such as manganese, tungsten, nickel, or chromium. It enhances the effect of these other alloys and helps to improve the physical properties of the metal. Generally it is used in quantities of less than 0.50 per cent, but even in these small amounts it is responsible for many marked improvements in the quality of iron and steel.

One of the most notable functions of vanadium is its effect in improving the dynamic properties of steel, such as fatigue and impact resistance. It also gives an inherently fine grain size to both steel and iron.

In high-speed tools, vanadium contributes wear resistance and red hardness. It is also an important alloy in many types of permanent magnet steels. These and many other types of special-purpose steels contain more than 0.50 per cent vanadium to enhance certain properties.

Dynamic Strength for Steels

The principal effect of vanadium in engineering steels is that of refining grain size. It is usually added in amounts of 0.10 to 0.25 per cent.

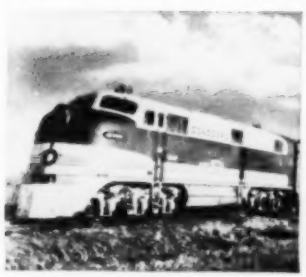

Fig. 1. Steels in which vanadium is an alloy have outstanding dynamic strength. That is why they are frequently used in such heavy-duty service as springs and axles in diesel locomotive trucks.

In the lower carbon ranges, vanadium steels are especially suited for carburizing and are used for such applications as hand tools, bearings, and pistons. Vanadium-bearing steels can also be nitrided effectively.

Vanadium contributes fatigue and impact resistance and also strength and ductility to spring steels. The famous chromium-vanadium (SAE 61xx series) and manganese-vanadium spring steels are outstanding examples of this use. Besides being used as springs, these steels are frequently used for axles, shafts, and other highly stressed moving engine parts.

Red Hardness in Tools

Practically all fine tool steels contain vanadium. In high-speed steels, vanadium content usually ranges from about 0.50 to 2.50 per cent, although higher percentages are sometimes used. Other alloy tool steels usually contain from 0.20 to 1.00 per cent vanadium.

Vanadium is a strong carbide-former and forms very hard and stable carbides. These vanadium-carbides are probably the main reason for the excellent wear resistance and edge-holding properties of vanadium tool steels. The persistence of the vanadium-carbides is largely responsible for the cutting qualities at red hardness of high-speed tool steels.

Adds Strength to Cast Iron

In amounts of 0.10 to 0.15 per cent, vanadium increases the strength of cast iron from 10 to 25 per cent, and adds a considerable amount of toughness. Cast iron containing vanadium is especially valuable in such applications as steam locomotive cylinders, valve and piston bushings, piston rings, and similar parts. In steam engines and diesel motors, vanadium cast iron cylinders greatly outlast those of ordinary cast iron. Chromium-vanadium cast iron rolls, containing up to 2 per cent chromium, have been used successfully in steel mills for a great many years.

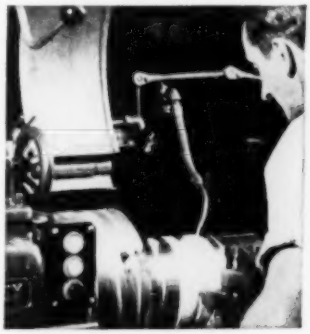

Fig. 2. Nearly all fine tool steels contain vanadium. It promotes fine grain size, high wear resistance, and greater control of hardenability. Vanadium also contributes to the red hardness of high-speed tool steels.

Cast iron in which vanadium is the sole alloying element is used primarily in applications where temperatures are moderately high and in heavy sections requiring uniform hardness without brittleness.

ELECTROMET Vanadium Alloys

ELECTROMET produces three grades of ferrovanadium in various sizes for the production of vanadium-bearing steels and irons. Each grade has a definite range of carbon and silicon contents and is especially adapted to assure the best results in the different requirements of iron and steelmaking.

Write for a copy of the booklet, "ELECTROMET Products and Service." It contains many useful facts about the use of ferrovanadium. The booklet also describes over 50 other alloys and alloying metals produced by ELECTROMET.

The term "Electromet" is a registered trademark of Union Carbide and Carbon Corporation.

Journal of Metals

ALUMINUM Co. of America last month unveiled its 15,000 metric ton aluminum forging press that is in operation at the company's Cleveland works. This press which was in operation in Germany from 1940 until the end of the war was built by Schloemann Co., Dusseldorf, and is second in size in this country only to the American built 18,000 ton press of Wyman Gordon.

This 15,000 ton aluminum forging press leased by Alcoa from the Air Force is the second largest operating in the United States.

Shortly after VE Day, Russia grabbed off the largest of Germany's heavy forging presses, a 35,000 ton job, and put it to work producing large aluminum sections for planes. The United States got two 15,000 ton presses, of which Alcoa's is one. It has been rumored that a 53,000 ton press was also built by Schloemann and is now operating in Russia.

Representative Gross (Rep. Iowa) recently blamed the Air Force for permitting the U. S. to lag behind Russia in building up air power by not having the German presses in operation sooner, and for being so slow in providing for new presses. Several presses were ordered some time ago (JOURNAL OF METALS, February 1951) with an estimated 18 months delivery, but they are still not in sight. However, it has been said that no actual work is waiting for the proposed presses—sections that could utilize the full potentialities of the giant presses are only on the drawing boards or experimental work. Underway also is a heavy furnace program—large furnaces designed to provide a steady supply of hot blanks for the presses.

The original press program called for a 75,000 ton forging press, but while design will be completed, production has been shelved. Present plans include eight aluminum forging presses. Loewy Construction Co. will build a 35,000 and 50,000 ton press for Wyman Gordon's Grafton plant; Mesta Machine Co. will build a 50,000 ton press for Alcoa, Cleveland; United Engineering & Foundry Co. will build two 35,000 ton presses, one for Harvey Mfg. Co., and one for Alcoa, Cleveland. Baldwin-Lima-Hamilton will build a 25,000 ton press for Harvey, and E. W. Bliss a 25,000 and a 35,000 tonner for Kaiser Aluminum & Chemical Corp., Newark, Ohio.

Of the nine extrusion presses to be built, all but one are for aluminum. Loewy Construction Co. will build seven of the presses of which two will be specials—a 13,300 ton Schloemann press for Alcoa, Lafayette, Ind.; and a 12,000 ton press for steel extrusions for Curtiss Wright, Buffalo, N. Y. Lombard Corp. will build the remaining two presses. Distribution and capacity of the presses will be: Reynolds Aluminum Co., Phoenix, Arix., 8000 and 12,000 tons; Harvey Mfg. Co., 8000 and 20,000 tons; Kaiser Aluminum & Chemical Corp., Halethorpe, Md., 8000 and 12,000 tons; and Alcoa, Lafayette, Ind., 20,000 tons.

◆◆◆◆◆◆◆◆

SUPREME Court Justice Hugo S. Black transcended the steel situation and reached well beyond it to other facets of society which have been debated by many Americans during the past and current generation. While primarily denying any President the right to take over the steel industry without Congressional authorization, it also in essence forbids a chief executive from taking similar action relative to other private organizations and quasi-public institutions as newspapers and radio stations.

Many clear thinking people have been of the opinion that the United States has, until now, been taking the road which leads away from the principles of 18th and 19th century liberalism. For them, the Supreme Court decision is a victory. Government participation in private affairs, they feel, should be limited to necessary regulation required for protection of the rights granted by the Constitution.

The Union and the companies have arrived at the point where they are quite willing to thrash things out without the good offices of Government. The advantage of a speedy settlement to both sides is obvious. The decks have been cleared of legal obstacles which impeded any real progress. The unfortunate aspect is that the defense effort must suffer. At the time of the Supreme Court decision, the steel industry was producing at more than 110 million tons per year, well over official rated capacity. The eventual goal for 1952 of 117 million tons seemed far away when Phil Murray called his men out of the plants. However, the odds against reaching the target are not insurmountable, and the industry may yet reach its objective.

◆◆◆◆◆◆◆◆

THE qualities of leadership, responsible for the magnificent pioneering era in American history, are rapidly departing from the scene of U. S. endeavor. American industry is faced with a dearth of young men with executive ability. Few young men today show signs of the talent needed to take

over the work when men now in positions of leadership retire. Recently, Benjamin Fairless, president of U. S. Steel, also was elected chairman of the board, on the retirement of Irving S. Olds. Perhaps the dual position was necessitated by the scarcity of men of the caliber of Olds and Fairless.

Executive training programs are part of the organization of many major corporations. Somehow, they have failed to produce men capable of stepping into the higher echelons. They fall far short of developing the man of vision who can plan for the future, instrument the needs of the present, and still maintain the equilibrium needed for sensible management. The nation must find many, many leaders, or else the economic structure will become unwieldy and collapse. At a time when the nation needs legions, it is producing only squads.

◆◆◆◆◆◆◆◆

ALCOA plans to operate its Rockdale, Texas plant on lignite, when construction is completed. According to I. W. Wilson, Alcoa president, the cost of natural gas has reached the point where other production factors outweigh any saving which might be made by its use. The price of natural gas has more than doubled in the last two years, and has made the use of lignite economical where transportation costs reduce the overall cost of production. Certainly lignite is more expensive than northwest water power, but the location of the new Texas plant makes it possible to take advantage of favorable transportation conditions. The possibility of extracting tar and tar acids from lignite before use in aluminum reduction also adds to its economic desirability.

Wilson also has taken a stand on the proposed aluminum expansion program. He feels that enlarged production facilities must await future markets. In addition, he feels that the Government would have to resort to subsidation if a new producer is to be brought in.

In the meantime, the government expansion policy remains clouded. In one instance, two cabinet officers made statements in contradiction to each other. Commerce Secretary Charles Sawyer sided with DPA. Sawyer said the U. S. "should get all the aluminum we can, as fast and as cheaply as we can, wherever we can, including Canada."

Interior Secretary Chapman, in a letter to the Joint Committee on Defense Production, favored encouragement of new, independent and domestic producers. Sawyer, though, viewed the proposed Alcan arrangement as a good one. Under the plan, at least 80,000 tons of aluminum would be offered to the U. S. this year and 90,000 in 1953. In 1954, offerings would increase and the U. S. would assume a liability to purchase. The contract would run until 1958—an item not to the liking of Chapman.

◆◆◆◆◆◆◆◆

NATIONAL Production Authority's present report on the substitution program indicates the conservation program has aided the defense effort immeasurably without upsetting the normal markets for the materials substituted. Realizing that any general trend toward substitution of one metal for another is likely to alter a particular market, NPA has moved cautiously and only when the needs of the production program warranted it. W. H. Wiewel, assistant administrator, Metals and Minerals Bureau, NPA, said the shortages will probably grow less acute within the next year or two. As current expansion programs are completed, considerable metal will be released to normal markets.

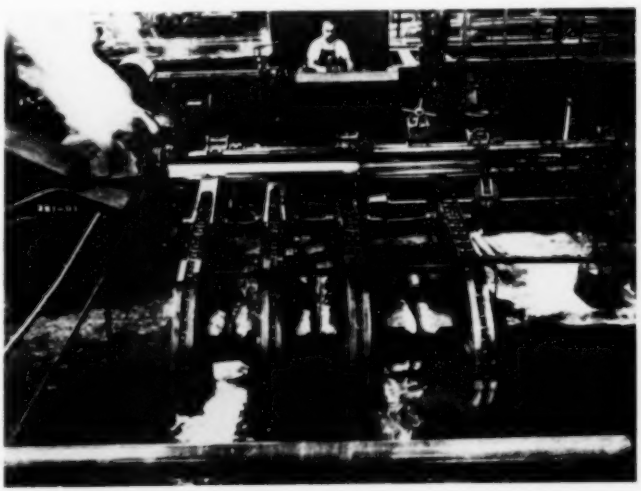

Copper billets from 3 to 9 in. in diam and weighing up to 1000 lb, are heated in a rotary furnace to about 1500 F, and move into this billet piercer at Chase Brass & Copper Co., Waterbury, Conn.

In less than 1 min, the hot billets are rotated and driven ahead by tapered rollers which open up the end of the billet to form a cavity, a mandrel moves in the rotating billet until a rough, hollow tube is formed, and the tube is conveyed through a water quench. The rough tubes are then cold drawn down to desired size.

MIGHTY FINE FOR MIXERS

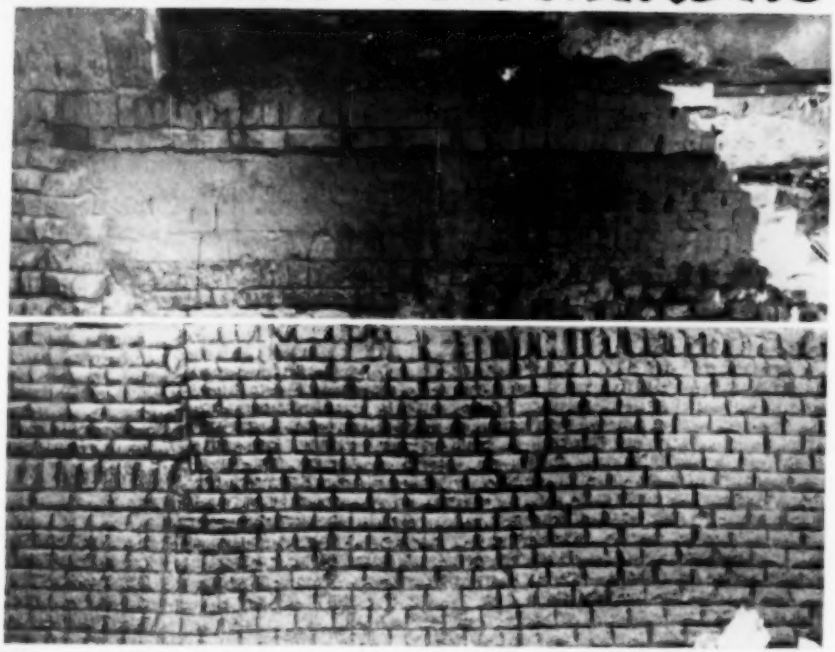

Area below white line is TASIL brick and cement in front-wall of 1300 ton mixer after handling 827,000 tons during 18 month period. High duty fireclay brick in less vulnerable area above white line, show severe erosion.

TASIL LASTS TWO CAMPAIGNS

Taylor Sillimanite (TASIL) Brick, laid in TASIL No. 302 Heat-Setting Cement, were used to "*balance*" the refractory lining of a 1300-ton Hot Metal Mixer which began operation in June, 1950. TASIL was used to strengthen the vulnerable areas of the front-wall, backwall and endwalls, and the pour-out spout jambs, sidewalls and bottom.

When this mixer came down in April, 1951, after approx. 450,000 tons had been through it, the TASIL Brick in the front and backwall were in such excellent condition they were *left in for the second campaign*. The TASIL in these areas had lost only 2 to 2½".

The second campaign ran from April to December, 1951, handling approx. 377,000 tons. Total for the two campaigns on the TASIL front and backwall are impressive:

MONTHS SERVICE: 18
TONNAGE HANDLED: 827,000 (approx.)

A five-campaign average for Blast Furnace Quality Firebrick linings in this mixer was 225,000 tons.

Results such as this continue to prove that TASIL "Balanced" linings are unsurpassed, from the standpoint of over-*all life and economy*. Use TASIL Brick in the areas of severe erosion—Fireclay Brick in the remainder of the lining—*all* laid in TASIL Cement. Call in a Taylor representative for a factual discussion of the TASIL possibilities in your plant.

Exclusive Agents in Canada:
REFRACTORIES ENGINEERING AND SUPPLIES, LTD.
Hamilton and Montreal

The CHAS. TAYLOR SONS Co.
A SUBSIDIARY OF NATIONAL LEAD COMPANY
REFRACTORIES SINCE 1864 • CINCINNATI • OHIO • U.S.A.

THE DRIFT OF THINGS

by Edward H. Robie

Engineers' Centennial

THIS summer, in Chicago, will be celebrated the "Centennial of Engineering" and half a hundred engineering societies will have meetings of one kind or another in the two weeks following Labor Day. It is really the 100th anniversary of the founding of the American Society of Civil Engineers. Centennial of Engineering is merely a convenient label to put on the celebration of 100 years of engineering progress in this country since the ASCE was founded. Engineering, of course, is much older than is thus indicated—thousands of years older. But Americans have a penchant for dramatizing progress by celebrating assumed anniversaries. Four years ago a special 3c stamp was issued on which a Brahma chicken was prominently displayed, with the legend, "1848-1948. Centennial of the American Poultry Industry." We feel reasonably sure that the first dozen eggs was sold considerably earlier than that.

Until a hundred or so years ago engineers were generally classified as either military or civil. Apparently a group of civil engineers met for the first time in Augusta, Ga. but no records were kept and the first meeting of which we have definite knowledge was at Barnum's Hotel in Baltimore, Feb. 11, 1839. Forty engineers were present and they decided to form a society. Among the aims of these engineers was "the greatest amount of useful effect at the smallest cost," which is as good a slogan for the engineer of today as it was 113 years ago. It was mentioned that the existence and prosperity of the society depended in no small degree on "the personal conduct and exertions" of the members. "Talents and respectability are preferable to numbers . . . from too easy and promiscuous admission, unavoidable, and not infrequently incurable, inconveniences perplex most societies."

The name American Society of Civil Engineers was selected. It was recommended that "architects and eminent machinists" be admitted to only associate membership. The founding committee recommended that every Member and Associate be required "to produce to the Society at least one unpublished communication in each year, or present a scientific book, map, plan, or model not already in the possession of the Society under penalty of $10." Apparently the society was too exclusive and the penalty for the unproductive member a bit too steep, ten bucks being what it was in those days, so the society died a-borning. An effort was, however, made to set up four engineering societies on a geographical basis, with one covering New England and New York; the second, Pennsylvania, New Jersey, Maryland, Delaware, and Virginia; the third all the states south of Kentucky and Virginia; and lastly "Kentucky and the Northwestern States." Something along this line was accomplished when the Boston Society of Civil Engineers was founded in 1848.

Efforts to organize a national society were finally successful in 1852 when the American Society of Civil Engineers and Architects was founded. There was but one grade of membership, to which were eligible "Civil, Geological, Mining, and Mechanical Engineers, Architects, and other persons who, by profession, are interested in the advancement of science." Those educators of the present day who take a dim view of the curricula labeled "geological engineering" can thus see that geological engineers were at least given early recognition.

In 1853 the Society held eight meetings, with an average attendance of six, and in all only 14 different members came to the meetings. In 1854 only six meetings were held, and attendance was less than in 1853 so resident dues (for those within 50 miles of New York) were reduced from $10 to $5 and non-resident dues from $5 to $3. This was done to "render membership less onerous, and with the hope that by so doing new members might be induced to seek a connection with the Society . . . the labors of the members more than their money is wanted to make the Society useful."

The Society had no headquarters so it was proposed to rent a room convenient to the office of some member who might be willing to supervise it, the annual rental of the room not to exceed $250, and the cost of furnishing not more than $150.

After its meeting on Mar. 2, 1855 the new Society was dormant for 12 long years, during which period the Civil War was fought. It came to life, with two rooms as headquarters in downtown New York, in 1867. Dues were put back up to $10 and $5, and the assets of the Society were $1592.07. The next year the words "and Architects" were deleted from the Society's name, but it remained a society for all engineers even after the mining engineers formed the AIME in 1871. In 1855 a member of the Society asked "whether any Transactions of the Society have been published or intended to be" (grammar was evidently not pure even in those days) but it was not until 1872 that the Civils published their first volume of Transactions. That was only one year before the first volume of AIME Transactions was published. A members' badge was not adopted until 1884 though the AIME had previously adopted one, and the American Society of Mechanical Engineers, founded in 1880, likewise. The Electricals did not form a separate society until 1884, and used the Civils quarters for several years. The Chemicals did not branch off on their own until 1908.

On Feb. 14, 1903 Andrew Carnegie wrote the following letter:

"Gentlemen of the American Society of Civil Engineers, American Society of Mechanical Engineers, American Institute of Mining Engineers, American Institute of Electrical Engineers, and the Engineers' Club: It will give me great pleasure to give, say, one million dollars to erect a suitable Union Building for you all, as the same may be needed. With best wishes, Truly yours, Andrew Carnegie." The societies were required to purchase suitable property on which to erect the building. The final amount that Mr. Carnegie gave was $1,050,000, and the present Engineering Societies Building was dedicated on Apr. 16 and 17, 1907. The Civils did not move in and become one of the four "Founder Societies" until about ten years later.

We are indebted to a history of the ASCE prepared by Edward C. Thoma for most of the above information. With the present building soon to celebrate its 50th anniversary, what we engineers now need is another Andrew Carnegie. Unfortunately the political climate is not now so favorable for accumulating large fortunes which may be available for such purposes as it was a half century ago.

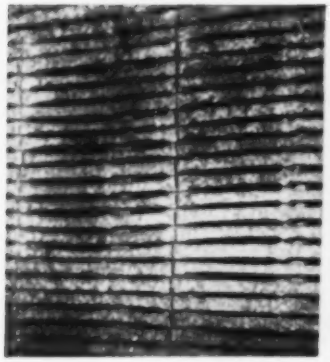

COMPARISON OF GRATE MATERIAL

Gray iron sintering grates, at left, show bad scaling and warpage after a single month of use. Note good shape of Ductile Iron grates, above, after same service. They greatly outlasted gray iron grates.

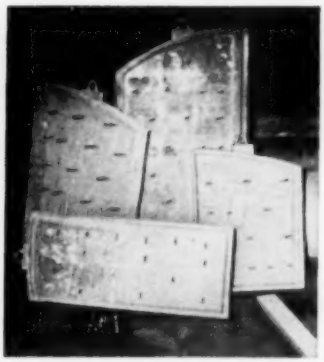

DUCTILE IRON FURNACE DOORS SAVE MONEY, TIME AND LABOR—In ordinary iron, exposed to high temperature, internal oxidation easily penetrates along paths of flake graphite, thus causing destructive growth. Penetration is curbed in Ductile Iron, since its graphite is wholly in spheroidal form.

DUCTILE IRON Sintering Grates and Furnace Doors

excel in elevated temperatures

Performance Records Show Outstanding Heat-Resistance of this New Material.

Tests show that iron containing graphite wholly in spheroidal form provides notably greater growth resistance than ordinary gray iron.

FOR INSTANCE: Gray iron and Ductile Iron grate bars in the Greenawalt sintering system of a merchant pig-iron producer gave the following performances:

At the Canadian Furnace Company, Ltd., in Port Colborne, Ontario . . . from date of their installation, August 1950, to June 1951 . . . no Ductile Iron grates needed replacements although 150 gray iron grates had to be replaced after 6 weeks' service.

The sinter-plant foreman stated, "*The Ductile Iron grates still seem to be as good as new.*" Cast by Lakeside Foundry, Ltd., of Port Colborne, these Ductile Iron grates also out-performed steel grates tested previously.

ANOTHER EXAMPLE: The forging furnaces of a leading steel plant now have Ductile Iron doors supplied by United Engineering and Foundry Company, Pittsburgh 22, Pa. Gray cast iron doors which were subjected to 24 hours' continuous service daily, heat-cracked after an average life of about four weeks. A trial lot of annealed Ductile Iron doors lasted 17 weeks . . . or more than four times as long as those of gray cast iron.

APPLICATIONS: As cast, as well as heat-treated Ductile Iron parts . . . serving at elevated temperatures in scores of machinery, engine and furnace applications . . . provide a growth-resistance heretofore unavailable in gray cast iron.

AVAILABILITY: Send us details of your prospective uses, so that we may offer a list of sources from some 100 authorized foundries now producing Ductile Iron under patent licenses. Request a list of available publications on Ductile Iron . . . mail the coupon now.

The International Nickel Company, Inc.
Dept. JOM, 67 Wall Street, New York 5, N. Y.
Please send me a list of publications on:
DUCTILE IRON

Name _____ Title _____
Company _____
Address _____
City _____ State _____

THE INTERNATIONAL NICKEL COMPANY, INC. 67 WALL STREET NEW YORK 5, N. Y.

Douglas Aircraft Co., Inc., will use about 88 pct titanium for skin covering of DC-7 engine nacelles. The use of titanium sheet represents the first time the metal has been employed in the airframe of a commercial aircraft. A 300-lb weight saving is expected because of the substitution for aluminum alloys and stainless steel.

Recovery of germanium from smelter dusts is being investigated by the Union Miniere Du Haut Katanga. A report to the ECA indicates that germanium oxide can be recovered from the dust and smoke of roasting zinc ores.

Apex Metal Products Corp., Cleveland, wholly owned subsidiary of Apex Smelting Co., has the exclusive license for the continuous casting of aluminum and other nonferrous metals under the Goss patents. The new process is said to represent the shortest distance from molten metal to the forge hammer.

Ordinary steel box strapping is being used by Solar Aircraft Co., for sawing stainless and other high alloy sheets. A much greater work life for the blades compared with that for regular saw tooth blades is reported by the company. The toothless blades harden and roughen within the first few seconds of cutting, and form their own oxygen scoops.

The Atomic Energy Commission reports the use of industrial radiography on a wide range of metals at lower costs may be possible through utilization of atomic waste products.

Mutual Security Agency approved a $8.47 million loan authorization to the Sollac Steel Combine for expansion and modernization of a light flat rolled steel plant in northeastern France. The hot strip mill is expected to produce an estimated 800,000 to 1 million tons of flat rolled steel products annually. Production is aimed at Western Europe's defense effort.

Completion of the third electrolytic aluminum furnace at the Toeging plant, of the Vereinigte Werke A. G., of Berlin and Bonn, brings the plant to its prewar capacity of 42,000 tons of primary aluminum. The present monthly output is about 3700 tons. Bauxite supplies have been assured for many months in advance.

Davy & United Engineering Ltd. of Great Britain, received the Karabuk Iron & Steel Works contract for extension and modification of the Turkish firm's 28-in. blooming and section mill plant. The pact involves the supply of more than 1000 tons of mill machinery and hydraulic equipment. The Karabuk installation is the only integrated steel plant in Turkey.

Italian firms are buying Japanese steel in quantity for the first time since the war. The Japanese product is slightly lower in price and delivery is quicker than from American suppliers.

Diamond Alkali Co., Cleveland, acquired metal cleaning processes owned by Spence Metals Research Co., Pittsburgh. Spence has developed several methods for desanding ferrous and nonferrous castings, and the cleaning and descaling of stainless steels. Diamond has supplied the basic alkali material used in the cleaning processes, and is carrying on research on application of the cleaning salts.

Conservation of and/or Substitution for Critical Jet Engine Materials

by N. E. Promisel

ONE of the most critical factors in the pattern of greatly expanded production for national defense, is the availability of materials to meet current and projected demands. The measures taken against spurious shortages were initially felt in this country in 1951, and former defense mobilizer C. E. Wilson said that the pinch will continue into 1953, and in some cases such as copper, into 1954. The most talked about material in critical supply is steel, because of its wide use for civilian goods, rather than a real quantitative shortage. Steel, copper, and aluminum are basic materials with a broad impact on military and civilian goods. Together they furnish a basis for the Controlled Materials Plan. Some very critical materials are less often discussed, but their scarcity spells future trouble in jet engine production. Here one of the major contrasts with World War II is found, because of demand for materials to operate under prolonged severe and complex stresses at extreme temperatures. Jet engine technology has imposed impressive requirements for scarce metals and advanced metallurgical thinking.

Steel cannot be disassociated from manganese, so vital in the industry as an alloying element, deoxidizer, and a neutralizer for sulphur. About two thirds of U. S. supply comes from India, Union of South Africa, and the Gold Coast. The intense production effort and paucity of domestic sources make this an extremely strategic material and have necessitated a program of stockpiling, conservation, and development of relatively low grade ores in this country. Substitutes for manganese in steel, such as titanium and zirconium, are being explored, with promising indications that at least partial substitution may be possible, subject to economic considerations.

Industrial expansion involves complex considerations if the program is to be well balanced. Production of materials needed for greater weapon output often means problems of machine tools and sources of power. The machine tool problem, is currently a major factor inhibiting increased military production.

Major factors to be considered in determining the classification of a material as critical are:

1—Strategic nature of source location, including importation hazards.

2—Reliability of sources, including their number and political factors.

3—Adequacy of natural resources, i.e., total material availability anywhere.

4—Availability of usable substitutes.

5—Adequacy of processing facilities, including power.

6—Expected M-day availability in stockpile.

7—Percentage of total requirements to be supplied by stockpile.

Scarce materials such as nickel, cobalt, molybdenum, and tungsten are allocated among 13 countries of the free world by an International Materials Conference.

Critical Jet Engine Materials

In jet engine production many of the acute shortages threaten to become severe. Fulfillment of these needs can have an overall impact on the entire materials field. In spite of substitution and other devices serving to reduce the demand the pressure for improved engine performance implies future

N. E. PROMISEL is Head, Materials Branch, Bureau of Aeronautics, Navy Dept., Washington, D. C. The opinions expressed herein are those of the author, and not necessarily those of the Dept. of Defense.

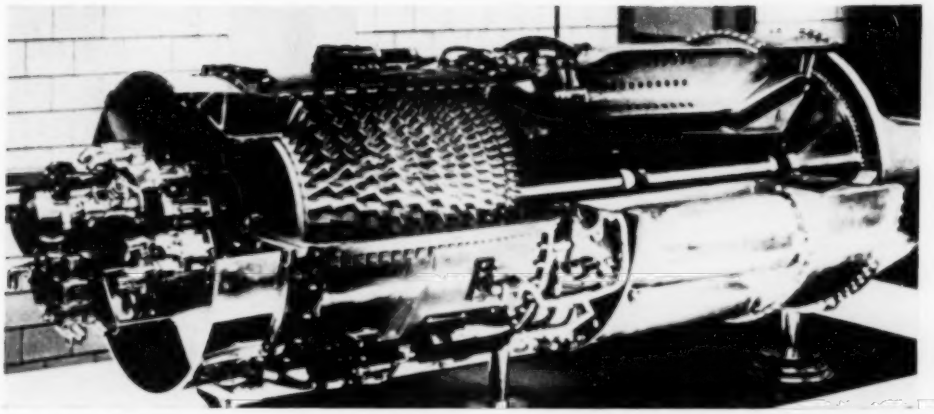

Fig. 1—Photograph of an axial flow type jet engine. To meet the specific requirements of different sections and components of the engine, many different materials are used. Temperatures range from below 0° to above 2000°F.

requirements for better materials to operate at higher temperatures.

Current jet engines require materials operating at temperatures ranging from below 0° to above 2000°F, over time intervals from an occasional brief hot-spot to perhaps 1000 hr. Stresses and operating conditions dictate consideration of stress rupture, creep, fatigue, notch sensitivity, toughness, impact, corrosion (in various forms), erosion, oxidation and other properties.

An axial flow type jet engine will be briefly reviewed. Alloy references in Tables I and II are illustrative only and are neither complete in alloys under each type nor in the elements listed for each alloy. In the jet engine Fig. 1, the air enters into the compressor, which operates at moderate temperature. Some compressor disks are aluminum alloy and the hotter ones are stainless steel, titanium, or low alloy steel. The rotating blades usually are of low-nickel or nickel-free stainless, types 431 and 410 respectively. The stationary vanes may be of stainless types 302, 410 or 431, or iron-copper powder metallurgy compacts, or even high tensile, low alloy steel. From the compressor, the air eventually finds its way to the burner area, where after fuel admixture and combustion, the hot gases expand through the turbine blades.

The combustion chambers are made of high alloy sheet (such as type 310 stainless or Nimonic 75) to resist high thermal stresses and fatigue. The turbine disk operates at high stress but as the temperature is only slightly more than 1000°F, reasonably lean alloys can be used. In some cases composite disks of low alloy core and higher alloy welded rim may be employed. The turbine blades represent the severest combination of temperature and complex stresses in the engine and require the richest alloys. The guide vanes also operate at very high temperature and thermal shock, but do not present the stress problem of the rotating blades. Finally, there is the exhaust system and tail cone, where fatigue and temperature must be combatted.

Table I shows the standard AISI stainless steels. All contain chromium, most contain nickel, and in some cases titanium, columbium, molybdenum, and tungsten. The last three alloys illustrate the types used for medium high temperatures and high stresses, as in turbine disks. Note the prevalence of chromium and nickel, and then to varying degrees columbium, molybdenum, tungsten, and cobalt. These alloys contain large quantities of iron, 40 to 50 pct.

Table II illustrates the alloys for highest temperatures and stresses. Again, chromium is present in all, as is nickel. Nickel and cobalt have replaced all the iron, with additions of the other high temperature elements—molybdenum, tungsten, and columbium.

Table I. Composition of Basic Types of High Temperature Alloys*, Pct

	Cr	Ni	Co	Mo	W	Cb	Ti
High Iron Types (balance mainly iron)							
AISI 302	17 to 19	8 to 10	—	—	—	—	—
AISI 310	24 to 26	19 to 21	—	—	—	—	—
AISI 316	16 to 18	10 to 14	—	—	—	—	—
AISI 321	17 to 19	8 to 11	—	—	—	—	0.75 max
AISI 347	17 to 19	9 to 12	—	—	—	1.00 max	—
AISI 410	11.5 to 13.5	—	—	—	—	—	—
AISI 430	14 to 18	—	—	—	—	—	—
AISI 431	15 to 17	1.25 to 2.50	—	—	—	—	—
19—9DL	19	9	—	1.3	1.2	0.4	0.2
Type A	20	20	20 to 30	3 to 10	2.5 to 5	0 to 1	—
Type B	15	26	—	1.5 to 3	—	—	—
Type C	13	13	10	2	2.5	3	—

* Only major critical elements listed.

Table II. Composition of Basic Types of High Temperature Alloys*, Pct

	Cr	Ni	Co	Mo	W	Cb
High Cobalt Type						
AMS [illegible]	20.5	20.5	45	4	4	4
AMS [illegible]	21.5	bal.	55		7.5	—
AMS [illegible]	27	3	62	6	—	—
High Nickel Types						
AMS [illegible]	15	72	—	—	—	0.7
Type A	20	56 to 59	10 to 14	3 to 10	—	—

* Only major critical elements listed.
† Aeronautical Material Specifications (SAE).

From these typical alloys, it is evident that at least six strategic elements may be selected: Cobalt, columbium, nickel, chromium (metallurgical and chemical), tungsten, and molybdenum.

Of the critical metals listed, columbium is a common ingredient of many of the best alloys. A major consumer is type 347 stainless steel, where columbium stabilizes the alloy against high temperature attack, by preferential combination with the carbon present. Columbium is imported from Nigeria and the Belgian Congo, and the availability of known practical, natural resources is limited.

Cobalt, up to the advent of the jet engine, was used conservatively in a limited number of applications, where special properties jutisfied its cost. Metallic uses have been in magnets, cutting tools and hard surfacing materials, low expansion alloys for joining metal to heat resisting glass and in recent years in heat resisting alloys. The major sources of cobalt are the Belgian Congo and Northern Rhodesia. Although natural resources are not limited as those of columbium, the increased demand for use in jet alloys makes cobalt one of the most critical materials of all.

One has but to review the many alloys in which nickel is found to realize its strategic importance. It is an important addition to low alloy steels (particularly for low temperature toughness) and in high alloy steels, notably the austenitic stainless group. It is used in cast iron, in nickel base alloys like Inconel and Monel and in numerous other nonferrous alloys, in electrical resistance alloys, in all heat resisting alloys, as a protective coating by electrodeposition, in magnets, as a catalyst and other applications. The relative abundance of this metal in Canada avoids the necessity for making it No. 1 on the shortage parade. The Nicaro deposits in Cuba should add an important 10 pct to the Free World's supply this year. Since columbium, cobalt, and tungsten are considered to be more sensitive strategically, conservation measures have been taken in the direction of using nickel to replace these metals. As a result, it is expected that military demands for nickel, particularly for jet use, will increase.

Tungsten is obtained from a number of sources outside this country, although important Montana mines are expected to produce late in 1952. Large quantities come from South America, Australia and some parts of Europe. Its extensive use in heat resisting alloys, high speed cutting tools and tungsten carbide and dependence on inadequate imports make this element critical. Molybdenum is included in the list, although it is primarily a domestic product. Its extensive use in low alloy steels, in which it is an important contributor to hardenability, its common presence in heat resisting materials and its significant potentialities for use alone or as a base for alloys for extremely high temperatures are the main factors dictating its importance in the military program. Scarcity is primarily because the richer ores were consumed in World War II, necessitating exploiting the leaner ores for anticipated requirements.

It might appear that all high temperature materials are so tight that the situation is hopeless insofar as substitution is concerned. It is true that it is often difficult to determine proper substitution. A number of lists have been published by non-government sources purporting to show quantitatively the relative scarcity of the elements mentioned. In general, these lists do not agree. Variations in the lists can be expected for use in procurement for stockpiling, for immediate production, for long range production planning, or for research and development. At the moment, nickel might appear to be the most critical element of all. Yet from a long range point of view this is not the case and columbium and cobalt are strong competitors for top ratings among the high temperature elements. Chromium can be considered to be the least critical of this group. Chrome stainless, containing no nickel, was recently removed from allocation under CMP to the status of a non-controlled material. The matter of justified use and substitution becomes even more involved when the partial interchange of several critical elements, the question of scrap and its reuse, the effect of substitution on requirements for different types of production equipment (casting versus forging) and other related factors are considered.

Conservation

Conservation embraces many approaches, which might be grouped as follows:

1—Substitution of less critical materials.

2—Scrap recovery.

3—Repair, reuse and increased life and efficiency of components.

4—More efficient manufacturing processes to reduce quantity of scrap.

5—Improved control of composition to avoid unnecessary surplus of critical ingredients.

6—Redesign of components to require less critical materials, in quantity or type.

It has been stated that the largest single outlet for columbium was in type 347 stainless steel, Table I. Three possible substitutes are available: Titanium stabilized stainless, type 321; use of tantalum to replace part of the columbium; and use of low carbon (0.03 pct max) unstabilized stainless steel. It is believed in most cases the two steels, 321 and 347, can be used interchangeably, although shop practice may require some modification. Retention of columbium may be justified for applications sensitive to continued high stresses at high temperatures, that are marginal in high temperature creep, or which cannot risk the presence of inclusions or stringers, and possibly severe chemical exposures. Such cases, however, (except for welding electrodes) are generally in the minority. The second substitute, tantalum, is used extensively in the approximate ratio of 2 to 1, columbium to tantalum. This substitution is desirable because of important ore supplies and residues containing columbium and relatively high in tantalum. The third substitute, low carbon stainless, has merit where corrosiveness and high temperature attack are not likely to be severe and where

the characteristics of a stabilized material, to a mild degree, are required.

It will be noted from Tables I and II that only type C of the high iron series and AMS 5765 of the high cobalt series contain high columbium. For the former, type B promises to be a suitable substitute and for the latter the high nickel alloys look promising, provided the increase in nickel can be tolerated.

Nickel in partial or total replacement, has been the major substitute for cobalt in alloys. This is particularly true for the wrought alloys. In the case of castings, cobalt seems to play an important role in contributing to ductility at low temperature. However, several new casting alloys look promising where cobalt has been reduced to about a third, with substantially higher nickel and tungsten. Here is an example where redesign, to minimize stress concentration and notch effects, might make possible the use of more brittle, very low cobalt or cobalt-free alloys. Also, better control of applications to avoid exposure to temperature and stress surges would increase likelihood of substitution. Simplifying design of turbine blades to permit rolling or extrusion of blade shapes is an example of conservation by minimizing machining and related losses. In the case of magnets, high purity powdered iron compacts and ferromagnetic oxide compacts offer possibilities where maximum magnetic energy is not necessary. In soft magnets, use of electromagnets are a possibility. The reuse of salvaged magnets in electronic components is also worthwhile. In cutting tools a high speed vanadium steel may be useful although this material may be difficult to grind. To a certain extent, nickel and possibly iron may be substituted for cobalt as a binder for carbides, particularly if the material is used as a cutting tool at only moderate temperatures. As in the case of columbium, some of the new materials discussed also could conserve cobalt.

Some specific substitute possibilities for nickel are:

For 18-8 Type Stainless—Nickel-free stainless of the 400 series (Table I) often may be substituted. Type 430 shows good resistance to high temperature scaling and oxidation, although lacking certain chemical resistance and high temperature strength. However, it welds well, can be worked easily, has lower thermal expansion, and finishes up well. Where necessary to enhance corrosion resistance of the nickel-free stainless steel, protective coatings may be applied, which may consist of ceramics or even nickel itself. Type 431, containing approximately 2 pct nickel, has corrosion resistance intermediate between the no-nickel and 18-8 types. Still another type of stainless that could be used is the type in which manganese replaces 4 pct of the nickel, with resulting comparable properties. However, the increased consumption of manganese would be an important factor. Aluminized carbon steel has been used for some high temperature shrouds. Clad steels are also distinct possibilities and may offer advantages over stainless since the core material may be selected for special properties, such as high thermal conductivity, and the cladding designed for protection. Most of the substitutes have been used in jet engine applications.

For Low-Alloy, High Strength, Nickel-Bearing Steels—The outstanding possible substitute is boron-treated steel. In a suitably melted steel, boron even as low as 0.001 pct contributes substantially to hardenability, thus permitting savings not only in nickel but also in molybdenum and chromium, with a possible saving of about half the critical alloy content. There is no shortage of boron for this purpose. Mill production of these steels has doubled since last August, currently being about 50,000 tons per month. The major worry of uniformity is disappearing as melting experience (particularly concerned with deoxidation) and proper use-experience progresses. Its limitations must be recognized: Effect of carbon content on hardenability contribution: avoidance of excess boron, about 0.005 and 0.008 pct being desirable maxima for high and low carbon steels; the need for thorough quenching and good heat treating practice; lack of suitability for high temperatures and deleterious effect of heating above 1600°F; increased sensitivity to temper brittleness unless precautions are taken, and other considerations. Data on aircraft quality grades, under fatigue, strength, notch and weld conditions are unavailable but an extensive program is underway. Table III gives possible alternate boron and lean steels which may be considered for conserving the alloying content of steels.

Fig. 2—An aluminized outer burner casing formed of AMS 5040 (SAE 1010) steel offers excellent corrosion resistance up to 600°F.

For Nickel Coatings—Nickel deposits are a common method of protecting steel from corrosion. Nickel is particularly valuable under chromium. Use of such coatings on substitutes for stainless alloys is justified where other coatings are not suitable. The possible embrittling effect of nickel plating on these substitutes must be considered. The newer technique of deposition by chemical reduction, without current—electrodeless nickel—appears promising. Under chromium, there is no wholly satisfactory, economical substitute. Sometimes omission of any underplate with increased thickness of chromium is preferable. Zinc and cadmium are both good protectors of steel, at least up to about 600°F. Surface treatments in chromate and other solutions enhance their value and promote paint adhesion. Baked resins and enamels offer further possibilities, particularly over a phosphated surface. Silicone-alkyd paints operate up to moderately high temperature, possibly up to 800°F. Metal spray, such as aluminum, has been used successfully as shown in Fig. 2. In all cases consideration must be given to the corrosion environment, wear and abrasion resistance, dimensional tolerances and effects upon the base metal. For

Table III. Possible Alternate Low Alloy Steels

	AISI No.	Composition, Pct C	Mn	Si	Ni	Cr	Mo
for S.S.	43BVxx 51100 94100	0.08 to 0.13	0.45 to 1.00	0.20 to 0.40	1.65 to 2.00	0.40 to 0.60	0.08 to 0.30
for S.S.	81Bxx 41100 48100 86100 87100	0.32 to 0.55	0.70 to 1.00	0.20 to 0.35	0.20 to 0.40	0.30 to 0.60	0.08 to 0.15
for S.S.	TS81xx 97100	0.43 to 0.70	0.70 to 1.00	0.20 to 0.35	0.20 to 0.40	0.30 to 0.55	0.08 to 0.15
for S.S.	86Bxx 98600	0.43 to 0.48	0.75 to 1.00	0.20 to 0.35	0.40 to 0.70	0.55 to 0.75	0.08 to 0.15
for S.S.	TS86xx 43100 47100 81100	0.13 to 0.53	0.70 to 1.00	0.20 to 0.35	0.40 to 0.70	0.55 to 0.75	0.08 to 0.15
for S.S.	94Bxx 84000 86000 86100 87100	0.13 to 0.20	0.75 to 1.00	0.20 to 0.35	0.30 to 0.60	0.30 to 0.50	0.08 to 0.15
for S.S.	98Bxx 61500	0.13 to 0.43	0.65 to 0.85	0.20 to 0.35	0.70 to 1.00	0.70 to 0.90	0.15 to 0.25

B indicates presence of boron, V indicates presence of vanadium, TS indicates tentative standard.

high temperature applications, ceramic coatings have been developed, each geared to the particular type of basis material and type of application. Ceramic coated, mild steel exhaust system parts have replaced stainless in some aircraft. Ceramic coatings on stainless have extended the life of parts significantly. A popular shock resisting coating is National Bureau of Standards Ceramic No. A417 applied in thicknesses of 0.001 to 0.003 in.

New Basic Materials

Although several new alloys have been alluded to a number of new materials that look promising are still in the development stage. Titanium and its alloys, of course, furnish the outstanding example of new material for operation up to about 700° or 800° F. Titanium is characterized by high strength, low specific gravity, excellent resistance to corrosion, good retention of properties at moderate temperatures and abundance in nature. High cost, limited production, difficulty in machining, broaching and grinding and alloy welding are some current problems that remain to be solved. In the high temperature range, work on chromium base alloys progresses, with promise of surpassing present alloys if melting and ductility problems can be overcome. Molybdenum and molybdenum-base alloys offer another fertile field, particularly for the higher temperature ranges. Here too are problems of availability, ductility and protection against oxidation.

There is an extremely important group of ceramic-metal combinations, called ceramels or cermets, that offer real promise in some high temperature applications. In this group are carbides, borides, nitrides, oxides and other transitional compounds, cemented with a variety of binders such as iron, cobalt, and nickel. One type that is receiving considerable attention contains mainly titanium carbide with nickel-cobalt binder. Such materials show good strength at very high temperatures, oxidation resistance, and thermal shock resistance. Ductility is generally limited but redesign will expedite adoption. Another recently introduced material is chromium carbide, which exceeds stainless and tungsten carbide in resistance to corrosion and high temperature oxidation.

Other Conservation Approaches

The return of clean, identified scrap to the alloy producer often accomplishes more conservation than an extensive substitution program. Arrangements are being made for the return of overseas scrap. Of great importance is the improvement of manufacturing operations to reduce scrap production. Casting and closed-die forging to close dimensions, to minimize machining, are illustrations of this. The use of built-up welded sections is another approach. Extrusion of precise shapes offers additional advantages. It is interesting to note the introduction into this country of the French Ugine-Sejournet extrusion process for hollow and solid shapes of steels and many other materials, using molten glass as a lubricant and as an insulator to protect the dies and equipment. Use of powder metallurgy techniques is being actively explored, particularly for producing permeable bodies that can be cooled by passage of a liquid or gaseous fluid. Cooling by such methods, or by flow through hollow parts, offers one of the most promising approaches for redesign to permit lower alloyed materials. Sometimes critical material can be conserved by ingenuity in heat treatment. Where high hardness is needed only locally or on the surface, low alloy steel or carbon steel may be used and induction hardened as necessary. Compression in the surface adds to the merit of the hardness obtained. Automotive crankshafts and axles of carbon steel have been successfully treated this way. Hot peening of Martempered or step-quenched leaner steels has been proposed as a means of obtaining compressive surface stresses combined with hardness.

The importance of reviewing every application using significant quantities of critical materials to determine whether the need for them actually exists is emphasized, not forgetting, however, that there is false economy if replacement or maintenance increases, the futility of the whole product if it fails to operate satisfactorily when needed, and the implications of such a failure.

OXYGEN IN STEELMAKING

by D. J. Girardi and D. C. Hilty

Because of the importance of oxygen in steelmaking and its influence on the properties of the finished steel, an Oxygen Symposium was held at the AIME Annual Meeting. This is a resume of the more important points brought out by the various papers.

OXYGEN, its effects and control in steelmaking is of vital concern to almost every ferrous metallurgist and steelmaker. More recently, the direct utilization of oxygen as a tool for accelerating steel melting operations through oxygen enrichment of the fuel, and by injection of oxygen into the molten bath to assist in carbon removal has further added to this interest. Many laboratories and operating organizations are conducting research on the technical and practical problems of steel deoxidation and the effective application and control of oxygen. The latest results of these investigations were brought to the attention of the American iron and steel industry when the Physical Chemistry of Steelmaking Committee of the Iron and Steel Div. of AIME sponsored a Symposium on Oxygen in Steelmaking at the AIME Annual Meeting in February. The program was organized by N. J. Grant representing the Physical Chemistry of Steelmaking Committee in cooperation with Walter Crafts, Program Chairman for the Iron and Steel Div.

Ferrous Oxide in Slags

The first session was held under the Chairmanship of N. J. Grant, Massachusetts Institute of Technology, and D. E. Babcock, Republic Steel Corp. A paper, by E. T. Turkdogan and J. Pearson of the British Iron and Steel Research Assn., presented by R. Schuhmann of Massachusetts Institute of Technology, dealt with the activity of ferrous oxide in slags. The authors reviewed and re-evaluated previously published data on oxygen solubility in molten iron and the effect of temperature and slag composition on the activity of FeO. The activity of ferrous oxide in any slag was calculated by dividing the oxygen content of the iron in equilibrium with it by the oxygen content of iron in equilibrium with essentially pure liquid iron oxide. It was established that ferrous silicate slags do not behave ideally, and the effect of temperature on the activity of ferrous oxide and silica in this system appears to be uncertain. In silicate and phosphate free slags the ferrous oxide activity is less than unity, probably because of ferrite formation. In the usual acid and basic steelmaking type slags the iron oxide shows positive deviation from ideality and does not appear to be affected by temperature between the limits of 1550° and 1650°C. Fluoride increased the activity of ferrous oxide in all slags studied.

A new iso-activity diagram for the ternary system $(CaO + MnO + MgO) - FeO - SiO_2$ was constructed.

D. J. GIRARDI is associated with Timken Roller Bearing Co., Canton, Ohio, and D. C. HILTY is with Union Carbide & Carbon Research Laboratories, Inc., Niagara Falls, N. Y.

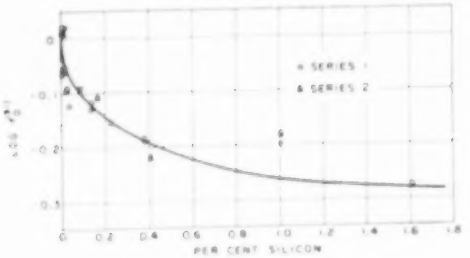

Fig. 1—Effect of silicon content on the activity coefficient of oxygen in liquid iron at 1600°C.

This diagram deviates somewhat from that of Taylor and Chipman in that the iso-activity lines are located differently and the locus of the inflexion points of these curves is not a straight line as suggested by Taylor and Chipman.

Distribution of Manganese

H. B. Bell, A. B. Murad, and P. T. Carter of the Royal Technical College, Glasgow, Scotland had examined the distribution of manganese between molten iron and FeO-MnO-SiO_2 slags not saturated with silica and reported their results in a paper presented for the authors by W. O. Philbrook of Carnegie Institute of Technology. They evaluated the apparent K_w of the reaction,

$$(FeO) + [Mn] = (MnO) + [Fe]$$

and found that it varied with the basicity of the slag, thus confirming the observations of other investigators.

By assuming the activity of FeO in the slag equal to the mol fraction of FeO, and by employing the K_w value of Chipman, Gero, and Winkler as the true K_w for pure FeO-MnO slags, the authors estimated the activity of MnO. By determining the activity of SiO_2 through the Gibbs-Duhem relation, corrections to these MnO activity values were made. A comparison of the activity values with those obtained by Schuhmann and Ensio for FeO-SiO_2 slags, and with estimated CaO and SiO_2 activities in CaO-SiO_2 slags, showed that they were in agreement with the known cation-oxygen bond strengths for calcium-manganese, and iron.

From their results, Bell, Murad, and Carter calculated the manganese, silicon, and oxygen contents of molten iron in equilibrium with various FeO-MnO-SiO_2 slags. These calculations, however, did not show good agreement with the experimental observations of Hilty and Crafts.

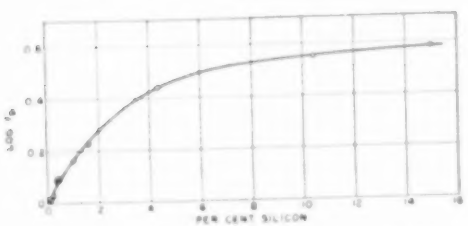

Fig. 2—Effect of silicon content on the activity coefficient of silicon in liquid iron at 1600°C.

Silicon-Oxygen Equilibrium

The next paper was a preprinted one on the silicon-oxygen equilibrium in molten iron by N. A. Gokcen and John Chipman of the Massachusetts Institute of Technology. Through the use of controlled atmospheres of steam and hydrogen that were useful in previous investigations of this type, small melts of Fe-Si-O alloys were equilibrated with the atmosphere in silica crucibles and then quenched in hydrogen and analyzed. By means of this technique a detailed study was carried out at 1600°C and up to 15 pct silicon of equilibrium in the reactions:

$$SiO_{2(s)} = Si + 2O \qquad [1]$$

$$SiO_{2(s)} + 2H_2 = Si + 2H_2O \qquad [2]$$

$$H_2 + O = H_2O \qquad [3]$$

Rate of reaction experiments lasting up to 16 hr indicated that the rate controlling process was the transfer of oxygen at the gas-metal interface and that the reaction at the metal-silica interface was more than sufficiently rapid to keep pace with it.

From the known equilibrium constant of eq 3 the activity coefficient of oxygen was determined and found to be strongly lowered by silicon as illustrated by Fig. 1. It also was found that the activity of silicon is highly dependent on the silicon content as shown in Fig. 2. The deoxidation constant, [pct Si]·[pct O]², was observed to be 2.8×10^{-3} at 1600°C in close agreement with the constant determined by Hilty and Crafts and also that of Körber and Oelsen. This constant, however, is not a true equilibrium constant because the activity coefficients are far from unity. The activity coefficients vary so that one compensates the other and results in a nearly constant product for practical purposes.

The effect of silicon on the oxygen content of liquid iron at 1600°C is shown in Fig. 3. The results did not confirm the break in the Si-O curve that was reported by Hilty and Crafts, but otherwise, the agreement with the Hilty and Crafts data is excellent.

The equilibrium at 1550° and 1650°C was also studied and resulted in the following free energy equations for reactions (1) and (2):

$$SiO_{2(s)} = Si + 2O, \quad \Delta F^\circ = 146{,}500 - 56.3\,T$$

$$SiO_{2(s)} + 2H_2 = Si + 2H_2O_{(g)}, \quad \Delta F^\circ = 82{,}000 - 27.3\,T$$

The [pct Si]·[pct O]² products were 1.2×10^{-3} at 1550°C and 5.5×10^{-3} at 1650°C, also in close agreement with Hilty and Crafts.

Oxygen Equilibria

The subject of oxygen equilibria under both acid and basic slags and the carbon-oxygen reaction in steelmaking was discussed by P. Herasymenko who presented a somewhat different approach to the problem. Based on his experience in acid open hearth steelmaking he assumed that an oxygen diffusion layer exists at the hearth-metal interface, but he considered that there is no need to assume the existence of an oxygen concentration gradient in the metal at the slag-metal interface. The experi-

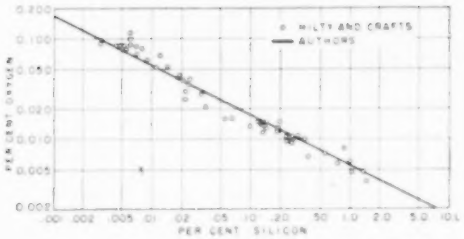

Fig. 3—Effect of silicon on the solubility of oxygen in liquid iron at 1600°C.

mental data can be understood better if it be assumed that the oxygen in the bulk of the metal is in equilibrium with the oxygen activity of the slag. Distinguishing between the oxygen content of the metal and oxygen activity, then the oxygen content of a carbon containing steel will be lower than the oxygen content of a carbon-free steel in equilibrium with the same slag because carbon increases the activity of oxygen. Applying this concept to existing experimental data covering a wide range of slag and metal compositions, Herasymenko supported his view that the distribution of oxygen between slag and metal is attained easily and that the activity coefficient of oxygen increases with increasing carbon content.

Taken as a whole, the group of papers presented in the Wednesday afternoon session indicated that the silicon-oxygen relation in molten iron is now reasonably well established, but that in spite of the large amount of research that has been done in the past on slag-metal equilibria and oxygen distribution, understanding of this complex subject is far from complete.

Chromium Distribution

Discussion of the strictly physicochemical aspects of oxygen in steelmaking was continued with G. Derge of Carnegie Institute of Technology and D. J. Girardi of Timken Roller Bearing Co. presiding. The concluding paper of this session, however, on stainless steel melting illustrated how fundamental data of this type can be applied to the solution of practical steelmaking problems.

The importance of chromium control in the manufacture of low alloy steels both from the standpoint of residuals and furnace operation is well recognized. A contribution to a better understanding of chromium distribution between liquid iron and molten basic slags of the open hearth type was presented by N. J. Grant, Earl Roberts, and John Chipman of the Massachusetts Institute of Technology. Based on 60 to 80-lb laboratory heats made in an induction furnace, the chromium distribution between molten iron of less than 0.01 pct carbon and basic slags of the simple CaO (MgO) —SiO_2—FeO type was determined at equilibrium in the temperature range 1526° to 1714°C. Chromium in the metal was from 0.03 to 0.60 pct under slags containing from 2 to 20 pct Cr_2O_3.

It was shown that Cr_2O_3 in basic slags behaves most probably as a basic oxide equal to CaO and MgO on a molar basis. Determination of the basic character of Cr_2O_3 was possible by using the desulphurization *standard* line of Grant and Chipman as a function of excess base.

The chromium distribution ratio, defined temporarily as the ratio of the mol fraction of Cr_2O_3 in the slag over the percent chromium, squared, in the metal when plotted against the mol fraction of FeO in the slag shows that the largest single factor affecting the chromium distribution is the FeO of the slag. Basicity has a small effect, the very basic slags showing more chromium in the metal than the very acid slags for a given FeO content. The results are shown in Fig. 4.

Assuming the reaction

$$FeO \cdot Cr_2O_{3(s)} = Fe_{(l)} + 2\underline{Cr} + 4\underline{O}$$

and assuming weight percent values for chromium and oxygen due to the dilute solution involved,

$$K' = [\text{pct Cr}]^2 \times [\text{pct O}]^4$$

K' at 1595°C = 2.55×10^{-8} compared to Chen and Chipman's value of 2.44×10^{-8} for a true K.

Fig. 5 shows the log K' vs 1/T plot for the above reaction from which

$$\log K' = -\frac{49{,}600}{T} + 20.15$$

Electrical Conductivity

Electrical conductivity data on slag systems hold considerable interest from the fundamental viewpoint of furthering the understanding of slag structures and reactions. John Chipman, John W. Tomlinson, and H. Inonye of Massachusetts Institute of Technology presented electrical conductivity data on liquid iron oxide, the system FeO-SiO_2 up to 42 mol pct silica, and melts containing 5 atomic pct of MnO, CaO, TiO, Al_2O_3 and SiO_2 coexisting with iron. The measurements were made in a dry nitrogen atmosphere and at temperatures up to 1500°C. The melts that were investigated obeyed the formula

$\kappa = A^{-\frac{E}{RT}}$ and the energy of activation ranged from 5 to 17 kcal per mol.

Liquid iron oxide is a semiconductor and its specific conductivity increases from 269 ohm^{-1} cm^{-1} at 1400°C to 324 ohm^{-1} cm^{-1} at 1500°C. The value of

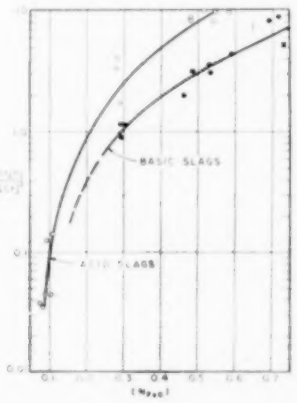

Fig. 4—Effect of FeO in the slag on the distribution of chromium between slag and metal.

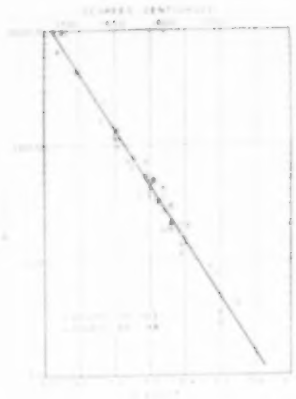

Fig. 5—Influence of temperature on the chromium oxygen reaction in liquid iron containing small amounts of chromium.

the specific conductivity reported by Fischer and vom Ende at 1400°C is approximately 8 ohm^{-1} cm^{-1}. Preliminary investigation by the authors indicated that an accurate determination of the lead resistance was necessary and that the maximum accuracy of the measurements was obtained when the ratio of the lead resistance to that of the melt was as small as possible. Since no value of the lead resistance was reported by Fischer and vom Ende the authors could not account for the discrepancy.

The addition of 5 atomic pct of the various oxides decreased the conductivity of the iron oxide melt in all cases. The decrease in the conductivity with the addition of various oxides ranged from 50 pct in the case of SiO_2 to 10 pct in the case of MnO at the same temperature. It was found that a dilution effect may be operative, but such a process cannot explain maxima and minima as found by several authors. Neither is the conductivity in the binary melts investigated a function of the basicity.

A strong negative deviation from additivity was found for the conductivity of the iron oxide-silica system as a function of composition. A logarithmic decrease of the specific conductivity was noted to 25 mol pct silica. No maxima or minima were found in the isotherms at 1300°, 1400°, and 1450°C.

Fig. 6—The Fe-S-O liquidus diagram.

Fe-S-O System

The types, distribution, and amount of inclusions in any given steel are closely allied with both the oxygen and sulphur contents of the metal, so that the term deoxidation as conventionally applied in steelmaking refers not only to the control of oxygen and oxide inclusions but to collateral modifications of sulphide inclusions as well. Consequently, in order that better understanding of the mechanism of deoxidation and inclusion formation may be developed, quantitative data for the fundamental iron-sulphur-oxygen system are desirable. Such data were presented by D. C. Hilty and Walter Crafts of the Union Carbide & Carbon Research Laboratories, Inc.

Mixtures of iron oxide and iron sulphide were melted in small iron crucibles at various temperatures in an argon atmosphere so that equilibrium between the melts and solid iron was substantially obtained. The melts were quenched in water from the equilibrium temperatures and were examined chemically and microscopically. For temperatures above the melting point of iron, a rotating crucible high-frequency furnace technique was employed. From the observations, the solidification diagram for the iron corner of the Fe-S-O system shown in Fig. 6, was plotted. There is a ternary eutectic at 67 pct iron, 24 pct sulphur, and 9 pct oxygen and approximately 920°C. A liquid miscibility gap extends into the system from the iron-oxygen side to a sulphur content of 21.5 pct with a minimum point at approximately 81.5 pct iron, 16.5 pct sulphur, 2 pct oxygen, and 1345°C.

In liquid iron, increasing sulphur concentration first slightly decreases the solubility of oxygen (up to about 0.10 pct sulphur) and then rapidly increases it. This effect of sulphur on the solubility of oxygen in liquid iron is shown at several temperatures in Fig. 7.

Metallic Oxidation in Cr Steel Melting

The concluding paper of this session was of more immediate practical interest than the preceding ones, and represented a transition step in the application of the physical chemistry of steelmaking to operating problems. In the melting and refining of chromium steels the oxidation of carbon to a low level is accompanied by the oxidation of chromium and iron in considerable amounts. For the subsequent recovery of chromium and associated iron from the slag, the amounts of metal oxidized must be known for efficient reduction and control of composition. Further, to arrive at an accurate understanding of the process, so that chromium-bearing scrap can be used effectively, information is required on the relation between composition of the charge and weight of metal oxidized in reaching the desired carbon content. Hilty and Crafts were joined by G. W. Healy of the Electro Metallurgical Co., a div. of Union Carbide & Carbon Corp., in presenting a report of their investigation of metallic oxidation in chromium steel melting.

By means of the observations of Chen and Chipman and the thermodynamic data given in *Basic Open Hearth Steelmaking* the following relation was calculated for melts containing small amounts of

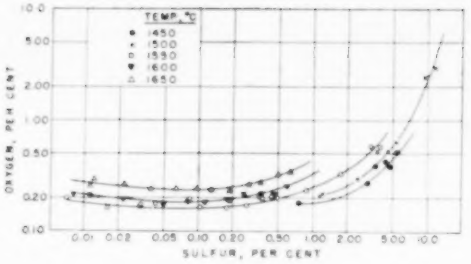

Fig. 7—Effect of sulphur on the solubility of oxygen in liquid iron.

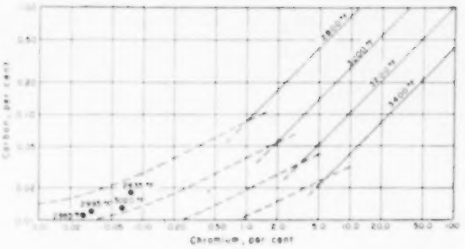

Fig. 8—Approximate chromium-carbon-temperature relations for all chromium contents of interest in the melting of chromium steels.

chromium and carbon, assuming a CO pressure of one atmosphere:

$$K = \frac{\text{pct Cr}}{(\text{pct C})^x}; \log K = -21250/T + 13.88.$$

With the use of this relation and its graphical extrapolation to the limiting carbon content at zero chromium the original chromium-carbon relation in chromium steel refining published by Hilty in 1949 was extended to low-chromium and carbon contents as illustrated by Fig. 8. It was considered that within the concentration limits usually encountered the amount of manganese in chromium steel heats is equivalent to a similar quantity of chromium and should be added to the chromium for practical applications of Fig. 8.

From observations on a number of arc furnace heats covering a wide range of chromium concentrations and temperatures it was shown that the ratio of chromium (plus manganese) to iron in the slag of a chromium steel heat depends almost entirely on the ratio of chromium (plus manganese) to iron in the metal. Through this relationship an expression for calculating the metallic oxidation during the oxidizing period of a heat if only the chromium and manganese contents of the charge and in the bath at the end of the oxidizing period are known was derived. Oxidation calculated according to this expression correlated well with that observed on arc furnace heats.

By employing Fig. 8 for estimation of the chromium (plus manganese) content of the bath after oxidation the quantity of metallics oxidized for charges of varying chromium contents oxidized to specified carbon and temperature levels were calculated with the results shown in Fig. 9. The amount of metallic oxidation (chromium plus manganese plus iron) is dependent upon the amount of chromium in the charge and the carbon content and temperature of the bath at the end of the oxidizing period. This is of particular interest in the manufacture of very low-carbon grades of stainless steel, because it would appear that if the charges for such heats contain more than a small amount of chromium, metallic oxidation may be excessive because of practical operating limitations on the temperatures that can be attained safely in normal electric furnace practice.

Sampling and Analysis for O

The final session, under the Chairmanship of D. L. McBride and R. E. Birch, dealt with the problems of sampling and analysis of liquid steel for oxygen and with the question of plant usage of gaseous oxygen for decarburization. The subject of sampling liquid steel for dissolved oxygen was presented in a paper by G. F. Huff, G. R. Bailey, and J. H. Richards of the U. S. Steel Co. An improved bomb-sampling device as shown in Fig. 10 was discussed. The improvements are all designed to provide better protection against slag contamination than that afforded by the conventional bomb.

The question of the size of the aluminum wire used as a deoxidizer in the bomb was investigated and the results indicated that wire diameters of 0.012, 0.050, and 0.081 in. had no significant effect. Also, the reproducibility of vacuum-fusion analysis within a sample and between duplicate samples was very good.

The relationship of the oxygen concentration in an open hearth heat to the carbon content and to the

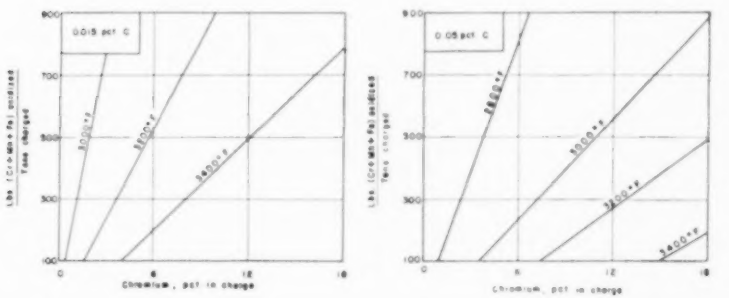

Fig. 9—Influence of final carbon content, charged chromium, and temperature on the amount of metallic oxidation occurring in the refining of chromium steels.

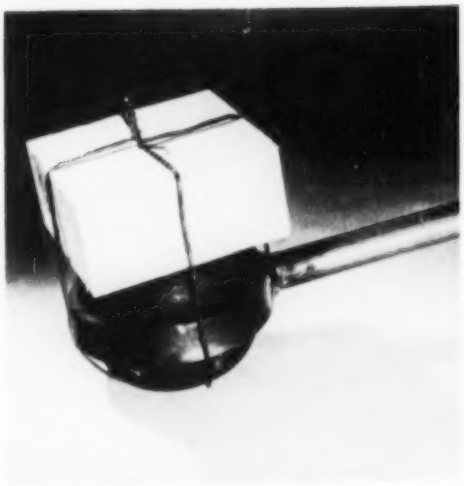

Fig. 10—Modified bomb assembled and ready for sampling

slag composition was reviewed, and it was shown that the oxygen dissolved in the bath as determined by this new bomb technique is more nearly in equilibrium with carbon at carbon levels greater than 0.10 pct, and is more nearly in equilibrium with the slag at carbon levels below 0.10 pct.

The question of oxygen determinations by the vacuum-fusion method on high sulphur irons such as those studied in the paper given by D. C. Hilty and W. Crafts was investigated by H. L. Hamner and R. M. Fowler of the Union Carbide & Carbon Research Laboratories, Inc. They found that the evolved carbon monoxide was contaminated with carbon disulphide and carbonyl sulphide. If not removed, these sulphur compounds would cause the oxygen results to be high. The authors described a procedure for removing sulphur compounds by hydrogenation to hydrogen sulphide and absorption in lead acetate. Table I shows the magnitude of interference found in the case of high sulphur irons.

Table I. Effect of High Sulphur on Oxygen by the Vacuum Fusion Method

Sample	Sulphur, Pct	Oxygen Regular Method, Pct	Modified Procedure, Pct
1	0.022	0.194	0.193
2	0.042	0.174	0.173
3	0.049	0.180	0.175
4	0.061	0.206	0.184
5	0.117	0.185	0.180
6	0.44	0.271	0.209

Oxygen and Air Lancing

The next two papers dealt with the practical production problem of carbon removal in molten baths with gaseous oxygen. The use of oxygen and air lances in the British steel industry and the results of some cooperative research undertaken by the British steel firms and the British Iron and Steel Research Assn. were discussed by D. J. O. Brandt of the British Iron & Steel Research Assn. in a paper summarized and presented for the author by J. H. Zimmerman of Linde Air Products Co. The data obtained for carbon removal from molten steel with the oxygen and the air lances were brought to a common basis in order that comparisons could be made with a reasonable degree of accuracy. These comparisons indicated that the overall action of the lance for carbon removal is the same in all cases. The rate of carbon removal, at high-carbon levels was initially slow, accelerating to a maximum, and then decreasing again as the carbon was reduced to low levels. To remove carbon to very low levels, a high rate of oxygen input was required. The action of the lance was strongly influenced by the condition of the slag, and Brandt indicated that evidence pointed toward the fact that the chemical action of the lance was via the iron oxide generated in the slag and metal. In comparing results of oxygen lancing in the electric furnace vs the open hearth, the lance appeared to operate at about 70 to 75 pct of stoichiometric efficiency in the case of the electric furnace and at 200 to 300 pct efficiency in the case of the open hearth. This difference in efficiency is undoubtedly caused by the presence of an oxidizing slag and an oxidizing atmosphere in the open hearth furnace. The importance of agitation under oxidizing conditions is further strengthened in that the air lance may assist carbon removal at a stoichiometric efficiency of over 300 pct on a lightly loaded furnace. In the case of baths containing 18 pct chromium, about three times more oxygen is required to remove carbon.

Further information on some phases of oxygen injection for carbon removal that have posed questions and problems was reported by W. R. Lysobey of the Air Reduction Co. An investigation on the use of the oxygen lance on blast furnace iron for silicon reduction indicated that the oxidation reaction was local in nature. A good portion of the oxygen appeared to be exerting solely a physical thrust against the metal and this produced waves of molten metal that broke over the rim of the open ladle. Injecting a total flow of 16,900 cu ft of oxygen in 75,000 lb of iron contained in the ladle brought about a change in silicon content from 1.24 to 0.74 pct, a change in manganese from 1.62 to 1.08 pct and the carbon content after the oxygen treatment was 4.40 pct. Calculations indicated an oxygen utilization efficiency of only 30 pct. This work illustrated that the use of an oxygen lance was not a practical method of removing silicon, manganese, or carbon from blast furnace iron. Some work has been reported whereby oxygen was efficiently utilized in basic iron by using a porous plug as the injection device.

The above investigation and other work on silicon containing baths has indicated that in the case of the silicon-iron-carbon system the degree of oxygen utilization is influenced by the concentration of silicon in the bath.

Acknowledgments

The authors of this review wish to express their appreciation to all of those who participated in the Symposium for their courtesy in making copies of their papers available to us even before submitting them for regular publication.

Physical Conditions in the Combustion and Smelting Zones Of A Blast Furnace

by J. F. Elliott, R. A. Buchanan, and J. B. Wagstaff

High speed photography through blast-furnace tuyeres showed coke particles moving rapidly. Model studies showed a raceway was formed and gave quantitative results which were correlated with actual blast furnaces. Another study showed the similarity between hanging and the flooding of a packed column. This was explored by models.

THE combustion zone before the tuyere in an iron blast furnace is a vital region because here are generated: 1—most of the gases on which the furnace depends to carry out its basic operation of reducing iron ore to the metallic state, and 2—the major fraction of the heat required in the nearby regions of the furnace for the various reduction reactions, the fusion of the slag, and the melting of the iron. Since the greater part of the coke is consumed in this region, the descent of the burden must be greatly affected by the characteristics of the tuyere zone. This region then would seem to be a profitable field for study.

Fortunately, a view into this important zone is available to the operator through the tuyere peep sight. Here he sees relatively dark pieces of coke "dancing" in the blast. What he sees is of considerable help in interpreting the behavior of the furnace at a given time but the very rapidly moving particles and the intense radiation obscures what is happening very deep in the zone.

This investigation was initiated in the hope that a better understanding of the combustion region could be obtained by using a high speed camera with a maximum speed of 3000 frames per sec. It seemed the best practical method of "slowing down" this characteristically violent action within the highly luminous field. Model studies and tuyere probing also have been used to aid in explaining the observed phenomena.

Above the combustion zone, but below the fusion zone, there is probably a region in which the coke is comparatively stationary. Here are zones in which the gases must flow up through the granular bed counter to descending liquid slag and metal. There is no easy way to observe this zone in a blast furnace, but model studies have been of some help in explaining the nature of the zone and the laws governing the flow of the fluids involved.

The whole problem is difficult and involved and any approach to a complete solution may require long investigation. This preliminary report has been written, therefore, because it is believed that appreciable progress has already been made that would be of interest to others.

J. F. ELLIOTT, Junior Member AIME, formerly with United States Steel Co., is now with Inland Steel Co., East Chicago, Ind., and R. A. BUCHANAN and J. B. WAGSTAFF are associated with the Research Laboratory, United States Steel Co., Kearny, N. J.

Discussion on this paper, TP 3333C, may be sent, 2 copies, to AIME. Manuscript, April 7, 1952. Los Angeles Meeting, February 1953. Paper also presented at the Blast Furnace, Coke Oven and Raw Materials Conference, March 1952.

Tuyere Studies, Chemistry and Kinetics

It is well known from the early work of Kinney and coworkers[1,2] that combustion of carbon before the tuyeres appears to occur in two zones:

$$\text{Zone A:}\quad C + O_2 = CO_2;\ \Delta H_{-} = -14{,}108 \text{ Btu per lb of carbon} \quad [1]$$

$$\text{Zone B:}\quad CO_2 + C = 2CO;\ \Delta H_{-} = +6{,}183 \text{ Btu per lb of carbon} \quad [2]$$

Zone A (Fig. 1) is close to the tip of the tuyere and zone B is somewhat farther back; there being a transition region in which both reactions occur. It is interesting to estimate the rate at which coke is burned before a tuyere with a wind rate of 90,000 cfm in a modern furnace having 18 tuyeres. Approximately 0.55 lb of carbon is consumed by eq 1 per tuyere per sec. A like amount disappears by eq 2 for a total consumption of 1.11 lb per sec per tuyere. Assuming the coke is 85 pct C and has a bulk density of 30 lb per cu ft, this figure can be converted to a total of 1.30 lb of coke with a bulk volume of 0.043 cu ft disappearing per sec per tuyere.

At the temperatures prevailing in the combustion zone (according to Kozlovich,[3] the maximum is about 3400°F), the rate at which carbon is con-

Fig. 1—Combustion zones as found by Kinney.

sumed is probably controlled by gaseous diffusion rates, relative air velocity past the particles, and surface exposed (particle size). Chemical considerations such as fuel reactivity and reaction rates probably are of secondary importance. In general, at temperatures prevailing in the blast furnace, Tu, Davis, and Hottel[7] found that the rate of combustion of carbon in air is roughly proportional to the absolute temperature. It is sufficient to note here that in the combustion zone the rate at which carbon in the coke is consumed is strictly a function of the rate at which oxygen is supplied, and the size of the combustion zone is controlled by the physical forces involved. The present study is primarily an effort to determine certain physical characteristics of this zone and of the melting zone immediately above it. The chemical factors have been neglected except insofar as they affect the temperatures and volume of the materials.

Experimental Work, Tuyere Studies

High Speed Pictures. A series of high speed color motion pictures have been taken through the tuyeres of a number of blast furnaces. The speeds run between 800 and 3000 frames per sec, which give a time magnification range of 50/1 to 188/1 in the scene viewed. The camera is sighted axially through the tuyere opening using a special peep sight fitted with a silica glass. The camera used was a 16-mm Kodak high speed camera and the film Kodachrome type A.

Although there have been several showings of a group of these films, a general summary of what the camera sees may be useful. The film shows a procession of angular particles dropping down into the air jet of the tuyere. As the jet impinges on them, they are flung violently to the rear of the region viewed. This region is rather congested with these particles, all of which are moving away from the camera. The small particles appear to travel at a relatively high speed and the larger particles move considerably more slowly. The time in the air jet ranges from approximately 0.1 sec for 2½ in. particles down to about 0.01 sec for ¼ in. particles. So that the rate of burning of coke (0.043 cu ft per sec = 74 cu in. per sec) is small compared with the quantity of coke moving in front of the tuyere.

The brightness of the particles seen on Kodak color film shade from an apparent black to almost white and careful observation has shown no apparent change in the brightness of a particle in its journey through the blast. Brightness is seemingly randomly distributed with regard to size. This brightness of a particle is probably due principally to its temperature, the brighter ones simply being hotter.

Identification of most of the particles seen in the films was obtained by photographing a furnace while filled with a coke blank and comparing the field observed with a furnace normally burdened. For this comparison, pictures were obtained at plant A on Nov. 14, 1949, after the furnace had been on wind for less than 5 hr after a prolonged bank. Six of the 16 tuyeres were open and the blast through the tuyere examined was approximately 33 pct above the normal operating rate. It was almost certain that in this test only coke was in front of the tuyeres. Fig. 2 compares frames from the high speed movies taken under normal operation and under this unusual condition. It is realized that neither of these "still pictures" adequately represents the movie film; only a view of the actual film is convincing. However, an approximate idea of the similarity of the two films can be obtained. Both films show rough, angular particles and there is the rather rare occurrence of dark, frangible particles. With virtually no difference in the appearance of the banked and normal furnaces, it is concluded that the majority of particles at the tuyere zone are pieces of coke. It is probable that the frangible material consists of partially reduced ore or slag-forming materials.

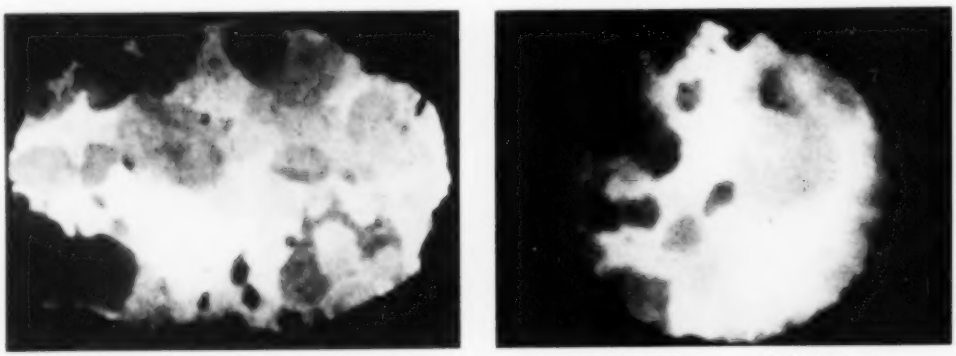

a—Through tuyere on furnace in normal operation.

b—On furnace with coke blank.

Fig. 2—Stills from high speed movie.

The films also tend to show a higher incidence of massive lumps at the tuyere zone in an irregularly working furnace than in one moving smoothly. These sometimes burst under the impact of the jet and spew forth bits of coke and ore. The dark coloring indicates a relatively low temperature within the lump. One explanation is that during irregular operation there is a greater chance for a small pocket of coke and ore to be walled off by partially solidified slag. Then this lump may be thrust by a slip into the combustion zone before being smelted. Sometimes these larger pieces fail to break up when they enter the raceway; they seem to be too big to be blown round, so they settle to the bottom of the visible region and slowly melt away. Careful examination of pictures of such lumps suggests that they are agglomerates formed within the furnace.

In viewing the films, the observer has the impression that the coke particles are moving backward into a rather large void. There is also the vague impression that just within view behind the moving particles is a highly luminous wall. With no depth index, it is impossible to judge the size of this void or the distance to the wall. Close observation shows that there is a general tendency for particles in motion to rise slightly as they are blown rearward and some of the larger ones even roll upward as though being pushed up an inclined plane. This last effect, coupled with the fact that some of the coke particles dropping in front of the tuyeres are very bright, leads to the postulation that circulation of coke is about a vertical circle with the jet roughly tangent to the lower edge, as shown in Fig. 3.

Model Performance: There seems to be no ready means for observing a vertical cross-section of the combustion zone of a furnace in the plane of the tuyere axis. Therefore, a model (Fig. 4) was constructed to simulate this view of the furnace. It consisted of two parallel plates of glass 30 in. sq, which were held in a vertical position 4 in. apart by a wooden frame around the two sides and bottom. A tuyere, 1.17 in. in diam, was positioned at one edge of the model so that the axis of the emergent jet was on the midplane between the two glass plates. The tuyere could be located either 6 or 12 in. from the bottom of the model and its axis was 2° from horizontal. By filling the model with a bed of granular solids and blowing a jet of air from the tuyere into the bed, the behavior of the particles could be observed through the glass plates.

Considerable thought was given to the best way to make a model to reproduce blast-furnace conditions. At first, it seemed that all dimensions should be scaled down proportionately and the Reynolds number of the jet maintained the same. Unfortunately, this results in extremely high velocities approaching that of sound when the size of the tuyere is reduced to "laboratory" proportions. It therefore seemed advisable to maintain the particle size about the same and use suitable velocities to attempt to keep the Reynolds number of the air flow around the particle constant. It was then necessary to accept

Table I. Oak Particles in Slice Model Bed

Percentage by Number	Particle Size and Shape	Shape Factor, Long Side: Short Side
90	¾ in. cubes	1:1
10	¾ × ¾ × 1½ in. right prisms	2:1

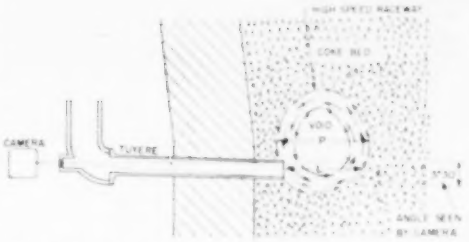

Fig. 3—Vertical section showing mechanically active zone before tuyere.

a major difference in the ratio of particle to jet diameter. It seemed reasonable to expect that, at least qualitatively, the particles should behave similarly whether the jet to particle diameter was 1:1 or 6:1. For the short time that a particle of coke remains in the tuyere jet, it appears that the forces on it because of the jet predominate as compared with gravitational forces.

Although the problem of similarity would have been simplified by the use of a bed of coke, this was not feasible experimentally, chiefly because of photographic limitations. Instead a bed of oak blocks was used, as described in Table I, to conform approximately with the size of coke appearing in the furnace combustion zone. The oak had a density of approximately 57 lb per cu ft and the bulk density of the particles poured slowly into a container was approximately 30 lb per cu ft. In these respects, the bed of oak blocks was similar to a bed of coke lumps.

Fig. 5 shows the model filled and ready for a run. The behavior of the bed is recorded by camera and the flowmeters and gages are positioned so that they also can be recorded. A grid of 1-in. squares on transparent film is attached to the viewing window for a frame of reference. Below a certain flow rate, the particles of oak do not move. As the air rate is increased, a critical point is passed and the particles begin to teeter on their corners and edges. A slightly higher rate sets the particles in a turbulent motion and with still higher rates a void is formed that is roughly circular in cross-section with the jet tangent to the lower edge. Around the outer edge of the void is a raceway of high-speed particles (Fig.

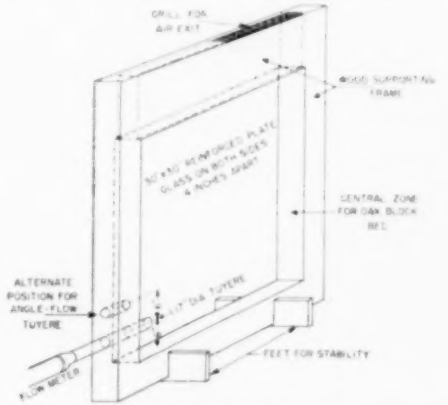

Fig. 4—Simplified sketch of slice model.

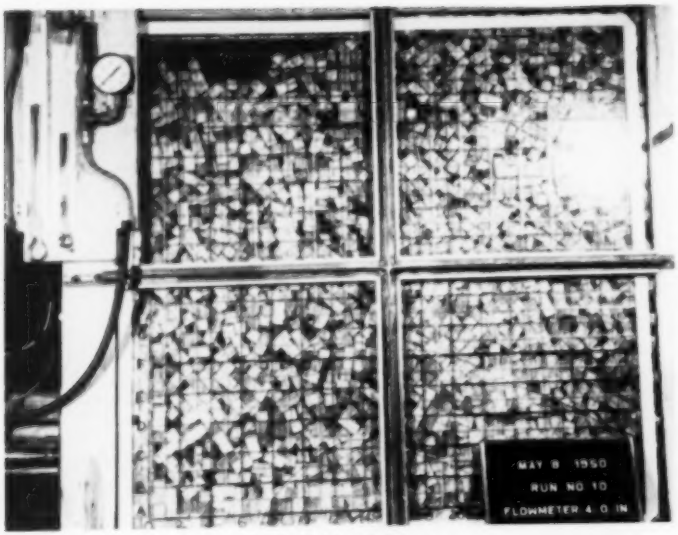

Fig. 5—Model ready for run.

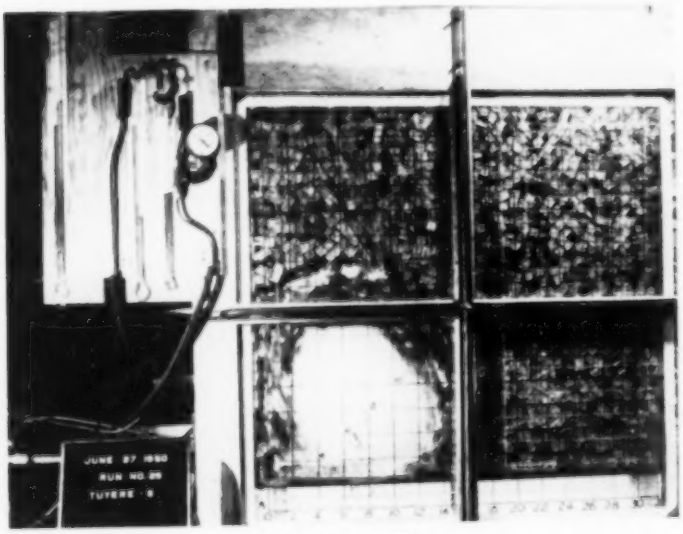

Fig. 6—Model in operation.

61. These particles are caught in the jet and are carried backward and upward as the jet is deflected upward by the solidly packed bed about the active zone. They work their way across the roof of the zone where the air escapes and then descend along the wall to re-enter the jet. The raceway is continually exchanging particles with the surrounding bed.

Air escapes from the zone upward through an area that is as long as the full penetration of the air jet into the bed and is the full width of the model. As the air flow increases, the jet readily increases the diameter of the circulating zone by eating into the solidly packed bed. Above the minimum flow rate at which a full raceway forms, the zone stabilizes quickly at a given flow rate and is reproducible.

It is recognized that this model does not precisely represent the furnace combustion zone because it is substantially two-dimensional instead of three. In addition, there is no attempt to evaluate the effect of combustion on the gas volume and velocity in the

real furnace. However, many points of similarity exist between the high speed pictures taken down the tuyere of a blast furnace and those taken of the model. It therefore appears that circulation of coke about a sizable void must occur before the tuyeres in a blast furnace with a wind rate above a certain minimum.

Circulating Zone in Furnace: With the presence of a raceway and a void before the furnace tuyere demonstrated, the question arises as to its size. Some indication is given by Sweetser[7] (and by many other furnacemen who have probed tuyeres), who describes the rod test and quotes Ora E. Clark as finding that the distance that a rod could be easily pushed into a furnace varied from about 4 ft just before cast to 7 ft 9 in. just after. Within the past two years, furnaces have been probed with a water-cooled rod as a part of this study. An interesting feature of the probing is that the rod tends to sag of its own weight when resting free in the combustion zone, but as it is pushed farther back and strikes stationary solid material, the end is deflected upward as though it were sliding up an inclined plane. The results of the probing indicate that the raceway before the tuyeres in modern large furnaces at full wind is approximately 40 in. in diam.

Correlation of Raceway Size: In order to correlate the size of the raceway with the air flow through the jet, two lines of argument seem reasonable, one based on conservation of energy and the other on conservation of momentum. In the first, the kinetic energy of the jet is considered to be dissipated, since the gases leave the raceway comparatively slowly. This gives a correlation of raceway diameter against the rate of expenditure of kinetic energy (power dissipation) in the jet. That is to say,

$$P = f\left(\tfrac{1}{2}\frac{M}{t}V^2\right)$$

where: P is the raceway diameter; M, the mass of air entering in time t; V, the linear velocity of jet; and f indicates a function.

On this basis, Fig. 7 has been drawn up showing the effect of kinetic energy of the blast on the diameter of the raceway. Three independent types of information have been included: 1—measurements on a model, 2—data obtained by probing actual blast furnaces, 3—information taken from published analyses of gas in blast furnaces.

Discussing first the data from the model, the mass air flow was obtained from an orifice plate flowmeter and the air velocity at the end of the tuyere was computed from the mass flow, air temperature, and static pressure just within the nose of the tuyere. It was assumed that the static pressure in the raceway was equal to that in the tuyere and that the kinetic energy of the gas leaving the raceway was small as compared with the kinetic energy of the tuyere jet. The data are consistent and reproducible to within approximately 1 in. of penetration. The band is narrow except at low flow rates where the penetration was small and difficult to measure accurately. Three tuyeres were used, all of which had the same nozzle area, that of a 1.17 in. diam circle—a straight tuyere, an elliptical tuyere, and a 22° angle-flow circular tuyere, which could be positioned downward or upward. These were designed to simulate the principal types of tuyeres in common usage. The elliptical tuyere yielded points within the band for straight round tuyeres but the 22° angle-flow tuyere showed slightly less penetration. Air flow in the 1.17 in. diam tuyere varied between 0.1 to 0.6 lb per sec and the air temperature between 60° and 170° F. The variation in air temperature was due to the variation in the ambient temperature and heating of the air blast during its compression. Air temperature entered the correlation only as it affects the velocity of the blast leaving the tuyere. Loss of sharp corners on the blocks because of collisions with each other did not alter their behavior.

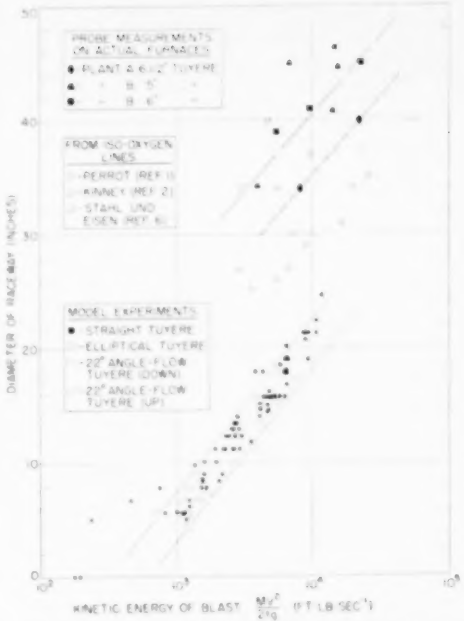

Fig. 7—Raceway correlation based on kinetic energy of blast.

Data from actual furnaces have also been plotted in Fig. 7. The power of the tuyere jet is computed on the assumptions that: 1—the velocity in all tuyeres is equal and uniform over the cross-section of the tuyere; 2—the pressure drop from the stock to the tuyere tip was negligible; 3—the temperature drop in the blast-distribution system was negligible. Calculations are based on the blast temperature, pressure, and volume recorded on the furnace instruments. Tuyere pressure, as measured by a static tube, was 1.6 to 1.9 psi less than recorded by the instruments, because of pipe losses and conversion of static head to dynamic head. The diameter of the raceway was taken to be 12 pct greater than the probe measurement because the probe did not measure the full diameter of the raceway, Fig. 3.

Included in Fig. 7 are points for other furnaces that have been studied for gas distribution in the tuyere zone.[1,2,6] The 1 pct oxygen contour has been used as an index of blast penetration for these furnaces, as it can be argued that a small amount of oxygen must remain in the gases in the raceway. This index may indicate a slightly greater penetration than that which actually occurs but it is probable that the error in fixing the position of a given gas contour line is in the realm of several inches, which may account for some of the spread of the

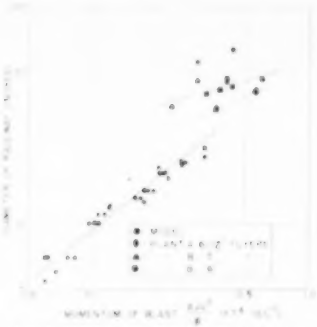

Fig. 8—Raceway correlation based on conservation of momentum

plotted data. Air blown as computed from the carbon balance for each furnace is used in the calculations.

The trend line drawn through the furnace data parallel to the band for the model appears to represent the points fairly well. The lower portion of the line probably swings sharply to the left toward the vertical axis. It is to be noted that the zero point—that is, the point at which the raceway just begins to form—does not lie in the line of the other points. This zero point was found to be difficult to reproduce in the model work and probably depends considerably on the packing of the particles around the tuyere. It may well be that the laws governing the size of the raceway do not hold in the limiting case of zero size.

A second method of correlating the size of the raceway may be obtained by considering the principle of conservation of momentum. It may be that the raceway diameter is determined by the ratio of the jet momentum and the opposing force that is assumed to be the product of the pressure and the surface area of the raceway. Then:

$$\phi L \pi P = A_p V^2$$

where L is the thickness of the model, A, the area of the jet, ρ, the density of the air leaving the jet, and ϕ, the pressure on the system. Fig. 8 shows a logarithmic plot of P vs. $A_p V^2/\phi$. L is a constant for the model. For the sake of clarity, not all the data from the model have been included, but the trend of the points is obvious. From the curve:

$$P = f\frac{(A_p V^2)^{0.5}}{\phi}$$

If the raceway is free to expand in three dimensions in the blast furnace, the corresponding equation is:

$$\phi \pi P = \frac{A_p V^2}{\phi}$$

when $$P = \left(\frac{A_p V^2}{\phi}\right)^{0.5}$$

Unfortunately, the data on actual furnaces are meager and only two sets of figures for the change in penetration with wind rate are available. These were obtained by putting a water-cooled probe through the tuyere and measuring the distance it could be inserted beyond the end of the tuyere before it struck the stationary bed of coke.

Two sets of data are available; the first at plant A when readings at two wind rates were recorded and the second at plant B. At the latter, more readings were taken but the practice on that furnace was unusual and the operation was somewhat rough. It was found on one of the tuyeres that the probe would penetrate large distances (5 ft and more), which could not be accounted for by the wind rate. It would be possible to explain these results if the coke failed to feed regularly into the raceway. There is, however, no reason to suppose that the smaller readings were unreliable. There are, therefore, two estimates available for the slope of the line of P against $\frac{A_p V^2}{\phi}$ on the logarithmic plot of Fig. 8, 0.35 and 0.47. It is unfortunate that the agreement is not better but these slopes are about half the value of 0.75 obtained with the two-dimensional model.

With the information available, it is not easy to say which method for correlating the raceway diameter (that is, the penetration of the blast into the furnace) is the better. Neither of these correlations takes account of the particle size of the material in the raceway and there is some evidence to indicate that this cannot be neglected, although it is not easy to obtain a reliable estimate of the particle size of the coke in a blast-furnace raceway. A further difference between the model and the furnace is the combustion and consequent release of energy. The greater part of the energy of combustion is released in the raceway and may well have some effect.

No information is yet available on the conditions in the furnace between two adjacent tuyeres. The camera can see only an angle of 3°, so that the line of sight is limited to the region directly in front of the tuyeres. The model was a narrow vertical slice of the mechanically active zone and could give no indication of the width of the raceway. Therefore, until further information is available it is possible only to guess whether there are "pillars" of comparatively stationary coke between adjacent raceways.

The chemically active combustion zone probably extends beyond the mechanically active zone. The void and raceway undoubtedly are occupied by gases high in O_2 and CO_2; thus the mechanically active zone conforms to Kinney's zone A (Fig. 1). Even though much of the gas flows rapidly upward, a portion of it must flow laterally into the surrounding coke bed because the tuyere zone is at a somewhat higher pressure than the surrounding region. These gases must continue to consume carbon, though the rate be relatively slow, in the surrounding bed. This corresponds to Kinney's zone B and, as a result, the inert region, or the so-called "dead man," lies somewhat farther into the furnace than the stationary coke bed at the back of the mechanically active region.

Melting Zone

It is reasonable to suppose that there is a region at some distance above the raceways where the slag-forming constituents fuse and form a liquid. Possibly the reduced iron melts in about the same region of the furnace. It follows then that these liquids trickle down through the comparatively stationary coke between the fusion zone and the raceway. In this zone, hot gases are therefore passing up through a bed of granular solids countercurrent to liquids coming down.

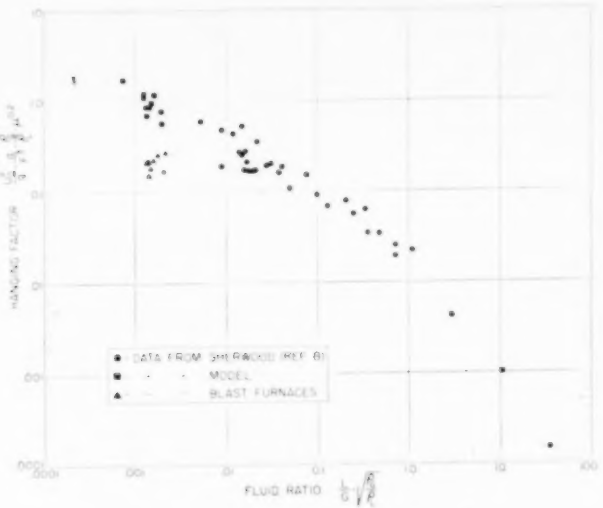

Fig. 9—Correlation of flooding of packed columns.

a—Cross sectional area of column, sq ft.
F—Fraction of free volume in packing, cu ft per cu ft of tower volume.
g—Acceleration of gravity, ft per sec per sec.
G—Superficial mass velocity of gas (U_{s_g}), lb per sec per sq ft.
L—Superficial mass velocity of liquid (Q_{s_l}), lb per sec per sq ft.
Q—Superficial liquid velocity, ft per sec.
S—Surface area of packing, sq ft per cu ft tower volume.
U'_{s_g}—Superficial gas velocity (based on empty tower), ft per sec.
μ—Viscosity of liquid, centipoises.
ρ_l—Density of liquid, lb per cu ft.
ρ_g—Density of gas, lb per cu ft.

This theory makes no assumption about the distance between the top of the raceway and the fusion zones. McCutcheon, Marshall, and Barnes[7] found evidence from a small, slowly quenched furnace that melting occurred close to the tuyere zone. They make no correction, however, for the collapse of the raceways when the wind was turned off and for the effects of drainage of any fused material during the early part of the quench. It is necessary therefore to exercise caution when discussing the condition in the tuyere zone of the furnace during actual operation based on their evidence from the quenched furnace.

Work done on packed absorption towers with a liquid passing down countercurrently to vapor moving up suggests that a system of this type works smoothly under changing conditions of flow until a critical stage is reached. At this point the liquid no longer flows smoothly down the column but is held in the interstices of the packing and may even be carried back upward, that is, the column "floods."

Assume that in a blast furnace the conditions of flow in the coke bed just below the fusion zone are similar to those in an absorption tower. Consider what could happen if for a given rate of liquid flow the critical upward flow of gas was reached. Instead of working their way downward through the channels in the coke bed, either or both the liquid metal and bosh slag would "hang up" and lodge in the coke-bed interstices. If the gas flow were sufficiently high, either or both of two liquids might in some locations actually be carried back upward. There is a considerable temperature gradient in the column in the vicinity of the fusion zone and the liquids moving upward into the colder regions would solidify in the voids of the coke bed. This would reduce to a marked extent the permeability of these locations to gas flow and would force the gases normally traversing them into other regions. This in turn could cause "flooding" and plugging of these regions, with further disruption of the gas flow. The whole process is unstable and once started tends to build up. It is easy to visualize an irregularity occurring, with the result that the blast pressure builds up, the column begins to hang, and unsteady operation with slips ensues. In extreme cases, an impermeable layer could form completely across the furnace, interrupting production.

Sherwood, Shipley, and Holloway[8] in 1938 made a detailed study of the flooding of packed columns by pouring a variety of liquids through various packings against different ascending gases. They obtained a correlation shown in Fig. 9, which applied to a wide range of data on both small and large towers.

Fig. 9 represents a complex arrangement of variables and merits further discussion. The ordinate, which has been called the "hanging factor" for this report, is composed of four factors multiplied together. The first, $\frac{U'^2_{s_g}}{g}$, is essentially the square of the gas velocity. The second, $\frac{a}{F^3}$, is the factor in the correlation that describes the nature of the particles and packing. Since the surface area of the particles increases rapidly when the particles are reduced in size and the void fraction appears as a cube, this factor is sensitive to small changes in the nature of the packing. The third factor is the ratio of the

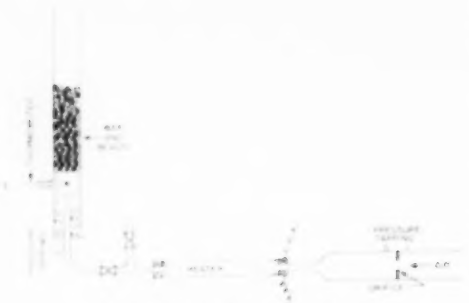

Fig. 10—Model for flooding experiments

density of the gas and liquid involved. The viscosity of the liquid has small significance in the correlation. Slight changes in temperature and composition, however, can change the viscosity of slags from 2 to 50 poises and in that case the effect of viscosity is considerable even when taken only to the 0.2 power.

The abscissa of Fig. 9 is essentially the ratio of the mass flow of liquid to gas multiplied by the root of the same density ratio as appeared in the ordinate. For convenience it has been called the Fluid Ratio.

In a blast furnace, the ratio of liquid to gas flow is smaller than that used in much of the previous work,[7] so that interest centers around the left end of the curve. Here the flooding conditions can be summarized by saying that flooding tendencies will be increased by higher gas velocity, increased by a more viscous slag, and decreased by large, uniformly sized coke. The effect of the density of gas and slag is more difficult to describe but a decreasing gas density is beneficial. However, changes in gas density are more than offset by the corresponding change in gas velocity for a given wind rate.

It is evident that there is a remarkable agreement between these factors affecting flooding and the factors commonly supposed to influence the hanging tendency of a furnace. It might therefore be argued that hanging is often associated with flooding of the coke column below the fusion zone of the furnace. However, direct proof of this is difficult to obtain. Indirect evidence may be obtained by the use of models.

Model Studies, Melting Zone: It seemed reasonable that the phenomena of hanging could be simulated by blowing hot air through a column filled with a mixture of wax particles and a neutral packing such as glass beads. This was done in the apparatus shown in Fig. 10. Small pieces of Ceresin wax were mixed with 5 mm glass beads in a 2 in. glass tube. Air between 90° and 130°C was blown through the bed, which was supported on wire mesh.

With low air rates, the wax melted and ran down the column. As the air rate was increased to a critical value, the liquid no longer ran smoothly down the column but held up in the voids of the bed and at slightly higher rates splashed back up the bed and froze. In this way, large impervious masses of wax and beads could be formed. Once a small scab formed, there was a strong tendency for it to grow, presumably because the air velocity was increased in the remainder of that particular cross-section of the tube. This was not quite true for experiments for which only a little wax was mixed with a large volume of beads. Here it sometimes happened that there was so little wax in the neighboring areas that the scab cleared itself.

In all cases, there was an appreciable hold-up of liquid in the column and this ran out if the air supply was turned off. This seemed analogous to the commonly observed phenomena that slag tends to drip past the tuyere when the wind is taken off a furnace.

In order to investigate the hanging condition, a series of runs was made with a given wax charge and at different air rates, in order to find the rate for which the bed just formed a scab. The points for these critical velocities have been included in Fig. 9, where they form an extension to the curve of Sherwood, Shipley, and Holloway. Some difficulty was experienced in deciding what was a flooding condition, particularly with lean mixtures of wax in the beads, so that there is considerable scatter in the values obtained. A further uncertainty is the viscosity of the wax as the temperature of the liquid in the critical region is uncertain.

The estimation of the liquid flow was carried out by measuring the rate of rise of the fusion zone through the uniform mixture of wax and beads and deducing the amount of liquid wax formed from the ratio of wax to beads in the original charge. It was not easy to determine the position of the fusion zone at any particular instant and the length of this zone varied somewhat, being longer for runs with lower air temperatures, 95° to 100°C, than for higher temperatures, 120° to 135°C. The rate of rise was obtained by averaging the figures for several runs. Measurements were taken on both top and bottom of the fusion zone.

In view of these sources of inaccuracy, it was to be expected that the results would show considerable scatter, but obviously they fall in line with the more complete work of other authors. It therefore seemed unnecessary to make a more detailed study of all the variables concerned, at least at the present stage of the work. It also seemed reasonable to conclude that the formation of these scabs or impervious masses of beads and wax was associated with the flooding of the bed just below the scab.

Furnace Performance: If the phenomena just described occur in a blast furnace, the cause of hanging must be sought in the conditions immediately under the fusion zone. Data on this zone are extremely meager and this attempt to apply the correlation given to furnace conditions involves the following assumptions, which were necessary to obtain the points for furnaces included in Fig. 9:

1—Temperature of the gas (N_2 + CO only) is 1500°C (2732°F).

2—Pressure of gas is the pressure in the blast main less 3 psi. Measurements indicate that about $1\frac{1}{2}$ to 2 psi is lost in the mains and a drop of $1\frac{1}{2}$ psi between the tuyere and the fusion zone was assumed.

3—Gas ascends uniformly across the furnace. The superficial velocity was calculated from the cross-sectional area of the empty stack at the mantle.

4—Viscosity was obtained by calculating the bosh slag and estimating the viscosity by reference to the McCaffery charts[7] for 1400°C (2552°F).

5—Surface area and void fraction of the coke are the same as that given in a recent survey for the district in question.

6—Although two liquid phases, metal and slag,

are present, slag is assumed to be the only one participating in the flooding action. The much lower viscosity and higher density of iron indicate that it would flood at a much higher wind rate than slag.

It is obvious that these assumptions are sweeping. No. 5 assumes not only that the coke put into the furnace had the same sizing as that used as the basis of the survey but also that there was no degradation in the furnace, since the survey was made on coke entering the furnace. While this is incorrect, there does not seem to be any better basis available for calculation.

Assumption No. 3 merits some discussion. In order to assess the superficial linear velocity of the gases, an effective cross-section of the furnace must be assumed. An accurate assumption involves much more knowledge of the shape of the "dead man" and of the flow path of the gases up the furnace than is currently available. It seemed reasonable that the critical cross-section of the furnace was well above the tuyeres but probably not above the mantle. The mantle area was therefore used in the calculation. It is appreciated that the gases probably do not flow uniformly up through the furnace at the mantle but any correction would amount to little better than a guess, so no correction was applied. Errors due to the incorrectness of Nos. 3 and 5 are in the same direction, i.e., they would tend to move the points downward on Fig. 9 and may well be contributing causes of this group of points lying well below the general curve.

It should be realized that this correlation is a complex one and the

$$\text{Hanging Factor} \frac{U_{sl}}{g} \cdot \frac{a}{F^2} \cdot \frac{\rho_g}{\rho_l} \cdot \mu \ldots$$

involves many properties of the system. The fluid ratio $\frac{L}{G}\sqrt{\frac{\rho_g}{\rho_l}}$ is a comparatively simple expression but its influence on flooding is minor under blast-furnace conditions. It therefore seems that one of the limitations of blast-furnace operation is the flooding of the coke just above the tuyere level with liquid slag. This does not seem to have been generally realized up to the present.

If this explanation is correct, it is at least possible to give one firm specification of the coke required in the blast furnace. For optimum conditions, the coke when at the bottom of the furnace just above the tuyere zone should have a minimum value of $\frac{a}{F^2}$; that is, a small surface area per unit volume as obtained with large lumps and a large void fraction as obtained in uniformly sized material. This verifies the blast-furnace man's experience that his coke should be large and uniformly sized.

The theory also indicates that the liquid bosh slag should be as fluid as possible. This seems to be most easily brought about by the addition of MgO where necessary. McCaffery[9] shows that 10 pct MgO in the slag greatly reduces its viscosity.

Conclusions

This study of the tuyere zone of the blast furnace has shown, with reasonable certainty, by means of model studies and of high speed photography, that in a normally functioning furnace there is a rapidly moving raceway of gases and coke before each tuyere. This is contrary to the frequently held concept that there is a relatively stationary bed of coke and other solids slowly descending in the tuyere zone. The diameter of the raceway ranges from 2½ to 5 ft in full-scale furnaces. The work reported has not yet progressed to a stage where all factors controlling the size of the raceway can be completely defined and as yet little is known of the width of these raceways.

The work has given a new meaning to the expression "penetration of the blast," as it is reasonable to conclude that the most important effect of changing the penetration is not chemical but physical, the effect of changing the raceway diameter. Undoubtedly this has an appreciable effect on the flow of gas farther up the stack but how much is unknown. Probably it also affects the flow of solids and liquids down the furnace to some degree.

There is some evidence to suggest that the size of the raceway in an irregularly operating furnace is somewhat variable and erratic. Suppose that for some reason the coke is prevented from entering the raceway for a short time; as, for example, would occur if the coke arched across above the raceway. Then the raceway is bound to increase in size because the coke is continuously consumed. This may be a contributing factor in the erratic results found in plant B, Figs. 7 and 8.

The data and argument presented strongly suggest that "flooding," which is characteristic of gases and liquids flowing countercurrently in a packed column, may be an important factor in causing irregular blast-furnace operation. This flooding by slag of the coke bed just below the fusion zone may contribute appreciably to hanging in the lower part of the furnace. It is to be noted that probably there are a number of causes of scabs and accretions on the furnace walls. Obviously, the scabs formed in the furnace stack are due to other causes and it is only the scabbing or "tightening" in the lower part of the furnace that can be directly related to flooding of the coke bed.

Acknowledgments

The authors wish to express their appreciation to J. J. Oravec and W. G. Forster for their enthusiastic assistance with the experimental work reported. They are appreciative of the help, patience, and understanding of the personnel of various blast-furnace plants of the United States Steel Co. where furnace studies were carried out, particularly at Edgar Thomson Works, Ensley Works, Gary Works, and Geneva. They are also grateful to L. S. Darken and B. M. Larsen for many helpful criticisms and suggestions.

References

[1] G. S. Perrott and S. P. Kinney: *Trans.* AIME (1923) **59**, p. 543.

[2] S. P. Kinney, P. H. Royster, and T. L. Joseph: U. S. Bur. Mines *Tech. Paper* 391 (1927).

[3] I. F. Kozlovich: *Stahl* (USSR) (1947) **7**, No. 7587.

[4] C. M. Tu, H. Davis, and H. C. Hottel: *Industrial and Engineering Chemistry* (1934) **26**, p. 769.

[5] R. A. Sweetser: *Blast Furnace Practice*. (1938) New York. McGraw-Hill Book Co.

[6] Blast Furnace Committee, Vereindeutscher Eisenhuttenleute: *Rept.* No. 227. *Stahl und Eisen* (1947) **66/67**, p. 277.

[7] K. C. McCutcheon, W. E. Marshall, and H. C. Barnes: JOURNAL OF METALS (April 1951) p. 304.

[8] T. K. Sherwood, G. H. Shipley, and F. A. L. Holloway: *Industrial and Engineering Chemistry* (1938) **30**, p. 765.

[9] R. S. McCaffery and Coworkers: AIME *Tech. Pub.* 383 (1931).

Distribution of Manganese and Oxygen Between Molten Iron and FeO-MnO-SiO_2 Slags

by H. B. Bell, A. B. Murad, and P. T. Carter

The distribution of manganese and oxygen between molten iron and FeO-MnO-SiO_2 slags not saturated with SiO_2 has been determined and used to calculate activities of MnO and SiO_2 in MnO-SiO_2 slags. These were found to be intermediate between the corresponding activities in FeO-SiO_2 and CaO-SiO_2 slags.

THE equilibrium constant for the reaction between molten iron containing manganese and slags containing FeO and MnO, namely:

$$FeO(slag) + Mn = MnO(slag) + Fe(liquid)$$

is most conveniently represented by:

$$K_{Mn} = \frac{(MnO)}{(FeO)\,[Mn]}$$

[Fe] is omitted, since for dilute solutions of manganese in iron, a_{Fe} is approximately constant. When activities are used for (MnO), (FeO) and [Mn], K_{Mn} is a true equilibrium constant and will apply to all types of slags, but when weight percentages are used, the values obtained for K_{Mn} for different slags vary considerably.

The equilibrium between iron containing manganese and relatively pure FeO-MnO slags has been investigated by several workers,[1-4] the most recent investigation reported is that of Chipman, Gero, and Winkler.[4] Their results, corresponding to slags containing up to 4 pct SiO_2, were represented by the equation:

$$\log K_{Mn} = \frac{6440}{T} - 2.95$$

In this case both slag and metal may be assumed to be ideal solutions, therefore the values of K_{Mn} so derived represent the true constant for the manganese reaction. As the molecular weights of MnO and FeO are almost equal, weight concentration of these oxides may also be used in the above expression.

Acidic oxides such as SiO_2 and P_2O_5 affect the activities of FeO and MnO differently, so that when total concentrations by weight of FeO and MnO are used in the above expression for K_{Mn} the values obtained are no longer constant. These will be denoted by K'_{Mn}. Körber and Oelsen[2] investigated the manganese reaction using silica-saturated iron-manganese-silicate slags and found:

$$\log K'_{Mn} = \frac{7940}{T} - 3.172$$

This corresponds to K_{Mn} values much higher than those obtained for pure oxide slags. The results of Körber and Oelsen, and Chipman, Gero, and Winkler are summarized in Table I.

Table I. Results Obtained on Oxide Slags

Temperature, °C	K_{Mn}		
	SiO_2-saturated Slags	Oxide Slags	Oxide Slags
1550	15.5	2.5	3.77
1600	12.0	2.0	3.00
1650	9.0	1.7	2.46

In the present investigation it was decided to study the manganese reaction using iron-manganese-silicate slags not saturated with silica, and which fell mainly between the orthosilicate join $2FeO \cdot SiO_2$—$2MnO \cdot SiO_2$ and the FeO-MnO side of the ternary system FeO-MnO-SiO_2. It has been shown[5] that the phases present in solidified slags of this part of the diagram are (FeO, MnO) and ($2FeO \cdot SiO_2$, $2MnO \cdot SiO_2$) solid solutions. Such an investigation would be of interest in deoxidation and also gives information on activities in liquid slags. This equilibrium has not as yet been investigated successfully. Hilty and Crafts[1] attempted to examine this reaction in a rotating crucible furnace, but were unable to obtain suitable slag samples. In the present investigation one series of experiments was carried out in a rotating crucible furnace, because the success of Taylor and Chipman[5] with such a furnace in their study of oxygen distribution between molten iron and (CaO, MgO)—FeO-SiO_2 slags suggested that it would minimize contamination of the slag by the crucible material. A second series was carried out using a wire-wound resistance furnace.

Rotating Crucible Furnace Experiments

In all cases the metallic charge consisted of 800 to 1000 g Armco iron containing 0.02 pct C, 0.03 pct Mn, and traces of Si. Manganese and silicon additions consisted of electrolytic manganese (99.9 pct

H. B. BELL and P. T. CARTER, Member AIME, are associated with the Metallurgy Dept., Royal Technical College, Glasgow, Scotland, and A. B. MURAD, formerly with the Royal Technical College, is now in Cairo, Egypt.

Discussion on this paper, TP 3269C, may be sent, 2 copies, to AIME by Sept. 1, 1952. New York Meeting, February 1952.

Mn), silicon metal (98 pct Si, 0.76 pct C, 0.8 pct Fe, and traces of Al, Ca, and Ti) or Mn-Si alloys prepared from these components. Slag additions consisted of the purest available silica sand (99.9 pct) and oxides of iron and manganese (Fe_xO_y, MnO, Mn_3O_4). Hand-rammed magnesia crucibles fired at about 1500°C were used. Details of the furnace, which was in many respects similar to that of Taylor and Chipman, are given in Fig. 1. Melting took place in a stream of purified nitrogen. In the early experiments it was found that the slag did not remain in the molten metal cup but crept up its walls towards the rim leaving the bulk of the metal uncovered, and prevention of crucible attack was not attained. Hilty and Crafts[4] also found this to occur with manganese oxide and silicate slags. An effort to keep the slag down by applying a strong jet of nitrogen directed at the slag which collected around the upper rim of the rotating metallic cup was also unsuccessful, and the experimental procedure was modified as follows.

The metal was melted and the crucible rotated for 30 min. Iron oxide, partitioned from the metal or perhaps formed by reaction of the metal with MgO, entered the pores of the crucible around the (subsequent) slag line and made the surface less porous to slag. This procedure appeared to slow down subsequent slag attack and penetration. Rotation was then stopped and additions made through a refractory tube passing from the top down to the crucible. Before removing the glass window to introduce the tube, the nitrogen flow was increased. The temperature was held constant for 30 min after the slag was completely molten, which according to Körber and Oelsen[5] and Winkler and Chipman,[6] is sufficient to establish equilibrium between metal and slag. Temperature was measured by the immersion method using a platinum-platinum-13 pct rhodium thermocouple protected by a silica sheath.

Sampling: Slag samples obtained by dipping an iron rod into the slag were invariably contaminated with metal, especially when the slag layer was very thin. Consequently the charge was allowed to solidify inside the crucible, and samples were taken from the solid metal and slag. A slag layer 3 to 5 mm thick was easily separated from the metal. Most of the melts in this investigation were carried out at about 1550°C, and as the melt solidified within 10 to 15 sec of switching off the current, it was assumed that no significant change in the equilibrium had occurred at such a high rate of cooling. This method of sampling may not be so reliable for temperatures far removed from the melting point of iron, as it could result in too high values for K'_{w_o}. It does, however, minimize the possibility of mechanical entrapment of slag particles in the metal sample which may occur during suction methods of sampling.

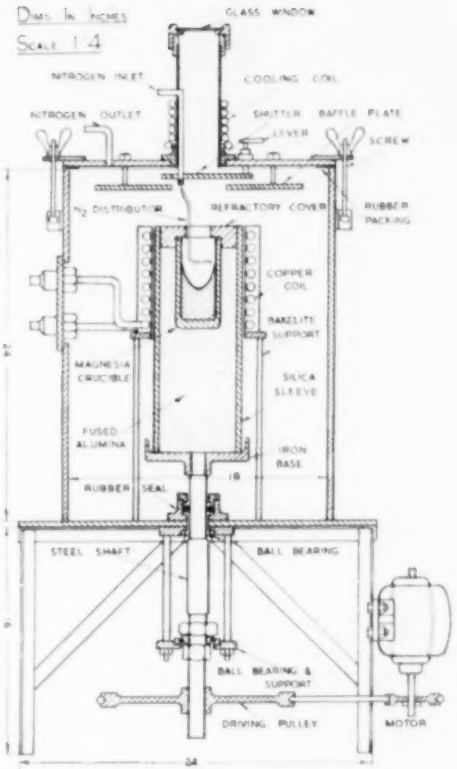

Fig. 1—Rotating crucible furnace.

Table II gives details of slag and metal analyses, temperatures and corresponding K'_{w_o} values for nine heats carried out by this method.

Resistance Furnace Experiments

Because of the slag penetration into the magnesia crucible which always occurred to some extent, even without rotation, and the possible effect this might have on the equilibrium, a series of experiments was carried out in which the charge was melted in slip-cast magnesia crucibles in a wire-wound resistance furnace. These crucibles were impervious to slag, although solution of MgO still occurred. Temperatures were taken using a platinum-platinum-13 pct rhodium thermocouple placed just beneath the crucible. After 1 hr at 1550° ± 5°C, slag samples were taken on the end of a brass rod, and metal samples by means of a Taylor sampler. The results obtained are given in Table III.

Results and Discussion

In Fig. 2, K'_{w_o} is plotted against the silica content of the slag as given by Tables II and III. The values of K_{w_o} obtained by Chipman, Gero, and Winkler[6] for FeO-MnO slags containing 1 to 4 pct Si, and by Körber and Oelsen[5] for silica-saturated slags are also indicated. The results in Table III may show a slightly lower trend than those obtained with the

Table II. Results of Experiments in Rotating Furnace

Heat No.	Temperature, °C	Metal Analysis, Mn	Metal Analysis, Si	Metal Analysis, O	Slag Analysis, FeO*	Slag Analysis, MnO	Slag Analysis, SiO$_2$	Slag Analysis, MgO	K'_{w_o}
1	1650	0.05	<0.005	0.144	55.5	24.2	13.0	6.8	8.8
2	1670	0.04	<0.005	0.130	51.0	16.7	24.5	7.2	8.2
3	1640	0.22	<0.005	0.077	24.3	42.7	27.2	7.9	7.3
4	1550	0.05	<0.005	0.097	44.0	29.8	20.9	5.3	13.5
5	1550	0.12	<0.005	0.057	27.2	42.0	23.8	7.3	12.9
6	1550	0.005	<0.005	0.135	75.1	3.6	16.3	5.5	9.6
7	1562	0.08	<0.005	0.070	42.8	28.4	19.9	8.1	8.4
8	1550	0.16	<0.005	0.150	73.5	23.0	1.7	2.1	3.2
9	1558	0.056	<0.005	0.077	31.8	25.8	35.8	6.7	14.4

* FeO determined from total iron.

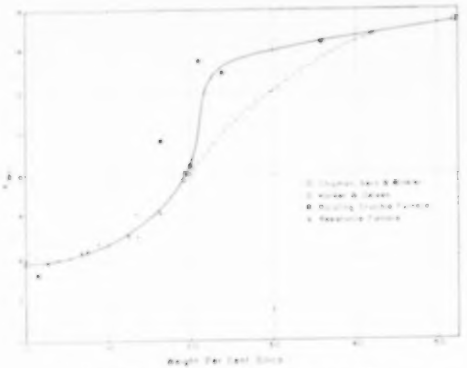

Fig. 2—Effect of silica content of slag on K'_{Mn}

rotating crucible furnace, but the results of both sets of experiments have been represented by one curve.

The increase in K'_{Mn} with silica content of the slag is similar to that observed by Krings and Schackmann[7] for melts made in alumina crucibles and containing 15 to 30 pct Al_2O_3, and to that calculated by Murray and White.[8] The increase must, of course, be attributed to the effect of silica on the activity of one or both of MnO and FeO in the slag. The curve drawn in Fig. 2 is in agreement with Chipman, Gero, and Winkler's value of 3.8 at 1550°C for pure oxide slags, and this value has been adopted in the following calculations.

Since:

$$3.8 = \frac{(a_{MnO})}{(a_{FeO})\,[\%Mn]}$$

and

$$K'_{Mn} = \frac{(MnO)}{(FeO)\,[\%Mn]} = \frac{(a_{MnO})\,\gamma\,FeO}{\gamma\,MnO\,(a_{FeO})\,[\%Mn]}$$

$$3.8 = \frac{\gamma\,MnO}{\gamma\,FeO}$$

Taylor and Chipman[1] determined the activity of FeO in a slag from the oxygen content of the molten iron with which it was in equilibrium, and showed that in the FeO-SiO_2 system, a_{FeO} is equal to its molar concentration. Recently Schuhmann and Ensio[9] found some divergence from ideality at about 1350°C, but this was only slight at silica contents below about 30 pct. Since FeO-MnO slags also behave ideally with respect to FeO, it might be expected that FeO-MnO-SiO_2 slags would behave similarly. This is not necessarily true, however, and caution must be exercised in making such predictions for a ternary system from a knowledge of activities in the binary systems. Thus the determinations of Taylor and Chipman[1] of a_{FeO} in CaO(MgO)-FeO-SiO_2 slags, illustrated in Fig. 3a, indicate that although in the FeO-SiO_2 and CaO-FeO systems, the activity of FeO approximately equals its molar fraction, its activity in the ternary system can be considerably different. This is because CaO and SiO_2 cannot be considered as separate constituents, but show a strong tendency to orthosilicate formation. In a system MO-FeO-SiO_2 in which MO behaved exactly like FeO, truly ideal behavior for FeO would be expected as shown in Fig. 3b. In the FeO-MnO-SiO_2 system, MnO shows a tendency to silicate formation less than that of CaO, but more marked than that of FeO, and behavior intermediate between that of the ideal case and that shown by the CaO(MgO)-FeO-SiO_2 system, as shown in Fig. 3c, would be expected. Unfortunately the limited number of determinations is not sufficient to detect the deviation from ideality expected, the experimental points shown in Fig. 4 appearing to indicate ideality. They indicate a distribution ratio $\frac{[\%O]}{(FeO)} = 0.20$ at 1550°C, as compared with 0.185 of Taylor and Chipman[1] and 0.26 given by Körber and Oelsen.[6]

Assuming that FeO behaves ideally in FeO-MnO-SiO_2 slags, the change in K_{Mn} caused by the addition of silica may be attributed entirely to a change in the activity of MnO, if it is also assumed that dilute liquid Fe-Mn solutions behave ideally. The activity coefficient of MnO in a slag would then be equal to:

$$\gamma\,MnO = \frac{3.8}{K'_{Mn}}$$

where K'_{Mn} is the value taken from Fig. 2 for the

Table III. Experiments Carried Out in Resistance Furnace

Heat No.	Metal Analysis, Wt Pct Mn	Metal Analysis, Wt Pct Si	Slag Analysis, Wt Pct FeO*	Slag Analysis, Wt Pct MnO	Slag Analysis, Wt Pct SiO_2	Slag Analysis, Wt Pct MgO	K'_{Mn}
11	0.020		77.0	14.5	3.8	4.0	3.8
13	0.04	0.005	70.1	12.1	7.5	9.7	4.3
14	0.12	0.005	58.0	23.1	6.6	9.1	4.25
15	0.40	0.005	27.1	58.0	8.8	5.1	4.65
16	0.40	0.009	29.5	32.5	13.6	4.6	3.0
17	0.20	0.005	40.9	41.1	12.6	4.9	3.0
18	0.22	0.005	32.9	44.0	10.4	8.1	6.1
19	0.052	0.005	52.8	12.1	13.5	15.1	6.1
20	0.085	0.007	38.1	30.2	19.4	9.7	8.1

* Not determined from Metal Data.

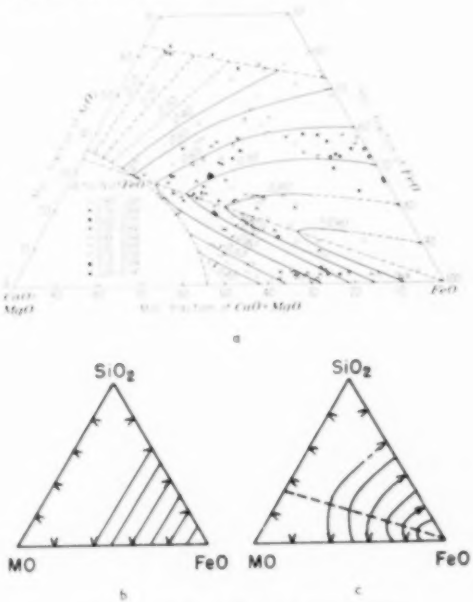

Fig. 3—Activity of FeO in simple ternary systems.

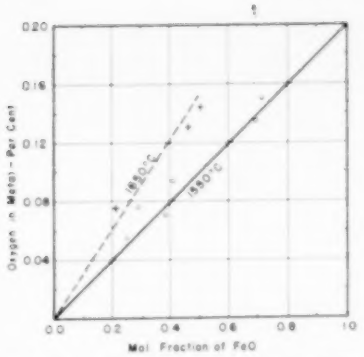

Fig. 4—Relation between oxygen content of metal and FeO content of slag

corresponding silica content of the slag. The values so obtained for γ MnO are given in Table IV.

In cols. 5 and 6 these values of γ MnO have been used to obtain approximate values for a_{MnO} in the MnO-SiO_2 system, although it should be remembered that at 1550°C slags of high MnO content would be partially solid and therefore these figures relate to supercooled liquids in this range. The values for a_{MnO} were used to determine a_{SiO_2} (standard state = pure cristobalite) in the MnO-SiO_2 system by application of the Gibbs-Duhem relation. The values of a_{SiO_2} so obtained indicated that the figures for K'_{MnO} taken from Fig. 2 at 25 and 30 pct SiO_2 were too high, values of 10.5 and 11.9, respectively, probably being more correct. The dotted curve through these points in Fig. 2 again suggests that the values of K'_{MnO} obtained in the rotating furnace are too high. Both the corrected and uncorrected values of a_{SiO_2} are given in Table IV.

Data for the activities of MnO and SiO_2 in MnO-SiO_2 slags (as defined above) are plotted against N_{SiO_2} in Fig. 5. The curves of Schuhmann and Ensio[11] for a_{FeO} and a_{SiO_2} in FeO-SiO_2 slags, and curves for a_{CaO} and a_{SiO_2} in CaO-SiO_2 slags (again corresponding to supercooled liquids at high CaO contents) are also included. Values for a_{CaO} were calculated by assuming a linear variation from $a_{CaO} = 1$ at $N_{SiO_2} = 0$, almost to $a_{CaO} = 0$ at $N_{SiO_2} = 0.33$, and using the figures given by Rosenqvist[12] at less basic compositions. The activity of silica was calculated using the Gibbs-Duhem relation. It will be seen that the relative positions of the activity curves are in agreement with the known cation-oxygen bond strengths for calcium, manganese, and iron.

Table IV. Activity Coefficients for Manganese Oxide in Slag

				MnO-SiO_2 System				
				Uncorrected			Corrected	
SiO_2 Pct	N_{SiO_2}	K'_{MnO}	γ_{MnO}	N_{SiO_2}	a_{MnO}	a_{SiO_2}	a_{MnO}	a_{SiO_2}
0	0.00	3.8	1.00	1.00	1.00	0.00	1.00	0.00
5	0.06	4.0	0.95	0.94	0.89	0.0001	0.89	0.0001
10	0.11	4.6	0.83	0.89	0.74	0.002	0.74	0.002
15	0.17	5.9	0.64	0.83	0.54	0.013	0.54	0.013
20	0.22	8.5	0.45	0.78	0.35	0.050	0.35	0.052
25	0.28	13.4	0.29	0.72	0.20	0.40	0.26	0.23
30	0.33	14.0	0.27	0.67	0.18	0.51	0.21	0.39
40	0.44	14.6	0.26	0.56	0.146	0.73	0.146	0.72
50	0.54	15.45	0.246	0.46	0.113	0.99	0.113	0.99
52	0.56	15.5	0.245	0.44	0.108	1.00	0.108	1.00

K_{MnO} in Steelmaking Slags: In basic slags, K_{MnO} is approximately the same as in pure oxide slags, as SiO_2 and P_2O_5 may be regarded as completely combined with CaO. They would then have little or no effect on the activities of MnO and FeO. At lower basicities, when insufficient CaO is present, the activity of MnO is lowered more than that of FeO, and K_{MnO} rises, as was shown by Darken and Larsen's[5] examination of steelmaking slags, and the experiments of Tammann and Oelsen.[10] A four-fold increase in K_{MnO} (i.e., from 3.8 to about 15.5) would be the maximum expected as the slags became more acidic.

Calculation of Manganese and Silicon Contents of Molten Iron in Equilibrium with FeO-MnO-SiO_2 Slags at 1550°C: Manganese: The manganese concentration can be calculated from the equation:

$$[\% \text{ Mn}] = \frac{\gamma \text{MnO}(\Sigma\text{MnO})}{3.8\,(\Sigma\text{FeO})} = \frac{(\Sigma\text{MnO})}{K'_{MnO}(\Sigma\text{FeO})}$$

where (ΣMnO) and (ΣFeO) are the total manganese and ferrous oxide contents of the slag (or deoxidation product), respectively.

Silicon: Körber and Oelsen[7] found that for silica-saturated slags containing about 50 pct SiO_2, the equilibrium constant for the reaction:

$$2\text{Fe (liquid)} + SiO_2 = 2\text{FeO (slag)} + \underline{\text{Si}}$$

could be expressed by:

$$K_{Si} = \frac{(\Sigma\text{FeO})^2[\% \text{ Si}]}{4.5 \text{ at } 1550^\circ\text{C}}$$

$$\text{Actually } K_{Si} = \frac{(a_{FeO})^2[\% \text{ Si}]}{(a_{SiO_2})}$$

and Körber and Oelsen's expression for K_{Si} assumes that: 1—The activity of FeO equals its percentage by weight. 2—Dilute solutions of silicon in iron obey Henry's law. 3—The activity of SiO_2 is unity.

The silicon content of the metal in equilibrium with a given FeO-MnO-SiO_2 slag at 1550°C can be calculated if it is assumed that a_{FeO} is proportional to the weight concentration of FeO, and also that a_{SiO_2} can be interpolated from the silica activity curves of Fig. 5, i.e.:

$$[\% \text{ Si}] = 4.5\frac{(a_{SiO_2})}{(\Sigma\text{FeO})^2}$$

Fig. 6 compares some of the recently published data of Hilty and Crafts[9] on deoxidation with silicon and manganese with those calculated from the

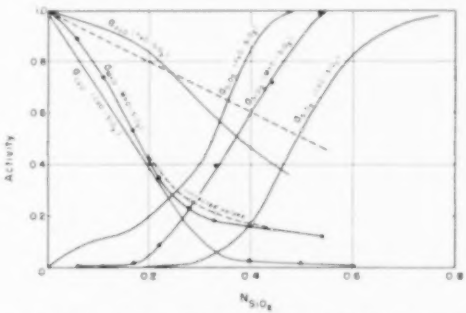

Fig. 5—Activities of metallic oxide and silica in the binary systems FeO·SiO_2, MnO·SiO_2, and CaO·SiO_2

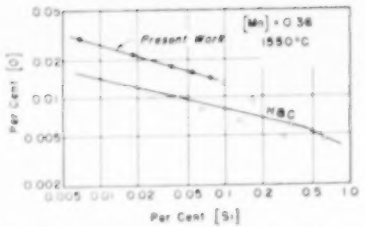

Fig. 6—Comparison of present results with those of Hilty and Crafts.

present work at 1550°C and presented in Table V. Fig. 6 shows that the oxygen contents of Hilty and Crafts are considerably lower.

For any given manganese content in iron, the highest silicon content is obtained when a silica-saturated FeO-MnO-SiO$_2$ slag which is in equilibrium with that manganese content. According to Table V, percentages of silicon higher than 0.078 pct cannot exist with 0.36 pct Mn under equilibrium conditions. Fig. 6 shows silicon contents up to 1 pct in Fe containing 0.36 pct Mn. Hilty and Crafts also reported silicon contents up to 1 pct in Fe containing as little as 0.04 pct Mn. It is probable, therefore, that in many of Hilty and Craft's experiments, an excess of deoxidizing elements had been added but no liquid slag was present to remove this excess.

The above results could be used to prepare charts showing the manganese, silicon, and oxygen contents of metal in equilibrium with a given FeO-MnO-SiO$_2$ slag. It is felt, however, that it would be unwise at this stage to make such lengthy calculations in view of the incompleteness of the experimental data. Nevertheless approximate calculations for any given slag composition can easily be carried out, as was done in the preparation of Table V.

Summary

The manganese equilibrium between molten iron and FeO-MnO-SiO$_2$ slags has been examined at 1550°C for slags not saturated with silica, using both a rotating crucible furnace and a wire-wound resistance furnace. The former appeared to give too high values for K'_{Mn}. This may have been due to the effect of the continuous absorption of slag by the crucible used, or the sampling techniques. It was not found possible to prevent contact between slag and crucible in the rotating crucible furnace.*

* It can be shown mathematically that the height of rise of the rotating liquid is independent of its density, so that if surface and interfacial tension effects are excluded the slag must come in contact with the crucible. Success with the rotating crucible furnace depends on having a slag with a high contact angle and interfacial tension against molten metal, and a metal which "wets" the crucible.

The K'_{Mn} values obtained were used to determine a_{FeO} in the slag, assuming that a_{MnO} was equal to its molar fraction. Determination of a_{SiO_2} using the Gibbs-Duhem relation enabled slight corrections to be made to the original a_{FeO} values. A comparison of the activity values with those obtained by Schuhmann and Ensio for FeO-SiO$_2$ slags, and estimated CaO and SiO$_2$ activities in CaO-SiO$_2$ slags, showed that they were in agreement with the known cation-oxygen bond strengths for calcium, manganese, and iron.

It is possible to calculate with reasonable accuracy from the results the manganese, silicon, and oxygen contents of molten iron in equilibrium with FeO-MnO-SiO$_2$ slags containing less than 25 pct SiO$_2$, and approximate values may be obtained for more acid slags.

Table V. Compositions of Metal and Slag in Equilibrium at 1550 C

Metal Analysis, Wt Pct			Slag Analysis, Wt Pct		
Mn	Si	O	FeO	MnO	SiO$_2$
0.36	0.078	0.0140	7.0	42.4	50
0.36	0.050	0.0132	8.0	46.4	45
0.36	0.037	0.0123	9.0	50.4	40
0.36	0.021	0.0098	11.2	53.8	35
0.36	0.007	0.0065	16.2	53.8	30

Acknowledgment

The authors would like to record their appreciation of the friendly advice and criticism of Professor R. Hay.

References

(1) C. H. Herty, Jr.: Chemical Equilibrium of Manganese, Carbon and Phosphorus in the Basic Open Hearth Process. *Trans.* AIME (1926) **73**, pp. 1107-1131.

(2) W. Krings and H. Schackmann: The Equilibrium FeO + Mn ⇌ Fe + MnO at 1550°C-1560°C. *Ztsch. anorg. allgem. Chem.* (1931) **202**, pp. 99-112.

(3) F. Körber and W. Oelsen: The Relation between Iron containing Manganese and Slags consisting almost entirely of Manganous and Ferrous Oxides. *Mitt. Kaiser-Wilhelm Inst. Eisenforschung* (1932) **14**, pp. 181-204.

(4) J. Chipman, N. Gero, and T. B. Winkler: The Manganese Equilibrium under simple Oxide Slags. *Trans.* AIME (1950) **188**, pp. 341-345; JOURNAL OF METALS (February 1950).

(5) F. Körber and W. Oelsen: The Principles of Deoxidation with Manganese and Silicon. *Mitt. Kaiser-Wilhelm Inst. Eisenforschung* (1933) **15**, pp. 271-309.

(6) P. T. Carter and A. B. Murad: Unpublished work.

(7) D. C. Hilty and W. Crafts: Solubility of Oxygen in Liquid Iron containing Silicon and Manganese. *Trans.* AIME (1950) **188**, pp. 425-436; JOURNAL OF METALS (February 1950).

(8) C. R. Taylor and J. Chipman: Equilibria of Liquid Iron and Simple Basic and Acid Slags in a Rotating Induction Furnace. *Trans.* AIME (1943) **154**, pp. 228-245.

(9) T. B. Winkler and J. Chipman: An Equilibrium Study of the Distribution of Phosphorus between Liquid Iron and Basic Slags. *Trans.* AIME (1946) **167**, pp. 111-133; METALS TECHNOLOGY (April 1946).

(10) P. Murray and J. White: Equilibrium Relationships in Systems containing Iron Oxide and their bearing on the problem of the Constitution of Liquid Open Hearth Slags. *Discussions* Faraday Soc. (1948) No. 4, pp. 287-296.

(11) R. Schuhmann and P. J. Ensio: Thermodynamics of Iron-Silicate Slags: Slags Saturated with Gamma Iron. *Trans.* AIME (1951) **191**, pp. 401-411; JOURNAL OF METALS (March 1951).

(12) W. Krings and H. Schackmann: The Effect of Temperature and Additions on the Equilibrium FeO + Mn ⇌ Fe + MnO. *Ztsch. anorg. allgem. Chem.* (1932) **206**, pp. 337-355.

(13) T. Rosenqvist: A Thermodynamic Study of the Reaction CaS + H$_2$O ⇌ CaO + H$_2$S and the Desulphurization of Liquid Metals with Lime. *Trans.* AIME (1951) **191**, pp. 535-540; JOURNAL OF METALS (March 1951).

(14) L. S. Darken and B. M. Larsen: Distribution of Manganese and of Sulphur between Slag and Metal in the Open-Hearth Furnace. *Trans.* AIME (1942) **150**, pp. 87-112.

(15) G. Tammann and W. Oelsen: The Distribution of Associated Elements between Steel and Slag in the Steelmaking Process. *Archiv Eisenhüttenwesen* (1932) **5**, pp. 75-80.

Thermodynamics of Iron-Silicate Slags: Slags Saturated With Solid Silica

by E. J. Michal and R. Schuhmann, Jr.

Experimental measurements are reported for the oxygen pressures of iron-silicate slags in equilibrium with solid silica. CO_2-CO mixtures were bubbled through the slags in silica crucibles to find equilibrium values of p_{CO_2}/p_{CO} over the entire composition range of silica-saturated slags at 1250°, 1300°, and 1350°C. From the data, the activity vs. composition relationships were calculated for O, FeO, and Fe.

SLAGS composed primarily of silica and iron oxides have particular practical importance in copper smelting, in acid steelmaking, and in accounting for the service behavior of silica refractories. These slags all contain both ferrous and ferric iron, so that, strictly speaking, they are ternary or three-component liquid solutions. For convenience, the components may be taken as the three oxides, FeO, Fe_2O_3, and SiO_2. The constitution of the FeO-Fe_2O_3-SiO_2 system at slagmaking temperatures has been studied in a recent investigation described in a separate paper.[1] This work showed the compositional ranges of iron-silicate melts at temperatures up to 1450°C and also the temperature-composition relationships for melts in equilibrium with various solid phases, including iron, wüstite, magnetite, and silica. Broadly speaking, the compositions of iron-silicate melts at a given temperature should be thought of as varying over a two-dimensional field. In the first place, the silica/total iron oxide relationship varies from maximum silica for silica-saturated melts to minimum silica for wüstite-saturated melts or, at higher temperatures, to zero silica for straight iron oxide melts. In copper smelting, for example, the converter slags approach the low silica limits while the reverberatory-furnace slags have intermediate silica contents, perhaps approaching silica saturation in some circumstances. Liquids formed in the pores of silica refractories presumably are close to silica saturation. The second type of composition variation is in the ferric/ferrous relationship, which depends on how oxidizing or how reducing the process conditions are. Relatively reducing slags, such as acid-steelmaking slags, are lower in ferric oxide and approach saturation with metallic iron. Oxidized slags, such as copper-smelting slags, contain larger percentages of ferric oxides and approach or reach saturation with magnetite. Since these two kinds of compositional variations are closely related to two general properties of interest for all metallurgical slags, basicity, and oxidizing power, it is hoped that the thermodynamic study of iron-silicate slags eventually will throw further light on the significance and nature of these long-recognized but as yet poorly understood slag properties.

Measurements of oxygen activity as a function of slag composition, using CO_2-CO gas mixture to fix oxygen activities, afford an experimentally convenient approach to the study of the thermodynamic properties of iron-silicate slags. In a preceding investigation,[2] this approach was used in a systematic study of iron-silicate slags in equilibrium with solid iron. The present paper gives the results of a similar study of the iron-silicate slags in equilibrium with solid silica. The experimental work consisted in the determination of CO_2:CO ratios in gas mixtures at equilibrium in the system:

gas: liquid slag: silica

Determinations were made at temperatures from 1250° to 1350°C for slags ranging in composition from iron saturation to magnetite saturation. Also, equilibrium CO_2:CO ratios and slag compositions were determined for the univariant systems:

gas: liquid slag: silica: γ iron
gas: liquid slag: silica: magnetite

Experimental Methods

The experimental procedure was essentially the same as that used in the previous study of iron-silicate slags saturated with solid iron,[2] but in order to work with the silica-saturated slags an all-silica crucible assembly was used. A liquid slag was prepared from pure prefused stock materials and brought to equilibrium with the silica crucible at the desired temperature. Then a mixture of CO_2 and CO was continuously bubbled through the melt

E. J. MICHAL, Junior Member AIME, is Research Metallurgist, National Lead Co., South Amboy, N. J., and R. SCHUHMANN, JR., Member AIME, is Associate Professor, Dept. of Metallurgy, Massachusetts Institute of Technology, Cambridge, Mass.

Discussion on this paper, TP 3331D, may be sent, 2 copies, to AIME by Sept. 1, 1952. Manuscript, Jan. 28, 1952. New York Meeting, February 1952.

This paper is based on a thesis submitted by Mr. Michal in partial fulfillment of requirements for the degree of Doctor of Science to Massachusetts Institute of Technology.

Fig. 1—Silica crucible assembly

1—Gas mixture inlet
2—Glass prism
3—Gas mixture outlet
4—Access tubes
5—Rubber gaskets
6—Brass head
7—Cooling water in and out
8—Outer silica crucible
9—Crushed silica packing
10—Gas bubbling tube
11—Inner silica crucible

and the CO_2-CO ratio in the mixture was adjusted until analyses of the gases entering and leaving the melt became and remained the same, indicating equilibrium between gas, slag, and crucible. After equilibrium was established, the slag was sampled and analyzed for FeO, Fe_2O_3, and SiO_2.

The starting materials, overall equipment arrangement, furnace, temperature controller, gas trains, and analytical methods were substantially the same as described in the preceding paper.[1]

Silica Crucible Assembly: Common laboratory forms of silica glass were found to behave very poorly as containers for iron-silicate slags, even if the slags were completely saturated with silica before the refractory was brought into contact with the slag. Slag penetration and devitrification, accompanied by deterioration in mechanical properties, ended all runs with ordinary crucible arrangements before gas-slag equilibrium determinations could be made. Eventually, however, the all-silica crucible and reaction chamber shown in Fig. 1 was developed and proved satisfactory, except that its fabrication required many man hours of painstaking work.

The silica reaction chamber was fabricated in an outer translucent silica tube 1½ in. in ID and 18 in. long. A double silica bottom was welded into this tube to form a large crucible, in which was placed a small inner crucible 1 in. in ID and 4 in. high. Ground fused quartz was packed between the inner and outer crucible. The small inner crucible supported on its rim a double access-tube assembly consisting of two quartz tubes ½ in. in diam welded together at the bottom in such a manner as to form a cover for the inner crucible. The space between the access tubes and the tall outer crucible was packed with coarsely crushed, fused quartz to serve as thermal insulation. An outlet at the top of the large crucible furnished a means of bleeding the equilibrium CO_2-CO mixture through this packing to flush out air. The top of the outer crucible was sealed by a water-cooled brass head and rubber gaskets, making a gas-tight assembly. The double access tube extended through the brass head and permitted the introduction, through one of the access tubes, of a 3/16 in. bore silica gas-bubbling tube. The other access tube was used for charging and sampling of slags, and temperature measurement. Welding and fabricating of the silica crucible assembly was done with gas-oxygen and oxygen-acetylene torches.

The crucible assembly was supported on insulating firebrick within a porcelain tube which extended vertically through the resistance furnace. The small inner silica crucible was positioned at the thermal center of the furnace, and the outer crucible extended through a water-cooled brass head at the top of the porcelain furnace tube. The atmosphere between the porcelain tube and the outer silica crucible was maintained at the same gas composition as the atmosphere being used within the silica crucible.

Each crucible assembly served for a run of several days during which a number of gas-slag equilibrium determinations were made. At the end of a run the innermost crucible and the silica packing were almost entirely permeated with slag, and in several cases the slag had nearly penetrated through the outer crucible as well.

Temperature Measurement: Slag temperatures were measured with an optical pyrometer sighted on the surface of the slag. The optical pyrometer was calibrated against a platinum-platinum-rhodium thermocouple* in a silica protection tube immersed in the slag. The calibration experiments covered the experimental temperature range from 1250° to 1350°C and the entire slag-composition range, and gave corrections of from 18° to 24°C to be added to the optical pyrometer reading. Accordingly, a correction of 20°C was added to all optical readings to obtain the temperature values reported in the data. The overall accuracy of the final temperature measurements is considered as ±5°C.

* Standardized at the melting point of gold.

Temperature explorations within an empty crucible assembly at about 1100°C showed uniformity of temperature to within ±3°C in the lower 3 in. of the crucible.

Gas Analysis: The CO_2-CO mixtures entering and leaving the slag in the reaction chamber were analyzed by the gravimetric method used in previous work,[1] which consisted in absorbing CO_2 in an ascarite-anhydrone train, oxidizing the CO in a copper oxide furnace, and then absorbing the resulting CO_2 in a second ascarite-anhydrone train. The gas mixtures varied from about 90 pct CO, 10 pct CO_2 to 0.5 pct CO, 99.5 pct CO_2, a much wider range than in the previous work. Accordingly, a careful study was made of the possible errors in the method, especially for mixtures low in CO. Possible sources of error investigated were: 1—weighing and manipulations of absorption tubes, 2—incomplete absorption, 3—incomplete flushing, 4—variations in blanks, 5—impurities in gas mixtures. These investigations, plus the internal consistency of the analyses found in calibrating the CO and CO_2 flowmeters in the gas

mixer, showed that the gas analyses were reliable to within ±0.05 pct CO over the entire range of gas compositions used in the investigation. The test for gas-slag equilibrium was the comparison of analyses for the gases entering and leaving the melt. With an accuracy of ±0.05 pct CO in individual gas analyses, it is estimated that the accuracy in finding the equilibrium gas composition for a given slag by the trial-and-comparison procedure was about ±0.1 pct CO for gases of low CO content and about ±0.3 pct CO for gases high in CO.

Sampling of Slags. Slag samples weighing about 30 g each were taken by suction into a length of 7 or 9 mm Vycor tubing. Before being inserted in the furnace, the sampler was flushed with the CO_2-CO mixture being fed to the furnace. The entire sampling operation was carried out in a rapid sequence, with only a few seconds' cooling in the upper part of the furnace tube before the sample was taken into the room. After cooling to room temperature, the Vycor broke cleanly away from the slag sample. No attack was ever observed on the Vycor tubing.

Experimental Results

The gas-slag equilibrium data are given in Table I. These determinations cover the entire range of compositions of silica-saturated slags at 1250°, 1300°, and 1350°C. In terms of silica and total iron oxide contents, these slags do not show much variation, from 30 to 40 wt pct SiO_2 and from 60 to 70 wt pct FeO + Fe_2O_3. However, the important composition variable in silica-saturated slags is the state of oxidation of the slag, and this can be expressed in several different ways. For example, the Fe_2O_3 content varies from 0.76 to 22.23 pct and the ratio of ferric iron to total iron varies from 0.0115 to 0.296. The equilibrium CO_2:CO ratio is, of course, another measure of the state of oxidation of the slag and at 1350°C for example varies from 0.1186 to 124. This approximately 1000-fold variation in CO_2:CO ratio corresponds to a 10^3 fold change in oxygen pressure, clearly showing the sensitivity of the oxidizing or reducing character of the slag to variations in the Fe_2O_3 content.

Table I. Silica Saturated Slags, Complete Experimental Data

Point No.	Temperature, °C	Slag Composition by Chemical Analysis,* Pct Fe_2O_3	Slag Composition by Chemical Analysis,* Pct FeO	Slag Composition by Chemical Analysis,* Pct SiO	Gas Composition by Analysis Pct CO	Gas Composition by Analysis p_{CO_2}/p_{CO}
3	1249	0.76	59.94	39.28	11.8	0.1312†
6	1291	1.02	59.41	39.54	19.6	0.244
4	1291	1.03	60.04	38.91	19.8	0.247
8	1296	1.76	59.65	38.65	39.7	0.636
9	1296	2.75	58.65	38.60	59.7	1.40
10	1300	4.36	58.94	37.60	80.6	4.15
11	1347	4.09	57.53	38.38	80.4	4.10
12	1350	2.76	57.86	39.38	60.2	1.51
13	1345	1.93	58.14	39.93	40.2	0.672
14	1345	1.22	58.61	40.17	20.1	0.252
15	1347	0.76	59.05	40.19	10.6	0.1186†
17	1248	0.83	60.80	38.37	13.0	0.1494†
19	1248	0.88	60.86	38.26	19.5	0.242
20	1246	1.78	60.35	37.87	39.5	0.654
21	1247	3.45	59.30	37.25	59.3	1.45
22	1246	3.80	59.50	36.70	80.3	4.07
24	1247	8.49	56.81	34.70	94.8	18.2
26	1246	8.76	56.09	34.33	94.6	17.5
28	1246	9.07	56.11	34.82	95.2	19.8
30	1245	12.85	53.60	33.57	97.35	36.7
31	1245	12.32	54.42	33.26	97.5	39.0
34	1302	11.91	53.62	34.47	96.9	31.2
35	1302	14.54	52.32	33.14	97.8	44.4
36	1302	9.27	55.35	35.38	94.8	18.2
37	1302	14.99	51.42	33.59	98.0	49.0
38	1351	10.02	53.76	35.40	96.15	25.0
39	1353	20.24	48.83	30.93	98.9	90.0
42	1302	15.24	52.47	32.29	97.7	42.5
43	1251	13.69	53.61	32.70	97.5	39.0
45	1354	17.89	49.53	32.58	98.55	68.0
47	1349	22.23	47.57	30.20	99.2	124.0‡
48	1299	18.09	50.37	31.54	98.5	65.6‡
49	1252	14.45	53.18	32.34	97.8	44.4‡
50	1253	14.23	53.33	32.42	97.8	44.4
51	1253	12.30	54.45	33.25	97.2	34.7
52	1252	10.44	55.33	34.23	96.0	24.0
53	1252	7.30	57.05	35.45	92.0	11.5
55	1302	7.64	56.18	36.18	92.0	11.5
57	1348	8.54	54.55	36.91	90.5	9.4
58	1252	4.64	58.72	36.63	80.0	4.0
59	1251	3.69	59.82	37.18	60.0	1.5
60	1298	16.93	51.37	31.70	98.6	70.4

* Recalculated to 100 pct total.
† Points at silica and ↄ iron saturation.
‡ Points at silica and magnetite saturation.

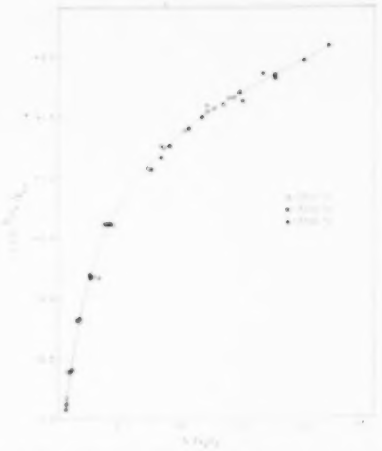

Fig. 2—Silica saturated slags. Log p_{CO_2}/p_{CO} vs. pct Fe_2O_3.

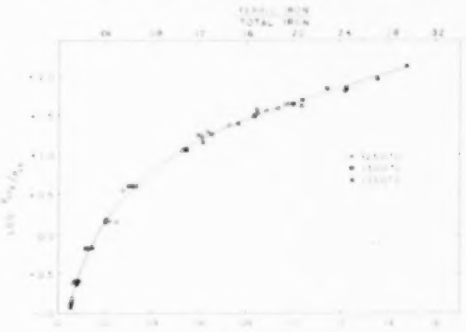

Fig. 3—Silica saturated slags. Log p_{CO_2}/p_{CO} vs. $N_{Fe_2O_3}/N_{FeO}$.

In the lowest state of oxidation at a given temperature (points 5, 15, 17 of Table I) the slags are in equilibrium with metallic iron as well as silica, and attempts to reduce the slags further will only form iron and silica. In the highest state of oxidation at a given temperature (points 47, 48 and 49) the slags are in equilibrium with solid magnetite and further oxidation would convert them into magnetite and silica.

The experimental data are given in Figs. 2 and 3 as plots of log p_{CO_2}/p_{CO} against various measures of slag composition; wt pct Fe_2O_3, the ratio ferric iron/total iron, and the ratio $N_{Fe_2O_3}/N_{FeO}$. The ratio $N_{Fe_2O_3}/N_{FeO}$ is especially useful in thermodynamic calculations and is calculated by expressing the chemical analysis in terms of mol fractions of the three components

Fig. 4—Silica saturated iron silicate slags. Log p_{CO_2}/p_{CO} vs. $10^4/T$.

FeO, O_2, and SiO$_2$. Thus N_{O_2}/N_{Fe} is the ratio of the number of mols of oxygen in excess of that required to form FeO and SiO$_2$ to the number of mols of FeO, calculating all the iron as FeO. As can be seen in Fig. 3,

$$\frac{N_{O_2}}{N_{Fe}} = \frac{1}{2} \text{ ferric iron}$$

For iron-silicate slags at equilibrium with solid silica, specification of temperature and a single composition variable such as pct Fe_2O_3 or N_{O_2}/N_{Fe} automatically fixes the entire slag composition, as can be proved by the Phase rule.

In both Figs. 2 and 3 it can be seen that the data for all three temperatures fall on the same curve within experimental error, so that for a given pct Fe_2O_3 or given N_{O_2}/N_{Fe} in silica-saturated slags, the CO_2/CO ratio does not vary appreciably with temperature. This is a coincidence and it is likely that more precise data or data over a wider temperature range would show some small variations of p_{CO_2}/p_{CO} with temperature. In this connection, it might be also noted that Darken and Gurry[7] found relatively small variations of p_{CO_2}/p_{CO} with temperature for pure Fe-O melts.

The ratio p_{CO_2}/p_{CO} and the oxygen pressure of the slags are seen to be very sensitive to content of ferric iron at low values of pct Fe_2O_3 or N_{O_2}/N_{Fe}. In this range, for example, p_{CO_2}/p_{CO} increases about tenfold as the Fe_2O_3 content increases from about 0.8 pct to about 2.5 pct. This sensitivity to ferric iron content is probably not confined to the particular iron-silicate slags studied in this investigation.

p_{CO_2}/p_{CO} Relationships for the Univariant Equilibria: Fig. 4 is a p_{CO_2}/p_{CO} vs. $1/T$ diagram which summarizes the results of the present investigation along with previous data on the limits of the field of stability of silica-saturated slags. Darken[1] first pointed out the three important univariant equilibria in which the liquid slags are in equilibrium with two solid phases: silica and magnetite, silica and fayalite, and silica and iron, respectively. For conditions of p_{CO_2}/p_{CO} and T falling outside the area enclosed by these three curves in Fig. 4, no stable slags saturated with silica can exist.

The relation of p_{CO_2}/p_{CO} to temperature for the univariant equilibrium

gas: slag: silica: γ iron

was determined by Schuhmann and Ensio,[2] who produced silica-saturated slags in iron crucibles. In the present investigation the measurements were repeated in silica crucibles, using iron wire in excess to produce iron saturation, and checked well with the previous work in iron crucibles. The newer work in an all-silica reaction chamber was more satisfactory than the previous work in all-iron systems in that no difficulty was experienced with carbon deposition by the reaction: $2CO \rightarrow CO_2 + C$.

No new data were obtained for equilibria with solid fayalite, so curve "5"-"2" in Fig. 4 is based on Darken's[1] data entirely.

For the univariant equilibrium:

gas: slag: silica: magnetite

the present investigation consistently gave lower p_{CO_2}/p_{CO} values than the previous work of Darken.[1] Accordingly various supplementary experiments were made to check this portion of the work. At all three experimental temperatures, attempts to establish gas-slag equilibrium at CO$_2$/CO ratios higher than those reported in Table I simply led to formation of more magnetite, with no increase in the equilibrium p_{CO_2}/p_{CO} value. As a further check, experiments were conducted by an entirely different technique, as follows: A small sample of slag taken from a run near magnetite saturation was placed in a platinum crucible and then suspended in a tube furnace at controlled temperature in a stream of the CO$_2$-CO gas mixture. After 18 hr the sample was quenched in the cold part of the furnace tube and then removed, mounted in bakelite, polished, and examined microscopically for primary magnetite. At a given temperature, runs were made at several CO$_2$/CO ratios, and the value of p_{CO_2}/p_{CO} was found which was just sufficient to form crystals of primary magnetite in the slag. At 1350°C, primary magnetite formed with gas mixtures containing 0.72 pct and less CO but did not form with gas mixtures containing 0.92 pct or more CO. These experiments check the figure of 0.8 pct CO for magnetite saturation found by the slag-bubbling technique. Similarly at 1250°C, the equilibration tests in platinum crucibles showed the magnetite-saturation gas composition to be between 2.25 and 2.42 pct CO whereas the slag-bubbling technique gave 2.2 pct CO.

The dashed lines within the slag field of Fig. 4 represent the p_{CO_2}/p_{CO} vs. $1/T$ relationships for silica-

Fig. 5—Effect of log p_{CO_2}/p_{CO} and temperature on solubility of silica.

saturated slags of several arbitrarily selected values of N_{FeO}/N_{SiO_2}. Each of these lines is horizontal, because, as shown in Fig. 3, p_{CO_2}/p_{CO} did not vary with temperature within the experimental error. The value of log p_{CO_2}/p_{CO} for each line was read from the smoothed curve of Fig. 3.

Silica Solubility in Iron Silicate Slags: Although the silica contents of the silica-saturated slags do not vary widely, as pointed out before, they do show a trend which might be of practical importance under some circumstances. Fig. 5 shows the effect of the CO_2/CO ratio on the solubility of silica at 1250°, 1300°, and 1350°C. The silica solubility at a given temperature decreases as the slag becomes more oxidizing, and the decrease is most rapid in the upper end of the range of p_{CO_2}/p_{CO} values. These results might be described by saying that on a weight basis ferric oxide is less effective than ferrous oxide as a flux for dissolving silica.

Thermodynamic Calculations

Calculations of Thermodynamic Activities: For calculation of equilibrium relationships in chemical reactions involving slags or slags with other phases, it is desirable to know how the activities of important slag components vary with composition. The experimental data of this investigation give in the p_{CO_2}/p_{CO} ratios a relatively direct measure of oxygen activity, and these ratios can be combined with established equilibrium data for the gas-phase reaction $CO + \frac{1}{2}O_2 = CO_2$ to calculate equilibrium values of oxygen pressure (p_{O_2}) for the slags studied. Also, for the experiments with silica-saturated slags, the activity of silica is known directly and is equal to unity if the standard state of silica is taken as pure solid silica (tridymite at the temperatures of this investigation). However, in addition to these directly determined activities, the data when combined with previously available data using standard thermodynamic relations also afford indirect determinations of the activities of other slag components, such as FeO and Fe. Table II gives the activities of various slag components at selected values of N_{FeO}/N_{SiO_2} calculated from the experimental data of this investigation as represented by the smoothed curve in Fig. 3. The activity data at 1300°C are also plotted in Fig. 6. The calculations are outlined in the following paragraphs.

Oxygen pressures (p_{O_2}) were calculated from the p_{CO_2}/p_{CO} ratios by the equation:

$$\log p_{O_2} = 2 \log (p_{CO_2}/p_{CO}) - \frac{29{,}270}{T} + 8.921 \quad [1]$$

This equation expresses the equilibrium conditions for the reaction $2CO + O_2 \rightarrow 2CO_2$ and is based on data selected by Darken and Gurry[7] (see footnote on p. 1402 of reference).

Activities of FeO were calculated by a Gibbs-Duhem integration. Taking the components of the slags as FeO, O, and SiO_2:

$$N_{FeO}\, d \log a_{FeO} + N_O\, d \log a_O + N_{SiO_2}\, d \log a_{SiO_2} = 0 \quad [2]$$

For silica-saturated slags a_{SiO_2} is constant, so $d \log a_{SiO_2} = 0$. Also, since a_O is proportional to p_{CO_2}/p_{CO}, $d \log a_O = d \log (p_{CO_2}/p_{CO})$. Applying these relations:

$$\int d \log a_{FeO} = -\int \frac{N_O}{N_{FeO}}\, d \log (p_{CO_2}/p_{CO}) \quad [3]$$

This integration is readily carried out graphically, the change in log a_{FeO} between any two values of p_{CO_2}/p_{CO} being found simply as the area under the curve of N_O/N_{FeO} plotted against log p_{CO_2}/p_{CO}. In the previous study of iron-saturated slags, the standard state for FeO at which $a_{FeO} = 1$ was taken as the pure Fe-O melt (0 pct SiO_2) in equilibrium with γ iron. On this basis it was found that a_{FeO} for slags saturated with both γ iron and silica was given by:[7]

$$\log a_{FeO} = \frac{300}{T} - 0.590 \quad [4]$$

This equation was used to evaluate a_{FeO} for the

Table II. Activities in Silica-Saturated Iron-Silicate Slags

$a_{SiO_2} = 1$ (tridymite)

Standard States:

$a_{FeO} = 1$ for pure Fe-O melt (0 pct SiO_2) in equilibrium with γ iron

$a_{Fe} = 1$ for γ iron

N_{FeO}/N_{SiO_2}	log p_{CO_2}/p_{CO}	p_{CO_2}/p_{CO}	log p_{O_2}	p_{O_2}, atm	log a_{FeO}	a_{FeO}	log a_O	a_O
				1250°C (1523°K)				
0.0061*	−0.818	0.152	−11.953	1.17×10^{-12}	−0.392	0.406	0	1.000
0.01	−0.35	0.447	−10.966	1.08×10^{-11}	−0.396	0.402	−0.469	0.340
0.02	0.17	1.479	−9.950	1.10×10^{-10}	−0.403	0.395	−0.986	0.103
0.03	0.55	3.55	−9.198	6.35×10^{-10}	−0.413	0.387	−1.386	0.0411
0.04	0.815	6.53	−8.668	2.15×10^{-9}	−0.422	0.378	−1.661	0.0218
0.06	1.21	16.22	−7.878	1.32×10^{-8}	−0.442	0.362	−2.075	0.0084
0.0901†	1.647	44.4	−7.004	9.9×10^{-8}	−0.476	0.334	−2.547	0.00284
				1300°C (1573°K)				
0.0058*	−0.879	0.132	−11.445	2.59×10^{-12}	−0.399	0.399	0	1.000
0.01	−0.35	0.447	−10.587	4.50×10^{-11}	−0.403	0.395	−0.532	0.294
0.02	0.17	1.479	−9.347	4.50×10^{-10}	−0.411	0.388	−1.060	0.087
0.03	0.55	3.55	−8.587	2.58×10^{-9}	−0.420	0.380	−1.449	0.0356
0.04	0.815	6.53	−8.057	8.76×10^{-9}	−0.430	0.372	−1.723	0.0189
0.06	1.21	16.22	−7.267	5.40×10^{-8}	−0.449	0.355	−2.138	0.0073
0.10	1.85	44.7	−6.387	4.10×10^{-7}	−0.484	0.328	−2.612	0.00244
0.122†	1.817	65.6	−6.053	8.85×10^{-7}	−0.502	0.315	−2.798	0.00159
				1350°C (1623°K)				
0.0057*	−0.935	0.116	−10.904	1.04×10^{-11}	−0.405	0.393	0	1.000
0.01	−0.35	0.447	−9.814	1.53×10^{-10}	−0.409	0.390	−0.589	0.258
0.02	0.17	1.479	−8.774	1.68×10^{-9}	−0.417	0.383	−1.117	0.076
0.03	0.55	3.55	−8.014	9.68×10^{-9}	−0.427	0.375	−1.507	0.0312
0.04	0.815	6.53	−7.484	3.28×10^{-8}	−0.436	0.367	−1.781	0.0166
0.06	1.21	16.22	−6.694	2.02×10^{-7}	−0.455	0.350	−2.196	0.0064
0.10	1.85	44.7	−5.814	1.53×10^{-6}	−0.496	0.320	−2.670	0.00214
0.148†	2.060	124.0	−4.928	1.18×10^{-5}	−0.543	0.285	−3.168	0.00068

* Slags saturated with γ iron.
† Slags saturated with magnetite.
‡ Atmospheres.

silica-saturated slags in equilibrium with γ iron, and the values thus obtained served as the starting points or lower limits for the integration of the data of the present investigation according to eq 3.

Activities of iron (a_{Fe}), referred to solid γ iron as a standard state, were calculated using the equilibrium constant for the reaction:

$$FeO\,(liquid) + CO = Fe\,(\gamma) + CO_2 \qquad [5]$$

From the previous paper on iron-saturated slags[7] the equilibrium constant for eq 5 is given by:

$$\log k = \frac{2640}{T} - 2.157 \qquad [6]$$

Thus, a_{FeO} was calculated from a_{Fe} and p_{CO_2}/p_{CO} by:

$$\log a_{FeO} = \log a_{Fe} - \log\left(\frac{p_{CO_2}}{p_{CO}}\right) + \frac{2640}{T} - 2.157 \qquad [7]$$

Free Energy of Formation of FeO. The experimental data of the present investigation afford an independent determination of the standard free energy of formation of FeO, from γ iron and oxygen, and this determination gives a good cross-check with the results of Darken and Gurry.[7] The measurements of oxygen activity over the composition range from γ iron saturation to magnetite saturation give, through the Gibbs-Duhem integration, values of a_{FeO} at magnetite saturation. The oxygen pressures (p_{O_2}) at magnetite saturation are calculated from the measured values of p_{CO_2}/p_{CO}. The activity of FeO (a_{FeO}) will be unity at magnetite saturation.*

* Actually, a_{FeO} referred to a standard state of pure solid FeO, will be slightly less than unity at magnetite saturation because the magnetite under these conditions would have a slight excess of oxygen compared to FeO.

Accordingly, for the reaction of formation of FeO:

$$3Fe\,(\gamma) + 2O_2 = Fe_3O_4\,(solid)$$

$$k = \frac{a_{Fe_3O_4}}{a^3_{Fe}\,p^2_{O_2}}, \text{ and}$$

$$\Delta F^\circ = -RT \ln k$$
$$= RT(\ln a_{Fe_3O_4} - 3 \ln a_{Fe} - 2 \ln p_{O_2})$$

In Table III, the values of ΔF° at 1250°, 1300°, and 1350°C calculated by this equation using data in Table II are compared with values of ΔF° calculated from the data of Darken and Gurry. The checks are quite satisfactory, especially considering the differences in experimental methods and the fact that one set of measurements was made on liquid slags containing silica while the other set was made on solid iron oxides in the absence of silica.

Summary

Equilibrium p_{CO_2}/p_{CO} ratios were determined experimentally for liquid iron-silicate slags in equilibrium with solid silica at temperatures from 1250° to 1350°C. Gas mixtures of varying CO_2-CO ratios were bubbled continuously through the liquid slag, and analyses of ingoing and outgoing gases were made to establish equilibrium. These silica-saturated slags ranged in composition from 30 to 40 wt pct SiO_2, balance iron oxides. The principal composition variable was the state of oxidation of the iron, and the FeO content varied from a minimum of about 0.8 wt pct for iron-saturated slags to a maximum of 14.5 wt pct and more for magnetite-saturated slags. The equilibrium values of p_{CO_2}/p_{CO} covered substantially a 1000-fold range, from 0.119 to 124.

Measurements of p_{CO_2}/p_{CO} ratios and slag compositions for the univariant equilibrium gas:slag:silica:γ iron checked well with the previously reported data of Schuhmann and Ensio. For the univariant equilibrium gas:slag:silica:magnetite, the measured p_{CO_2}/p_{CO} ratios were somewhat lower than those reported previously by Darken.

From the experimental data, calculations were made of the thermodynamic activities of FeO and Fe. Also, the data afforded a new determination of the free energy of formation of magnetite which checked with previous determinations of Darken and Gurry.

Table III. Standard Free Energy of Formation of Magnetite, Cal Per Mol

	1250°C	1300°C	1350°C
Present investigation	−150,890	−147,370	−143,780
Darken and Gurry	−150,440	−147,250	−143,620

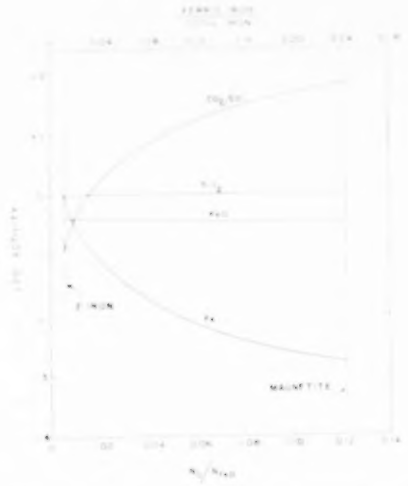

Fig. 6—Activity composition relations in silica saturated slags at 1300°C.

References

(1) R. Schuhmann, Jr.: A Survey of the Thermodynamics of Copper Smelting. *Trans.* AIME (1950) **188**, pp. 573-584; JOURNAL OF METALS (June 1950).

(2) R. Schuhmann, Jr., R. G. Powell, and E. J. Michal: Constitution of the FeO-Fe_2O_3-SiO$_2$ System at Slag-making Temperatures. Unpublished.

(3) R. Schuhmann, Jr., and P. J. Ensio: Thermodynamics of Iron-Silicate Slags: Slags Saturated with Gamma Iron. *Trans.* AIME (1951) **191**, pp. 401-411; JOURNAL OF METALS (May 1951).

(4) L. S. Darken and R. W. Gurry: The System Iron-Oxygen: II. Equilibrium and Thermodynamics of Liquid Oxide and Other Phases. *Journal* Amer. Chem. Soc. (1946) **68**, pp. 798-816.

(5) L. S. Darken: Melting Points of Iron Oxides on Silica; Phase Equilibria in the System Fe-Si-O as a Function of Gas Composition and Temperature. *Journal* Amer. Chem. Soc. (1948) **70**, pp. 2046-2053.

(6) L. S. Darken and R. W. Gurry: The System Iron-Oxygen. I. The Wustite Field and Related Equilibria. *Journal* Amer. Chem. Soc. (1945) **67**, pp. 1398-1412.

Deleading Zinc Concentrate

At the

Parral and Santa Barbara Mills

by C. L. Boeke and G. G. Gunther

THE zinc deleading processes at the Parral and Santa Barbara mills are described separately to provide a basis for comparison. Although the two procedures are fundamentally alike, there are some differences in application to meet specific conditions.

The Asarco mill at Parral in the State of Chihuahua is a flotation plant treating 1450 metric tons per day of complex sulphide copper-lead-zinc ores. In general, the procedure used for selective separation of the minerals into a copper, a lead, and a zinc concentrate follows the usual practice.

First, a bulk copper-lead concentrate is floated and then separated into a final copper and a final lead concentrate by the sulphurous acid process. A small tonnage of high grade gravity lead concentrate is tabled from the bulk copper-lead cleaner tailing before it is reground so as to avoid undesirable overgrinding and sliming of this portion of the lead mineral. Next, a zinc concentrate is floated from the lead rougher tailing and, as described later, is separated into a final lead product and a final zinc concentrate. Finally, the zinc rougher tailing receives a strong scavenger float to remove all recoverable middling values for regrinding and return to the flotation circuits. The slime is separated from the scavenger flotation product, and only the sand portion goes to the regrind section. The minerals in the separated slime are extremely resistant to all methods of selective separation and pose one of the major problems awaiting solution. Nevertheless, the slime shows a profit when mixed with either the lead or the zinc concentrate, except when metal prices are very low, so it is accepted as a final product for lack of a more profitable method of handling it. In contrast, the minerals in the reground sands of the

C. L. BOEKE, Member AIME, is Mill Superintendent, Cia. Minera Asarco, S. A., Parral, Chihuahua, Mex., and G. G. GUNTHER is Mill Superintendent, Cia. Minera Ascaro, S. A., Santa Barbara, Chihuahua, Mex.

Discussion on this paper, TP 3287BD, may be sent to AIME. Manuscript, August 27, 1951. Mexico City Meeting, October 1951. Los Angeles Meeting, February 1953.

Table I. Parral Mill Products—Second Quarter of 1951

Product	Assays, Grams		Assays, Pct					Recoveries, Crude Ore Content, Pct					
	Au	Ag	Pb	Cu	Zn	Fe	Insol	Au	Ag	Pb	Cu	Zn	Fe
a—Rich copper-lead flash	7.81	1804	40.7	12.0	4.5	11.2	1.6	45.5	66.0	68.9	74.3	4.6	19.6
b—Impure rich copper concentrate, flash	2.94	671	6.1	30.1	2.8	26.2	1.6	5.3	6.3	3.3	32.2	0.7	10.8
c—Impure rich lead concentrate, flash	0.37	2447	61.55	4.9	6.4	3.4	1.0	40.0	29.7	65.6	22.1	3.9	3.8
d—Lead-zinc-iron concentrate, flash	17.42	2296	31.4	1.3	3.9	4.2	0.7	2.9	2.0	2.7	0.2	0.1	0.2
e—Lead-zinc-iron concentrate, flash	7.30	1805	42.1	5.2	16.1	8.0	2.0	6.1	7.8	8.1	4.1	1.7	1.5
f—Lead-zinc concentrate, flash	6.86	2349	58.05	4.9	7.0	5.8	1.0	49.0	63.3	70.4	26.4	5.7	7.5
g—Total lead concentrate	2.80	810	7.0	1.1	19.5	10.6	12.0	4.1	3.3	2.3	1.6	3.6	6.3
h—Scavenger lead product, flash													
i—Lead-bulk lead concentrate													
j—Lead-zinc concentrate before deleading	7.43	1936	40.4	4.1	10.1	8.4	4.3	53.1	72.8	78.7	28.0	9.3	13.8
k—Zinc concentrate after deleading	1.67	274	4.5	1.2	52.8	5.5	5.4	18.7	16.9	12.1	13.6	79.9	14.9
l—Deleading agent													
m—Zinc concentrate, flash	1.24	156	1.6	0.9	55.3	5.3	3.5	13.6	9.1	4.6	9.5	78.2	13.4
n—Tailing, flash	0.26	21	0.57	0.1	0.83	2.5		28.0	11.8	14.0	10.3	11.8	62.0
								100	100	100	100	100	100

a—Flash and products b to e are combined in a thickener to form a single concentrate before filtering.

scavenger product are highly amenable to separation and recovery.

The assays and recoveries for the products removed in various stages from the Parral mill circuits are listed in Table I.

One deviation from ordinary procedure is the retreatment of the final zinc concentrate for the recovery of lead. This is accomplished by depressing the zinc minerals with cyanide and zinc sulphate and then refloating to remove a lead concentrate.

Certain characteristics of the minerals in the Parral mill feed make such a deleading process necessary and advantageous. The ore supply comes from various veins that contain minerals covering a wide range of floatability. In addition, the veins that supply the major part of the tonnage have been cut by a fault which created an extensive shattered zone in which the minerals are in various stages of alteration. As a consequence, the lead minerals in the mill feed include a large proportion of easily floated clean galena, mixed with more refractory and partially altered minerals, which do not float readily. The separation of lead from zinc is complicated further by the ever-present problem of the slimed minerals, which do not respond satisfactorily to the procedure that is best suited for selective recovery of the granular portion.

It is evident then that part of the lead mineral is readily floatable and can be separated easily and cleanly from the zinc, another part has the same degree of floatability as the zinc and requires special treatment for selective separation, while the remaining and most refractory part is less floatable than the zinc and can be recovered only by a strong scavenger flotation of the zinc circuit tailing.

Table II. Deleading of Zinc Concentrate at Parral Mill

Product	Zinc Conc, Grams, Pct	Assays, Grams		Assays, Pct			
		Au	Ag	Pb	Cu	Zn	Fe
Zinc concentrate	100.00	1.67	274	4.5	1.2	52.8	5.5
Lead-zinc concentrate before deleading	7.04	7.43	1936	42.9	4.2	10.3	8.9
Deleaded zinc concentrate	92.96	1.24	156	1.6	0.9	55.3	5.3
	Recoveries Based on Zinc Concentrate, Pct						
	Au	Ag	Pb	Cu	Zn		
Zinc concentrate	100.0	100.0	100.0	100.0	100.0		
Lead-zinc concentrate before deleading	31.0	49.4	67.0	36.0	2.2		
Deleaded zinc concentrate	69.0	50.6	33.0	64.1	97.8		

Such conditions preclude a reasonable recovery of the lead in a single flotation operation without floating an excessive amount of zinc. This led to experiments with a zinc concentrate deleading circuit in 1945, with such beneficial results that the procedure has been continued without interruption since that time. The advantages of the deleading process are as follows:

1—It simplifies the operation of the lead flotation circuit by making unnecessary any attempt to float the more refractory portion of the lead mineral at the expense of floating an excessive amount of zinc. Instead, a high grade lead concentrate low in zinc is floated, thereby dropping more of the zinc mineral into the lead circuit tailing for recovery in a zinc concentrate.

2—The lead mineral that floats in the zinc circuit has the same degree of floatability as the zinc mineral, and the segregation and treatment of minerals in the same restricted range of floatability favors a more effective separation. Even a slight deactivation of the zinc makes it less floatable than all of the lead mineral within this limited range. Such favorable conditions for separation cannot be established in the lead rougher circuit where the most refractory portion of the lead mineral is still present.

3—A high concentration of cyanide is used on the relatively small tonnage of zinc concentrate for maximum deactivation of the zinc, and it would not be economically permissible to use the same concentration of cyanide for the large tonnage in the lead rougher circuit to deactivate the zinc to the same degree. For example, 3.5 lb of cyanide and 2.0 lb of zinc sulphate per ton of zinc concentrate are used in the zinc deleading circuit at Parral, equal to 0.3 lb of cyanide and 0.2 lb of zinc sulphate per ton of crude ore mill feed. The high concentration of cyanide in the deleading circuit requires only one twelfth of the quantity that would be needed to establish the same concentration in the lead rougher circuit, and the cyanicides in that circuit make the cyanide less effective than when it is used on the clean zinc concentrate.

Cyanide and zinc sulphate are the only reagents used in the deleading circuit. The residual reagents in the feed to the circuit provide all the activation and froth needed to float the lead, but on occasions a small amount of alcohol frother is used to help carry the lead through the cleaner cells. Thickening and long conditioning were found to be detrimental to the separation, although some benefit is derived from a brief contact with cyanide and zinc sulphate

to permit their complete diffusion throughout the pulp before flotation. The feed has a slight natural alkalinity of pH 7.8, and experimental additions of lime have had no noticeable effect on the separation.

As shown in Table II, the deleading procedure recovers 67.0 pct of the lead content of the zinc concentrate with a loss of only 2.2 pct of the zinc content, and based on the crude ore mill feed, see Table I, this is equivalent to a recovery of 8.1 pct of the lead with a loss of only 1.7 pct of the zinc. The percentage of gold, silver, and copper removed with the lead makes the procedure still more desirable when the zinc concentrate is sold on a schedule that pays for the zinc content only.

Table III shows the percentage of crude ore lead content in the zinc concentrate before and after the zinc deleading circuit was placed in operation. During 1942, 1943, and 1944, when lead was recovered in a single step in the lead flotation circuit only, from 6.5 pct to 7 pct of the crude ore lead content remained in the zinc concentrate, and it could be kept at that point solely by floating from 12 pct to 13 pct of the crude ore zinc content with the lead concentrate. After the introduction of zinc deleading in 1945, the lead in the zinc concentrate gradually decreased to less than 4 pct of the crude ore content, with at the present time the inclusion of less than 10 pct of the crude ore zinc content in the combined lead products, see Table I. This represents a 2.5 pct increase in lead recovery in conjunction with a 2.5 pct decrease in zinc recovery in the lead concentrate, and at the same time, the zinc dropped from the lead concentrate improved the recovery in the zinc concentrate by an equal amount.

The concentrating plant of the Asarco's Santa Barbara unit is located near the village of Santa Barbara, which lies in the foothills of the Santa Barbara mountain range in the southcentral part of the State of Chihuahua at an elevation of 6300 ft. The prevailing rock in the district is shale which has been intruded by rhyolite and basalt dikes. This shale is cut by numerous veins that have been mined since early colonial times. The work of the Spaniards was limited to the oxide portion of the veins, which extends several hundred feet below the outcrops except in those areas where erosion has been excessive. At the present time, mining is confined to the deeper sulphide areas of the veins. Ores from five different mines make up the mill feed, and the principal minerals are lead, mainly occurring as galena, copper in the form of chalcopyrite and to some extent as chalcocite, and zinc as a marmatitic sphalerite, all associated with pyrite and some gold and silver in a siliceous gangue.

For a number of years, and till the middle of 1949, the flowsheet of the mill followed the conventional lines of most plants practicing selective flotation of lead and zinc. As additional features, this flowsheet included—and still includes—gravity concentration of the lead liberated in the primary grinding circuit, a lead-copper separation process by means of sulphurous acid, and a scavenger circuit following the zinc float.

In view of the fact that most of the Santa Barbara ores presently treated show varying degrees of alteration and oxidation of the mineral surfaces and, with few exceptions, cannot be classed as clean ores as regards selectivity and floatability of the lead and zinc constituents, they require strong flotation conditions in the lead circuit for optimum lead-copper recoveries and the subsequent production of a zinc concentrate of acceptable grade. It is obvious that this procedure tends to float a good deal of zinc into the lead concentrate, especially when the ore is very refractory. In the past, these zinc losses, and the resulting comparatively low grade lead concentrates, were tolerated as long as the value of the refractory lead recovered was greater than the value of the zinc that had to be taken into the lead concentrate and thus was lost as a pay product.

Table III. Crude Ore Lead Content in Zinc Concentrate After Zinc Deleading Circuit

Procedure	Year	Crude Ore Lead Content Remaining in Zinc Conc., Pct
Zinc concentrate, not deleaded	1942	6.5
	1943	7.0
	1944	6.7
Deleading started July 30th	1945	4.8
Zinc concentrate, deleading circuit in continuous operation	1946	4.3
	1947	4.1
	1948	4.3
	1949	3.9
	1950	3.6

Early in 1949, however, the amounts of refractory material in the various ores delivered to the mill increased to such an extent that it became more and more difficult to produce marketable lead and zinc concentrates and maintain recoveries. In spite of the customary strong flotation conditions in the lead circuit, a good deal of the lead and also copper dropped into the zinc section and floated there under the activating influence of the copper sulphate but to the detriment of the grade of the zinc concentrate produced. Attempts to retard this lead in the zinc circuit with potassium bichromate and to float it in the scavenger circuit were not successful. Therefore it was decided to try a deleading retreatment of the final zinc concentrate along the lines developed in the Parral mill. When it was possible to show that the lead could be floated away successfully from the zinc after the latter had been depressed with cyanide and zinc sulphate, this deleading operation became part of the regular flowsheet in July 1949. The immediate result of this procedure was a noticeable improvement in the zinc concentrate grade through the removal of considerable amounts of lead, copper, and iron minerals from the original zinc concentrate with relatively low losses of zinc in the refloat lead concentrate. In turn, the lead and copper values thus recovered and added to the original lead-copper concentrate correspondingly increased the recoveries in the lead and copper circuits.

As soon as the deleading operation had been firmly established, it became possible to change the conditions in the original lead float. Instead of attempting to recover as much lead as possible in the lead circuit, the operators were instructed to disregard the lead section tailings, to produce a high grade lead concentrate of minimum zinc content and to allow the refractory lead minerals to pass into the zinc circuit for their subsequent recovery in the refloat circuit.

The overall effect of the refloat operation and typical results obtained are shown in Table IV.

Table IV brings out the fact that the refloat operation not only produces a relatively high grade final zinc concentrate and a lead-copper concentrate of acceptable grade, but also recovers 84 pct of the total lead in the mill feed with a loss of only 2.1 pct of the total zinc. The value and effectiveness of the refloat circuit are thus clearly emphasized. At the same time assays of the zinc concentrate before the deleading reflect the operation of the original lead circuit and indicate the amounts of lead and copper that were allowed to drop into the zinc section. It is obvious that, without a deleading circuit, a zinc concentrate assaying 5.4 pct lead, 1.6 pct copper, and only 50.2 pct zinc would not be produced for financial reasons, even if such a concentrate were acceptable to the smelter, and that the lead circuit would be operated so as to produce a greater recovery of the lead and copper values, which naturally means a lower grade concentrate and a higher loss of zinc.

It is to be understood that the figures in Table IV represent average results only. It will be readily seen that the overall value of the entire refloat operation increases as the refractoriness of the ore treated increases, whereas with cleaner ores the results are less spectacular.

In the zinc deleading operation as practiced at Santa Barbara the primary zinc is double-cleaned in a ten-cell No. 24 Denver Sub-A machine, and then is pumped to an eight-cell No. 24 Denver Sub-A machine. A rougher lead concentrate is taken from cells No. 3, 4, 5, and 6 to be cleaned in No. 2 cell and recleaned in No. 1 cell. The rougher concentrate from the last two cells of the machine is returned to No. 4 cell. The double-cleaned lead concentrate joins the original lead-copper concentrate for further treatment in the lead-copper separation section, the tails of the machine constituting the final zinc concentrate.

Principal reagents added ahead of the pump are cyanide, zinc sulphate, and lime. Minor amounts of xanthate, cresylic acid, and of an alcohol frother are added at the machine as needed. Approximate reagent requirements per ton of primary zinc concentrate feed to the refloat section are: 2.3 lb cyanide, 4.4 lb zinc sulphate, 3.2 lb lime, 0.03 lb xanthate, and 0.01 lb each cresylic acid and Du Pont frother B-22.

Cost of operating the section, including reagents, power, and maintenance, amounts to approximately 9c to 10c per ton of crude ore milled.

Both cresylic acid in the rougher and alcohol frothers in the cleaner section have been found necessary and, if judiciously used, helpful. Obviously, overfrothing is to be avoided not only in the refloat circuit but also in the primary zinc rougher and

Table IV. Overall Effect of Refloat Operation and Typical Results

	Assays					
	Grams		Pct			
	Au	Ag	Pb	Cu	Zn	Fe
Zinc concentrate:						
Before deleading	1.2	294	5.4	1.6	50.2	7.5
After deleading	0.8	171	1.1	1.1	54.5	7.2
Refloat lead concentrate	4.6	1364	42.6	6.6	12.9	10.2

	Recoveries in Refloat Lead Concentrate, Pct					
	Au	Ag	Pb	Cu	Zn	Fe
Based on deleading section feed	31.0	46.4	67.0	30.5	2.2	10.3
Based on mill feed	6.1	7.8	8.1	4.1	1.7	1.5

Table V. Comparison of Parral and Santa Barbara Deleading Results

	Assays					
	Grams		Pct			
	Au	Ag	Pb	Cu	Zn	Fe
Zinc concentrate before deleading:						
Parral	1.7	274	4.5	1.2	52.6	5.5
Santa Barbara	1.2	294	5.4	1.6	50.2	7.5
Zinc concentrate after deleading:						
Parral	1.2	158	1.6	0.9	55.3	5.3
Santa Barbara	0.8	171	1.1	1.1	54.5	7.2
Lead concentrate from zinc concentrate:						
Parral	7.4	1005	42.8	5.2	16.3	8.0
Santa Barbara	4.6	1364	42.6	6.6	12.9	10.2

	Recoveries in Refloat Lead Concentrate, Pct					
	Au	Ag	Pb	Cu	Zn	Fe
Based on deleading section feed:						
Parral	31.0	46.4	67.0	30.5	2.2	10.3
Santa Barbara	39.6	47.9	81.4	38.7	2.6	14.0
Based on mill feed:						
Parral	6.1	7.8	8.1	4.1	1.7	1.5
Santa Barbara	2.9	6.6	6.4	6.7	2.1	2.4

cleaner section. The importance of the latter factor was demonstrated in the plant some time ago when Aerofloat No. 242 was tried in the zinc rougher float as a substitute for the standard xanthate collector. It was found that the frothing properties of this reagent, even if used in less than the necessary amounts, were so pronounced as to make the refloat circuit uncontrollable in a very short time.

pH Control

For reasons as yet unknown, the great amount of laboratory work done to study the effect of lime has, so far, failed to furnish the necessary data on which definite conclusions may be based, and a good deal more work will be required to answer the fundamental question as to whether lime should be used or not. Results obtained in the plant show that, without lime, the operation of the refloat section becomes rather unstable and erratic, a fact also borne out in some of the laboratory series where the absence of lime led to poor lead-copper recoveries because of a pronounced lack of selectivity. On the other hand, quite a few test series showed a normal float and an acceptable lead-zinc separation when no lime was used. Notwithstanding this erratic and as yet unexplained behavior of the different mill pulps tested, certain general trends resulting from the use of lime may be summarized as follows. Up to a pH value of 9 or 9.5, recoveries of lead and copper are better than those obtained at a pH value of 8 which is the natural pH of the primary circuit in the plant. As the pH value of the refloat is raised above 9.5, the floatability of the lead and copper begins to decrease, and in the case of the copper, sometimes so rapidly as to lead to a definite rejection. Zinc rejection improves as the pH value of the float increases. From the few data presented it is obvious that the use of lime in the refloat circuit is, if anything, critical, and requires a careful study and balancing of all the factors involved in each individual case.

A comparison of the Parral and Santa Barbara deleading results is shown in Table V.

The results obtained at Parral and Santa Barbara indicate that a zinc concentrate deleading process may be a valuable means of improving concentrate grades and recoveries wherever a poor lead-zinc selectivity poses a major metallurgical problem.

Chlorination of Zirconium Oxide

by W. W. Stephens and H. L. Gilbert

Production of anhydrous zirconium tetrachloride by direct chlorination of a zirconium oxide-carbon mixture in a silica-brick-lined chlorinator is described. Theory and thermodynamics of reactions are discussed. A pilot-model chlorinator and full-scale production equipment are described and operating data are included.

ANHYDROUS zirconium tetrachloride required as a starting material in the Kroll process for production of ductile zirconium has been produced in this country principally by chlorination of the carbide or "carbonitride" made by reduction of zircon sand concentrates with carbon in the arc furnace. This process and the equipment used have been fully described.[1] It is well known that zircon or baddeleyite ores may be chlorinated directly with chlorine in the presence of carbon, and this one-step approach would seem at first glance to be preferable to the two steps involved in the carbide-chloride operation. As previously discussed[1] considerations leading to adoption of the longer process were:

1—Chlorination of the carbide proceeds rapidly at temperatures below 500 C, whereas temperatures above 900 C were considered necessary for chlorination of zircon-carbon mixtures.

2—The highly exothermic nature of the carbide-chlorine reaction makes it self-sustaining, while heat must be supplied continuously in direct chlorination of the ore.

3—Silicon was thought to be chlorinated along with zirconium in the direct chlorination of zircon, leading to high chlorine consumption. In production of carbide in the arc furnace, silicon is driven off as silicon monoxide and does not enter the chlorinator.

4—For efficient direct chlorination, the ore must be finely ground and intimately mixed with carbon, and the mixture briquetted.

5—Direct chlorination requires a much larger chlorinator for a given production capacity than chlorination of carbide.

Recently it has become necessary to produce large quantities of zirconium metal from a chemically purified zirconium oxide. Since the cost of the latter is high, the relatively high losses encountered in production of carbide in the arc furnace could not be tolerated, and a graphite resistor furnace[2] was developed for production of carbide, which was then chlorinated in equipment previously used for chlorinating arc-furnace carbide. This method of operation was quite satisfactory, and losses in the carbiding step were minimized. However, operating costs were relatively high, and the process did not lend itself particularly well to large-scale operation because of the multiplicity of small units required and the hand labor needed to load, unload, and maintain the furnaces. To chlorinate the carbide, a vertical-shaft chlorinator was used in which the charge was heated with a central split graphite-rod resistor.[3] Operation of this chlorinator was somewhat less satisfactory with the resistor furnace carbide than it had been with the arc-furnace carbide due, principally, to the differences in physical properties of the carbide. The arc-furnace carbide is obtained as a fused metallic-appearing mass which can be crushed to $-\frac{1}{4}$ in. with production of a minimum of fines, whereas the resistor-furnace product is lightly sintered and produces a large proportion of fines in crushing and handling. These fines tend to pack in the chlorinator and promote channeling, which results in poor chlorine efficiency and low capacity. Data based on production of 22,000 lb of chloride from resistor-furnace carbide in this equipment are shown in Table I.

Table I. Production of Zirconium Tetrachloride from Resistor-Furnace Carbide

Product	Product Weight, Lb	Contained Zr, Lb	Recovery, Pct Zr	Recovery, Pct Cl
Input				
Zirconium carbide		10,970.4		
Chlorine	39,965			
Output				
$ZrCl_4$	22,075	8,640.0	78.80	43.8
Residues		1,839.5	16.75	
Losses		490.9	4.45	68.4

Average Zr content of residues = 48.84 pct
Average power consumption = 0.81 kw-hr per lb $ZrCl_4$

Necessity for increasing production of chloride from about 2,000 to 15,000 lb per week led to further investigation of possible methods for direct chlorination of the oxide or oxide-carbon mixtures. Direct chlorination of the pure oxide presents much less difficulty than chlorination of zircon sand or oxide ores. The oxide is easily ground to −200 mesh, and no silica is present to cause excessive consumption of chlorine or contamination of the product.

Theoretical Considerations

The principal chemical reactions involved in chlorination of mixtures of zirconium oxide and carbon may be written as follows:

$$\tfrac{1}{2}\,ZrO_2(c) + C(c) + Cl_2(g) = \tfrac{1}{2}\,ZrCl_4(g) + CO(g) \quad [1]$$

$$\tfrac{1}{2}\,ZrO_2(c) + CO(g) + Cl_2(g) = \tfrac{1}{2}\,ZrCl_4(g) + CO_2(g) \quad [2]$$

$$\tfrac{1}{2}\,ZrO_2(c) + \tfrac{1}{2}\,C(c) + Cl_2(g) = \tfrac{1}{2}\,ZrCl_4(g) + \tfrac{1}{2}\,CO_2(g) \quad [3]$$

W. W. STEPHENS, Member AIME, is Chief, Rare Metals Branch, Region II, and H. L. GILBERT is Chemical Engineer, Northwest Electrodevelopment Laboratory, U. S. Bureau of Mines, Albany, Oregon.

Discussion on this paper, TP 3332D, may be sent, 2 copies, to AIME by Sept. 1, 1952. Manuscript, Jan. 23, 1952. New York Meeting, February 1952.

Papers by authors of the U. S. Bureau of Mines staff are not subject to copyright.

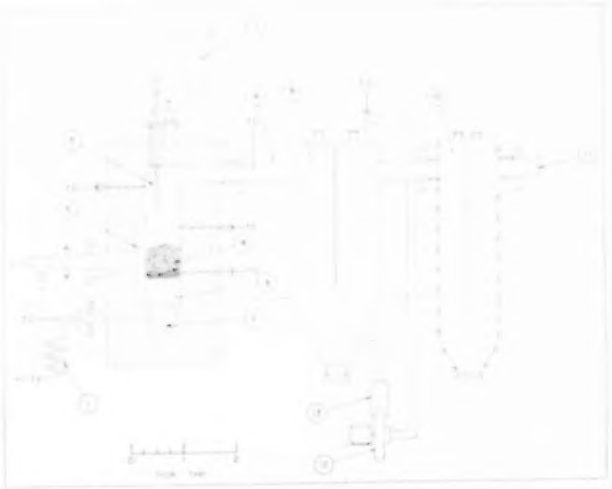

Fig. 1—Experimental chlorinator

TC—Thermocouple positions
1—Chlorine gas preheater
2—Charcoal diffuser bed
3—Resistor carbon
4—Charge of briquettes
5—Graphite electrode
6—Split graphite pipe top heater
7—Feed hopper
8—Nichrome heater for crossover pipe
9—Nickel lined condenser
10—Water cooled iron aftercondenser
11—Exhaust to scrubbers
12—Condenser heating air blower
13—Nichrome air heater

It may be seen that reaction 3 is the sum of reactions 1 and 2. The heats and free energies of reaction for these equations were calculated using the most recent data available[7] and are shown in Table II for the temperature range of 800° to 1400° K (527° to 1127° C). These data indicate that reaction 3 may be expected to predominate at low temperatures, while reaction 1 will predominate at high temperatures. In fact, as pointed out by Doerner,[7] the equilibrium of the reaction $C + CO_2 \rightleftharpoons 2CO$ determines the CO/CO_2 ratio in the reaction products, assuming the presence of excess carbon. Thus the CO reaction might be expected to predominate over the CO_2 reaction in a ratio of about 2:1 at 715° C and 99:1 at 1000° C. Although reactions 2 and 3 are more desirable than reaction 1 from the standpoint of heat requirements and carbon consumption, the extent to which they can be utilized is limited by practical considerations.

It was felt that the principal problem involved in the design of equipment for efficient, large scale chlorination would be to obtain even distribution of heat in the charge so as to utilize the full cross-sectional area of the bed for chlorination. The central split graphite-rod heating element used in the 12 in. ID chlorinator previously described[4] showed little promise as a method for heating larger equipment, and the problems involved in constructing and maintaining a multiple electrode furnace of this type were considered prohibitive. Heating of the charge by mixing oxygen with the chlorine fed to the chlorinator as practiced at the Leverkusen Works of the I. G. Farbenindustrie[5] was felt to be undesirable from the standpoint of increasing the volume of exhaust gas and leading to excessive carry-over of oxide and increased losses of chloride.

A shaft-type chlorinator in which the charge itself was used as a resistance-bed heating element appeared to have some promise of fulfilling the requirements. Measurements of the electrical resistance of a bed of briquettes made up of finely ground oxide and carbon black in the required proportions for chlorination showed this method of heating to be feasible.

Table II. Thermodynamic Data for Chlorination Reactions, Calories Per Gram-Mol

Temperature, °K	Reaction 1		Reaction 2		Reaction 3	
	H	F	H	F	H	F
800	56	23,612	41,229	−30,797	20,930	27,293
1000	513	29,437	41,285	−20,343	20,969	29,229
1200	1041	35,208	41,338	−26,363	21,190	31,383
1400	1598	40,908	41,349	−22,302	21,472	33,840

Pilot-Model Chlorinator

A pilot-model chlorinator was constructed as shown in Fig. 1, using a mild-steel shell lined with silica brick to form a vertical shaft, with an inside diameter of 8 in. and height of 40 in. Three graphite plates 3 in. wide x 18 in. high were embedded in the lining at 120° intervals to serve as electrodes, and power was supplied by a 37 kva, 3-phase, 60-cycle transformer having secondary voltages variable from 10 to 30 v.

Nickel was used for the chlorine inlet, the charging port, and the chloride discharge pipe. The condenser was made of light-gage nickel with an iron jacket, the space between the jacket and the inner shell being baffled for circulating the air used to maintain the proper condenser temperature. An aftercondenser of water-cooled iron was added to

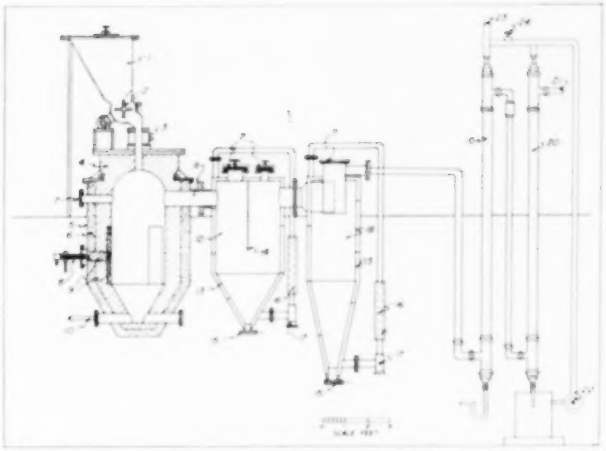

Fig. 2—Production chlorinator.

1—Feed hopper
2—Star valve feeder
3—Ball valve
4—Silica brick
5—Steel shell
6—Insulating brick
7—Clean out
8—Water-cooled copper electrode connector
9—Graphite electrode and nipple
10—Chlorine inlet pipe
11—Nickel cross-over pipe
12—Primary condenser
13—Condenser jacket
14—Baffle
15—Discharge valve
16—Air heater
17—Blower
18—Cyclone type aftercondenser
19—Water scrubbing tower
20—Caustic scrubbing tower
21—Exit gas outlet to stack
22—Caustic circulating pump
23—Waste water inlet
24—Caustic bleed line

minimize stack loss of chloride, which is troublesome in direct chlorination due to the presence of byproduct gas, principally carbon monoxide and carbon dioxide, which tends to sweep out fine particles of chloride.

To heat the upper part of the furnace shaft a small graphite resistor was installed. A chlorine gas preheater was made by coiling a length of thin wall ¼ in. nickel tubing into a helix and applying low voltage power to opposite ends of the tubing. A short coil of Nichrome resistance wire was wound on the exposed inlet to the nickel condenser to keep it free of chloride. Condenser heating-air temperature was maintained by a maze-type Nichrome-wire heater.

Waste gas was scrubbed in 4 in. diam pyrex glass towers packed for 48 in. with 1 in. porcelain Raschig rings. The first tower was supplied with waste cooling water from the chlorinator, while the second functioned with circulating 2 N sodium hydroxide solution.

Initial operating tests showed that the cold zirconium oxide-carbon briquettes did not conduct well enough to heat up rapidly, so a bed of ¼ in. mesh resistor carbon was incorporated in the heating plans.

In operation, the chlorinator shaft was first loaded through the charging port with ⅜ in. mesh softwood charcoal up to the lower end of the graphite electrodes. Next 2 to 4 in. of resistor carbon was tamped in. This was followed by a 12 to 14 in. depth of the 1 in. diam x ¼ in. thick briquettes of zirconium oxide-carbon mixture. Chlorine was admitted through the inlet at the lower end of the shaft to purge the chlorinator and condenser of air, and the electrical power turned on. Representative power inputs and temperatures attained in normal operation are given in Table III.

When the desired temperature was attained, chlorine flow was adjusted to 5 lb per hr, the metering of which was controlled by a flow gage. Immediate reaction was noted by an increase in the temperature of the top of the shaft and in the condenser. During active chlorination, the heat transferred to the condenser by condensing chloride made additional heating unnecessary, but a high volume of circulating air was maintained to prevent local overheating of the condenser. Chloride condensed with an indicated condenser-shell temperature of 180° C is dense, granular, and free-flowing, a highly desirable condition for subsequent operations.

In early runs, considerable difficulty was occasioned by disintegration of the briquettes in the charge, the resultant dust causing channeling of the chlorine and poor efficiencies. Furthermore, the oxide is quite abrasive, and briquetting in a conventional-type press resulted in rapid wear of punches and dies. Fortunately, a briquetting machine of the Belgian roll type was available, and the very hard, dense briquettes made with this equipment proved to be quite satisfactory. Briquettes made in this

Table III. Power Input and Temperatures Attained in Operating Pilot-Model Chlorinator

	Power, Kw	°C Temperature,
Chlorine preheater	0.25	200-300
Charge area	5.5	900-1150
Top of shaft	3.5	400-600
Cross-over pipe	0.5	400-500
Condenser air heater	2.0	180-200

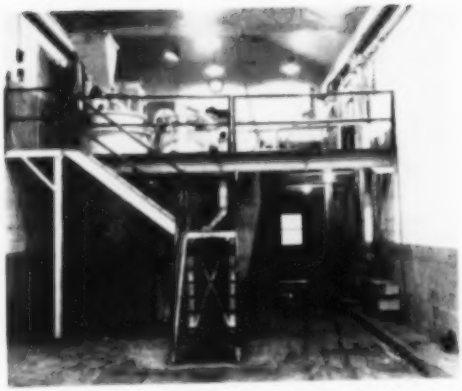

Fig. 3—Equipment installed in chlorination plant. Identification of equipment may be made by comparison with Fig. 2

manner were almond-shaped, with dimensions of approximately 1⅝x1x¾ in. It was found that continuous addition of briquettes to maintain a relatively shallow bed gave equal efficiency and much less channeling than when operating with a deep bed. Briquettes were added manually from a closed hopper connected to the top of the chlorinator by a section of 3½ in. diam rubber tubing, which permitted the operator to gage the amount being fed.

A number of test runs were made in this equipment under varying conditions. The results of these tests showed that 85 to 90 pct of the zirconium in the feed material could be recovered as chloride with reasonable chlorine utilization and capacities of approximately 17.5 lb of chloride per hr per sq ft of bed area. Best results were obtained with briquettes made up of 81 pct −200 mesh zirconium oxide, 15 pct −200 mesh carbon black, and 4 pct dextrine as a binder, with water added as required. It is to be noted that this amount of carbon considerably exceeds the stoichiometric amount required, even assuming that no carbon dioxide is formed. It has been shown several times, however, that lower carbon additions result in production of excessive amounts of white residues indicating a deficiency of carbon. Residual moisture in the briquettes and water formed by decomposition of the binder account for the oxidation of a portion of the excess carbon. Carbon dioxide formed in one area of the bed may react with carbon in higher temperature areas with the result that the charge in these areas may be deficient in carbon.

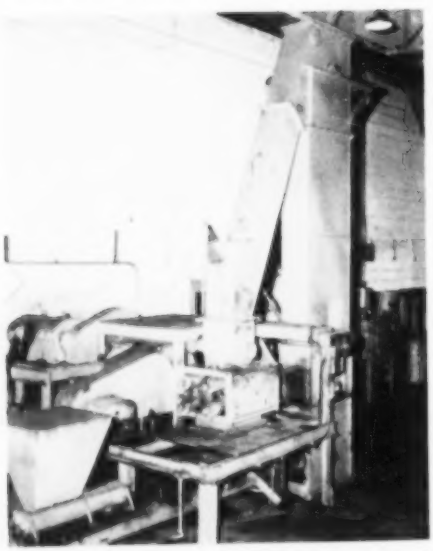

Fig. 4—Briquetting roll with automatic screening and recycling system

Full Scale Production Equipment

Based on the assumption that the capacity of this type of chlorinator should be proportional to the cross-sectional area of the bed within reasonable limits, a production plant was designed with two chlorinators each with a 26 in. bed diameter. Design of these chlorinators as shown in Fig. 2 follows closely that of the pilot model. The general layout of the two production chlorinators is shown in Fig. 3.

Principal differences from the pilot-model chlorinator lie in engineering improvements and modifications required by the greater size. Structural materials are predominantly the same. Briquettes are prepared in the same Belgian roll mentioned previously, with the addition of an automatic screening and recycling system as shown in Fig. 4 to break up, and return for rebriquetting, all briquettes that are not dense and hard. Briquettes are dried in a forced-draft electric drying oven. The finished product is shown in Fig. 5. A crew of two men can produce 2600 lb of briquettes in 8 hr.

Liquid chlorine is supplied from 1 ton cylinders to an electrically heated hot-water chlorine evaporator. All chlorine handling equipment except the short inlet section is of iron.

No charcoal or resistor carbon is employed in loading the large chlorinators. The prepared briquettes are added mechanically by means of a star valve on the closed hopper. The feeding tube and star valve are kept free of chloride by a continuous small flow of inert gas into the hopper. The rate of addition of briquettes is controlled to maintain the measured bed level below the bottom of the crossover pipe to the condenser. The feed hopper is easily reloaded with the chlorinator in operation by closing the ball valve below the feeder to prevent back flow of chloride through the hopper.

Power for each chlorinator is supplied by three 1000 amp welding transformers, feeding through tapped autotransformers which may be adjusted to apply 50 or 25 pct of the output voltage of the welding transformers to the chlorinator electrodes. Individual control of the power input to each electrode is obtained by varying the setting of the welding transformers, using remote controls on the operating panel.

The chlorine preheater, top heater, and condenser inlet heater used on the small scale chlorinator were found not to be required on the large equipment.

The condenser is constructed with an inner shell of $\frac{1}{8}$ in. nickel sheet. An outer shell of black iron forms a jacket through which air may be circulated for heating or cooling. One change required in operating on this scale was the installation of a cyclone-separator-type aftercondenser to minimize losses of chloride. This aftercondenser is also heated by cir-

culating hot air in the space between the steel outer shell and nickel inner shell.

Gas scrubbing is accomplished in two 6 in. diam pyrex glass towers packed for 8 ft with 1 in. Raschig rings. The use of waste water alone for preliminary scrubbing resulted in damage to the sewer system, and a continuous stream of dilute sodium hydroxide solution from an 8000-gal storage tank is now fed to both scrubbing towers.

Operating Data

Briquettes for chlorinator feed are made up from a mix containing 81 pct calcined zirconium oxide, 14.5 pct channel black, and 4.5 pct sucrose. The oxide is pulverized to 97 pct through 200 mesh in a swing-hammer pulverizer and mixed with the sucrose in a ribbon mixer. Water in the amount of 1.5 liters per 100 lb of dry mix is added, and the carbon is blended into the damp mix. This mix is aged for 24 hr to permit the moisture to diffuse and then briquetted. Briquettes are dried at 140°C.

The oxide used has an average zirconium content of 70 pct. The principal impurity is carbon. The channel black contains approximately 92 pct fixed carbon and 8 pct volatile matter.

Operating data for a typical month's operation of one chlorinator are given in Table IV.

Comparison with data given in Table I for chlorination of the resistor-furnace carbide indicates a considerable advantage to the direct chlorination operation. Actually, chlorination of the carbide probably could be carried out in the new chlorinators with efficiencies at least as high as for the oxide-carbon briquettes under suitable operating conditions, and somewhat higher rates of production might be attained. The principal advantage of direct chlorination lies in elimination of the carbiding step, with its relatively expensive equipment and high operating costs. It is estimated that operating costs for direct chlorination will be less than half of those for a carbide and chlorination operation of comparable capacity.

Direct chlorination in a silica-brick-lined shaft furnace does not cause undue attack upon the brickwork, probably because of the limited contact of the brickwork with carbon. The small amount of silicon tetrachloride produced is not condensed in the heated condenser but passes to the scrubbing towers.

Table IV. Operating Data, Large-Scale Chlorinator

Product	Product Weight, lb	Contained Zr, lb	Recovery, Pct Zr	Cl
Input				
Briquettes	27,654	15,696		
Zirconium sponge*	399	399		
Chlorine	31,000			
Total input		16,095		
Output				
Zirconium tetrachloride	37,962	14,858	92.3	74.7
Residues	1,527	717	4.5	
Chlorination loss		520	3.2	25.3
Total output		16,095	100.0	100.0

Power consumption: 1.58 kw-hr per lb $ZrCl_4$.
Direct operating personnel: 2 men per shift
(1 operator, 1 helper)
Normal rate of chlorine addition per chlorinator: 45 to 50 lb per hr
Operating temperatures, °C:

Chlorinator	
Lower zone	500–900
Middle zone	400–600
Upper zone	350–500
Condenser	150–200
After condenser	100–150

* Scrap sponge being recycled; not essential to direct chlorination.

Fig. 5—Briquettes of zirconium oxide-carbon mixture ready for chlorination.

No difficulty has been experienced in grinding the zirconium oxide to the fineness required for direct chlorination.

The size of our present chlorinators is not prohibitive, although the floor space required is greater than would be required for carbide chlorinators if the space for the carbide furnaces is not considered.

Acknowledgment

This paper is a report of one of the investigations carried out by the Rare Metals Branch, Bureau of Mines, Region II, Albany, Oregon, under the supervision of S. M. Shelton, Regional Director. The authors wish to make special acknowledgment of the services of Irwin J. Groce who was responsible for construction and operation of the pilot-model chlorinators and construction of the large-scale equipment and William F. Hergert under whose direction the large-scale equipment has been operated.

References

1. W. J. Kroll, A. W. Schlechten, and L. A. Yerkes: Ductile Zirconium from Zircon Sand. *Trans.* Electrochem. Soc. (1946) **89**, pp. 263-276.

2. W. J. Kroll, A. W. Schlechten, W. R. Carmody, L. A. Yerkes, H. P. Holmes, and H. L. Gilbert: Recent Progress in the Metallurgy of Malleable Zirconium. *Trans.* Electrochem. Soc. (1947) **92**, pp. 99-113.

3. W. J. Kroll, C. T. Anderson, H. P. Holmes, L. A. Yerkes, and H. L. Gilbert: Large Scale Laboratory Production of Ductile Zirconium. *Journal* Electrochem. Soc. (1948) **94**, No. 1, pp. 1-20.

4. W. J. Kroll, W. W. Stephens, and H. P. Holmes: Production of Malleable Zirconium on a Pilot-Plant Scale. *Trans.* AIME (1950) **188**, pp. 1445-1453; JOURNAL OF METALS (December 1950).

5. W. J. Kroll, W. W. Stephens, and J. P. Walsted: Graphite-Rod Hairpin-Resistor Reduction Furnace for High Temperatures. *Trans.* AIME (1950) **188**, pp. 1394-1395; JOURNAL OF METALS (November 1950).

6. All data for CO, CO_2, O_2, and Cl_2 as well as $\Delta H^\circ_{298.16}$ for ZrO(c) and $ZrCl_4$(c) from *Selected Values of Chemical Thermodynamic Properties*. Nat. Bur. Standards.

7. H°_T-$H^\circ_{298.16}$ and S°_T-$S^\circ_{298.16}$ for Zr(c) and ZrO_2(c) from Coughlin and King: *Journal* Amer. Chem. Soc. **72**, pp. 2262-2265.

8. H°_T-$H^\circ_{298.16}$ and S°_T-$S^\circ_{298.16}$ for $ZrCl_4$(g) calculated by K. K. Kelley, Chief, Minerals Thermodynamics Branch, Region III, Bureau of Mines, Berkeley, Calif.

9. H. A. Doerner, and W. F. Holbrook: Chlorination of Magnesia. U. S. Bur. Mines *R. I.* 3833 (December 1945) p. 12.

10. Ford H. McBerty: Anhydrous Chlorides Manufacture. F.I.A.T. Final Report No. 774 (1946) pp. 15-18.

Observations on Nodular Graphite

By H. M. Weld, R. L. Cunningham, and F. W. C. Boswell

Chemical analysis shows the partition of the magnesium addition between the metal and the graphite is independent of whether the graphite is in the form of nodules or flakes. The bright central spot observed in nodular graphite polished sections is shown to be due to the structure of the nodules.

DURING the past few years numerous papers have been published on the production[1] and heat treatment[2] of nodular cast irons. However, very little information is available on the structure of the nodules and the reason for their formation. It would appear that an explanation of the phenomenon of nodulation must await a detailed knowledge of the nature of the nodule. Disagreement exists among various workers on such a fundamental point as to whether or not a nodule actually contains a macroscopically visible, nongraphitic nucleus.[3-5] Work was initiated with a view to obtaining definite information on this and other aspects of the problem.

Chemical Separation and Analysis

Microscopic appearance had indicated[3] that a nongraphitic core might exist in nodules (Fig. 1). It appeared that a chemical comparison of separated nodules and flake graphite would be profitable, for if the core is nongraphitic a relatively large amount of certain elements would be found in the nodules as compared to the flake. This comparison could best be made by obtaining nodules and flake from the same melt of cast iron, part of which had been inoculated with a suitable addition reagent for the formation of nodules.

A 300 lb melt was produced. About half of this was inoculated in the ladle with an Fe-Si-Mg alloy to produce nodules and cast into keel blocks; the remaining half of the melt had silicon added in an effort to compensate for the silicon in the inoculant used in the other half of the melt and this was cast into similar keel blocks. The analyses of the resultant irons are given in Table I.

Nodules and flake were chemically extracted from 2 kg samples of metal as described in the appendix.

H. M. WELD, R. L. CUNNINGHAM, and F. W. C. BOSWELL are Physical Metallurgists, Mines Branch, Department of Mines and Technical Surveys, Ottawa, Ont., Canada.

Discussion on this paper, TP 3271E, may be sent, 2 copies, to AIME by Dec. 1, 1952. Manuscript, Oct. 2, 1951. Philadelphia Meeting, October 1952.

Published by permission of the Director General of Scientific Services, Department of Mines and Technical Surveys, Ottawa.

Table I. Analyses of Nodular and Gray Cast Iron

Element	Nodular Iron, Pct	Gray Cast Iron, Pct
C	3.16	3.36
Si	2.29	3.24
Mn	0.43	0.43
S	0.001	0.043
P	0.023	0.024
Mg	0.051	0.00025†
Ti*	0.011	0.008
Al*	0.055	0.048
Cr*	0.025	0.020
V*	0.004	0.004
Ni*	0.030	0.042
Cu*	0.09	0.10
Mo*	0.010	0.007
Sn*	0.013	0.013

* Determined by spectrographic analysis. In all, some 58 elements were checked.

† Estimated spectroscopically to be approximately 1/200 that found in nodular iron.

While this method dissolved the iron and chromium carbides, it did not dissolve the titanium, vanadium, and molybdenum carbides. These latter carbides could have been removed by nitric acid, but in other experiments it was found that it attacked pools of metallic iron entrapped in the nodules which had, until the nitric acid treatment, been protected from the attack of the sulphuric, hydrochloric, and hydrofluoric acids. It will be shown in the next section that entrapped iron exists in nodules but not in flake.

On microscopic examination many tiny irregular particles were observed to accompany both the nodules and the flake. These were identified by tabling a sample of nodules from which a sufficient fraction was obtained for X-ray analysis. A good pattern of titanium carbide was obtained indicating that this was the predominant compound present.

Since it was not possible to determine how completely the carbides could be removed mechanically and since their removal from flake is much more difficult, it was decided not to resort to any separation as this would render further comparisons more difficult. The samples were ashed in a combustion

boat, in an atmosphere of oxygen. The analyses and other pertinent data are given in Table II, from which it will be observed that titanium, vanadium, and molybdenum, whose carbides were not dissolved in the extraction process, were found in large quantities in the ash. Since magnetic measurements (to be discussed in the next section) showed that neither nodules nor flake contained any measurable amount of iron carbide, it is assumed that carbides of these other three elements did not exist to any extent within the graphite. Hence the data on these elements cannot be used to estimate the relative amounts within the different forms of graphite.

Where the recovery ratio is unity it indicates no preferred concentration of the element in either form of graphite. Hence any element whose ratio is near 1.0 would not be expected to be responsible for the differences in the formation.

It is shown in the next section that metallic iron is randomly trapped by the growing nodules only, thus accounting for the large iron ratio presented in Table III. As this iron contains the same proportion of silicon as the original melt, it is possible to correct the silicon recovery ratio to exclude this amount. The ratio for silicon then becomes 1.27. It is now seen that the recovery ratios for silicon, aluminum, tin, and chromium have a value of 1.0 within the limit of experimental error.

Likewise the manganese is partly tied up in inclusions of manganese sulphide which would be lost during the extraction and cleaning. The loss is only appreciable in the case of the gray cast iron which has 45 times as much sulphur as the nodular iron. The effect of this upon the recovery ratio has been to reduce it from 0.55 ±0.6 to 0.45 ±0.06.

For manganese and copper the ratios are 0.45 and 0.3, respectively, being significantly less than 1.0 and thus indicating a relative concentration of the sulphide-forming elements in the flake. The nickel ratio, 8.4 ±3.3, shows a relative concentration of this element in the nodules as compared to flake. However, the amount of nickel present is not sufficient to form microscopically visible nuclei. The nickel ratio suggests, however, that a nickel compound may serve as a submicroscopic nucleating agent.

From the recovery ratio of iron and the amount of iron recovered in the nodules it would at first appear from analytical data that either iron or an iron-rich compound comprised the nucleus. That this was not the case is demonstrated by work to be described in the next section.

Table II. Data on Samples

	Nodular Iron	Gray Cast Iron
Weight of metal	2650 g	2125 g
Weight of extracted sample	66.6 g (3.07 pct)	66.7 g (3.14 pct)
Weight of ashed sample	1.105 g (0.054 pct)	0.394 g (0.018 pct)

Analyses of Ash

Element	From Nodular Iron, Pct	From Gray Cast Iron, Pct
Fe_2O_3	40.5	7.74
SiO_2	3.56	5.85
MnO	0.39	2.00
S		
P	Trace	Faint trace
MgO	2.45	0.02*
TiO_2	32.3	58.4
Al_2O_3	0.88	2.22
Cr_2O_3	0.46	1.00
V_2O_5	3.25	3.62
Ni	0.020*	0.010*
CuO	0.46	4.58
MoO_3	3.90	4.65
Sn	0.2*	0.48*
B	Trace*	Trace*

* Indicates analysis by spectroscopy.

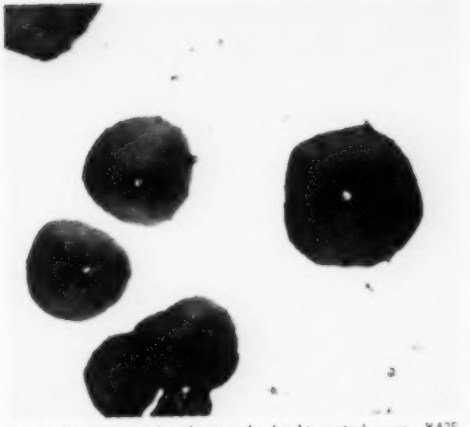

Fig. 1—Graphite nodules showing the bright central cores. X425.

Magnetic Properties of Nodules and Flake

During the course of a previous investigation in these laboratories it was found[2] that nodules extracted from nodular cast iron were feebly attracted by a magnet, whereas graphite flake extracted from commercial cast iron did not appear to be. It was decided to investigate the cause of this difference in behavior and to see if it was related to the formation of nodules. To obtain information on this magnetic material, advantage was taken of the fact that ferromagnetic substances possess a characteristic temperature at which their ferromagnetism disappears. This is commonly known as the Curie point.

A magnetic balance of the translation-bar type, equipped with a furnace, was constructed which was sufficiently sensitive to make possible the determination of the Curie points of the ferromagnetic material or materials in the degree of dilution in which they occurred in the nodules. In this instrument the force on the sample due to the interaction with the magnetic field is balanced by an opposing

Table III. Recovery of Elements from Nodules and Flake by Ashing (Based on the Analysis of the Two Cast Irons)

Element	From Nodular Iron, Pct	From Gray Cast Iron, Pct	Recovery Ratio: Nodules/Flake
Fe	0.016	0.001	16±2
Si (total)	0.037	0.016	2.30
Si (less amount dissolved in entrapped iron)			1.27±0.2
Mn	0.037	0.082	0.45±0.06
Mg	1.481	1.12	1.32±0.6*
Al	0.375	0.454	0.8±0.2*
Cr	0.686	0.643	1.0±0.25*
Ni	0.0360	0.0045	8.4±3.3†
Cu	0.219	0.675	0.3±0.1*
Sn	1.220	0.676	1.8±0.8†

* One spectrographic and one chemical analysis compared.
† Two spectrographic analyses compared.
‡ The estimation of error is based on the assumption that individual chemical analysis can be in error by 5 pct and that the spectrographic ratios for low concentrations on the same type of sample can be in error by 20 pct.

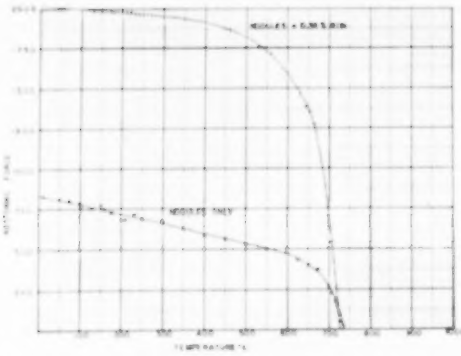

Fig. 2—Comparison of the magnetic properties of nodules and nodules plus 0.36 pct Fe. The presence of only one Curie point indicates that metallic iron is the only ferromagnetic substance present in the nodules.

force existing between a coil mounted on the beam and a fixed coil.

A sample of separated and cleaned nodules was placed in the specimen holder and the restoring current recorded as the temperature was slowly raised. A curve was obtained which showed no inflections up to about 700 C at which point it fell rapidly and approached zero. Because of the difficulty of obtaining an accurate temperature measurement of the sample on the balance beam, another sample was prepared by the addition of 0.36 pct of electrolytic powdered iron as an internal standard. As before only one Curie point was found, thus indicating that metallic iron was the only ferromagnetic material originally present in the sample. A comparison of the nodules before and after the addition of iron is shown in Fig. 2.

From the chemical analysis of ashed nodules, in which iron was reported as Fe_2O_3, the maximum amount of metallic iron that could be present in the nodules was calculated. A synthetic mixture of electrolytic iron powder and corn flour containing about the same proportion of free iron as that calculated for the nodules was made up. Magnetic measurements showed the restoring force to be about twice that found for the nodules. However, flake which contained about half as much iron showed no magnetic effect. The data is reported in Table IV. This would indicate in the nodules that either the particle size of the iron or the composition of the iron is sufficiently different from the electrolytic iron to cause this factor of two in magnetic properties, or else it may be concluded that a portion of the iron is contained in a nonmagnetic compound. Evidence for this latter suggestion comes from the fact that the flake which contains an appreciable amount of iron shows no ferromagnetic effect, in which case it must be concluded that the iron is all combined in a nonmagnetic compound. If a nonmagnetic iron compound exists in flake, then it seems reasonable to assume that some can also exist in the nodules. There may, of course, be a combination of the effects noted above.

Table IV. Results of Magnetic Measurements

Material	Weight G	Restoring Force (Arbitrary Units)	Restoring Force for 0.1250 G Sample (Arbitrary Units)
Nodule (Fe 0.467 pct)	0.1201	784	708
Core Flour (~ 0.48 pct Fe)	0.0960	1630	1435
Flake (Fe 0.241 pct)	0.0288	0	0

An attempt was made to determine the distribution of the iron in the nodules by the magnetic colloid technique. Separated nodules were mounted in lucite and polished. A drop of magnetic colloid was placed on the sample and covered with a glass cover slip. The sample was then mounted on a microscope, using an oil immersion lens, and a magnet was brought near the sample. It was found that over some of the nodules the magnetic power gathered in one or more minute clusters. When the magnetic field was removed, the powder would disperse but would gather to form the same pattern when the field was reapplied. The important fact was that the centers about which the magnetic powder gathered were distributed at random throughout the nodule and were not particularly associated with the central spot or the periphery. In view of the above evidence the difference in the magnetic properties of nodules and flake graphite cannot be interpreted as evidence for the existence of a nongraphitic core in the nodules. The ferromagnetic material in the nodules has probably been occluded in the nodules during the growth process.

Since the possibility existed that ferromagnetic particles might have been embedded in the surface of the nodules during the polishing process, a similar experiment was carried out using flake graphite. There was no evidence of magnetic inclusions. Further discussion of the above results will be given in a later section of the paper.

Microscopic Observations and the Central Spot

It is well known that if a polished surface of nodular graphite cast iron is examined in the light microscope, a small whitish central spot can be seen in many of the nodules. It has been suggested that this spot may be due to a nongraphitic core or nucleus in the graphite nodule.[1]

The electron microscope investigation of the nodules was originally undertaken in order to study the structure of this central spot in greater detail, and also to study its behavior under chemical attack. The nodules were studied using polystyrene-silica replicas, and it was found in agreement with other investigators that the nodules possessed a characteristic fine structure, except for the central spot which appeared as a relatively smooth, flat surface, usually with some evidence of fine-scale flaking, Fig. 3. Generally the boundary of this central area was indistinct, although occasionally the boundary was a reasonably well-defined polygon. The fact that a smooth central spot shows up in the electron micrographs has been interpreted[2,3] as evidence for a nongraphitic core. Other workers[4] have suggested that the spot may be due to the slip characteristics of the graphite and the structure of the nodule.

It appeared that this question could be finally settled by geometrical considerations, since if a core actually exists it is reasonable to assume that the proportion of nodules in a polished surface with exposed cores is very nearly equal to the ratio of the diameter of the core to that of the nodule. This is based on the assumption of nodules of uniform size,

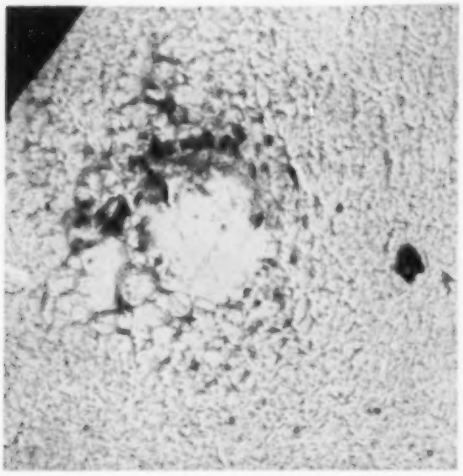

Fig. 3—Electron micrograph showing smooth central spot of nodule. X4500. Area reduced approximately 50 pct for reproduction.

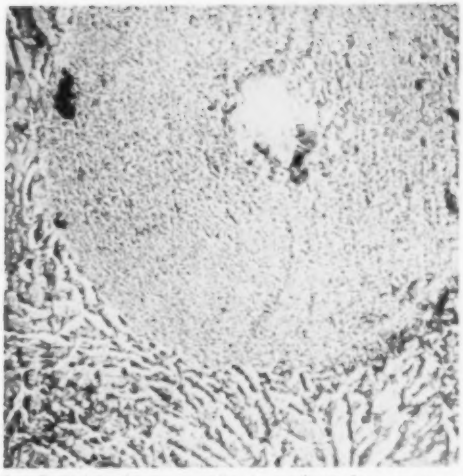

Fig. 5—Nodule showing variation in roughness from center to periphery. Electron micrograph. X1500. Area reduced approximately 50 pct for reproduction.

but the size distribution found in practice[4] would not seriously affect the conclusions.

Counts on several carefully polished samples indicate that about 60 pct or more of the nodules show a central spot, although in a poorly polished sample this figure may be much lower. Thus if the central spot is due to a nongraphitic core, it would be expected that the diameter of the core would be about 60 pct of the diameter of the nodule and the ratio of the average diameter of the visible spots to that of the nodules would be about 50 pct. Measurements of a large number of nodules having central spots showed the average core diameter to be only about 10 pct of the diameter of the nodules. This 5:1 disagreement shows that the assumption that the central visible spot is due to a real core of nongraphitic material is untenable. While the figures given will vary somewhat from specimen to specimen, the variations are insufficient to conceal the noted discrepancy.

Interpretation of Electron Micrographs

It has been known for some time, as a result of microscopic examination under polarized light, that nodules possess a radially symmetric structure.[3] Recent X-ray work[4] has verified that a nodule consists of a number of graphite crystallites, each slightly misaligned with respect to its neighbors and with its basal plane perpendicular to the radius which roughly passes through its base. With this model in mind many features of the microscopic observations can be explained.

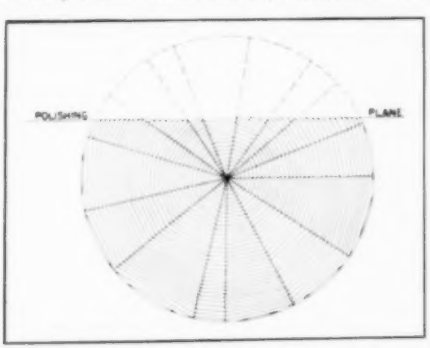

Fig. 4—Diagrammatic sketch indicating variation in surface structure across a polished section of a nodule due to the orientations of the radial crystallites.

If, during polishing, a nodule is sectioned between the periphery and the center, then the crystallite near the center of the section will have its basal plane nearly parallel to the polishing direction, but the surrounding crystallites will have their basal planes more sharply inclined to the surface, Fig. 4. It is a well-known property of graphite that the binding in the basal planes is very strong, while the binding between basal planes is weak. Thus during polishing it is believed that the graphite of the central crystallite is removed in flakes leaving a relatively smooth surface, while the surrounding graphite will be inclined to the polished surface and hence will be broken away in small chips leaving a relatively rough surface surrounding the central spot.

If a nodule is sectioned exactly through its center, all the graphite in the polished surface of the nodule would be oriented with basal planes perpendicular to the polished surface, and a uniform nodule should appear with no apparent "core." However, nodules which do not possess a smooth central spot occur more frequently than can be accounted for by this effect alone. It is possible that nodules built up of relatively few crystallites also may be polished so that no central spot is visible, even though they are not sectioned through the center. The reason for this lies in the fact that the angle between the basal plane of a crystallite and the polishing plane must be small if the surface of the crystallite is to be slipped off in flakes. As the number of crystallites making up a nodule decreases, the probability that the basal planes of one of the crystallites will make a sufficiently small angle with the surface to allow slip also decreases. Thus a nodule composed of a few large crystallites will often be polished so that no smooth central spot appears.

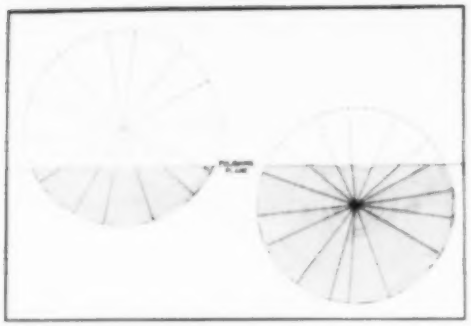

a b

Fig. 6—In case a, a flake can be removed smoothly from the central spot whereas in case b, a flake can be removed only with considerable disruption taking place at its edges.

From numerous observations it is believed that the maximum roughness is obtained when the angle between the basal planes and the surface is somewhat less than 45°. Thus in a nodule cut near the center a small smooth central spot is exposed, surrounded by a rough area which is in turn surrounded by a somewhat smoother one. This effect is sometimes observed, Fig. 5.

It may be noted that if the polishing plane cuts the nodules so that less than half of the sphere is left embedded in the iron, then the crystallites surrounding the central crystallite will have their basal planes so inclined to the polished surface that a flake can be removed from the central crystallite with a minimum of disturbance at its boundary, Fig. 6a. On the other hand if more than half of the nodule, Fig. 6b, is embedded the adjacent crystallites will tend to impede the slip of the basal plane of the central crystallite. This effect may account for the great variation observed in the amount of disturbance at the boundary of the smooth central area.

It is well known that the central spot shows up in light micrographs as a grayish-white spot considerably brighter than the surrounding graphite. This is believed to be due to the fact that the smooth central area reflects a considerable amount of light into the objective, whereas light incident on the surrounding slightly roughened graphite is largely scattered away from the objective lens.

The fact that scratches in a polished section are not observed to pass through the central spot has been taken as evidence that the central spot was due to the presence of a very hard nongraphitic material.[10] However, it is now believed that a scratch-forming piece of abrasive would merely remove a flake of graphite from the central crystallite rather than cut a scratch across the smooth area.

It has been observed[11] that generally larger cores were to be found in the smaller nodules in a given sample. This is to be expected on the basis of the model we have used since, when a nodule is sectioned near the periphery, the apparent diameter will be small while the "core" diameter will be near its maximum value for that nodule.

Although the smooth central spot often observed in nodules is in no way connected with a crystallization nucleus, it is possible that an invisible nongraphitic nucleus may exist. If it exists, it must be very small (< 0.5 microns diameter).

Conclusions

1—Metallic iron is randomly entrapped during the growth of nodules.

2—Flake and probably nodules contain a nonferromagnetic iron compound.

3—Aside from the entrapped iron there appears to be no element in sufficient quantity to account for a visible nucleus. However, this metallic iron is not associated with the central position.

4—Manganese and copper are relatively concentrated in flake graphite.

5—It is still possible that a submicroscopic nongraphitic crystallization nucleus exists in the nodule. Chemical evidence suggests a nickel compound.

6—Both the light and electron microscope appearance of nodules in polished section has been interpreted as due to the structure of the nodule and the anisotropy of graphite.

Acknowledgments

The authors are indebted to J. E. Rehder and staff for producing the samples of nodular and commercial cast iron, and for many helpful discussions of the problem, to J. A. Fournier and staff for the development of the methods for the extraction and cleaning of the graphite and for the various chemical analyses, and to the staff of the spectrographic laboratory.

Appendix
Extraction of Nodules and Flake from Nodular and Commercial Cast Iron

For extraction each batch consists of approximately 100 g of iron, cut into thin disks and placed in 300 cc of 2.5 normal sulphuric acid. When reaction has ceased, the solution and graphite are decanted, the remaining iron washed free of salts and the procedure repeated with fresh acid until all the iron has been dissolved.

As the graphite has a tendency to float, it is convenient to siphon off the clear solution of iron sulphate.

It is then twice treated with hydrofluoric acid to remove silica. This is followed by a treatment with hydrochloric acid to insure solution of any residual iron that may have been held by the silica. The residue is then filtered and washed free of acid and, as a precaution, it is, as required, treated with a mixture of hydrochloric and hydrofluoric acids and finally washed and dried at 100°C.

References

[1] H. Morrogh and W. J. Williams: *Journal* Iron and Steel Inst. (1949) **158**, p. 306.

[2] H. Morrogh and W. J. Williams: *Iron and Steel* (1948) **21**, p. 208.

[3] E. T. Myskowski and R. P. Dunphy: *Foundry* (1949) **77**, p. 72.

[4] C. K. Donoho: *American Foundryman* (February 1949) **15**, p. 30.

[5] D. Reese and P. Gagniben: *Foundry* (1949) **77**, p. 172.

[6] J. E. Rehder: *Canadian Metals* (May 1950) **13**, p. 16.

[7] J. E. Rehder: *Canadian Metals* (June 1950) **13**, p. 16.

[8] J. E. Rehder: *Trans.* American Foundrymen's Soc. (1950) **58**, p. 298.

[9] H. Morrogh and W. J. Williams: *Journal* Iron and Steel Inst. (1947) **155**, p. 321.

[10] A. L. DeSy: *Metal Progress* (1950) **57**, p. 774.

[11] J. E. Rehder: *American Foundryman* (1952) **21**, No. 2, p. 44.

[12] J. A. Fournier: Private communication.

[13] H. E. Stauss, F. W. Von Batchelder, and E. I. Salkovitz: *Trans.* AIME (1951) **191**, p. 249; JOURNAL OF METALS (March 1951).

Observations on the Tension Texture of Aluminum

by E. A. Calnan and Betty E. Williams

IN the development of a new treatment for the prediction of deformation textures,[1,2] it was noted that for no metals are there experimentally determined tension textures with which the predictions may be compared. There is a considerable knowledge of drawing textures and previous workers have been content to consider these as equivalent to tension textures for the purposes of comparison. It is shown, however, in the new treatment that the tension and drawing textures are not necessarily identical, the radial compression exerted by the dies in the drawing operation producing some modification of the tension texture. In particular for the face-centered cubic metals it is predicted that for drawing the final texture should be [111] with a spread towards [211] (a more detailed derivation of this texture has been made by Calnan[3]). This has been amply confirmed by experiment, see Hibbard.[4] For the pure tension case, however, the treatment predicts intermediate [111] and [100] textures leading to a [211] end-point, while all previous treatments have predicted the final texture as [111] with in some cases an additional [100] component. Thus evidence that the pure tension end-point is the [211], or at least that [111] and [100] are not the final textures, should provide a valuable test of the new treatment. Accordingly some experiments were made on aluminum.

Three aluminum specimens were examined in detail, one of cold-rolled high purity rod (99.99 pct), specimen A, and two of commercial extruded rod of purity 99.4 pct, specimens B and C. The initial annealing treatments were: A, 1½ hr at 400°C; B, 2 hr at 400°C; C, 1½ hr at 650°C. The principal difficulty is that of obtaining sufficient elongation before fracture occurs. This was overcome to some extent by giving a softening heat treatment, 1 hr at 300°C, after each 15 pct of extension. Vickers hardness measurements gave values before and after the softening treatment of about 30 and 28, respectively, in comparison with the initial value of about 19 corresponding to fully annealed material. From recent observations in this laboratory it is concluded that this small recovery corresponds to a polygonization process rather than recrystallization proper and consequently the preferred orientation is unaffected. At the higher extensions, however, some slight necking of the specimens took place and it was necessary to turn them down to a uniform cross-section before

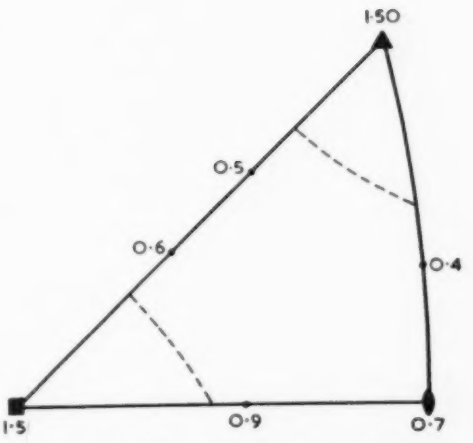

Fig. 1—Superpure aluminum, initial condition. Unit triangle showing ratios of the reflection intensities for plane normals parallel to the tension axis to the corresponding intensities of a random aggregate. Broken line is estimated position of ratio unity, the boundary of preferred orientation.

E. A. CALNAN and B. E. WILLIAMS are Members of the Staff of the Metallurgy Div., National Physical Laboratory, Teddington, Middlesex, England.

Discussion on this paper, TP 3330E, may be sent, 2 copies, to AIME by Dec. 1, 1952. Manuscript, March 14, 1952. Philadelphia Meeting, October 1952.

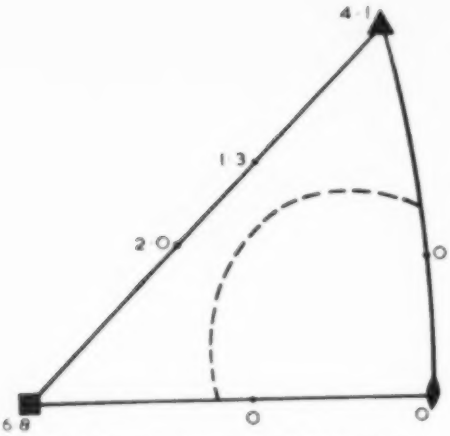

Fig. 2—Superpure aluminum after 75 pct extension.

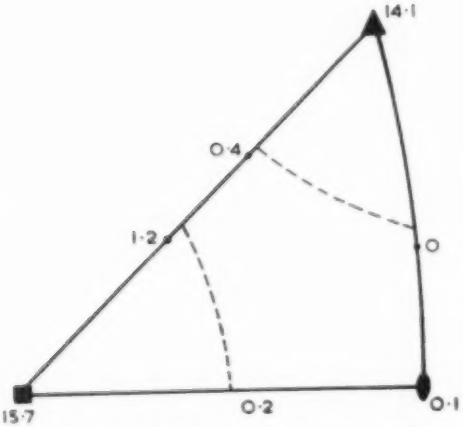

Fig. 3—Commercial purity aluminum rod, initial condition.

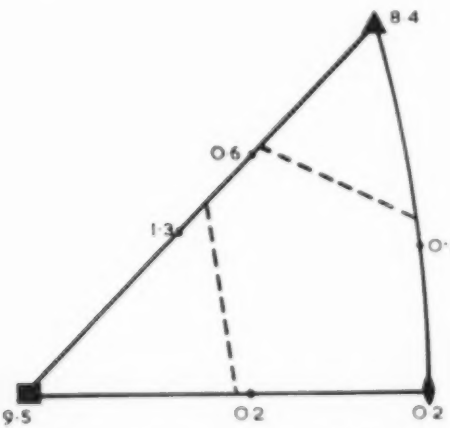

Fig. 4—Commercial purity aluminum rod after 50 pct extension.

continuing the extension. By this means a maximum of 75 pct extension was reached.

X-ray observations were made on cross-sections of the material, carefully sawed from the specimen before and after extension and polished on successively finer emery papers down to Huberts 00. Using a Geiger-Muller Counter Spectrometer the integrated intensities of the following reflections, 111, 200, 220, 311, 331, 420, and 422, were measured with the surface of the cross-section at the appropriate Bragg angle to the incident beam. In this way the intensities are proportional to the numbers of grains with the particular plane lying in the surface, i.e., with the direction of the same indices parallel to the tension axis. The intensities were compared with those from a lightly compressed block of aluminum powder which may be considered as a randomly oriented aggregate. Thus the ratio of specimen intensity to powder intensity indicates the degree of preferred orientation of the corresponding direction along the specimen axis. Fig. 1 shows these ratios for specimen A before extension and indicates a little preferred orientation. After 75 pct extension, Fig. 2, it will be seen that not only the [111] and [100] but also the [211] and [311] ratios have increased between three and four times at the expense of orientations around [110]. This increase is far more than the variation between different cross-sections of the same specimen which was found to be about 0.3 of the observed values. The effect of extension on the duplex [111], [100] texture of Fig. 2 is illustrated by the extruded rod specimen, B, Figs. 3 and 4. The interesting feature is that although no marked [211] texture has developed after 50 pct extension the [111] and [100] components are diminishing. This indicates that the final end-point is neither [100] nor [111] but, since the [311] and [211] are slightly increased, is probably somewhere in the region of these latter points. Specimen C gives some confirmation of this effect, for the initial condition shows a preferred orientation near [311] which is increased after 75 pct from a ratio of 1.1 to 9 while the [111] and [100] increase from 0.3 to 0.85 and 0.2 to 2.2, respectively.

Summary

While it appears that extensions sufficiently large to produce the final texture have not been attained there is evidence that the texture end-points of aluminum under pure tension are not the [111] or [100] directions as previously supposed but are somewhat on the [011] zone between these points.

Acknowledgment

The work described above has been carried out as part of the General Research Program of the National Physical Laboratory and this paper is published by permission of the Director of the Laboratory.

References

[1] E. A. Calnan and C. J. B. Clews: *Philosophical Magazine* (1950) **41** (7) p. 1085.
[2] E. A. Calnan and C. J. B. Clews: *Philosophical Magazine* (1951) **42**, p. 616.
[3] E. A. Calnan and C. J. B. Clews: *Philosophical Magazine* (1951) **42**, p. 919.
[4] E. A. Calnan and C. J. B. Clews: *Philosophical Magazine* (1952) **43**, p. 93.
[5] E. A. Calnan: Thesis, University of London (1952).
[6] W. R. Hibbard, Jr.: *Trans.* AIME (1949) **185**, p. 598; JOURNAL OF METALS (September 1949).

Preferred Orientations in Vanadium

by Carl J. McHargue and Joseph P. Hammond

THERE have been no publications on the wire texture, on the cold-rolled sheet texture, nor on the recrystallized sheet texture of vanadium. Since it has a body-centered cubic structure, it would be expected to show strongly preferred orientations such as are found in iron[1] and molybdenum.[2] The wire textures of body-centered cubic iron,[3] tungsten,[3] molybdenum,[3] tantalum,[3] niobium,[3] and brass[4] have been found to have [110] directions lying parallel to the wire axis. Wires of iron,[5] containing 1.95 pct V or 1.95 pct Si,[5] and steel[6] retain their texture upon recrystallization. Molybdenum[2] and tungsten[2] wires retain their texture after recrystallization at low temperatures. A [100] recrystallization texture has been reported for molybdenum[2] and for a Fe-Ni alloy (53 atomic pct Ni).[7]

The cold-rolled sheet texture for iron,[1] mild steel,[6] and molybdenum[2] is chiefly one in which the [110] directions lie parallel to the rolling direction and the (100) planes lie parallel to the rolling plane with a deviation from this position chiefly about the rolling direction as an axis.

This paper presents the cold-rolled and the recrystallized wire textures, and the cold-rolled and the recrystallized sheet textures for vanadium. The results show that the textures in vanadium are not significantly different from those reported for other body-centered cubic metals.

The vanadium used in this investigation was the so-called "ductile" vanadium which has a nominal composition within the following limits:[8] O, 0.05 to 0.12 pct; H, 0.001 to 0.004; N, 0.02 to 0.04; C, 0.03 to 0.07; and V, 99.8 to 99.9.

The wires were formed by rolling annealed rods of 0.280 in. diam to 0.028 in., a reduction in diameter of 90 pct. The wires were then electrolytically etched to 0.005 in. diam and used as such for specimens. Annealed sheet was reduced 95 pct in thickness from 0.100 to 0.005 in. with a two-high, 4-in. diam mill using reductions no greater than 10 pct per pass. In order to avoid temperature effects, the sheet was allowed to cool between passes. X-ray specimens were made in the form of posts from the sheet. The sheet was mounted in a fixture and the edges were polished using metallographic technique. Each edge was alternately polished and etched during the last stages in order that all worked material would be removed. These post specimens were approximately square in cross-section. The specimens to be recrystallized were wrapped in tantalum foil, sealed in evacuated quartz tubes, and annealed at 1600°F.

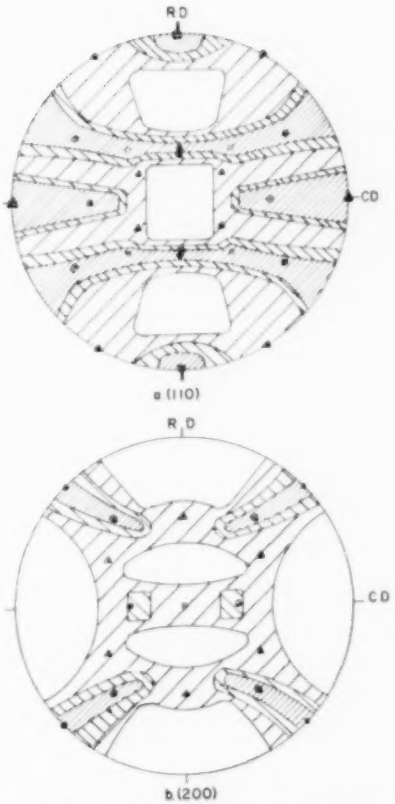

Fig. 1—Pole figure for vanadium cold rolled 95 pct. Circle—(112) [110]. Square—(100) [011]. Triangle—(111) [112].

The X-ray data were obtained from transmission shots made with a 0.030 in. pinhole camera, and molybdenum radiation with a zirconium filter inserted between the specimen and film. The grain size was sufficiently small in both the cold-worked and recrystallized material to give satisfactory results with the specimens stationary.

In order for the wire texture to be determined, transmission X-ray patterns were taken with the

C. J. McHARGUE, Student Associate AIME, is Research Associate, and J. P. HAMMOND is Associate Professor of Metallurgical Engineering, Dept. of Mining and Metallurgical Engineering, University of Kentucky, Lexington, Ky.

Discussion on this paper, TP 3324E, may be sent, 2 copies, to AIME by Dec. 1, 1952. Manuscript, Dec. 28, 1952. Philadelphia Meeting, October 1952.

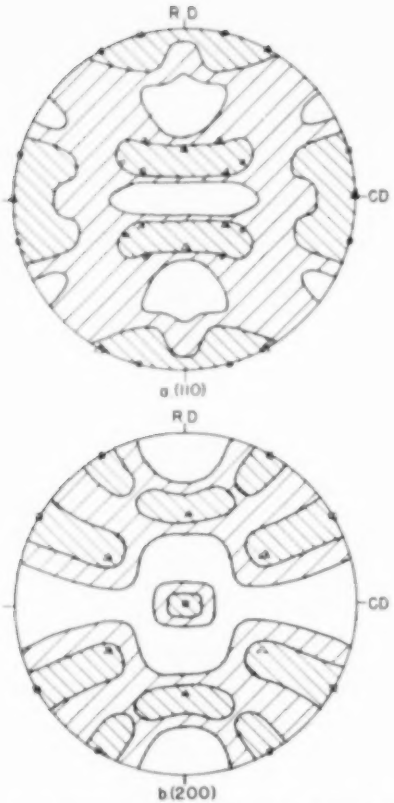

Fig. 2—Pole figure for vanadium recrystallized at 1600°F. Square position near (100) [011]. Triangle—(111) [112].

specimen tilted 10° from the perpendicular toward the beam. Analyses were made of the (002), (110), and (112) reflections.

The data for the sheet textures were obtained from exposures made with the beam normal to the rolling direction and 0°, 11°, 26°, 41°, 56°, 71°, and 79° to the cross direction. Exposures were also made with the beam normal to the cross direction and 0°, 11°, 56°, 71°, and 79° to the rolling direction. Additional shots were made where necessary in order to verify data in regions in which the orientation was uncertain. The intensities of the various portions of the diffraction rings were estimated visually, and the pole figures were plotted in the usual manner.

Discussion of Results

Wire Texture: The cold-rolled vanadium wire shows a simple [110] texture. The [110] direction lies parallel to the wire axis with a very small amount of spread from this position. This texture was retained upon recrystallization at 1600°F. These results are consistent with the fiber texture reported for other body-centered cubic metals and with that predicted by theory.[9]

Sheet Textures: The pole figures for cold-rolled vanadium sheet are shown in Fig. 1. The regions of highest intensity are satisfactorily explained on the basis of the orientations (100) [011] and (112) [110]. There is another component of the sheet texture which is described by the orientation (111) [112]. The texture could also be described as the (100) [011] orientation with scatter of ±55° in the cross direction. The deviation about the cross direction as an axis amounts to 8° to 10° each way.

Fig. 2 shows the pole figures for the recrystallized material. The principal orientations appear to be those which have the (100) and (111) planes parallel to the rolling plane and the [011] directions 15° from the rolling direction and the [112] directions parallel to the rolling direction. In other words, this texture is centered about the orientations (100) [011] 15° to the rolling direction, and (111) [112]. The (112) [110] component of the cold-rolled texture does not appear to be present either as such or rotated as the (100) [110] component. Thus, it seems that the recrystallized texture has one component which was present in the cold-rolled texture and another component derivable from a component of the cold-rolled texture by a rotation of approximately 15° about the normal to the rolling plane.

Both the deformation and recrystallization sheet textures are very similar to those reported for iron,[7] and the deformation texture is similar to that reported for molybdenum.[8]

Summary

1—The fiber texture is found to be a simple [110] texture for "ductile" vanadium in both the cold-rolled and recrystallized conditions.

2—The cold-rolled and recrystallized sheet textures are presented in the form of pole figures of the (110) and (200) planes. These data are similar to those reported for other body-centered cubic metals. The cold-rolled sheet texture is described by the three "ideal" orientations (100) [011], (112) [110], and (111) [112]. The recrystallized texture is described by (111) [112], and by (100) [011] rotated 15° about the normal to the rolling plane.

Acknowledgment

The authors wish to thank A. B. Kinzel of the Electro Metallurgical Division of the Union Carbide and Carbon Corp. for supplying the vanadium used in this investigation.

References

[1] G. Kurdjumov and G. Sachs: *Ztsch. Physik* (1930) **62**, p. 592.

[2] J. F. H. Custers and J. C. Riemersma: *Physics* (July 1946) **12**, p. 145.

[3] C. S. Barrett and L. H. Levenson: *Trans.* AIME (1939) **135**, p. 327.

[4] Z. Jeffries: *Trans.* AIME (1924) **70**, p. 303.

[5] M. Ettisch, M. Polyani, and K. Weissenberg: *Ztsch. Physik* (1921) **7**, p. 181.

[6] W. R. Hibbard, Jr., A. E. Roswell, and A. E. Schuetz: *Trans.* AIME (1951) **191**, p. 808; JOURNAL OF METALS (September 1951).

[7] C. S. Barrett: *Structure of Metals*, p. 424 (1943) New York. McGraw-Hill Book Co.

[8] N. P. Goss: *Trans.* A.S.S.T. (1929) **16**, p. 405.

[9] T. Fujiwara: *Proc.* World Eng. Congress, Tokyo. (1931) **36**, Part 4, p. 171.

[10] W. G. Burgers and F. M. Jacobs: *Metallwirtschaft* (1936) **15**, p. 1063.

[11] M. Gensamer and R. Mehl: *Trans.* AIME (1936) **120**, p. 277.

[12] A. B. Kinzel: *Metal Progress* (September 1950) p. 315.

[13] W. R. Hibbard, Jr., and M. K. Yen: *Trans.* AIME (1948) **175**, p. 126; METALS TECHNOLOGY (February 1948).

Principles of Zone-Melting

by W. G. Pfann

In zone-melting, a small molten zone or zones traverse a long charge of alloy or impure metal. Consequences of this manner of freezing are examined with respect to solute distribution in the ingot, with particular reference to purification and to prevention of segregation. Results are expressed in terms of the number, size, and direction of travel of the zones, the initial solute distribution, and the distribution coefficient.

IF a charge of binary solid-solution alloy is melted and then frozen slowly from one end, as for example in the Bridgman method of making single crystals,[1] coring usually occurs, with a resulting end-to-end variation in concentration. Such coring, or normal segregation, is undesirable where uniformity is an object. On the other hand, for certain systems, it can be utilized to refine a material by concentrating impurities at one end of the ingot.[2,3]

In the present paper a different manner of freezing will be examined with respect to the distribution of solute in the ingot. A number of procedures will be indicated which have in common the traversal of a relatively long charge of solid alloy by a small molten zone. Such methods will be denoted by the general term *zone-melting*, while the process described in the preceding paragraph will be called *normal freezing*. It will be shown that, in contrast to normal freezing, zone-melting affords wide latitude in possible distributions of solute. Segregation can either be almost entirely eliminated or it can be enhanced so as to provide a high degree of separation of solute and solvent.

A number of simplifying assumptions will be invoked which, while not entirely realizable in practice, nevertheless provide a suitable point of departure for more refined treatments. Moreover, our own experience with zone-melting has shown that, for certain systems at least, the analysis holds quite well. The present paper will be confined to a discussion of principles and a general description of procedures. Comparison with experiment is planned for later publication.

Normal Freezing

Before considering zone-melting, segregation during normal freezing will be reviewed briefly. If a cylinder of molten binary alloy is made to freeze from one end as in Fig. 1, there usually will be a segregating action which will concentrate the solute in one or the other end of the ingot. If the constitutional diagram for the system is like that of Fig. 2, then the distribution coefficient k, defined as the ratio of the concentration in the solid to that in the liquid at equilibrium, will be less than one and the solute will be concentrated in the last regions to freeze. If the solute raises the freezing point, then k will be greater than one and the solute will be concentrated in the first regions to freeze.

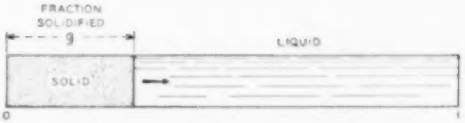

Fig. 1—Solidification by normal freezing (schematic).

The concentration in the solid as a function of g, the fraction which has solidified, can be expressed by the relation:

$$C = k\,C_o\,(1-g)^{k-1} \qquad [1]$$

where C_o is the initial solute concentration in the melt. Eq 1 is based on the following assumptions:

1—Diffusion in the solid is negligible. 2—Diffusion in the liquid is complete (i.e., concentration in the liquid is uniform). 3—k is constant.

Concentration curves representing eq 1 for k's from 0.01 to 5.0 are plotted in Fig. 3. This equation, in one form or another, has been treated by Gulliver,[4] Scheuer,[5] Hayes and Chipman[6] for alloys and by McFee[7] for NaCl crystals. It is derived in Appendix I. It should be pointed out that the k which is calculated from the phase diagram will be valid only in the ideal case for which the stated assumptions are correct. In all actual cases, the effective k will be larger than this value for solutes which lower the melting point, smaller for solutes which raise the melting point, and will probably vary during the beginning of the freezing process. For simplification it will be assumed that the ideal k is valid.

Zone-Leveling Processes

The processes of this part are designed to produce a uniform, or level, distribution of solute in the ingot.

Single Pass: Consider a rod or charge of alloy whose cross-section is constant and whose composition, C_o, is constant, although permissibly varying on a microscopic scale.* Such a charge might be a rapidly frozen casting or a mixture of crushed or powdered constituents. Cause a molten zone of

* More accurately, C_o must be invariant with x, but the concentration may vary throughout a given cross-section.

W. G. PFANN, Member AIME, is associated with Bell Telephone Laboratories, Murray Hill, N. J.

Discussion on this paper, TP 3326E, may be sent, 2 copies, to AIME by Dec. 1, 1952. Manuscript, Jan. 9, 1952; revised, April 24, 1952. Philadelphia Meeting, October 1952.

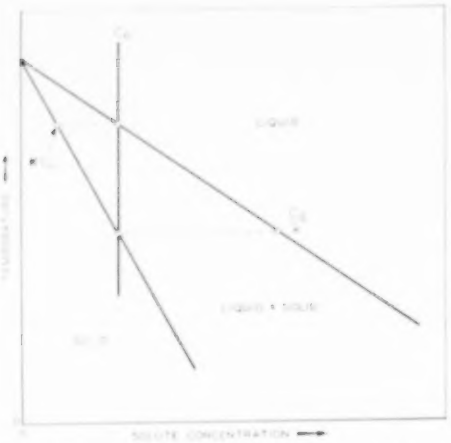

Fig. 2—Portion of constitutional diagram for a solute which lowers the freezing point of the solvent (schematic).

length l to traverse the charge, as shown in Fig. 4, l being constant and small compared to the length of the charge.

The course of segregation during this process may be visualized by reference to Fig. 2. As the molten zone advances it freezes out a layer dx of solid and melts a layer dx of the charge. The first solid to freeze, at $x=0$, is of concentration kC_o. For $k<1$, kC_o is less than C_o and hence the liquid is enriched. As the zone progresses the liquid continues to be enriched, although at a decreasing rate, until it attains concentration C_o/k. When this condition is attained the concentrations of solids entering and leaving the zone are the same and hence no further change of concentration occurs in the zone or in the solid freezing from it until the zone reaches the end of the charge. The remaining liquid then solidifies by normal freezing, as described by eq 1.

Thus, as shown in Fig. 5, simple zone-melting of a uniform charge results in an initial transition region; a region of uniform concentration which may have any desired length and an end region of length equal to one zone, in which normal freezing prevails. The concentration C at any length x in the zone-melted bar (except in the last zone) is given by:

$$C/C_o = 1-(1-k)e^{-kx/l} \qquad [2]$$

where x is the length solidified, measured from the starting end, and not the fraction solidified. The derivation of eq 2 was made by W. T. Read and appears in Appendix II. The underlying assumptions are those of normal freezing, with the addition that l is assumed to be constant.

Calculated curves of C vs. x/l according to eq 2 are plotted in Fig. 6 for k's from 0.01 to 5.0, for the particular case of a charge ten units long, unit zone-length, and unity C_o. Nine zone-lengths are depicted; the tenth solidifies by normal freezing. In connection with the curves of Fig. 6 it should be noted that:

1—As k increases, C approaches equality with C_o at lower values of x/l. For a given k, the percentage yield of uniform material can be increased by increasing the rod-length and by reducing l.

2—The difference between the mean and initial

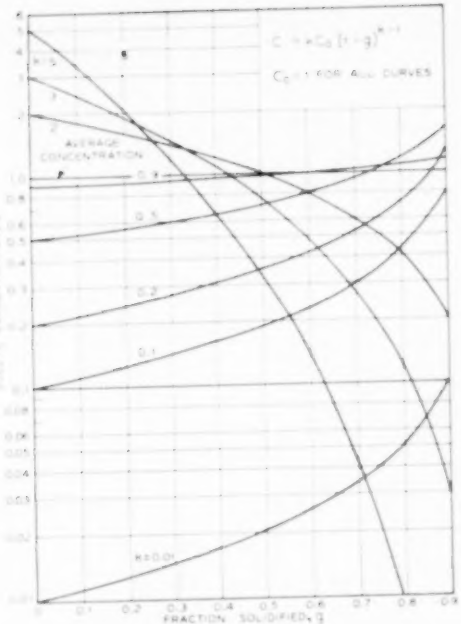

Fig. 3—Curves for normal freezing, showing solute concentration in solid as a function of g, the fraction solidified, calculated from eq 1 for various values of k, the distribution coefficient.

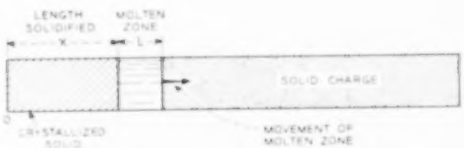

Fig. 4—Solidification by zone melting (schematic).

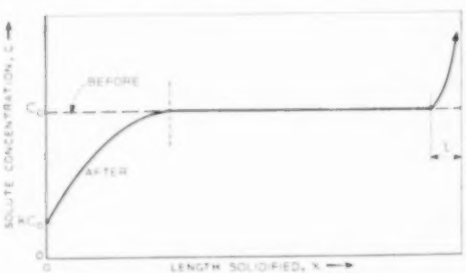

Fig. 5—Approximate concentrations before and after single-pass zone melting. Note region of uniform concentration after zone-melting.

concentrations is proportional to $(1-k)$ as in normal freezing.

3—While eq 2 and the curves of Fig. 6 are based on the four stated assumptions, *the basic feature of the zone-melting process, that is, the attainment of a limiting composition C_o, is relatively independent* of these assumptions. (Of course, fluctuations in k

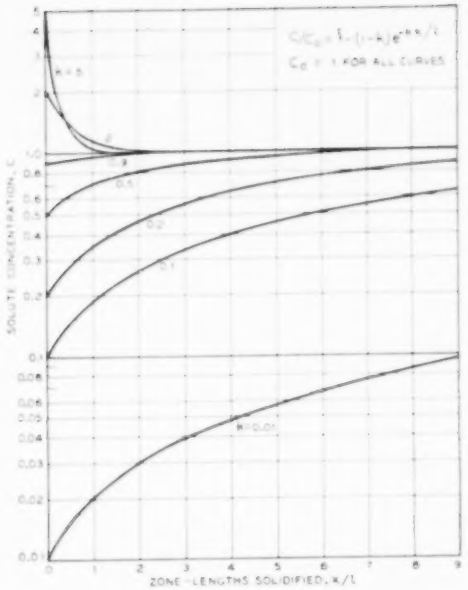

Fig. 6—Curves for zone melting, showing solute concentration in solid as a function of x/l, the zone-lengths solidified, calculated from eq 2, for various k's. Nine zone-lengths are shown.

or l after C_o has been reached will cause changes in C_o.)

4—For k's of about 0.2 or less the rod is not at all uniform.

Reverse Pass: It has been shown that zone-melting of a uniform rod results in two end-regions in which C differs considerably from C_o. An improvement in uniformity can be made by re-zone-melting in the reverse direction, from right to left. If C has essentially attained the value C_o at some point in the first pass, as in curve a of Fig. 7, then the distribution of solute after the reverse pass will be as shown qualitatively in curve b. The deviation at the right will be eliminated; that at the left will be re-reduced. Even if k is very small, ~0.01, and C_o is not attained in the first pass, it is found that reverse zone-melting results in substantially uniform composition in all but the last zone.

Repeated Pass: If a sufficient number of back-and-forth passes is made in a straight bar, all deviations from a uniform composition can be eliminated, except in the last zone to freeze. In this respect the molten zone may be likened to a weighted drag moved across soil in order to level it. The drag picks up soil at high spots, drops it at low spots. Similarly, the molten zone equalizes points of high and low concentration in the charge, the action being particularly effective if k is small. For a starting charge of mean composition C_o, not assumed to be uniform, and a charge of total length d, the final concentration, C_o, of the uniform rod is given by:

$$C_o/C_o = \frac{dk}{dk + L(1-k)} \qquad [3]$$

The final concentration in the molten zone will be C_o/k.

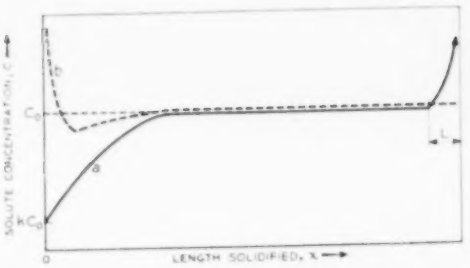

Fig. 7—Approximate concentrations after: (a) single pass zone-melting, (b) reverse zone-melting of (a).

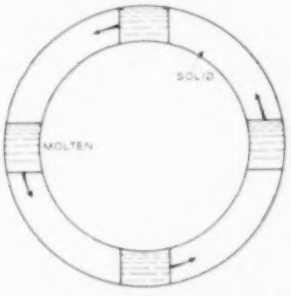

Fig. 8—Repeated-pass zone melting of circular charge. The final state is a uniform solute concentration in the solid equal to k times that in the molten zones.

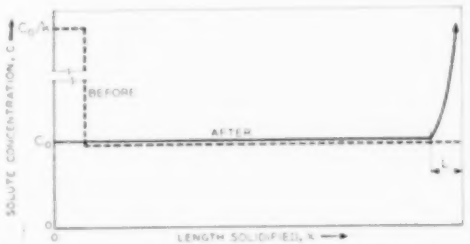

Fig. 9—Zone melting with starting charge, to eliminate initial transition region.

An alternate means of achieving the result expressed by eq 3 is to arrange the charge in the form of a closed ring, as in Fig. 8, and to cause one or more molten zones to travel around it. In the ring method, if more than one zone is used, l, in eq 3, should be the sum of their lengths.

Starting Charge: The initial transition region in single-pass zone-melting is a result of the fact that the molten zone must travel some distance before it accumulates enough solute to attain concentration C_o/k. This region can be eliminated by arranging the charge to have a concentration C_o/k in the first zone and C_o in the remainder,† as shown in Fig. 9.

† This fact was pointed out by W. Shockley (private communication).

Starting Charge into Pure Solvent: It may be seen from Fig. 6 that the initial transition region is

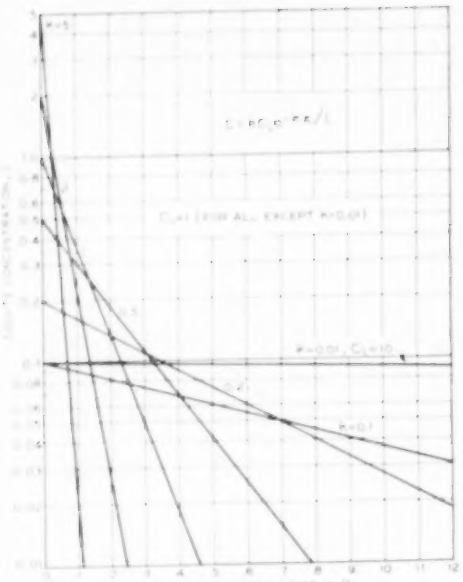

Fig. 10—Curves for zone melting into pure solvent, showing solute concentration in solid as a function of x/l, the zone lengths solidified, calculated from eq 4 for various k's.

extremely long for values of k of about 0.1 or less, and that segregation is quite severe in single-pass zone-melting. A method of zone-melting which is particularly effective in such instances is to place solute in the first zone only, the remainder of the charge being pure solvent. The concentration of the solid after one pass is given in all except the last zone by:

$$C = kC_o e^{-kx} \qquad [4]$$

where C_o is the concentration of the charge in the first zone. Calculated concentration curves for a range of k's are shown in Fig. 10. It may be seen that for k equal to 0.01 the concentration decreases only about 10 pct in ten zone-lengths.

Even such decrease can be entirely prevented by reducing the volume of the zone as it travels through the charge. For a charge of constant cross-sectional area, a, the concentration will remain constant, at the value kC_o, if the zone-length l is decreased in accordance with the equation:

$$l = l_o - kx \qquad [5a]$$

where l_o is the initial zone-length. If it is desired to maintain l at a constant value and decrease a, then a must vary in accordance with the equation:

$$a = a_o e^{Dx} \qquad [5b]$$

where:

$$D = \frac{1}{\log e\,(1-k)}$$

and a_o is the cross-sectional area at $x = 0$. It may be noted that eq 5a is applicable only to a charge of finite length, l_o/k, for at that value of x the zone-length becomes zero. Eq 5b in principle at least is applicable to a charge of infinite length. Both equations are valid only if $k<1$. Derivations of eqs 4, 5a, and 5b appear in Appendix III.

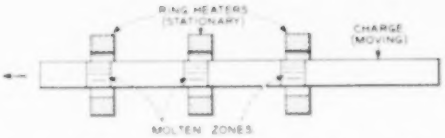

Fig. 11—Multiple-zone refining, using a straight charge. For $k<1$, the solute becomes concentrated in the end of the ingot, at the right.

Zone-Refining Processes

The processes of this part have the object of purifying a solvent material, or separating solute from solvent.

Utilization of segregation during normal freezing to purify part of an ingot is well known.[1,2] The process is particularly effective where k is small and diffusion in the solid is limited. A glance at the curves of Fig. 3 indicates that for k's less than about 0.1 most of the solute is concentrated in the last tenth of the ingot. Further purification can be obtained by cropping the solute-rich tip, remelting and refreezing. In principle any desired degree of purification can be obtained by a repetition of such steps.

Refinement can also be accomplished by zone-melting. A comparison of Figs. 3 and 6 shows that for small k's a considerable purification is effected by single-pass zone-melting, although on the average it is less than for normal freezing, for any given fraction of the charge. The particular merit of zone-refining becomes evident when repeated crystallizations are desired. By passing a bar through a series of heaters a number of molten zones can be made to traverse the charge in a single operation. Each zone picks up solute on its way through the charge and deposits it at the end of the charge. Thus, any desired number of refining steps can be obtained in a single operation, and without resort to the intermediate steps of cropping. Figs. 11 and 12 illustrate multiple-zone-refining for a straight and for a circular charge.

It is of interest to know the distributions of solute after two, three, or more zones pass through an initially uniform charge and also the ultimate distribution after a large number of passes. The latter is more easily determined and will be discussed first.

Consider a charge of length d and of mean composition C_o, with no restriction being placed on the distribution of the solute. Assume for purposes of

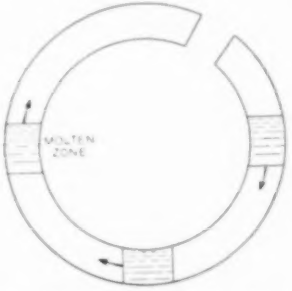

Fig. 12—Multiple-zone refining, using a charge in the form of an open ring.

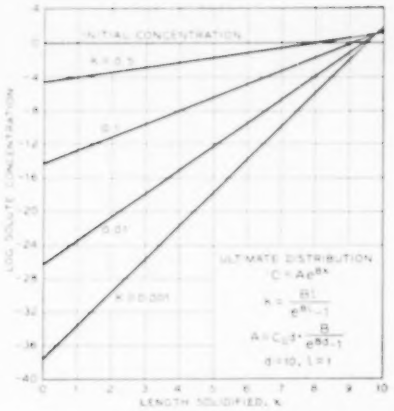

Fig. 13—Solute concentration curves showing the ultimate distribution after multiple-zone refining, calculated from eq 8, for various k's.

exposition that k is less than one. It is instinctively seen that after repeated passes in one direction a distribution will be reached which cannot be further changed. (The effect may be likened to piling a given amount of sand against a vertical wall—there will be a maximum attainable height.) Let this ultimate distribution be:

$$C = F(x) \qquad [6]$$

If a molten zone of length l is to pass through the bar without changing this distribution then the concentration of the solid freezing out of the zone at any point x must be given by eq 6. The concentration of the liquid in the zone is:

$$C_l = \frac{1}{l}\int_x^{x+l} C\,dx = \frac{1}{l}\int_x^{x+l} F(x)\,dx$$

assuming unit cross-sectional area. The concentration which freezes out at x is kC_l, from which:

$$F(x) = \frac{k}{l}\int_x^{x+l} F(x)\,dx \qquad [7]$$

The solution of eq 7 is:

$$C = Ae^{Bx} \qquad [8]$$

where:

$$k = \frac{Bl}{e^{Bl}-1} \qquad A = \frac{C_0 kB}{e^{Bl}-1}$$

Ultimate distributions calculated from eq 8 are plotted in Fig. 13 and it is seen that for small k's these are extremely steep. For example, if $k = 0.1$, $d = 10$, $l = 1$, the ultimate concentration at $x = 0$ is less than C_0 by a factor of about 10^{-4}. Eq 8 is actually an approximation because it cannot apply in the last zone, where normal freezing prevails, and the effect of the distribution in the last zone is reflected back into the preceding zones. However, this effect is small, especially at the pure end of the bar.

Since the concentration at the starting end is decreased by a factor of the order of k in each pass, it is evident from an inspection of Fig. 13 that at least 14 passes are required to approach the ultimate distribution.

A good approximation to the actual distribution after each of a number of successive single-zone passes readily can be obtained by a computation procedure suggested by R. W. Hamming in which the molten zone is assumed to advance in discrete steps of convenient size, say 0.5 zone-length, the concentration frozen out at each step being k times that in the zone. The result of such a computation is shown in Fig. 14 for three successive passes through an initially uniform charge, assuming $k = 0.1$. Also shown is the ultimate distribution.

Both refining and uniformity can be obtained by the repeated-pass methods described earlier in the paper, the purification being more effective for small k's. The ratio C_f/C_0 in eq 3 may be defined as the refinement ratio, R. For a given system R can be varied by controlling the fraction of the charge which is molten. For example, if $k = 0.01$, $d = 10$, then $R = 0.048$ for $l = 2$, 0.091 for $l = 1$.

Discussion

Possibly the most significant feature of zone-melting is its flexibility. The charge may be regarded as a medium and the molten zone as a distributor of solutes in the medium. Subject to the restriction that the concentration freezing out of the molten zone is k times that in the zone, and to certain other restrictions on solidification conditions, an operator can produce a large variety of useful distributions of solute in an ingot. Among the tools at his disposal are the arrangement of the starting charge, and the size, number, and direction of travel of the molten zones.

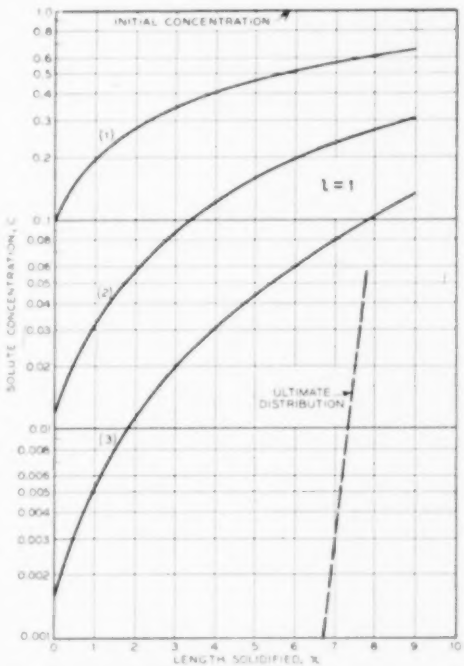

Fig. 14—Concentration curves, showing concentration of solute in solid as a function of x, the length solidified, after 1, 2, and 3 successive single-zone passes from left to right, through an initially uniform charge ten units in length, for unit zone-length.

While this paper is directed to metallurgists, the principles discussed in it are applicable to the freezing of any solid-solution system in which diffusion occurs much more readily in the liquid than in the solid. These methods may also be applied to solid-state transformations if the rates of diffusion of solute in the respective phases differ considerably.

The discussion of zone-melting has been confined to the categories of zone-leveling and zone-refining and a number of illustrative examples have been given in each. These by no means form a complete listing and many other variations are possible. For example, except in the part described under the subheading "Starting Charge into Pure Solvent," it has been assumed that l, the zone-length, is constant. However, by varying l as the zone travels, corresponding changes can be introduced in concentration. The descriptions have been confined to binary systems and ingots of bar form, either straight or ring shaped, but such restrictions are unnecessary.

Acknowledgments

The writer is greatly indebted to E. E. Schumacher and J. H. Scaff for discussions, advice and encouragement which have been important factors in bringing this work to fruition. He is indebted also to a number of colleagues at Bell Telephone Laboratories for valuable discussions, in particular to W. T. Read whose contributions to the mathematics have helped to crystallize much of the thinking.

Appendix I
Derivation of Eq 1

Freeze a unit volume of solution. Assume that during the freezing process there is no diffusion in the solid and complete diffusion in the liquid. Assume also that k the distribution coefficient is constant. Let:

- g = the fraction of the original volume which has frozen.
- s = the amount of solute remaining in the liquid.
- s_o = the total amount of solute.
- C = the solute concentration in the solid at the liquid-solid interface, in units of solute per unit volume of solution.
- C_l = the solute concentration in the liquid.

By definition:

$$C = kC_l$$

Since $C_l = s/1-g$

$$C = \frac{ks}{1-g}$$

After a fraction g has frozen, freeze an additional amount, dg. The concentration C in the frozen layer of volume dg is:

$$C = -\frac{ds}{dg}$$

Eliminating C and integrating gives:

$$\int_{s_o}^{s} \frac{ds}{s} = \int_{0}^{g} -\frac{k}{1-g}\,dg$$

From which:

$$s = s_o\,(1-g)^k$$

and:

$$C = -\frac{ds}{dg} = ks_o\,(1-g)^{k-1}$$

Since the original volume was unity, $s_o = C_o$, where C_o is the original solute concentration, and hence:

$$C = kC_o\,(1-g)^{k-1} \qquad [1]$$

This treatment neglects the change of density during freezing. It places no restrictions on the shape of the molten or solid portion during freezing.

Appendix II
Derivation of Eq 2, after W. T. Read

Assuming k, the distribution coefficient, and l, the zone-length to be constant, the concentration, C, of the freezing solid at any length x, measured from the beginning of the ingot, may be found as follows:

Let C_o = mean concentration of solute in charge, assumed to be invariant with x, and expressed in units of solute per unit volume of solution.

s = quantity of solute in zone at any x.

s_o = quantity of solute in zone at $x = 0$.

Advance the zone a distance dx. An incremental volume dx of solid will form, an equal volume dx of charge will melt (see Fig. 4). The quantity of solute frozen out is:

$$kC_l\,dx$$

where C_l is the solute concentration in the molten zone. But $C_l = s/l$, assuming unit cross-sectional area. The quantity entering the zone is $C_o dx$. The net change in s is therefore given by:

$$ds = (C_o - \frac{ks}{l})\,dx \qquad [A\text{-}1]$$

From which:

$$\frac{ds}{dx} + \frac{k}{l}s = C_o \qquad [A\text{-}2]$$

The solution of eq A-2 is:

$$se^{\frac{k}{l}x} - s_o = C_o \int_0^x e^{\frac{k}{l}x}\,dx = \frac{C_o l}{k}\left(e^{\frac{k}{l}x} - 1\right)$$

Since $s_o = C_o l$ then:

$$s = [C_o l + \frac{C_o l}{k}(e^{\frac{k}{l}x} - 1)]\,e^{-\frac{k}{l}x}$$

$$= C_o l \frac{k-1}{k} e^{-\frac{k}{l}x} + \frac{C_o l}{k}$$

Since $C = \frac{ks}{l}$:

$$C = C_o\,(k-1)\,e^{-\frac{k}{l}x} + C_o$$

or:

$$C/C_o = 1 - (1-k)\,e^{-\frac{k}{l}x} \qquad [2]$$

Appendix III
Derivations of Eqs 4, 5a, 5b

Eq 4: The conditions are the same as in Appendix II except that all of the solute is in the first zone at the start. The concentration C_o in the zone at $x = 0$ is therefore s_o/l. Advance the zone, at any x, a distance dx. Then:

$$ds = -\frac{ks}{l}\,dx$$

$$\int_{s_o}^{s} \frac{ds}{s} = \int_0^x -\frac{k}{l}\,dx$$

$$s = s_o\,e^{-\frac{k}{l}x}$$

Since:

$$C = -\frac{ds}{dx} \text{ and } C_o = \frac{s_o}{l}$$

$$C = kC_o\,e^{-\frac{k}{l}x} \qquad [4]$$

Eq 5a: Given that the cross-sectional area a is constant, find the dependence of l on x which will result in a constant value of C:

$$C = -\frac{ds}{adx} = \frac{ks}{al} = \text{constant} \qquad [A\text{-}3]$$

Since a and k are constant, then:

$$d\frac{(s)}{(l)} = 0$$

$$\frac{ds}{l} - \frac{sdl}{P} = 0$$

$$\frac{ds}{s} = \frac{dl}{l}$$

From eq A-3:

$$\frac{ds}{s} = -\frac{k}{l}dx$$

hence:

$$\frac{dl}{l} = -\frac{k}{l}dx$$

$$l = l_o - kx \qquad [5a]$$

Eq 5b: Given that l is to be constant, find the dependence of a on x which will result in constant C. Let a be designated $a(x)$; let v = zone volume:

$$C = -\frac{ds}{a(x)dx} = \frac{ks}{v} = \text{constant} \qquad [A\text{-}4]$$

where:

$$v = \int_x^{x+l} a(x)dx$$

and:

$$\frac{dv}{dx} = a(x+l) - a(x) \qquad [A\text{-}5]$$

Since k = constant:

$$d\frac{(s)}{(v)} = 0$$

$$\frac{ds}{v} - \frac{sdv}{v^2} = 0$$

$$\frac{ds}{s} = \frac{dv}{v}$$

From eq A-4:

$$\frac{ds}{s} = -\frac{ka(x)dx}{v}$$

hence:

$$dv = -ka(x)dx$$

$$\frac{dv}{dx} = -ka(x)$$

From eq A-5:

$$\frac{dv}{dx} = a(x+l) - a(x)$$

hence:

$$a(x+l) - a(x) = -ka(x)$$

$$\frac{a(x+l)}{a(x)} = 1-k \qquad [A\text{-}6]$$

The solution of eq A-6 is:

$$a = a_o e^{-Dx} \qquad [5b]$$

where:

$$D = \frac{1}{\log_e (1-k)}$$

References

1. P. W. Bridgman: *Proc. Amer. Acad. Arts and Sciences* (1925) **60**, p. 305.
2. R. H. McFee: *Journal of Chemical Physics* (1947) **15**, p. 856.
3. G. H. Gulliver: *Metallic Alloys* (Appendix) (1922) London, Chas. Griffin & Co.
4. E. Scheuer: *Ztsch. Metallkunde* (1931) **23**, p. 237.
5. A. Hayes and J. Chipman: *Trans. AIME* (1939) **135**, p. 85.

Technical Note

Recrystallization Textures in Copper Wire

by G. Bassi

RECENTLY Wallbaum[1] found that copper wires with different degrees of deformation up to 98.7 pct area reduction recrystallize giving a [112] texture, while deformation over 98.7 pct gives either a [100] texture at low temperatures or a [111] texture at high temperatures. Furthermore it was found that the recrystallization temperature as a function of deformation up to 98.7 pct decreases as expected, but increases over that deformation. Wallbaum concluded that the different textures have different recrystallization temperatures. The [112] texture has the lowest and [111] the highest. At the same time Bassi[2] found that for high deformation (over 99 pct area reduction) and for an annealing temperature of 400°C, the [100] texture first forms and with prolonged annealing time the [112] texture appears through grain growth. This secondary texture does not appear if the wire is annealed at 1000°C before the deformation.

From these two papers it might be concluded that the [112] texture can appear either as a primary or as a secondary texture after annealing. The texture formed in a special case depends on the previous history of the wire. Probably the texture of the wire prior to the last deformation is important. To investigate this, wires were produced by adequate deformation and annealing to give a [100], a [112], and a [111] texture. The wires then were given a series of different deformations and were annealed at various temperatures, after which the textures were studied.

Experimental Work

The copper used was electrolytic tough-pitch (Cu 99.90 pct and O. 0.04 pct). Three wires with the different initial textures were made in the following way: The [100] and [112] by drawing a 16 mm rod to 1 mm and annealing it 16 hr at 200°C and 2 hr

G. BASSI is associated with AB Svenska Metallverken, Vasteras, Sweden.

TN 115E. Manuscript, Feb. 15, 1952.

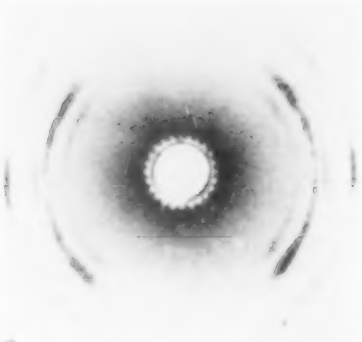

Fig. 1—1 mm wire annealed 16 hr at 200°C. [100] texture. No rotation of specimen. Incident beam perpendicular to wire axis. Unfiltered copper radiation. Specimen etched to 0.20 mm. Distance specimen-film: 26 mm.

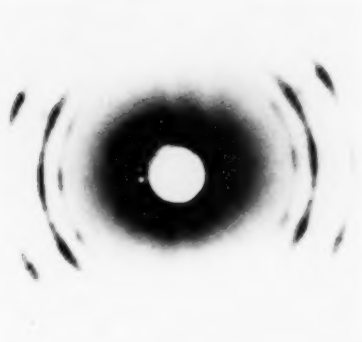

Fig. 2—1 mm wire annealed 2 hr at 400°C. [112] texture. Rotation of specimen. Incident beam perpendicular to wire axis. Unfiltered copper radiation. Specimen etched to 0.20 mm. Distance specimen-film: 26 mm.

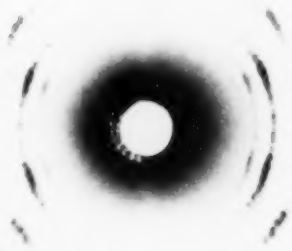

Fig. 3—1 mm wire annealed 1 hr at 950°C. [111] texture. Rotation of specimen. Incident beam perpendicular to wire axis. Unfiltered copper radiation. Specimen etched to 0.20 mm. Distance specimen-film: 26 mm.

at 400°C, and the [111] by drawing a 19 mm extruded rod to 1 mm and annealing it 1 hr at 950°C. The initial textures for the wires are shown in Figs. 1 to 3. Samples of the wires were then drawn with 10 to 99.7 pct area reduction and annealed 1 hr at 200°, 400° and 950°C. The examination of the textures was by X-ray analysis of the wire core.

Experimental Results

Deformation Textures: Up to a reduction of 80 pct the [100] and [111] textures appear relatively stable. The [112] texture however changes rather fast to the [111] orientation. Over 80 pct deformation, all three initial textures are changed to [111] + [100]. The wires were drawn at room temperature, but the same result is also obtained if the wires are drawn at −70°C.

Recrystallization Textures: Table I shows the influence of the initial orientation on the recrystallization textures.

From this the following can be concluded:

1—The [100] recrystallization texture depends mainly on the degree of deformation.

2—The [112] texture can only originate from the deformation of the [100] texture.

3—The [112] texture is a primary texture as long as the deformation is not sufficient to give the [100] texture. If a certain degree of deformation (about 90 pct) is exceeded, then the [100] texture originates first. With prolonged annealing time the [112] texture is formed by grain growth.

4—By deformation and following annealing of the [112] and [111] texture, no primary [112] texture originates. Consequently no secondary [112] texture forms by higher reduction, in spite of the formation of the primary [100] texture.

Table I. Influence of Initial Orientation on Recrystallization Texture

Initial Texture	Deformation, Pct	Temperature, °C		
		200°	400°	950°
[100]	10 to 90	Not recrystallized (rep. randomly)	[112]	[112]
[100]	90 to 99.7	[100]	[100] primary [112] secondary	[100] + [112] + [111]
[112]	10 to 90	Not recrystallized (rep. randomly)	Randomly	Randomly
[112]	90 to 99.7	[100]	[100]	[111]
[111]	10 to 90	Not recrystallized	Randomly	Randomly
[111]	90 to 99.7	Beginning of recrystallization to [100]	[100]	[111]

5—The [112] and [111] textures give a single [111] texture after a high deformation and annealing at high temperature.

6—Table I shows that wires with a second last annealing at high temperatures, 950°C for the wire with the [111] initial texture, will result in a higher recrystallization temperature than the wires with the [112] and [100] texture. The latter had a low second last annealing temperature. This might explain Wallbaum's findings that wires with a deformation in excess of 98.7 pct had a higher recrystallization temperature than wires with lower deformation.

Acknowledgment

The author wishes to express his gratitude to AB Svenska Metallverken for permission to publish the results. He is also indebted to B. I. Strom for the translation and helpful discussions and to H. Ohrlund for assistance with the experiments.

References

[1] H. J. Wallbaum: *Ztsch. Metallkunde* (1951) p. 207.

[2] G. Bassi: *Trans.* AIME (1951) **191**, p. 533; JOURNAL OF METALS (July 1951).

A Study of Grain Shape in an Aluminum Alloy

And Other Applications of Stereoscopic Microradiography

by W. M. Williams and Cyril Stanley Smith

THE quantitative study of grain shape in three dimensions has been a difficult one from the practical standpoint. Experiments on grain shape have usually been based on indirect observations of two-dimensional metallographic samples or on grains separated by intergranular corrosion or fracture. The latter method was used in particular by Desch[1] in 1919 in observing the shapes of β-brass grains which had been separated with mercury. The similarity in detail of shape and packing that exists between bubbles in a soap froth and metal grains was noted by Desch who remarks that: "Surface tension has an important share in determining the form of the crystal grains in a solidifying metal and such grains have a tendency to assume the shape of foam cells." More recently the relation between grain shape and grain growth has been studied by Harker and Parker.[2] The importance of surface tension forces in determining microstructure has been discussed by Smith,[3] and an analysis of the topological rules that apply to such structures has been made by the same author.[4] Biologists have made valuable contributions to the general problem of shape and form in an assembly of space-filling cells subject to surface tension forces. Particular mention must be made of the extensive researches of Lewis[5, 6] on botanical and anatomical tissues, and Matzke and Nestler,[7, 8] who have made painstaking studies of bubble shapes in different kinds of foam. The present paper introduces a new method of studying individual grains in particular alloys—a method which may well find use in other metallurgical researches, and which seems also to be applicable in biological problems.

Metal Grains in Three Dimensions

The individual grains in a piece of metal or the bubbles in a soap froth must satisfy two conditions—they must be in juxtaposition so as to fill space and their interfaces must conform to the laws of surface tension. If a further restriction is imposed, namely, that only one type of polyhedron be used, then the sole possibility is an assembly of "minimal" tetrakaidecahedra,[3] each polyhedron having eight doubly-curved hexagonal faces and six plane quadrilateral faces, the angles between adjacent faces being 120°. Such cells could be stacked on a body-centered cubic lattice and would be quite stable. For many years it was believed that soap bubbles actually possessed the shape of this ideal body, and the hypothesis was the starting point for several investigations on the shapes of soap bubbles, biological cells, and metal grains. These investigations have shown, what might have been obvious in the beginning, that if the condition of symmetry is relaxed the tetrakaidecahedron is almost never found. If we retain only the rule that all contacts should be in local surface tension equilibrium and that the assembly should fill space, metal grains may then take a nearly infinite variety of shapes and no single one may be regarded as an archetype. These two conditions, which are fully discussed in one of the previously mentioned papers,[4] lead us to think of a typical grain in an annealed metal as having the following characteristics:

1—A grain may have any number of faces, but usually between nine and eighteen. The faces (each of which is, of course, shared by two grains in the assembly) may have any number of edges, but usually between four and six. Pentagons are by far the most frequent.

2—In the assembly of grains each edge is shared by three faces and by three grains. Each vertex is a point shared by four grains, six faces, and four

W. M. WILLIAMS, formerly with the Institute for the Study of Metals, is now associated with Revere Copper and Brass Co., Rome, N. Y., and C. S. SMITH, Member AIME, is Director, Institute for the Study of Metals, University of Chicago, Chicago.

Discussion on this paper, TP 3275E, may be sent, 2 copies, to AIME by Dec. 1, 1952. Manuscript, Feb. 14, 1952. Philadelphia Meeting, October 1952.

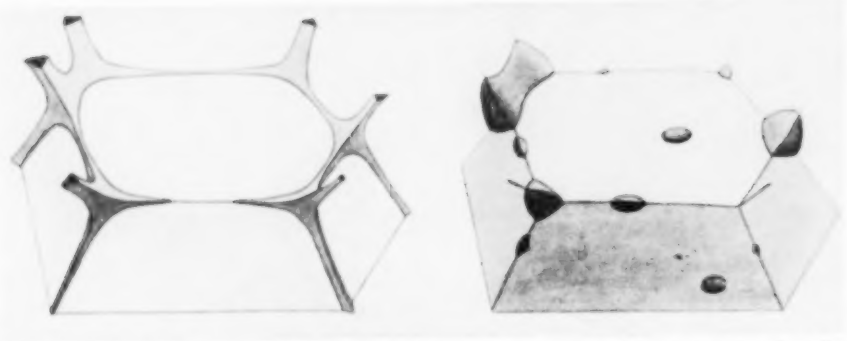

Fig. 1—Sketch showing the anticipated three dimensional distribution of a minor second phase in a polycrystalline alloy. Left, θ about 65°; right, θ about 120°. (Drawing by Barrett[3])

edges. On a single grain, separated from the mass, every vertex is three-rayed.

It is difficult to analyze these concepts in a pure metal because it is accessible only by two-dimensional sections, and extremely laborious successive sectioning is necessary to build up the complete three-dimensional picture. The examination of an intergranular fracture is woefully inadequate, and it seems to be virtually impossible by intergranular corrosion to obtain a complete sample of all of the grains in a given volume. However, it is possible by stereoscopic microradiography of a metal containing a small amount of a second phase to delineate grain edges to get a view of the extended structure and to analyze a sufficient mass of directly connected grains. When a minor second phase in a polycrystalline alloy has a dihedral angle, θ, between 180° and 60°, it will exist as discrete particles at grain corners, edges, and between adjacent faces. When θ is less than 60°, the second phase becomes continuous along all grain edges. As θ decreases, the phase spreads more and more over grain faces until at $\theta = 0°$, each grain is isolated from its neighbor by an envelope of the second phase. Fig. 1 is a drawing by Barrett taken from one of the previously mentioned articles,[3] and shows the distribution of a minor second phase for the two cases where θ is 65° and 120°, respectively. At 60° the gap shown in the face edge would close completely.

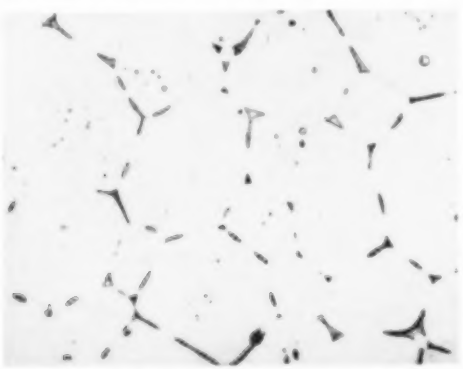

Fig. 2—Micrograph of the polished section of an Al-Sn alloy (5.2 pct Sn) after annealing at 580°C. Dihedral angle ~30°. About 4.5 volume pct liquid. Unetched. X70. Area reduced approximately 50 pct for reproduction.

The Al-Sn alloys are well adapted for such studies. In a study of their microstructure, Ikeuye and Smith[3] found that the dihedral angle of the tin-rich phase (liquid at the annealing temperature) varied from 55° at the eutectic temperature to 0° near the melting point of the aluminum in a manner related to the composition of the second phase. The alloys can be cast, rolled, and annealed easily, have typical polyhedral grain structure, and the difference in X-ray absorption makes radiography easy. They are, moreover, of some industrial importance as bearing materials.[3]

Stereoscopic Microradiography

The technique of microradiography has developed quite rapidly during the last few years,[5-8] and it is now possible even to study segregation in the brasses with the proper choice of radiation.[8] A valuable recent paper[7] reviews the different methods and discusses the variables involved, such as focal spot size, choice of radiation, and the relation of exposure time to the photographic emulsion used.

Stereoscopic principles seem not to have been previously applied in the field of microradiography although they have been successfully applied in many fields in science. In the medical and dental fields, in many branches of industry, and in aerial surveying, stereoscopic photographs at ordinary magnifications are standard. In electron microscopy stereoscopic views are commonplace in deciding the three-dimensional shape of particles and also lend themselves to the accurate determination of surface contours on replicas.[9] The simple rules of stereoscopy are just as easily applied to microradiography.

Method

For the present studies the experimental arrangement was as follows. A beam of "white" radiation from a tungsten target was directed at the specimen and the X-ray shadow registered on a piece of fine grained photographic plate placed in close contact behind the specimen. Two microradiographs were taken of each specimen, the specimen and plate being rotated through an angle of 4° to 6° between the two exposures. In the absence of a tube with a fine focal spot, a 1 mm pinhole was placed as close to the target as possible. The specimen-to-target distance was 10 in. and the tube operated at 50 kv, 20 ma. The exposure time depends not only upon these factors and the specimen absorption, but also upon the kind of photographic plate used. The two most satisfactory types of plate are Eastman-Kodak 649-0,

Table I. Analysis of Grain Shapes

Code No. (Arbitrary)	Total No. of Faces	Number of Faces with n Sides								$\Sigma(6-n)F_n$	Grain Size†
		$n=2$	$n=3$	$n=4$	$n=5$	$n=6$	$n=7$	$n=8$	$n=9$		
W44	6	—	—	6	—	—	—	—	—	12	C
W37	6	—	2	2	2	—	—	—	—	12	A
W5*	7	—	—	5	2	—	—	—	—	12	A
W34	7	—	—	5	2	—	—	—	—	12	A
W33	7	—	—	3	2	—	—	—	—	12	B
E35	7	—	1	3	3	—	—	—	—	12	B
W43	7	—	1	3	3	—	—	—	—	12	B
W4*	8	—	—	4	4	—	—	—	—	12	B
W2*	8	—	1	3	3	1	—	—	—	12	B
E19*	8	1	1	2	3	1	—	—	—	14	B
E4*	9	—	—	3	6	—	—	—	—	12	C
W10*	9	—	—	3	6	—	—	—	—	12	C
E21*	9	—	—	3	6	—	—	—	—	12	B
W19*	9	—	—	4	4	1	—	—	—	12	C
W26	9	—	—	4	4	1	—	—	—	14	A
E9*	9	—	—	5	4	—	—	—	—	12	B
W29	9	—	1	3	3	2	—	—	—	10	C
E6*	9	—	1	2	4	1	1	—	—	12	B
W13*	10	—	—	4	4	2	—	—	—	12	B
W14*	10	—	—	4	4	2	—	—	—	12	B
E27*	10	—	—	4	4	2	—	—	—	12	C
E42	10	—	—	4	4	2	—	—	—	12	B
W20	10	—	—	4	6	2	—	—	—	12	C
W23	10	—	—	4	4	2	—	—	—	12	B
W40	10	—	—	4	4	2	—	—	—	12	C
W41	10	—	—	4	4	2	—	—	—	12	B
W31	10	—	—	2	8	—	—	—	—	12	B
E29*	10	—	—	6	—	4	—	—	—	12	B
E40	10	—	1	4	2	3	—	—	—	12	C
E46	10	—	1	3	3	2	—	—	—	12	C
E44	10	—	2	2	3	2	1	—	—	12	C
E45	10	—	2	3	3	1	1	—	—	14	C
W7*	11	—	—	4	4	3	—	—	—	12	C
E14*	11	—	—	4	4	3	—	—	—	12	C
W16*	11	—	1	4	2	3	1	—	—	12	C
E26*	11	—	1	4	2	3	1	—	—	12	C
E12*	11	—	—	2	8	1	—	—	—	12	C
W24	11	—	—	5	2	4	—	—	—	12	C
E38	11	—	1	2	5	3	—	—	—	12	C
E26*	11	—	1	4	4	1	1	—	—	14	C
E28*	11	—	1	3	3	1	2	1	—	8	C
W8*	12	—	—	4	4	4	—	—	—	12	C
E17*	12	—	—	3	6	3	—	—	—	12	C
W12*	12	—	—	2	8	2	—	—	—	12	C
W35	12	—	—	3	3	3	1	—	—	12	D
E33	12	—	1	3	4	3	1	—	—	12	D
E11*	13	—	—	3	6	4	—	—	—	12	D
W39	13	—	—	1	10	2	—	—	—	12	D
E19*	13	—	—	3	7	2	1	—	—	12	D
W30	13	—	—	4	6	1	2	—	—	12	D
W22	13	—	—	4	5	3	1	—	—	12	D
E7*	13	—	—	6	3	1	3	—	—	12	D
W36	13	—	—	6	2	3	2	—	—	12	D
W18*	13	—	1	5	—	6	1	—	—	12	D
W6*	14	—	—	4	5	4	1	—	—	12	C
E36	14	—	—	4	5	4	1	—	—	12	C
W27	14	—	—	4	5	4	1	—	—	12	D
E15*	14	—	—	3	6	5	—	—	—	12	D
W25	14	—	—	5	4	5	—	—	—	14	D
E23*	14	—	—	2	9	2	1	—	—	12	E
E37	14	—	—	4	7	2	1	—	—	14	D
W15*	14	—	—	4	6	2	2	—	—	12	D
E31	14	—	—	3	2	5	2	—	—	10	D
E1*	14	—	2	4	3	1	3	1	—	12	D
E25*	15	—	—	4	5	5	—	—	—	14	D
W17*	15	—	—	3	6	5	—	—	—	14	C
W3*	15	—	—	2	9	3	1	—	—	12	D
E8*	15	—	—	3	7	4	1	—	—	12	D
E13*	15	—	—	5	4	4	2	—	—	12	E
W1*	15	—	1	2	6	5	1	—	—	12	E
E2*	15	—	1	3	4	6	1	—	—	12	D
E22*	15	—	2	4	6	2	2	—	—	16	D
E39	15	—	—	7	3	2	1	2	—	12	C
E18*	15	—	2	3	5	2	1	2	—	12	D
E5*	16	—	—	3	7	5	1	—	—	12	D
E34	16	—	—	4	7	4	1	—	—	14	E
W22	16	—	—	4	6	4	2	—	—	12	E
E6*	16	—	—	3	8	3	—	2	—	10	E
E16*	16	—	—	6	5	3	1	1	—	14	D
E30*	16	—	1	5	3	3	4	—	—	12	D
W11*	16	—	2	2	7	2	1	2	—	12	E
E24*	17	—	—	2	8	6	—	—	—	14	D
E32	17	—	2	4	5	5	2	—	1	12	E
W42	17	—	3	2	3	7	1	—	1	12	E
W38	18	—	—	3	9	3	3	—	—	12	E
W28	18	—	2	3	7	3	3	—	—	16	F
B*	19	—	—	3	7	8	1	—	—	12	E
W9*	19	—	1	3	5	5	2	1	—	14	F
E43	20	—	1	5	4	7	3	—	—	14	E
E41	20	—	1	4	6	6	1	2	—	12	E
W21	21	—	1	5	6	6	3	2	—	12	G

* Grains illustrated in Figs. 4 and 5.

† Grain size obtained by approximate matching of volume of stereo image of grains at magnification 30 with balls of varying dimensions. Size designated as follows:

0.106 mm. $<$ A $<$ 0.212 $<$ B $<$ 0.318 $<$ C $<$ 0.423 $<$ D $<$ 0.529 $<$ E $<$ 0.635 $<$ F $<$ 0.740 $<$ G $<$ 0.846 mm.

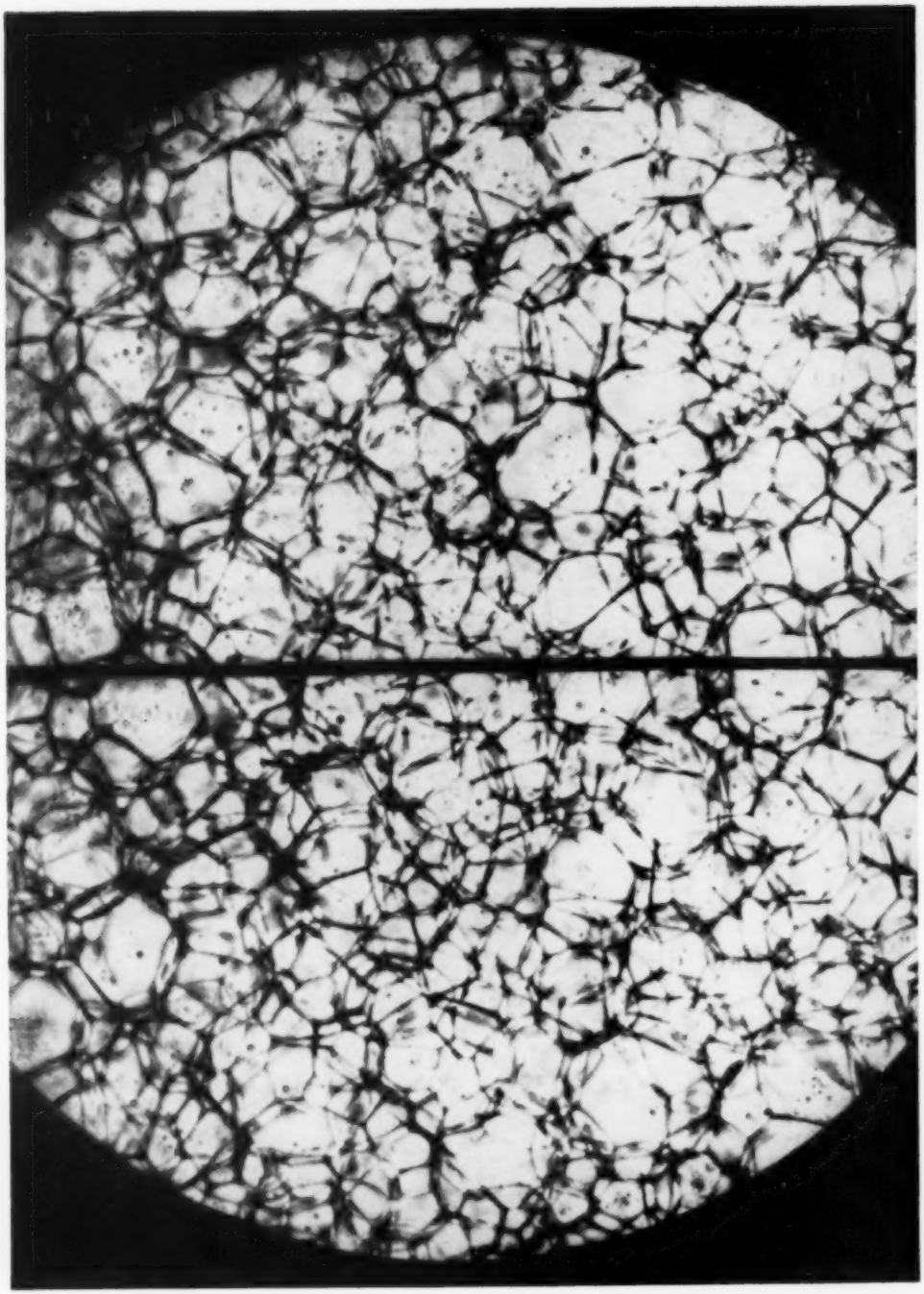

Fig. 3a

Fig. 3a and b—Stereoscopic view through a sample 1 mm thick of the Al-Sn alloy shown in Fig. 2. Stereo angle 6°. (Tin, dark.

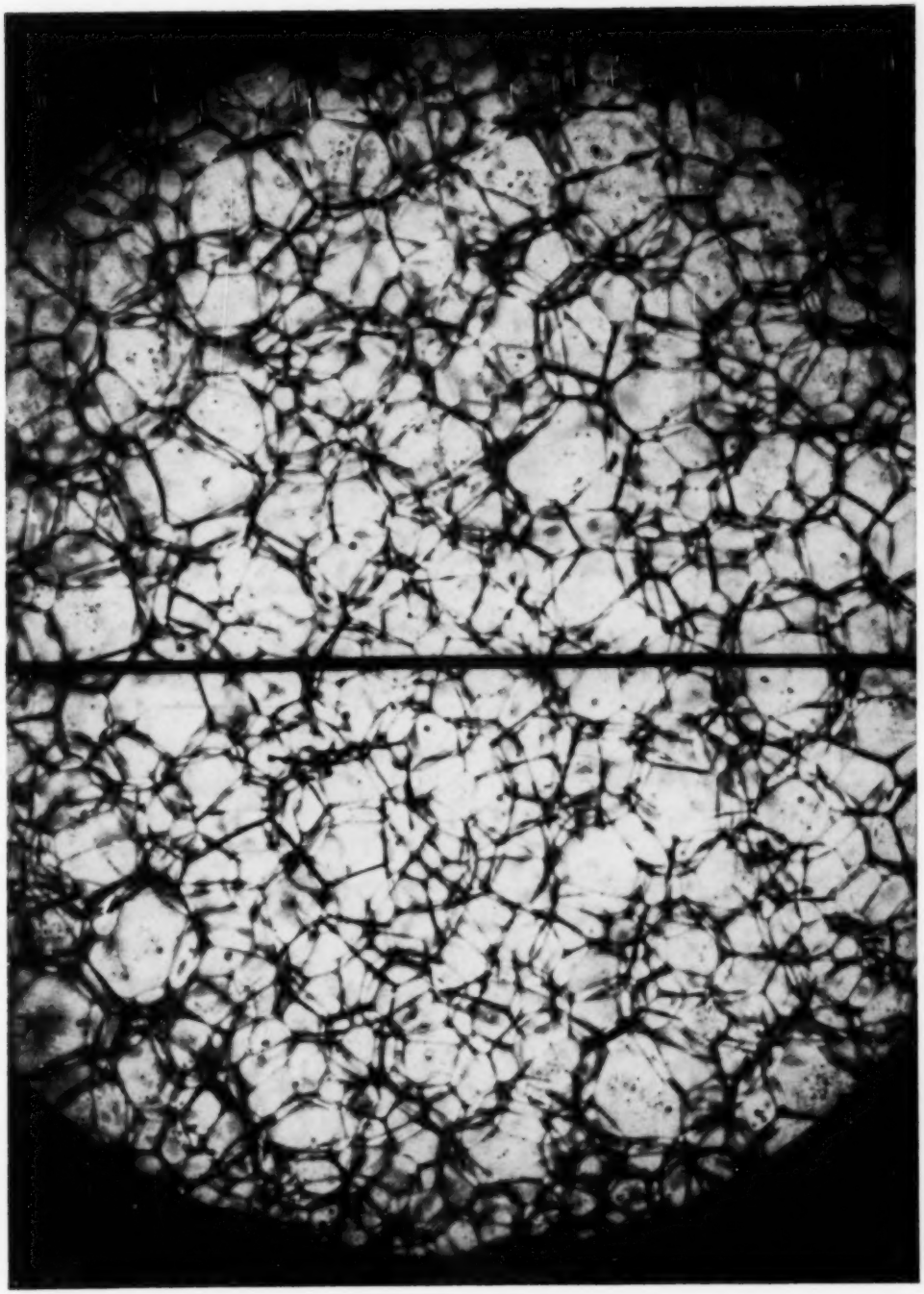

Fig. 3b

aluminum, light). X35. The pair of photographs should be viewed in a stereoscope of the type used in medical radiography.

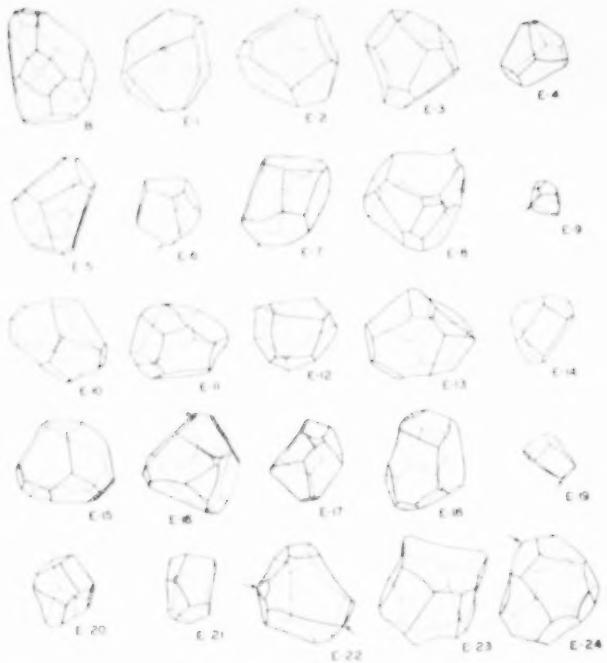

Fig. 4 — Camera lucida drawings of 25 grains. Arrows indicate abnormal vertices. X50. Area reduced approximately 60 pct for reproduction.

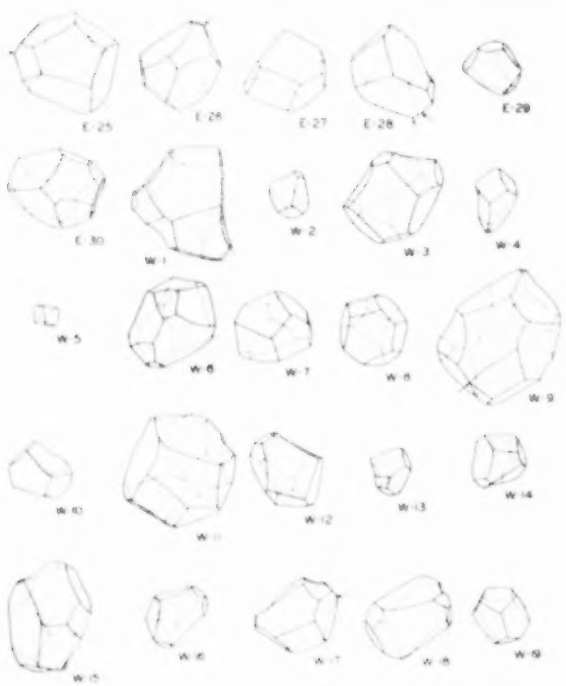

Fig. 5 — Camera lucida drawings of 25 grains. Arrows indicate abnormal vertices. X50. Area reduced approximately 60 pct for reproduction.

which may be enlarged up to X700, and Eastman-Kodak 548-0, which may be enlarged X400 before the photographic grain becomes objectionable. Typical exposure times with the X-ray conditions mentioned above, for a thickness of 1 mm of aluminum, were 1 hr for 649-0 plates and 30 min for 548-0 plates. Kodak D.19 contrast developer was used for both kinds of plates; development by inspection, usually 5 to 8 min.

Each pair of microradiographs obtained in this way was enlarged and photographed using a metallographic microscope with transmitted light, and the enlargements viewed in a stereoscope.

Preparation of Polycrystalline Al-Sn Alloy

For an analysis of grain shape, a specimen of Al-Sn alloy (nominally 5.2 wt pct or 1.2 atomic pct Sn) was cut from a swaged rod, annealed at 580°C for 16 hr and quenched. For radiography the sample was then sectioned and abraded down to a thickness of 1 mm, the final polish being on 4/0 emery paper. This gave a specimen about four grains thick. Metallographic examination (Fig. 2) showed, as anticipated, that the once-liquid tin phase was concentrated in triangular areas at grain corners (triangular prisms at edges in three dimensions) and that the dihedral angle was somewhat less than 60°. Some tin was in discrete spherical particles in the center of the grains, and other particles on grain faces appeared to be lens-shaped.

The specimen was radiographed as described above and enlargements of the radiographs made at X30. The stereoscopic pair of photographs, showing the whole area examined, is given in Fig. 3a and b. The viewing of these in a suitable stereoscope such as those found in medical radiography installations is strongly recommended for the structure is spectacular. Smaller photographs for use in a hand stereoscope are reproduced later in this paper*

* Many individuals can view these pairs without optical aid by allowing eye directions to drift apart until the right picture seen with the left eye fuses with the left picture seen by the right eye. To assist in establishing the correct registry the small black arrowheads have been placed in each photograph.

Analysis of Grain Shapes in the Alloy

The delineation of the almost pure aluminum grains by the tin-rich liquid phase was so unmistakable that it was possible to make an analysis of a large fraction of the grains in the sample shown in Fig. 3. By the use of a camera lucida or by projection on the ground glass of a photomicrographic apparatus, enlarged drawings were made of each of 91 contiguous grains in the sample and an analysis made of their shapes. The grains studied comprised almost all the complete grains shown in Fig. 3, but omitted those of which part was cut off by the surface. The grains analyzed therefore occupied an irregularly-shaped volume flattened in a direction normal to the plane of the photograph and lying transversely to the original direction of deformation in swaging. Care was taken to include every grain in the volume. In the examination of these grains it sometimes happened that a corner, or some other point of interest was obscured by another corner or edge immediately above it and in order to remove any uncertainties of this kind another stereoscopic view from a different standpoint was used. That is, if one stereoscopic view was made up of two microradiographs taken with the plane of the specimen at angle of 0° and 6° to the X-ray beam, a different view was obtained from a second pair made by combining the 6° photograph with a third

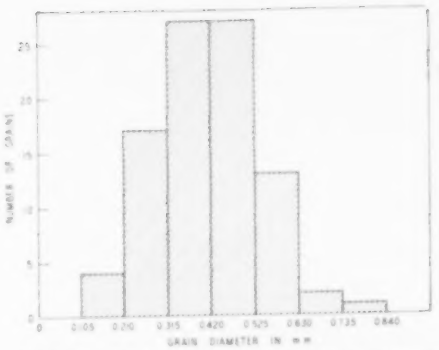

Fig. 6—Approximate distribution of grain sizes in the sample shown in Fig. 3.

one taken at 12°. Using both sets of photographs, the shape of every grain in the volume chosen could be drawn with certainty. The first 50 of the grains drawn are shown in Figs. 4 and 5, and illustrate the variety of shapes and sizes recorded. Stereoscopic pairs of drawings of two grains are shown later (Figs. 9 and 10).

The complete record of grain shape for the 91 grains is given in Table I, which shows for each grain the combination of faces, the number of faces and the approximate size. The grain size was obtained in the following way: A series of steel balls, ranging in diameter in $\frac{1}{8}$ in. steps from $\frac{1}{8}$ to 1 in., was compared with each grain in the enlarged three-dimensional image of the stereoscope, and that ball selected which matched most closely the apparent actual volume of the grain being examined. More exact measurement of maximum and minimum grain diameter would have been possible from the three-dimensional images but was not deemed necessary for the present purpose.† The grain size was designated *A* for a grain intermediate in size with a $\frac{1}{8}$ and a $\frac{1}{4}$ in. ball, *B* for a grain size between $\frac{1}{4}$ and $\frac{3}{8}$ in. and so on to *G* with a grain size between $\frac{7}{8}$ and 1 in. An attempt was made to match actual grain volumes with the balls, and the grain sizes

† This technique of matching a measured object of known dimensions with the stereoscopic image was borrowed from medical radiography. Obstetricians sometimes match a disk with the maximum dimensions of stereoscopic image of the head of a fetus and by experiment ascertain whether it can pass the available space between pelvic bones in order to decide whether a Caesarean operation is necessary. The authors are indebted to Dr. Harold W. Jacox of Columbia-Presbyterian Hospital, New York, for an outline of this technique. It is described in detail by H. C. Moloy and C. M. Steer: *American Journal of Obstetrics and Gynecology* (1950-60, No. 5, pp. 1135-1142.

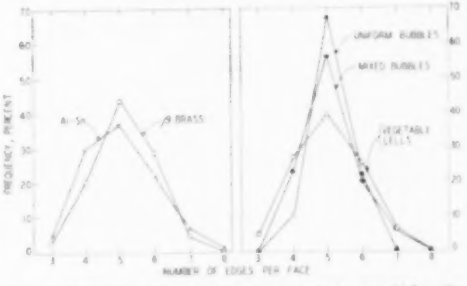

Fig. 7—Frequency of various polygonal faces in the Al-Sn alloy compared with those in soap froth, in vegetable cells, and in β brass.

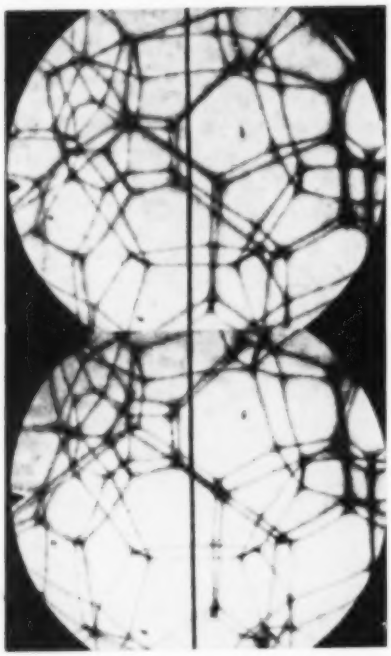

Fig. 8—Stereoscopic radiograph of a soap froth. Stereo angle 4°. X12.

listed in Table I therefore represent the approximate distribution of grain sizes in three dimensions. When an allowance is made for the magnification of the microradiographs (X30), it is seen that the range of actual grain diameters goes from 0.105 to 0.840 mm. The letter representing the approximate grain diameter of every grain is included in Table I, and it will be seen that, as might be expected, the grains of larger diameter are those with the greater number of faces. A frequency plot of the various sizes is shown in Fig. 6. Fig. 7 shows the frequency with which various polygons appeared among the grain faces. This also includes for comparison the data on bubbles of uniform and nonuniform size (from Matzke,[1] Matzke and Nestler[2]), vegetable cells (from Matzke[1]) and grains of β brass (after Desch[3]). In all cases the most frequently occurring type of face is the pentagon, with quadrilaterals and hexagons in close competition. The close similarity between metal grains and soap bubbles is further made evident by a comparison of the microradiograph of grains in Fig. 3 with the microradiograph[2] of soap bubbles shown in Fig. 8.

[2] This was radiographed under similar conditions to the Al-Sn sample except that the voltage was only 30 kv and lantern-slide plates were used since less resolution was needed. To increase contrast, potassium argentocyanide was added to the soap solution.

It will be seen from Table I that grains in the sample studied have from 6 to 23 sides and there is a wide variety of combinations of faces in the various grains. While some combinations appear more than once (notably the ten-hedron with four quadrilateral, four pentagonal, and two hexagonal faces which occurs eight times), no particular combination occurred so often as to constitute a "type." This is hardly surprising when the range of sizes that occurs and the random nature of contacts between grains are considered. The unit of structure is ideally not the grain but rather the tetrahedral junction of four grain edges which can be connected together in innumerable ways without structural symmetry or exact repetition of detail.

Departure from Ideal Surface Tension Array

In a sample like the present one, which has been annealed for a long time at a high temperature to allow grains to grow to a large size and the average curvature to become small, it would be expected that occasional corners would have abnormal junctions because of differences of surface energy or because of the presence of inclusions. These can be found either by direct examination of the corners as seen in the stereophotographs, or by topological checks on the shapes of individual grains.

Most of the corners in the specimen are composed of simple tetrahedral junctions of edges and most grains are of the simple surface tension type with

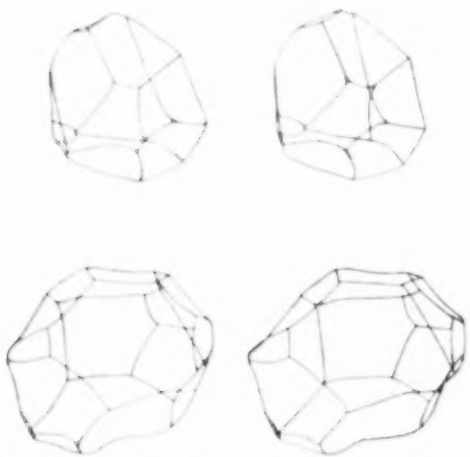

Fig. 9—Stereoscopic drawings of typical grains with normal three-ray vertices. X90. Area reduced approximately 60 pct for reproduction.

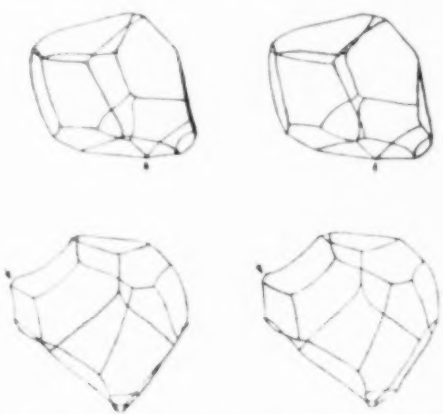

Fig. 10—Stereoscopic drawings of grains with abnormal corners. X90. Area reduced approximately 60 pct for reproduction.

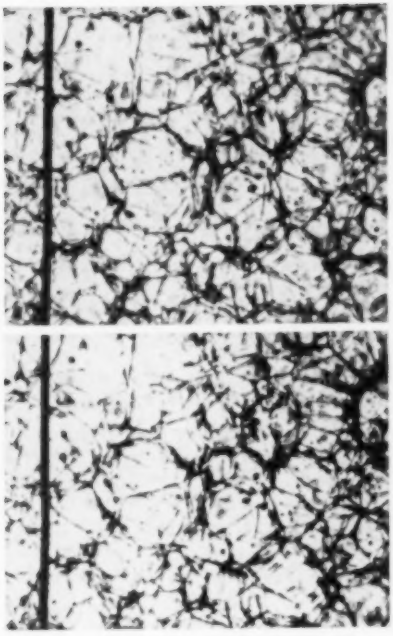

a—350°C. Dihedral angle 55°, 2.2 volume pct liquid.

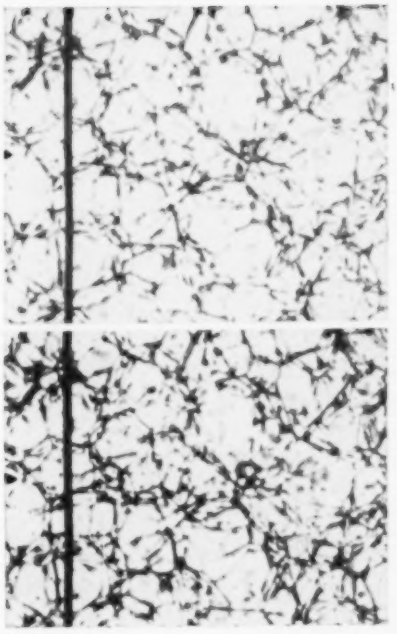

b—500°C. Dihedral angle 45°, 2.5 volume pct liquid.

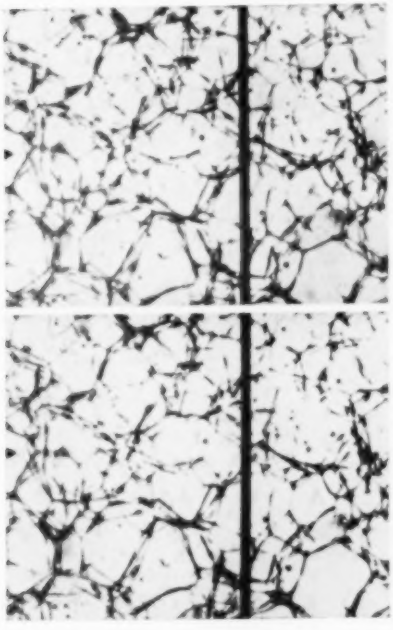

c—600°C. Dihedral angle 10°, 7.3 volume pct liquid.

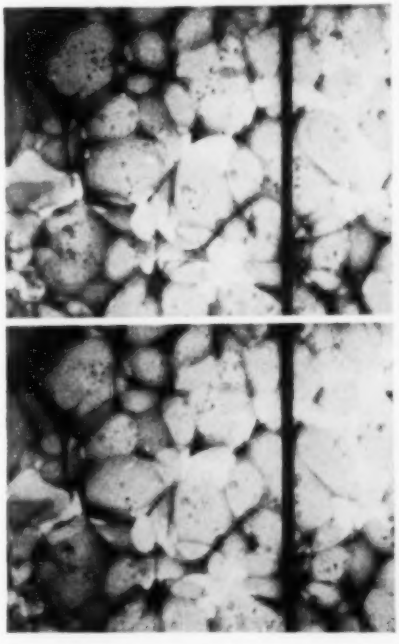

d—640°C. Dihedral angle 0°, 38 volume pct liquid.

Fig. 11—Stereoscopic microradiographs of Al-Sn alloy (5.2 wt pct Sn) quenched after annealing 16 hr at various temperatures. Stereo angle 4°. Specimens 1 mm thick. X25.

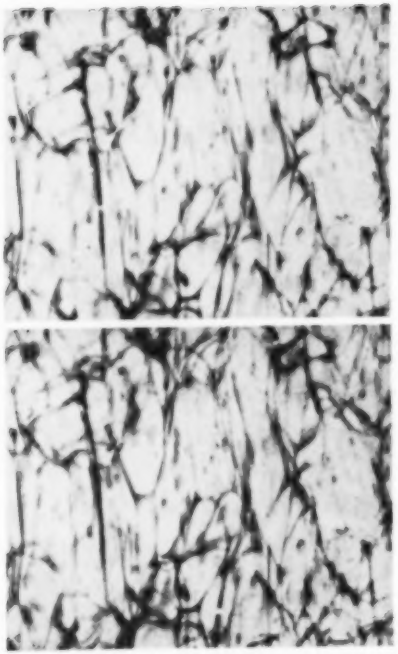

Fig. 12—Stereoscopic microradiograph of Al Sn alloy as Fig. 3, cold rolled to 66 pct reduction. Stereo angle 4°. X35

three faces and three edges meeting at each vertex, as shown on the typical grains in Fig. 9.

Close examination of the structure reveals, however, that there are nevertheless some corners which are abnormal in that more or less than four edges meet at a point. If the grains meeting at such a corner are drawn individually, this abnormal behavior will appear as an abnormal vertex, i.e., not three-rayed, on one of the separate grains. Fig. 10 shows two such abnormal grains, one resulting from five grains and five edges meeting in space instead of the usual four, and the other with a two-rayed vertex resulting from three edges meeting in space.

The number of abnormal corners throughout the assembly was 19. Since the total number of corners in the assembly (derived from Table II) was 475, the fraction of abnormal corners is 4 pct. A few of these may be corners where more than the usual number of edges have come together only temporarily during the process of grain growth, and on continued annealing the corners and edges would soon have readjusted themselves to the new stable surface tension configuration. The majority of the abnormalities, however, probably result from the grain growth blocking mechanisms mentioned above. The three-ray corners (two-ray vertices in separate grains) could only result from the action of inclusions.

The figures listed in Table I in the column under $\Sigma(6-n)F_n$ have the following topological significance.[7] If, on an isolated polyhedron, F_n is the number of faces having n sides, E the number of edges, and C the number of corners, then:

$$\Sigma F_n - E + C = 2 \quad \text{(Euler's law)}$$

Since each edge is shared by two polygons:

$$E = \frac{\Sigma n F_n}{2}$$

If consideration is limited only to those polyhedra which have three-rayed vertices, then:

$$C = \frac{\Sigma n F_n}{3}$$

and hence:

$$\Sigma F_n - \frac{\Sigma n F_n}{2} + \frac{\Sigma n F_n}{3} = 2$$

or, simplifying:

$$\Sigma(6-n)F_n = 12$$

This equation applies to grains with only three-rayed vertices and hence conformity to it by a given grain is a useful check of conformity to surface tension rules. As can be seen from Table I, most of the 91 grains examined satisfy this equation. However, there is a significant minority of nonconformists which result from the abnormal corners referred to above.

Table II shows the total numbers and frequencies of the different kinds of faces (see also Fig. 7) and the results calculated from these data, viz., the average number of edges per face, the average number of corners per cell, and the other quantities whose topological significance has been pointed out by one of the authors.[7] The value of n, the average number of edges per polygon, is calculated to be 5.02 and compares favorably with a soap froth or assembly of biological cells, although deviating from the figure of 5.14 for ideal stacking. The average number of faces to the average grain, considered as a separate polyhedron, is 12.48. The quantity $P/B - C/B$ (where C is the number of corners,* P the number of polygons, and B the number of bodies in the three-dimensional array) is unity when all the grains, taken separately, have three-rayed vertices, and $(6 - C/B)$ is a test of the departure from the most economical stacking of the grains and should be zero when there is maximum sharing of faces and corners. The value of $(P/B - C/B)$ in the present experiment is 1.02, confirming that the number of separated grains having abnormal ver-

Table II Summary of Grain Face Shapes and Average Topological Characteristics

n	ΣF_n	Pct	n			
			ΣnF_n	6029	n	5.02
			P	1130		
3	1	0.1				
4	40	3.8	P	1130		
5	309	29.6	B	2x91		6.24
6	617	59.2	C	6029		
7	248	23.8	B	12x91		5.22
8	31	4.2				
9	36	3.4	$\frac{C}{B}$			0.78
10	2	0.2				
			$\frac{P}{B} - \frac{C}{B}$			1.02
ΣF_n	1130	100.0				

* It should be pointed out that the value used is computed from the number of polygon corners on the assumption that the corners of six polygons meet at every corner in three dimensions. This is not strictly true, and it would have been preferable to have counted actual corners.

tices (i.e., those that are not three-rayed) is small. The value of $(6 - C/B)$ is 0.78, definitely larger than the values obtained on uniform bubbles or cells (0.149 and 0.107, respectively) and probably associated with the wide distribution of size of grain in the array.

Some Other Applications of Stereomicroradiography

Fig. 11 shows a series of stereomicroradiographs of the Al-Sn alloy (5.2 pct Sn) used for the main investigation described above, but quenched from different temperatures. As the annealing temperature increases from 350° to 640°C, the dihedral angle changes, at first slowly and then more rapidly, from approximately 55° to 0°, while the amount of liquid increases from 2.2 to 38 volume pct. The corresponding effect on the three-dimensional microstructure is shown in these pictures. At the lowest temperature, because of the presence of some boundaries of lower energy than the average, there are some dihedral angles less than 60° and some edges not fully penetrated by the liquid. As the annealing temperature increases, all edges are delineated by the liquid phase, which also spreads more and more over the faces until near the melting point the solid grains become rounded and seem to float in the liquid which surrounds them. The contraction which the liquid phase undergoes on quenching is evident from the specimen annealed at 640°C (Fig. 11d). The spheres of liquid trapped in the centers of the grains show transparent "bubbles" occupying about 10 pct of their volume—the contraction due to the change in density in going from liquid at 640°C to the eutectic temperature (232°C). There are also areas, white on the photograph, where all of the liquid between the grains has been drained away by shrinkage or simply by gravity.

Fig. 12 shows the same Al-Sn alloy that was used for the grain shape experiments described above but cold-rolled to 66 pct reduction in area after it had been annealed at 580°C. The distorted shape of each grain is clearly visible. By a sequence of such photographs at different reductions it is possible to measure the deformation of individual grains and to study the interaction of neighbors upon each other. In like manner the advance of a fatigue crack or the penetration of corrosion areas could be followed. The addition of the third dimension, as well as the fact that the new technique is nondestructive, will greatly facilitate many kinds of studies. It may even prove of value in biological investigations where, by the proper choice of radiation, aggregates of many cells may be studied more conveniently than by serial sectioning.

Summary

Using stereoscopic microradiography, the shape of 91 contiguous grains in a worked and annealed Al-Sn alloy have been analyzed and some topological quantities calculated. The alloy was selected because of the opacity of tin to X-rays and because the energy of its interface with aluminum crystals causes it to spread along the edges of every grain and so to delineate it clearly. The grain shapes are believed to be typical of polycrystalline metals annealed to a large grain size. It is shown that the grains are closely analogous in shape to soap bubbles in a froth where surface tension and space-filling alone determine the structure. The average grain has 12.48 faces and the average face has 5.02 edges. A small but significant fraction of corners is observed (4 pct) at which the number of meeting edges differs from that of the typical tetrahedral junctions resulting from equal surface tensions, which probably indicates both the presence of inclusions and the variation of grain boundary energy with orientation.

Other examples of stereomicroradiography are given showing the effect of surface tension and of deformation. The authors believe that stereomicroradiography will find increasing application in metallurgical research, for the addition of the third dimension adds enormously to the ease of understanding the true structure of a metal.

References

[1] C. H. Desch: The Solidification of Metals from the Liquid State. *Journal* Inst. Metals (1919) **22**, pp. 241-263.

[2] D. Harker and E. Parker: Grain Shape and Grain Growth. *Trans.* A.S.M. (1945) **34**, pp. 156-195.

[3] C. S. Smith: Grains, Phases and Interfaces—An Interpretation of Microstructure. *Trans.* AIME (1948) **175**, pp. 15-51; METALS TECHNOLOGY (June 1948).

[4] C. S. Smith: The Shape of Metal Grains, with Some Other Metallurgical Applications of Topology (and discussion). Symposium on Interfaces, October 1951. A.S.M.

[5] F. T. Lewis: The Typical Shape of Polyhedral Cells in Vegetable Parenchyma and the Restoration of that Shape Following Cell Division. *Proc.* Amer. Academy of Arts and Sciences (1925) **61**, pp. 1-34.

[6] F. T. Lewis: The Analogous Shapes of Cells and Bubbles. *Proc.* Amer. Academy of Arts and Sciences (1949) **77**, pp. 147-186.

[7] E. B. Matzke: The Three-Dimensional Shape of Bubbles in Foam—An Analysis of the Role of Surface Forces in Three-Dimensional Cell Shape Determination. *American Journal of Botany* (1946) **33**, No. 1, pp. 58-80.

[8] E. B. Matzke and J. Nestler: Volume-Shape Relationships in Variant Foams. A Further Study of the Role of Surface Forces in Three-Dimensional Cell Shape Determination. *American Journal of Botany* (1946) **33**, No. 2, pp. 130-144.

[9] Lord Kelvin: On the Division of Space with Minimum Partitional Area. *Philosophical Magazine* (1887) **24**, pp. 503-514.

[10] K. K. Ikeuye and C. S. Smith: Studies of Interface Energies in Some Aluminum and Copper Alloys. *Trans.* AIME (1949) **185**, pp. 762-768; JOURNAL OF METALS (October 1949).

[11] H. K. Hardy, E. A. Liddiard, J. Y. Higgs, and J. W. Cuthbertson: Improved Aluminum Bearings (Al-Sn and Al-Sn-Cu Alloys). *Metal Progress* (1951) **60**, No. 4, pp. 97-103.

[12] G. L. Clark and S. T. Gross: Technique and Applications of Industrial Microradiography. *Industrial and Engineering Chemistry* Anal. Ed. (1942) **14**, No. 8, pp. 676-683.

[13] S. E. Maddigan: Microradiography. *Industrial Radiography* (1946) **4**, No. 4, pp. 22-25.

[14] E. I. Salkovitz: Microradiography with Routine X-ray Equipment. *Metal Progress* (1946) **50**, No. 5, pp. 1091-1096.

[15] J. G. Kura, L. W. Eastwood, and J. R. Doig: Microradiography Applied to Leaded Copper-Base Alloys. *Foundry* (1951) **79**, No. 9, pp. 90-91.

[16] A. Taylor: Intense Gallium X-rays for Microradiography and Diffraction Investigations. *Nature* (1951) **168**, No. 4272, pp. 471-472.

[17] G. A. Homes and J. Gouzou: Les ressources de la microradiographie dans les problemes metallurgiques. *Revue Metallurgie* (1951) **48**, pp. 251-261.

[18] R. D. Heidenreich and L. A. Mathewson: Electron Microscopic Determination of Surface Elevations and Orientations. *Journal of Applied Physics* (1944) **15**, No. 5, pp. 423-435.

Titanium-Copper Binary Phase Diagram

by A. Joukainen, N. J. Grant, and C. F. Floe

ACCORDING to Guertler,[1] Smith and Hamilton were the first to study the Cu-Ti alloy system, but because of the presence of large amounts of impurities their data are inconclusive. Hensel and Larsen[2] in 1930 and Kroll[3] in 1931 determined the high copper end of the diagram. In 1939 Laves and Wallbaum,[4] in a short summary of compound determinations in titanium binary alloys, mentioned the existence of a face-centered cubic compound, Ti_2Cu, with 96 atoms per unit cell, and also a compound, $TiCu_4$, which was said to have a deformed hexagonal close-packed structure in which ordering had been observed. The existence of a compound, $TiCu_3$, was also found but the crystal structure was not determined.

Craighead, Simmons, and Eastwood[5] determined the effect of copper on the allotropic transformation in titanium. The investigation was limited to alloys containing from 0 to 5 pct Cu, using titanium of fairly high impurity content.

Experimental Procedure

The methods used for determination of the diagram included metallographic examination and X-ray and thermal analyses. The system was first worked out using the higher purity "Process A" sponge titanium and oxygen-free copper. The high titanium region was next determined more accurately using iodide titanium and vacuum-melted, oxygen-free copper.

Preparation of Alloys. The alloys were prepared by arc melting under prepurified helium atmospheres in water-cooled copper crucibles. The high purity iodide titanium alloys were prepared by melting three compositions along with a specimen of unalloyed titanium in a single charge. A multiple crucible was used which consisted of a copper plate with four cup-like depressions. The unalloyed titanium was melted first and acted as a getter for any oxygen and nitrogen in the melting chamber. Since these elements harden titanium, the hardness of the standard specimen was an index of the highest probable contamination of the alloy melts.

The sponge titanium alloy melts weighed from 100 to 200 g each and the iodide titanium melts from 20 to 25 g. In order to insure greater homogeneity most of the alloys were melted, turned, and remelted twice. The larger buttons made from sponge titanium were sectioned or crushed before remelting. These alloys up to 30 pct Cu were further homogenized by forging at 925°C. They forged readily up to 20 pct Cu but numerous cracks were formed in the alloys containing from 20 to 30 pct. Above 30 pct Cu the sponge titanium alloys were homogenized by heating for 200 hr at 850°C under prepurified helium. Similarly, the iodide-grade titanium alloys containing up to 3 pct Cu were homogenized at 1000°C for 24 hr and all others at 880°C for 200 hr.

Fig. 1—Typical thermal analysis cooling curves for Ti-Cu alloys. The percentage of copper in each alloy is indicated at the top.

A. JOUKAINEN is associated with Mechanical Section, Design Dept., E. I. du Pont de Nemours & Co., Inc., Wilmington, and N. J. GRANT and C. F. FLOE, Members AIME, are with the Dept. of Metallurgy, Massachusetts Institute of Technology, Cambridge, Mass.

Discussion on this paper, TP 3272E, may be sent, 2 copies, to AIME by Dec. 1, 1952. Manuscript, Dec. 13, 1951. Philadelphia Meeting, October 1952.

This paper represents part of a thesis by A. Joukainen submitted in partial fulfillment of requirements for the degree of Metallurgical Engineer to Massachusetts Institute of Technology.

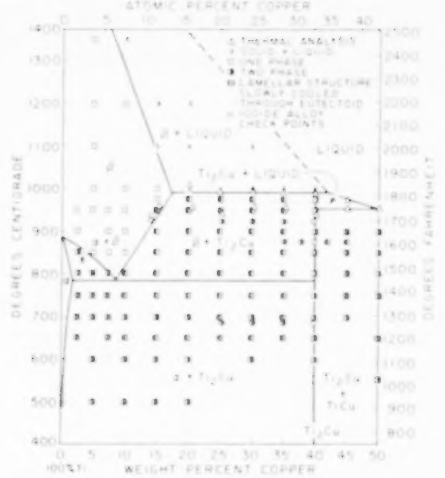

Fig. 2—Ti Cu phase diagram from 0 to 50 pct Cu. Alloys made from Process A sponge titanium and oxygen-free copper.

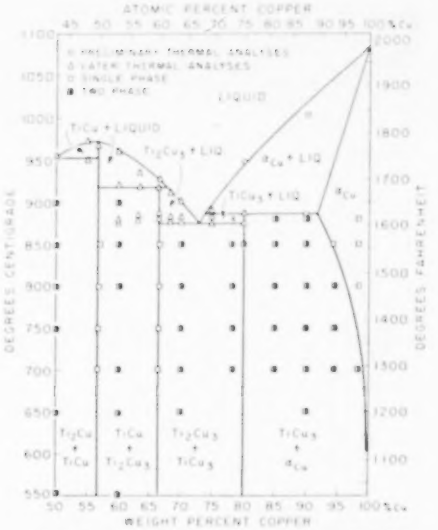

Fig. 3—Ti Cu phase diagram from 50 to 100 pct Cu. Alloys made from Process A sponge titanium and oxygen-free copper.

Analyses for copper on the homogenized alloys showed that the nominal composition was always obtained within less than 1 pct. Some of the forged alloys were also checked for nitrogen by wet analysis and showed values varying from 0.009 to 0.023 pct.

Heat Treatment of Alloys: For metallographic examination and X-ray analysis, specimens of the homogenized alloys were heated at various temperatures below the liquidus and either cooled slowly or quenched in water. This treatment made it possible to determine phases present at various temperatures. The sponge titanium alloys were heated in a tube furnace controlled to ±10°C using a prepurified helium atmosphere. To reduce contamination the procedure of evacuating to 10⁻³ mm of mercury and flushing with prepurified helium was repeated three times before each heat treatment.

The heat treatment of the iodide titanium alloys was accomplished by first sealing the specimens off in evacuated Vycor tubes. These were then heated in a laboratory muffle furnace, which was almost filled with refractory brick, leaving only a small cavity in the center for the Vycor tube and thermocouple. In this way the specimen temperature could be maintained at ±0.5°C. Quenching was accomplished by withdrawing the tube and breaking it under water.

Metallographic Examination: The heat-treated specimens were prepared for metallographic examination by standard methods. Alloys containing up to 60 pct Cu were etched with aqueous solutions of hydrofluoric acid and nitric acid. For higher copper alloys the most satisfactory etch was a solution of 5 pct hydrofluoric acid added to a solution of 2 g of potassium dichromate, 4 g of sodium chloride, 8 cc of sulphuric acid, and 100 cc of water.

X-Ray Analysis: X-ray diffraction patterns were

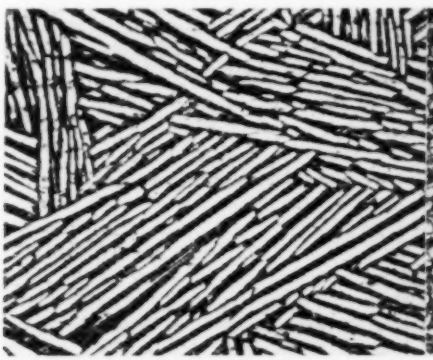

Fig. 4—Microstructure of a hypereutectoid alloy (4.85 pct Cu) consisting of primary α and a eutectoid of α and Ti Cu. Alloy homogenized at 900°C, slowly cooled to 750°C, held 25 hr, and brine quenched. X100.

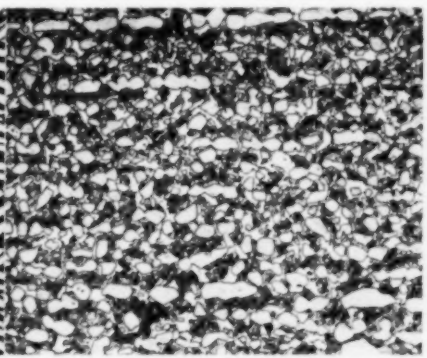

Fig. 5—Microstructure of a hypereutectoid alloy (14.5 pct Cu) consisting of primary Ti Cu and a eutectoid of α and Ti Cu. Alloy homogenized at 900°C, slowly cooled to 750°C, held 25 hr, and brine quenched. X100.

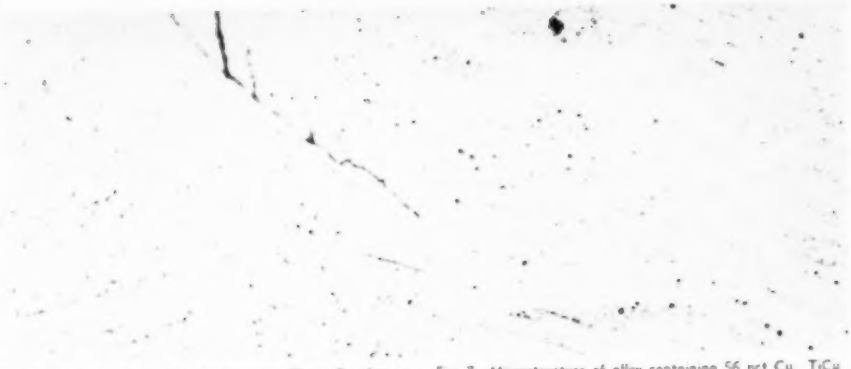

Fig. 6—Microstructure of alloy containing 40 pct Cu. Large grains of Ti_2Cu plus small particles of a second phase. Homogenized at 850° C for 200 hr and brine quenched. X100.

Fig. 7—Microstructure of alloy containing 56 pct Cu. TiCu plus small amounts of a second phase. Homogenized at 850° C for 200 hr and brine quenched. X100.

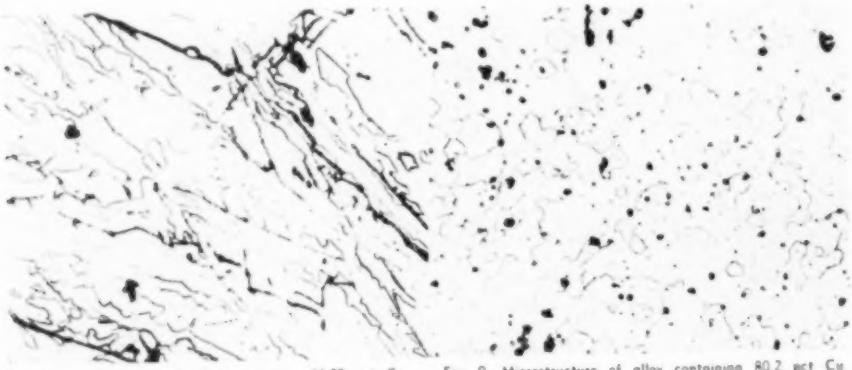

Fig. 8—Microstructure of alloy containing 66.25 pct Cu. Light grains of Ti_2Cu_3. Homogenized at 850° C for 200 hr and brine quenched. X100.

Fig. 9—Microstructure of alloy containing 80.2 pct Cu. Light grains of $TiCu_4$ plus small amounts of a second phase. Homogenized at 850° C for 200 hr and brine quenched. X100.

made using CuKα radiation. A range of angles of 2θ from 34° to 86° was obtained with a Norelco recording spectrometer. The specimens, which were the same as those used for metallographic examination, were rotated during exposure.

Thermal Analysis: Except for a few preliminary results in which induction melting was used, all thermal analyses were made in a Globar tube furnace under prepurified helium atmospheres. Specimens of approximately 20 g each were prepared by crushing arc-melted alloys. Melting was carried out in small, dense, stabilized zirconia crucibles embedded in alumina and contained within larger alumina crucibles. Tantalum sheet and sponge titanium were placed over the inner crucible to act as getters for oxygen and nitrogen. Temperatures were measured with a chromel-alumel thermocouple in an alundum tube.

No appreciable attack on the zirconia crucibles was observed and the alundum thermocouple tube was only lightly attacked. The upper surfaces of the melts were free of slag and bright in color.

All thermal analyses runs were repeated to give two heating and two cooling curves. Typical cooling cycles are shown in Fig. 1. In most instances the hysteresis on heating and cooling was less than ±5° C.

Experimental Results

Sponge Titanium-Base Alloys: Alloys were made up at intervals of 5 pct from pure titanium to pure copper. Intermediate alloys were also prepared, particularly in the vicinity of critical points. A summary of the results obtained for the high titanium side of the system is shown in Fig. 2 and for the high copper side in Fig. 3. A few iodide titanium specimens are also included. The structures indicated were determined on homogenized samples by both metallographic and X-ray analyses.

The eutectoid structures were developed by furnace cooling from the β or β plus Ti_2Cu fields. The reaction is sluggish and slow cooling rates are necessary to obtain equilibrium structures. Micrographs of typical alloys on both sides of the eutectoid point are shown in Figs. 4 and 5.

For phase determinations above the eutectoid temperature, X-ray analysis could not be used. Even

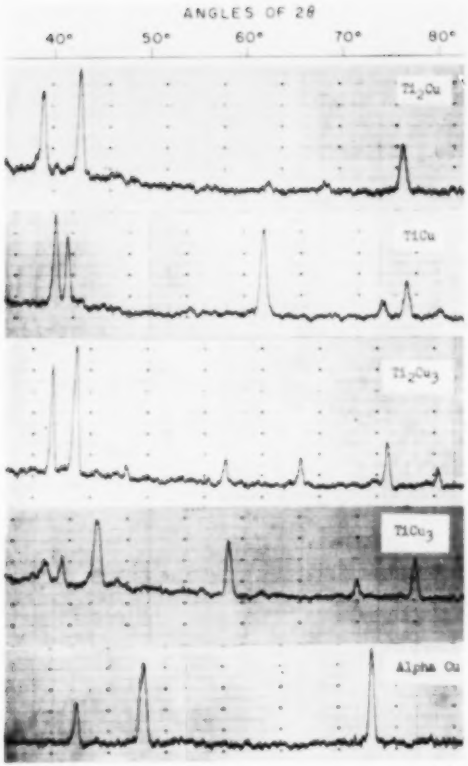

Fig. 10—X ray patterns of alloys at approximate composition of 40 pct Cu (Ti_2Cu), 57 pct Cu (TiCu), 66.5 pct Cu (Ti_2Cu_3), 80 pct Cu ($TiCu_3$), and 98 pct Cu (α Cu). Specimens homogenized 200 hr at 850°C and brine quenched.

the most drastic quenching of β solid solutions resulted in producing a supersaturated acicular α structure by a martensitic type reaction. Reheating of such structures below the eutectoid allowed Ti_2Cu to form, and all specimens up to 40 pct Cu (Ti_2Cu) treated in this manner gave X-ray patterns composed of lines for both α and Ti_2Cu.

Four intermetallic compounds were found in the system, Ti_2Cu, TiCu, Ti_2Cu_3, and $TiCu_3$. Difficulty was experienced in obtaining single-phase structures in the alloys of stoichiometric composition even after very long annealing treatments for all compounds except Ti_2Cu. The Ti_2Cu_3 compound in particular always showed a duplex metallographic structure even though X-ray analysis showed the presence of only one phase. As a check, a diffusion couple was made using iodide titanium and high purity copper. The assembly was heated at 838°C for 14 days in an evacuated Vycor tube followed by brine quenching. Metallographic examination showed the presence of four intermetallic compounds in addition to the two terminal solid solutions. Sectioning through the Ti_2Cu_3 region revealed a single phase which gave an X-ray pattern identical to that obtained for the duplex structure observed in the metallographic specimen. The conclusion is that the duplex structure results from the peritectic reaction which occurs during freezing of the compound and persists even after a single phase is reached.

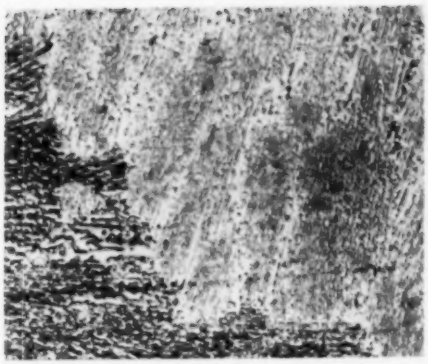

Fig. 11—Eutectic structure of an alloy containing 49.7 pct Cu. Small amounts of primary Ti_2Cu plus eutectic of Ti_2Cu and TiCu. X100.

Micrographs of structures that consist almost entirely of the compound phases are shown in Figs. 6 to 9. X-ray patterns for the four compounds are shown in Fig. 10.

The system has two eutectics, one at 50 pct Cu and one at 72 pct Cu. A typical structure for the slowly cooled 50 pct alloy is shown in Fig. 11.

Metallographic examination of the thermal analysis specimens made after a run showed nonequilibrium structures for all specimens in which peritectic reactions were involved. As a result of the sluggishness of the peritectic reactions, eutectics were frequently formed in alloys outside of the eutectic range. This resulted in points on the cooling curves, Fig. 1, which would not have been present under equilibrium conditions.

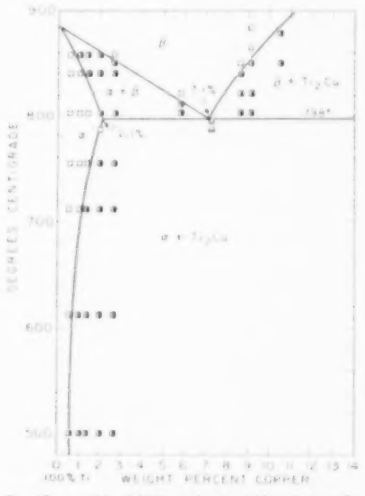

Fig. 12—α solid solubility and eutectoid region on the high titanium side of the Ti-Cu phase diagram as determined with iodide titanium alloys.

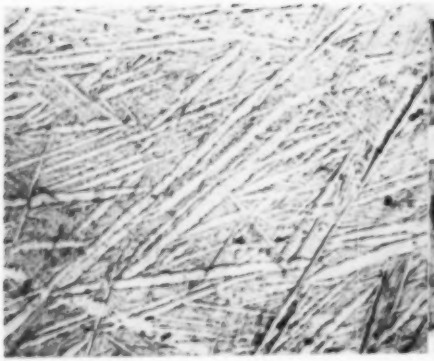

Fig. 13—α martensite structure in a 2.6 pct Cu alloy formed by quenching from the β field (858 C). X500.

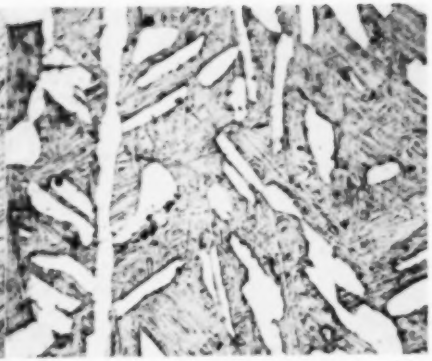

Fig. 14—Microstructure of a 2.6 pct Cu alloy formed by quenching from the $\alpha + \beta$ field (850 C). Primary α plus α martensite. X500.

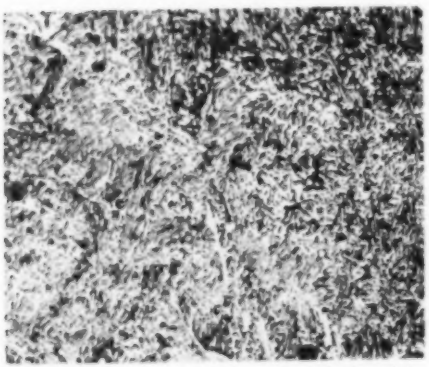

Fig. 15—Microstructure of a 7.2 pct Cu alloy formed by slowly cooling from the β field to 787 C, holding for 24 hr, and brine quenching. Small amounts of primary Ti_2Cu in a eutectoid of α and Ti_2Cu. X500.

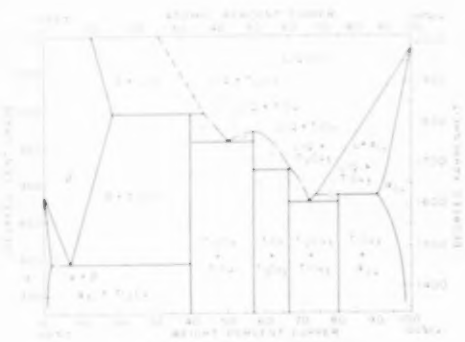

Fig. 16—Ti_2Cu binary phase diagram.

Iodide Titanium Alloys: A series of high purity alloys was prepared using iodide titanium and oxygen-free copper. The hardness of the standard sample is an indication of the purity as previously described. These alloys were used to check the high titanium side of the diagram, to locate the eutectoid point more accurately, and to determine the α solid solubility line. Results of metallographic and X-ray analyses on heat treated specimens are shown in Fig. 12.

Three typical microstructures of these alloys are shown in Figs. 13 to 15. Fig. 13 is the structure produced by rapidly quenching β solid solutions. A supersaturated solid solution of α is produced by a martensitic reaction. Fig. 14 is the structure produced by quenching from the $\alpha + \beta$ field. It consists of primary α crystals plus the acicular transformation product of β. Fig. 15 shows the eutectoid structure produced by isothermal transformation just below the eutectoid temperature.

Summary

The Ti-Cu phase diagram as determined in this investigation is shown in Fig. 16. Four intermetallic compounds were found: Ti_2Cu, TiCu, Ti_2Cu_3, and $TiCu_4$. There is a eutectoid reaction on the high titanium side of the diagram which offers possibilities for heat treatment of alloys by suppression of the β to α transformation.

Acknowledgment

The authors wish to express their thanks to the Air Materiel Command for sponsorship of this research program, as well as to C. C. Wang, Mrs. G. Johnson, and F. Cuff for various contributions during the course of the investigation.

References

[1] Guertler: *Metallographie* (1912) Berlin. Erster Band.

[2] Hensel and Larsen: Unpublished Research Report, R-7417-F, Westinghouse Electric and Manufacturing Co. (1930).

[3] Kroll: Vergütbare Titan-Kupferlegierungen. *Ztsch. Metallkunde* (1931) **23**, p. 33.

[4] Laves and Wallbaum: Kurze Originalmitteilungen. *Naturciss.* (1939) **27**, p. 674.

[5] Craighead, Simmons, and Eastwood: Titanium Binary Alloys. *Trans.* AIME (1950) **188**, p. 485; JOURNAL OF METALS (March 1950).

Effect of Molybdenum and of Nickel On the Rate of Nucleation And The Rate of Growth of Pearlite

by R. Wayne Parcel and Robert F. Mehl

THE rate of the decomposition of austenite in eutectoid steels, forming only pearlite, may be expressed fundamentally in terms of the rate of nucleation and the rate of growth of pearlite nodules. This matter has received much attention in recent years. (The basic references are listed in ref. 1; references of particular import to the present work will be given separately.)

Systematic data have been developed for plain carbon eutectoid steels.[2] Although the physical factors affecting the rate of nucleation, N, in case of plain carbon steels have presumably been identified, they cannot as yet be evaluated quantitatively.[3] Several somewhat successful attempts, however, have been made to calculate the rate of growth, G. In the latter case the important factors determining the edgewise growth of pearlite have been assumed to be: 1—the interlamellar spacing; 2—the concentration extremes and concentration contours of carbon in austenite in front of the growing pearlite interface; and 3—the rate of diffusion of carbon in austenite.*

* It was first pointed out in 1938 that G should vary inversely as the interlamellar distance and directly as the diffusion coefficient of carbon in γ Fe.[4] In discussion to that paper, Hultgren proposed that the concentration extremes are provided by extrapolation of A_1 and A_{1-2} curves in the Fe-Fe$_3$C system (see also ref. 12); this extrapolation has been employed by Zener[5] and by Brandt[6] in calculations of the rate of growth.

The only systematic data on N and G for pearlite in alloy eutectoid steels are those for Co-steels;[7] there are no data on alloy eutectoid steels in which the alloying element is known to decrease the rate of formation of pearlite, apart from a few scattering data reported earlier[8] for steels containing manganese. This paper reports a systematic study of N and G for eutectoid alloy steels containing molybdenum and nickel, respectively. In order to provide information of help in understanding the results, new data are presented on the effect of molybdenum on the interlamellar spacing of pearlite, S_o; data on the effect of nickel on S_o have already been published.[9]

The alloys used were in five groups:

1—Pure Fe-C-Mo alloys (Table I) were supplied by the Climax Molybdenum Company of Michigan, Detroit. They were made from Armco ingot iron of standard analysis, Acheson graphite, and ferromolybdenum, melted in silica-lined crucibles in a high frequency induction furnace. The ferromolybdenum was added to the melted steel, followed in 5 min by 0.08 pct Al. The ingot as-cast measured $2\frac{3}{4}$ x $3\frac{1}{4}$x10 in.; it was hot-forged at 1150°C to a bar 1 in. sq.

R. W. PARCEL is Research Metallurgist, Rem-Cru Titanium, Inc., Midland, Pa., and R. F. MEHL, Member AIME, is Professor of Metallurgical Engineering, Carnegie Institute of Technology, Pittsburgh.

Discussion on this paper, TP 3270E, may be sent, 2 copies, to AIME by Dec. 1, 1952. Manuscript, Nov. 14, 1951. Philadelphia Meeting, October 1952.

This paper is from a thesis by R. Wayne Parcel submitted in partial fulfillment of the requirements for the degree of Doctor of Science in Metallurgical Engineering to Carnegie Institute of Technology, June 1949.

Table I. Composition of Fe-C-Mo Steels

Code No.	Heat No.	Mo	C	Mn	Si
1	2858	0.12	0.78	0.019	0.030
2	2854	0.26	0.76	0.030	0.026
3	2859	0.28	0.75	0.021	0.016
4	2856	0.59	0.75	0.019	0.013
5	2857	0.67	0.75	0.018	0.015

2—Fe-C-Mn-Mo alloys (Table III) were made by the same company, in the same way.

3—Fe-C-Mn-Mo alloys (Table II) from the work of Blanchard et al.[3] were furnished by the same company.

4—Pure Fe-C-Ni alloys (Table IV) were prepared by the research laboratory of the International Nickel Co. in a manner identical to that in group I above.

5—Fe-C-Mn-Ni alloys (Table V) from the work of Pellissier et al.

It will be observed that in Table I both manganese and silicon are low; in Table II manganese is low but silicon is in the range common in forging steels; in Table III manganese is in the range of 0.33 to 0.60 pct with silicon in the range common in forging steels; in Table IV manganese is low and silicon

Table II. Composition of Fe-C-Mn-Mo Steel[3]

Code No.	Mo	C	Mn	Si	S	P
CL 1	0.017	0.77	0.71	0.29	0.029	0.011
CL 2	0.15	0.77	0.70	0.29	0.029	0.011
CL 3	0.32	0.78	0.73	0.28	0.029	0.011
CL 4	0.52	0.77	0.72	0.28	0.029	0.011
CL 5	0.77	0.79	0.76	0.27	0.029	0.011

though somewhat lower is in the common range; in Table V manganese is 0.49 and 0.46 and silicon is 0.55, somewhat higher than common.

There are systematic data on the constitution of the ternary system Fe-C-Mo,[4] but these data are unfortunately not voluminous in the iron corner. The isothermal transformation diagrams for alloys in this system have been studied comprehensively,[5] the absence of proeutectoid reaction in these diagrams was the criterion determining the compositions to be used in procuring alloys of eutectoid composition. The behavior of the actual compositions employed with respect to the presence or absence of proeutectoid constituents on isothermal reactions, especially in the ternary alloys, furnished direct evidence needed as to how closely the alloy approached the eutectoid composition.

The constitution of the ternary system Fe-C-Ni is not well known. Isothermal transformation diagrams are, however, available for commercial alloys (though not for pure alloys), which formed a basis for the selection of compositions.

Each alloy was also inspected for the presence or absence of proeutectoid constituents in isothermal reaction. They were all essentially eutectoid in

Table III. Composition of Fe-C-Mn-Mo Steels

Code No.	Heat No.	Mo	C	Mn	Si
18	2875A	0.15	0.80	0.33	0.21
16	2872B	0.13	0.83	0.52	0.20
19	2875A	0.31	0.82	0.60	0.20
21	2871B	0.31	0.85	0.37	0.19

Table IV. Composition of Fe-C-Ni Steels

Code No.	Heat No.	Ni	C	Mn	Si
1	17,392	1.16	0.80	0.04	0.15
2	17,471	1.54	0.76	0.03	0.16
3	17,473	2.04	0.75	0.029	0.12
4	17,381	2.48	0.75	0.024	0.16
5	17,468	2.95	0.73	0.022	0.17

nature, though in some cases a small amount of proeutectoid ferrite was observed at quite high isothermal reaction temperatures—not to a degree, however, to be important.

Characteristics of the Systems

Isothermal transformation diagrams of commercial Fe-C-Ni alloys have shown the effect of nickel to be a simple one: nickel merely displaces the curve, in both the pearlite region and the bainite region, to longer times; the knee of the curve is depressed to lower temperatures by increasing percentage of nickel, owing, presumably, to the lowering of the Ae_1 temperature. No special carbides of nickel appear in the compositions studied; the carbide is Fe_3C in type.

Isothermal transformation diagrams for alloys of Fe-C-Mo, and for commercial alloys (containing manganese, silicon, etc.) have been provided in relative abundance by the Climax group.[5] Molybdenum is known to displace the pearlite reaction to longer times and to somewhat higher temperatures, presumably because of the effect of molybdenum in raising Ae_1. When the percentage of molybdenum is greater than 0.50, the pearlite reaction exhibits its own knee, i.e., there is a temperature at which the rate of reaction is a maximum. The pearlite reaction is thus separated from the bainite reaction by an interval of slow reaction rate, for example, in the alloy with 0.52 pct Mo, molybdenum influences the rate of formation of bainite to a much lesser degree than it does pearlite. The ternary phase diagram Fe-C-Mo is complex; for our purposes we need merely note that the pearlite formed in alloys in the range of 0 to 0.50 pct Mo is composed of αFe and Fe_3C (with dissolved molybdenum), while in alloys containing more than 0.50 pct Mo the pearlite is composed of αFe and a different carbide—known as κ, face-centered cubic in structure, and presumably of the composition $(Fe, Mo)_3C$. It is known that as much as 1.13 pct Mo may dissolve in orthorhombic Fe_3C, and that the face-centered cubic carbide $(Fe, Mo)_3C$ may contain as little as 3.41 pct Mo and as much as 5.45 pct Mo. These are the composition ranges observed upon isothermal transformation, bearing little or no relationship to the equilibrium compositions[6] (also see ref. 1 for complete list of references on this subject).

Experimental Methods

Homogenization: The steels as-received were banded. For the molybdenum steels, assuming the worst possible distribution of molybdenum, i.e., that

Table V. Composition of Fe-C-Mn-Ni Steels

Code No.	Ni	C	Mn	Si	S	P
D5	1.06	0.84	0.49	0.55	0.04	0.013
D6	2.91	0.73	0.46	0.55	0.037	0.015

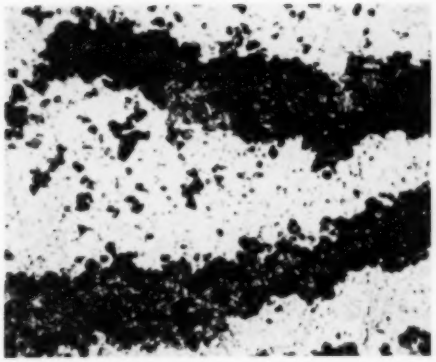

Fig. 1a—Specimen partly reacted without previous homogenization. Picral etch. X50.

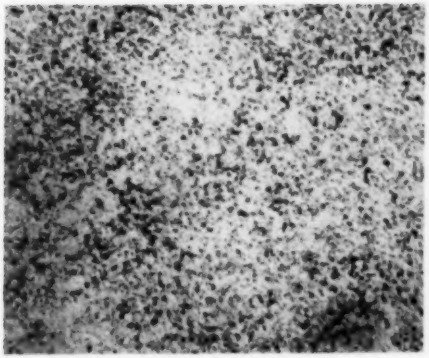

Fig. 1b—Same steel reacted after homogenization. Picral etch. X50.

along a line perpendicular to the banding, the concentration contour would be a square wave with wavelength equal to the observed band width, and with all alloy concentrated in one-half of a cycle, and employing the known value of the diffusion coefficient of molybdenum in γFe, calculation showed that 90 hr at 1300°C would reduce the molybdenum gradient to a value below that which was deemed important. On this basis all alloys were initially homogenized for 100 hr at 1300°C. The furnace atmosphere was dried nitrogen. The effectiveness of this treatment is shown in Fig. 1a and b. Decarburization was confined to a surface layer of inappreciable thickness. The molybdenum steels from the work of Blanchard et al. had been homogenized at 1200°C for 50 hr and were apparently free from important heterogeneity. The nickel steels were similarly treated, but employing a temperature of 1250°C instead, since some burning occurred at 1300°C.

Determination of Interlamellar Spacing: The method by which the interlamellar spacing was evaluated was that employed previously in this laboratory.[5] Apparent spacing values (those observed on the surface of polish) were obtained at 1200 diam on specimens reacted isothermally, using a micrometer eyepiece. The number of plates per eyepiece division was measured at 100 to 200 random points, and the data were considered ample when further measurements did not alter the distribution curve obtained (see ref. 7). The results of the calculations of true spacing, S_o, are given in Fig. 2. At higher molybdenum contents and lower temperatures the results were irregular owing to structural degeneracy, and are not plotted. It was observed that molybdenum increases the variability in S_o even more than it affects the average value of S_o (cf. ref. 6). The effect of nickel on S_o has been reported.[5]

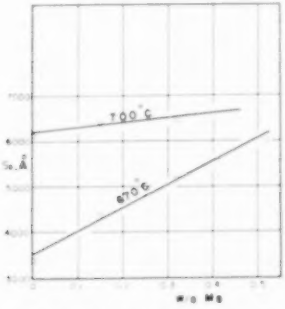

Fig. 2—Interlamellar spacing of pearlite as influenced by molybdenum.

Determination of G

The methods employed are those used earlier. In a series of identical specimens, partially reacted separately for increasing time periods, the diameter of the largest pearlite nodule in each specimen, presumably that nodule which nucleated first, was taken. These diameters plotted against time gave a straight line, the slope of which is G. In plain carbon eutectoid steels, G was found to be insensitive to austenitizing time and temperature, i.e., was not structure-sensitive. This is not to be expected in alloy steels, for the occurrence of undissolved carbide, containing much of the alloying element, would presumably increase the value of G from the true, low value, the effect of the alloying element not dissolved in the austenite on G having been lost. To appraise this possibility, G was determined as a function of the degree of austenitizing. The results are shown in Fig. 3; the abscissas are values of Dt, where D is the diffusion coefficient of molybdenum (or nickel) in γFe and t the time. This product should be a measure of the effectiveness of austenitizing (carbon diffuses very much more rapidly than the alloying elements). The ordinate values are the ratios of the observed G values to the final value. For the purpose of this diagram the final value is designated as G_∞—the final values used subsequently will be designated simply by the symbol G. The

Fig. 3—Effect of austenitizing on G for several of the steels used. Abscissa is Dt. Steels are, left to right, code numbers 31, 1', 2', 3' (Tables III and IV). Temperature 875°C for 31, 1200°C for rest.

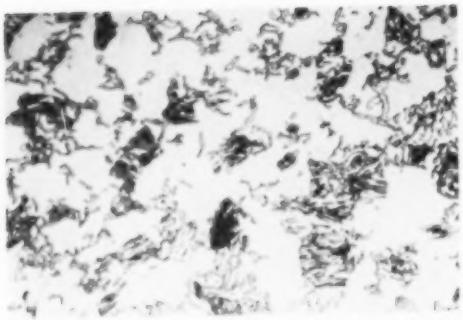

Fig. 4—Degenerate pearlite formed by partial isothermal reaction of Fe-C-Mo alloy. X1000. Area reduced approximately 75 pct for reproduction.

Fig. 5—Steel 31 (0.31 pct Mo, 0.57 pct Mn) reacted at 700°C. Picral etch. X2000. Area reduced approximately 75 pct for reproduction.

values of G are thus dependent upon the degree of homogenization; in plain carbon steels, such an analysis is unnecessary, for in this case the necessary homogenization time is of the same order as the time of heating. The homogenization times to attain a final value of N, N_∞, were found more than enough to reach a fixed value of G_∞. It was shown that, prior to isothermal reaction, austenitizing steels with low molybdenum content at 875°C for 90 min was adequate (as shown by experiments for shorter times at lower temperatures). Nickel steels were treated at higher temperatures, i.e., 1200°C for 4 min. This treatment was used also on the molybdenum steels though more than sufficient.

Determination of N

The methods employed are those used earlier.[1] The bulk of the work used "method 3" of Hull, Colton, and Mehl,[1] i.e., assuming nucleation to be general, assuming N to be constant with time, the value of N may be calculated from a knowledge of the half-time for isothermal reaction and of the pertinent value of G. The reaction equation for this case[5] can be plotted in double-logarithm form as a straight line of slope 4; the values obtained here gave a slope somewhat greater than 4 (owing to departures from the simplifying assumptions) but the curve was a straight line up to 0.80 reaction. A small amount of work was done using Scheil's method,[6] which gives the variation of N with t; the particular method employed in determining the N values reported hereinafter will be designated.

Experimental Results

Morphology. It was originally intended that this work should provide data on N, G, and S for relatively pure ternary alloys. In the case of the molybdenum steels, however, it was found that the steel of Table I upon isothermal reaction did not form a distinctly lamellar pearlite, but a degenerate pearlite, representing divorcement and resembling spheroidite, Fig. 4, for reasons that are not understood. These steels, surprisingly, would form distinctly lamellar pearlite on slow cooling (but not on extremely slow cooling); Fig. 4 shows the divorced pearlite formed isothermally and the lamellar pearlite formed on cooling; divorcement could be deliberately varied from 0 to 100 pct by allowing a given sample to transform isothermally for a while, when divorced pearlite appeared, then allowing it to complete its transformation on falling temperature. A single field would contain divorced pearlite formed during the first part of the treatment, and lamellar pearlite formed during the latter. Divorcement was studied for a full range of time and temperature, and for various austenitizing treatments. It was found to be unavoidable even with the most complete austenitizing. These circumstances forced us to abandon the "pure" Fe-C-Mo alloys.

It was found that eutectoid molybdenum steels with normal commercial amounts of manganese and silicon formed normal lamellar pearlite, Fig. 5, and accordingly the measurements were concentrated on these, Tables II and III.

Rate of Growth, G. The nodules of pearlite upon which measurements of G were made were nearly always, interestingly enough, single colonies, Fig. 5. It has been clear for some time[7] that the rate of edgewise growth $G_\perp$ (parallel to the lamellae) must be about equal to that sidewise growth, $G_\parallel$ (else the colonies would not be so nearly equiaxed as they are observed to be). The single-colony nodules of pearlite in molybdenum steels provided an opportunity for a direct measurement of $G_\perp$ and $G_\parallel$. Fig. 6 gives the measurements for steel 16 reacted at 691°C, a total of 59 measurements. Other measurements on molybdenum steels are given in Table VI.

An induction period is shown in all cases. Fig. 7, giving the G data for steel 31, illustrates this. The value of the induction period (hereinafter "I.P.") increases with decrease in G; Figs. 8 and 9 give this relationship for molybdenum and nickel steels, respectively. It was suggested many years ago,[8] in connection with the theory of age hardening, that the initial slow rate of a transformation may be associated with a time period required to establish the equilibrium state of concentration fluctuations at the reaction temperature; Turnbull[9] recently developed this idea on the basis of modern chemical rate theory, obtaining both an I.P. and an increase of N with time. On this basis, austenitizing two samples of the same steel at two different temperatures, would provide different values of the I.P., since the

Table VI. Ratio of Edgewise to Sidewise Growth of Pearlite in Molybdenum Steel

Steel	Mo, Pct	Temperature, °C	Ratio
16	0.16	691	1.71
16	0.16	691	1.35
31	0.32	691	2.29

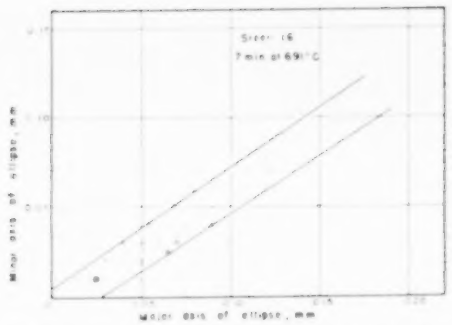

Fig. 6—Relationship between edgewise and sidewise growth. Major axis was always lengthwise of the pearlite plates. Molybdenum steel 16, Table VI.

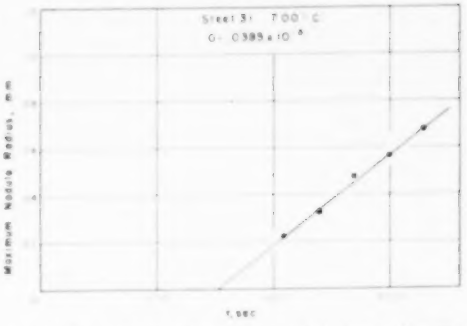

Fig. 7—Plot of nodule radius vs. time, which shows a long "incubation" period. Molybdenum steel.

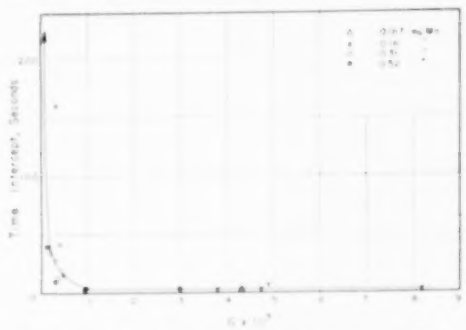

Fig. 8—Plot of "incubation" period as a function of G for molybdenum steels.

alloy starts reaction at different fluctuation states. The I.P. should be the greater in the sample austenitized at the higher temperature, since the degree of fluctuation is then less, the system thus possessing fewer embryos. Fig. 10 gives the results for molybdenum steel 31, with 0.31 pct Mo, one set of samples austenitized at 1200°C for 90 min and the other at 875° for 120 sec, both reacted at 600°C. The I.P. is obviously much shorter in the steel reacted at the higher temperature, as predicted; G is the same, as expected.

This behavior should be manifest in the isothermal reaction rate. One set of samples of steel 4, with 2.5 pct Ni, was austenitized at 1200° for 4 min and reacted at 625°C. A similar set was austenitized at 1200° for 4 min, transferred to 875°C for 10 min, and reacted as before at 625°C. Fig. 11 shows that the reaction rate is the greater in the latter case, as expected, though the difference is not great and the data not voluminous; if the result is valid, the difference lies in the respective values of N.

At the inception of the work, samples were obtained from Blanchard of his steels CL 1, CL 2, CL 3, and CL 4, in order to get some idea of the magnitudes of G, and the magnitude of the variation of G with alloy content; measurement of nodule radii upon growth at 650°C provided the data given in Fig. 12. Obviously, the effect of alloy is great enough to be beyond experimental error; these results may be taken as typical of all. The G values obtained for all steels are assembled in Fig. 13, in which log D is plotted against the atomic percentage of the alloying elements; to these are added the earlier approximate values for the effect of manganese.[4] All values at zero percentage alloying element are taken from the earlier work on plain carbon eutectoid steels,[5] choosing values from steels of the same manganese content as in the alloy concerned. It will be noted that the plot of log G against atomic percentage is a straight line in all cases, except for the molybdenum steels reacted at 625° and 600°C; stated differently, those values (two each, respectively) do not extrapolate well to zero percentage alloy.

Fig. 14 shows the values of G at different temperatures for molybdenum steels 16 and 31, as compared to the earlier steel,[5] Steel A, of comparable manganese content (the lower retrogressive part of the "Hull" curve, representing the growth of bainite, not pearlite, should be disregarded). Fig. 15 is the same type of plot, on a different scale, comparing molybdenum contents of 0.16, 0.31, 0.52, and 0.77 pct; the points on the 0.15 and 0.31 pct Mo steels are for the Climax steels.

Fig. 16 shows the values of G for the pure Fe-C-Ni alloys as a function of temperature. Except for the one point at 625° for the 2.5 pct Ni alloy, the effect of nickel in regularly decreasing G is evident. Fig. 17 is the same kind of plot, but the values are read from Fig. 16—the values are interpolated and averaged; the curve for the pure Fe-C alloy, Steel J, from earlier work,[5] is plotted for comparison (again, and for the same reason, the lower, retrogressive, part of the latter curve is to be disregarded).

Rate of Nucleation, N

The values of N, for molybdenum steels, obtained by dividing the average value of N_a (determined from the half-reaction time and the value of G, see above) by the grain-surface area, are plotted in Fig. 18 (cf. ref. 2). Steels 16 and CL 2 both contain 0.15 pct Mo, steel 16 has 0.52 pct Mn, and steel CL 2 has 0.70 pct Mn; steels 31 and CL 3 are similarly comparable. But it will be observed that the comparable pairs do not give good agreement; indeed the curve for N for a plain carbon eutectoid steel falls in the midst of the curves for the molybdenum steels. Presumably some steelmaking or processing variable is active here; steels 16 and 31, made in the same way at the same time, stand in the expected relationship, with N for steel 31 (with the higher percentage of molybdenum) standing lower than for steel 16; the same is true for the Blanchard steels CL 2 and CL 3. Evidently the effect of molybdenum on N must be appraised on closely comparable steels. The data

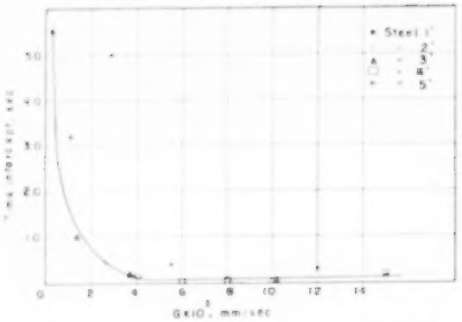

Fig. 9—Plot of "incubation" period as a function of G for nickel steels.

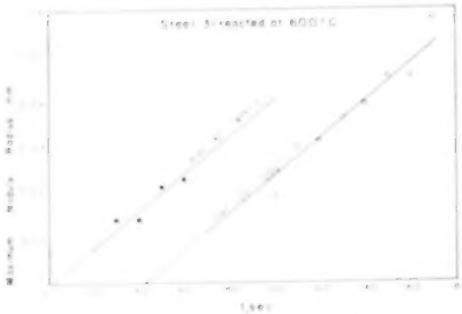

Fig. 10—Effect of austenitizing temperature on "incubation" time, G unchanged.

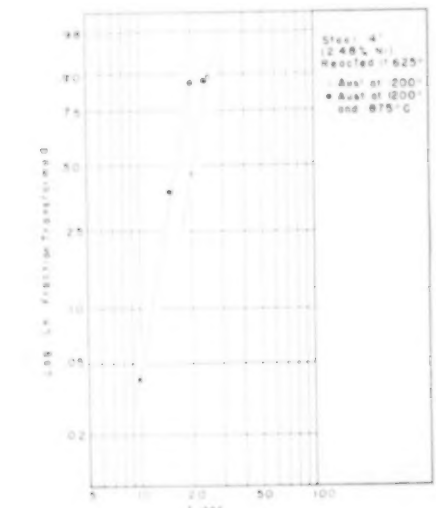

Fig. 11—Effect of austenitizing temperature on reaction time.

seem to suggest that G is unusually effective in determining the isothermal reaction rate. Presumably the Blanchard steels were more completely homogenized than steels 16 and 31; they had been rolled to strips ½x1/16 in. while steels 16 and 31 had been rolled to 1 in. squares. In any one set, the results are consistent; Fig. 19 shows N, values vs. weight percentage of molybdenum for the Blanchard steels. It is clear that there is a point of inflection near 0.4 pct, near that composition at which the nature of the carbide changes. A similar point of inflection occurs in the comparable curves for G, Fig. 13. Values of N, obtained by the complete method of Scheil and Langeweise, Fig. 20, for molybdenum steels, show that N varies with time, as observed for plain carbon eutectoid steels.[3]

The results of the determination of N, for nickel steels, by the method of half-reaction, are less satisfactory. Fig. 21, on which N, is plotted against weight percentage of nickel, shows a maximum at 2 pct Ni which is unlikely and doubtless reflects cumulative errors. Application of the Scheil and Langeweise method gave the values plotted in Figs. 22 and 23. Both figures show N, to decrease with increasing nickel, in accord with expectations.

Discussion

These results show that both N and G in eutectoid steels are decreased by molybdenum and nickel. The data are good for G, the data on N are good for molybdenum steels, but relatively poor (and in a measure contradictory) for nickel steels, owing, presumably, to heterogeneity. In all cases the active nucleus is carbide, for proeutectoid ferrite was observed not to accelerate the isothermal rate of reaction while proeutectoid cementite was observed to be a powerful inoculant (cf. ref. 1).

The value of N was observed to increase with time, approximately exponentially, for both molybdenum and nickel steels (Figs. 20, 22, and 23). This is the same result as reported for plain carbon steels, and presumably reflects the progressive change in the austenite matrix during isothermal reaction to pearlite, toward an equilibrium state of concentration fluctuations characteristic of the reaction temperature;[3] change in the initial fluctuation state by changes in austenitizing, alters the induction period and the reaction rate as would be expected on this basis.

Molybdenum has a great effect upon N, Fig. 19, decreasing N at 650 C in the composition range studied roughly by 10[6]. At roughly 0.4 pct Mo, near where the ϵ carbide appears, an inflection point occurs (Fig. 19), in all likelihood reflecting the occurrence of the new carbide as an active nucleus; this suggests that the actual nucleus is indeed the ϵ carbide. The shape of the N vs. T curve, Fig. 18, is similar to that for plain carbon steels, except that a maximum appears in the curve for 0.32 pct Mo (CL 31); steel 31, with 0.31 pct Mo, does not show a maximum, but might if lower temperatures had been studied. It is possible that this maximum merely reflects the intrusion of the bainite reaction, for the nature of the reaction products at low temperatures is difficult to identify.

The values of N for nickel steels as a function of the percentage of nickel, Fig. 21, are probably not reliable, as noted, though those as a function of time, Figs. 22 and 23, not affected by comparing steels of questionable comparability are probably quite valid.

Presumably N should respond to quantitative

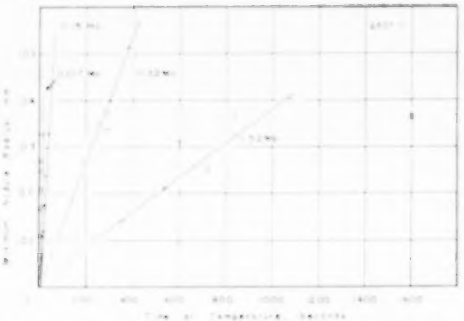

Fig. 12—Nodule radii as a function of time. Molybdenum steels at 650°C.

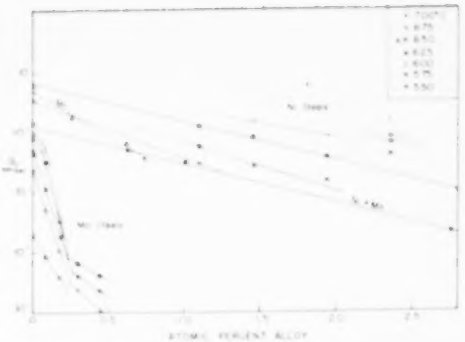

Fig. 13—Rates of growth as a function of composition at several temperatures for all the steels studied.

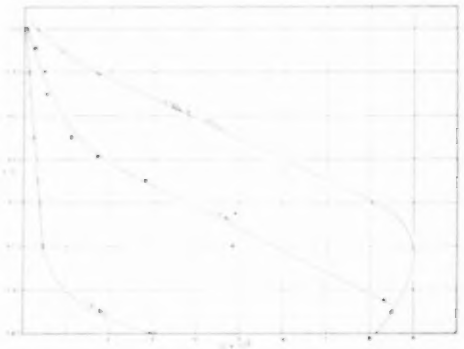

Fig. 14—Rates of growth for steels 16 and 31 compared to a carbon steel.

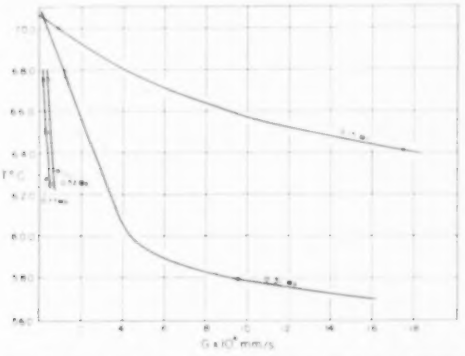

Fig. 15—Rates of growth of four molybdenum steels as a function of temperature.

treatment on the basis of nucleation theory. Qualitatively the presence of alloy should decrease the simple probability of the correct chance association of atoms to form a nucleus of the proper composition, assuming this to be different from the average composition, but the composition of the original nucleus is not known (and will be difficult to learn) —on partition data also the inclination is to assume, though with uncertainty, that the nucleus in molybdenum steels contains molybdenum while that in nickel steels does not contain nickel; nor is the composition of the austenite at the grain boundary (the Gibbs surface concentration effect), where nucleation is preferred, known, nor can it be readily inferred; nor are the surface energies, nor the effect of alloy upon the bulk free energy known; until these deficiencies are remedied, further speculation seems unpromising. The application of the principle of dihedral interphase angles, extensively developed by Smith,[11] upon proper experimentation should yield information on interface energies; B. H. Alexander[12] reports preliminary results. Measurements on the heat of transformation as affected by alloy should yield values from which approximate free energies could be calculated, much as Zener has done for plain-carbon steels;[7] such measurements on cobalt steels would constitute a fair test of the proposal[7] that cobalt increases the bulk free energy of the transformation and correspondingly increases N, and decreases S, with the result of increasing G.

The measured values of G are somewhat more responsive to study. These values may be determined with much precision; they are sensitive to austenitizing treatment, but there are methods which will fix a characteristic value of G, Fig. 3. The effect of austenitizing is less on G than on N, in qualitative accord with earlier experience with plain carbon steels.[7] Austenitizing times as short as 5 min at 875°C yield a rate of growth for a 0.31 pct Mo steel only twice that obtained after 4 min at 1200°C. Nickel steels require longer austenitizing times than molybdenum steels, perhaps reflecting the lower rate of diffusion of nickel in austenite.[13]

G values are constant with time, Figs. 7 and 10, as in plain carbon steels, which argues that growth in these alloy steels is also a steady state process. The effect of alloy upon G is very great in molybdenum steel, and in nickel steels, though not so great, is well beyond experimental error, Figs. 12 to 15. This is opposite to the diffusion coefficients of these elements in austenite, but parallels their carbide-forming tendency. Fig. 13 combines all results, and includes earlier approximate data on the effect of manganese.[7] It shows also the effect of manganese on nickel steels—the two curves for steels D5 and D6 (containing nickel and 0.46 pct Mn) and the simple nickel steel are parallel, manganese depressing G by the same amount (on this logarithmic plot) for all nickel contents. This is the same amount as observed for 0.46 pct Mn in ordinary

Fig. 16—Rates of growth of nickel steels, experimental points.

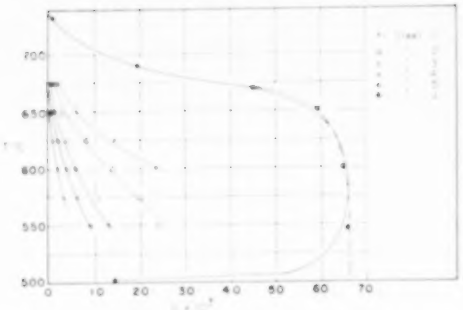

Fig. 17—Rates of growth of nickel steels. Values are by interpolation from Fig. 16. Steel J is high purity Fe-C steel.

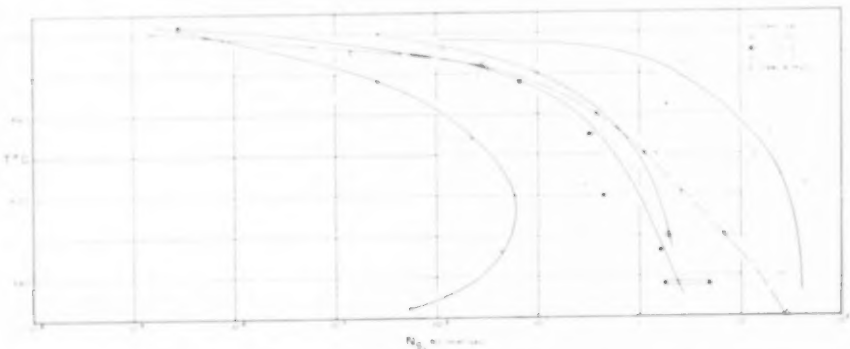

Fig. 18—N_v = rate of nucleation per unit grain boundary area per sec) as a function of temperature for molybdenum steels.

commercial plain carbon steels; the logarithms are thus additive, and the effects of different alloys presumably multiplicative. As Fig. 14 shows, the logarithm of G is a linear function of the percentage alloy.

It was proposed early[7] that the retarding effect of alloy addition upon the isothermal rate of formation of pearlite lies in a diminution in the N and G values, in the case of G perhaps because of the necessity for the diffusion of the slowly diffusing alloy addition, e.g., molybdenum. This has been questioned,[8] especially as the argument relates to G, on the basis that no reason exists to believe that pearlite should, on growing, await the diffusion of the alloy—the effect of alloy on the isothermal rate of reaction was attributed entirely to the effect on N. The present data, however, can leave no doubt but that G is indeed decreased by alloy addition, in the case of molybdenum greatly, Fig. 13. It was argued[8] that partition data do not prove the occurrence of segregation at the growing interface—the observed partition could well have occurred between ferrite and carbide behind the moving interface, though segregation during the formation of pearlite composed of ferrite and a special carbide, e.g., ϵ in molybdenum steels, was not (and could hardly be) questioned.

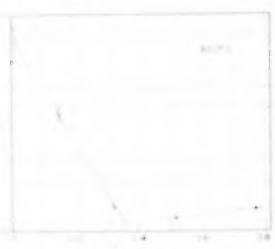

Fig. 19—N_v at 650 C as a function of molybdenum for Climax steels.

Partition data, however, seem more significant than this argument allows. Bowman[9] has studied the partition of molybdenum between carbide and ferrite in eutectoid steels reacted isothermally to pearlite and in the same steels quenched and tempered. Bowman's best data are those at 705 C (his data at 650 C are less definite owing to difficulties in separation of the two phases prior to analysis and owing to poor X-ray resolution upon diffraction). The carbide as isothermally formed pearlite (just fully reacted) in a 0.30 pct Mo steel was observed to be cementitic in lattice type, containing 1.1 to 1.2 pct Mo; in steels with 0.51 pct Mo or above, the carbide was the ϵ carbide, face-centered cubic in structure, represented by $(Fe,Mo)_2C$; the unit cell of the latter contains 116 atoms whereas Fe_3C contains 16 atoms; the ϵ carbide was observed to contain 3.4 pct

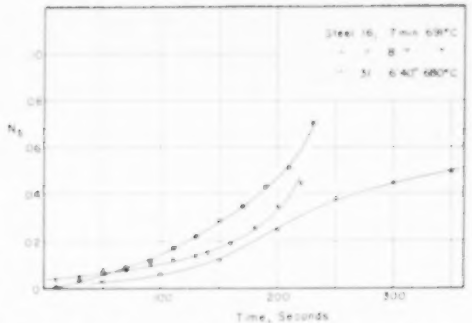

Fig. 20—N_s as a function of time for molybdenum steels by the method of Scheil.

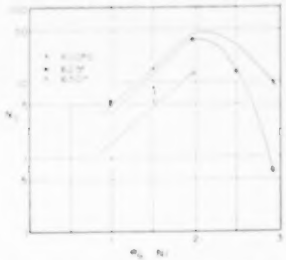

Fig. 21—N_s as a function of nickel content.

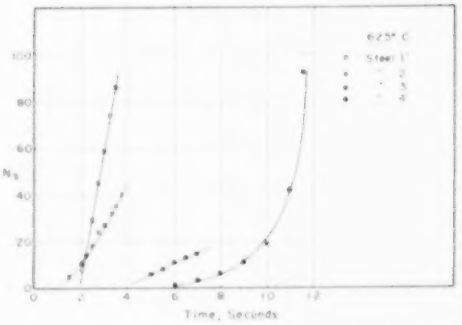

Fig. 22—N_s vs. time, by Scheil's method, for nickel steels at 625° C.

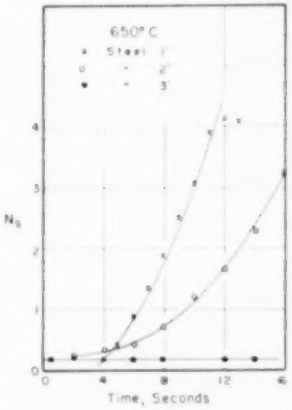

Fig. 23—N_s vs. time, by Scheil's method, for nickel steels at 650° C.

Mo or more (see above). The same steel quenched, and tempered at 705°C, similarly showed partition, increasing with increasing tempering time, but even after 250 hr at 705°, the degree of partition was markedly less than that observed in the isothermally reacted steel. These experimental facts argue that partition occurring in pearlite, behind the growing interface, is slow compared to that which occurs at the growth pearlite:austenite interface. Similar conclusions may be drawn from the work on partition in steels reacted 50 pct to completion. Kuo and Hultgren,[7] performing somewhat similar work on other steels, similarly report that silicon is absent from the carbide phase in both isothermally reacted and quenched and tempered steels, and that nickel shows early and extensive partition.

Moreover, if it is admitted that segregation must take place in steels with more than 0.50 pct Mo, in which the α phase occurs, and that this may be employed to explain the decrease in G, it is difficult to see why the same reasoning may not be employed for steels with a percentage of molybdenum just less than this, Fig. 13, for the curves of G vs. the percentage alloy are continuous, with a point of inflection. The occurrence of the branch of the G curve at high molybdenum contents shows, to be sure, that in this range the rate of growth of the α pearlite is greater than that of the extrapolated cementitic pearlite. There is no apparent way to rationalize the observed partitions; they are not the equilibrium values, and presumably are determined by kinetic as well as by thermodynamic factors. The data show that G is in fact decreased by the addition of alloy, for molybdenum, nickel, and manganese steels, and the weight of argument favors the segregation of the alloy by diffusion at the reacting interface.

It has been suggested that the "anomalous" increase in G caused by the addition of cobalt lies in the increase excited by cobalt on the bulk free-energy change in the austenite:pearlite transformation, resulting in a smaller S_o and thus a greater G value.[8] No direct data on the bulk free energy, as affected by alloy addition are available (though as noted above, some information on this could readily be obtained), but the theory demands that G should be linearly related to $1/S_o$. The data on cobalt steels support the idea qualitatively, in the sense that cobalt decreases S_o while increasing G, but the relation is not linear as proposed.

Comparable data on molybdenum, nickel, and manganese steels are given in Table VII. Again the direction of change in S_o is in conformity with the decrease in G, but G decreases much more than can be accounted for by change in S_o, and another effect must intrude, presumably alloy partition.

The problem of calculating G is very difficult in alloy steels. Although fair agreement is obtained for plain carbon steels between observed and calculated G values from concentration gradients de-

Table VII. Effect of Alloying Elements on Rate of Growth of Pearlite

	Temperature, °C	Increase in spacing Due to This Amount of Alloy	Decrease in G Due to This Amount of Alloy
Molybdenum, pct			
0.32	700	1.84×	10×
0.15	670	1.23×	5.1×
0.32	670	1.50×	23×
0.32	670	1.82×	85×
Nickel, pct			
1.06	625	1.63×	4.85×
2.90	625	2.48×	83×
Manganese, pct*			
1.5	625	2.22×	144×

* The manganese data are by extrapolation, so that the effect may be exaggerated.

rived from the Hultgren extrapolation and S_α and the diffusion coefficient of carbon in γ Fe, there are several points of arbitrariness in these calculations. The extrapolation of the ferrite and cementite composite phase curves lead to a very large concentration difference. If Zener[1] is correct, these extrapolated concentrations are in error because of the effect of the radius of the lamellae ends in lowering the A_{1-2} curve; the diffusion coefficient rises rapidly with percentage of carbon within the austenite field[2] and would presumably extrapolate to extraordinary values for the extrapolated concentration difference. Even assuming this, the differential equation representing diffusion flow, through a very complex concentration contour, is not available.

It was suggested by Onsager[3] that the high rate of diffusion of carbon in α Fe is the controlling factor in determining G. This assumed that transformation occurs first, and the diffusion of carbon later, within the α phase. Using Stanley's[4] new data on the solubility of carbon in α Fe and on the diffusion coefficient of carbon in α Fe, very rough calculation does not favor this mechanism over the more conventional one, assumed above. On the Onsager idea the cementite lamellae would be sharply pointed at the pearlite-austenite interface, with the cementite lamellae assuming their full thickness some distance from the interface, but recent studies in this laboratory,[5] on thousands of lamellae, do not confirm this.

For alloy steels, the matter is more complicated. It is known that the alloying elements do not effect the rate of diffusion of carbon in austenite appreciably,[6] from this point of view: both manganese and nickel slightly increase the diffusion coefficient of carbon in γ Fe[7] while molybdenum (by extrapolation) very slightly decreases it in the reaction temperature range of concern here.[8] According to Brandt,[9] possible changes in the concentration extremes are also inadequate. It is shown above that changes in S_α are not in themselves adequate. That these minor effects might additively produce the observed diminution in G seems unlikely in view of the extraordinary disparities shown in Table VII; these considerations suggest (though do not in themselves prove) that the slow rate of diffusion of the alloying element upon segregation during the growth of pearlite is at least one determining factor.

Summary

1—The rate of nucleation, N, and the rate of growth, G, of pearlite were measured over a temperature range in a series of eutectoid alloy steels containing 0 to 0.77 wt pct Mo and 0 to 2.95 wt pct Ni, for the alloy systems Fe-C-Mo, Fe-C-Ni, Fe-C-Mn-Mo, and Fe-C-Mn-Ni. The effect of molybdenum on the interlamellar spacing was measured.

2—Both N and G are decreased by molybdenum and nickel, at all temperatures, in all alloys.

3—G was found to decrease by orders of magnitude when the interlamellar spacing increased by factors of only 2 or 3; thus G is not determined primarily by the spacing.

4—G was found to decrease exponentially with increase in alloy content; combined effects of several elements on G are multiplicative. A change in slope in the curve of log G vs. percentage molybdenum was demonstrated, coinciding with the appearance of the noncementitic, ε carbide; a similar though less certain change in slope was found for N.

5—The evidence is strongly in favor of a segregation of the alloying element concomitant with the growth of pearlite in these alloy steels.

Acknowledgment

The authors wish to acknowledge the assistance given them by the International Nickel Co. at Bayonne, N. J., and the Climax Molybdenum Co., of Detroit, in furnishing materials. We wish also to express our gratitude to the Office of Naval Research which supported this work financially.

References

[1] R. F. Mehl: Third Hatfield Memorial Lecture. *Journal* Iron and Steel Inst. (1948) **159**, p. 113.

[2] F. C. Hull, R. A. Colton, and R. F. Mehl: *Trans.* AIME (1942) **150**, p. 185. See also, R. F. Mehl: Campbell Memorial Lecture. *Trans.* A.S.M. (1941) **29**, p. 813.

[3] R. F. Mehl: *Hardenability of Alloy Steels.* (1938) Cleveland. A.S.M.

[4] C. Zener: *Trans.* AIME (1946) **167**, p. 550; METALS TECHNOLOGY (January 1946).

[5] W. H. Brandt: *Journal of Applied Physics* (1945) **35**, p. 139; *Trans.* AIME (1946) **167**, p. 405; METALS TECHNOLOGY (December 1945).

[6] M. F. Hawkes and R. F. Mehl; *Trans.* AIME (1947) **172**, p. 467; METALS TECHNOLOGY (August 1947).

[7] G. E. Pellisier, M. F. Hawkes, W. A. Johnson, and R. F. Mehl: *Trans.* A.S.M. (1942) **30**, p. 1049.

[8] J. R. Blanchard, R. M. Parke, and A. J. Herzig: *Trans.* A.S.M. (1943) **31**, p. 849.

[9] T. Takei: *Kinzoku no Kenkyu* (1932) **9**, pp. 97, 142.

[10] F. E. Bowman and R. M. Parke: *Trans.* A.S.M. (1944) **33**, p. 481; F. E. Bowman: *Trans.* A.S.M. (1945) **35**, p. 112; (1946) **36**, p. 61.

[11] W. A. Johnson and R. F. Mehl: *Trans.* AIME (1939) **135**, p. 416.

[12] F. C. Hull and R. F. Mehl: *Trans.* A.S.M. (1942) **30**, p. 381.

[13] See references in R. F. Mehl and L. K. Jetter: Age Hardening of Metals. A.S.M. Symposium (1939).

[14] D. Turnbull: *Trans.* AIME (1948) **175**, p. 774; METALS TECHNOLOGY (June 1948).

[15] C. S. Smith: *Trans.* AIME (1948) **175**, p. 15; METALS TECHNOLOGY (June 1948).

[16] B. Alexander: Private communication.

[17] C. Wells and R. F. Mehl: *Trans.* AIME (1940) **140**, p. 279; (1941) **145**, pp. 315 and 329.

[18] J. L. Ham, R. M. Parke, and A. J. Herzig: *Trans.* A.S.M. (1943) **31**, p. 877.

[19] A. Hultgren: *Trans.* A.S.M. (1947) **39**, p. 915.

[20] C. Wells, W. Batz, and R. F. Mehl: *Trans.* AIME (1950) **188**, p. 553; JOURNAL OF METALS (March 1950).

[21] L. Onsager: Discussion, Symposium on Phase Transformations in Solids. Cornell University (1951).

[22] J. K. Stanley: *Trans.* AIME (1949) **185**, p. 752; JOURNAL OF METALS (October 1950).

[23] H. P. Tardif: Unpublished research, Carnegie Institute of Technology.

AIME OFFICERS
President—M. L. Hollis
Vice-Presidents—O. E. J. Hoppe, J. L. Gillson, Philip Kraft, Lewis S. Morris, L. F. Reinartz, E. W. Thomas
President-Elect and Treasurer—Andrew Fletcher
AIME STAFF
Secretary—E. H. Robie
Ass't. Secretaries—R. Allnutt, H. N. Aggarwal, C. V. Beall, E. J. Kennedy, Jr., Ernest Kirkendall, R. E. O'Brien
Ass't. Treasurer—J. J. Agel

aime NEWS

Reinartz Heads 1953 AIME Nominations Slate

LEO F. REINARTZ

For President-Elect

Leo F. Reinartz has been nominated for the Presidency of AIME in 1954. Mr. Reinartz is now vice-president, special operating development, Armco Steel Corp. He was born in East Liverpool, Ohio, and graduated from the Carnegie Institute of Technology as metallurgical engineer. He joined Armco in 1909 as a chemist and then became open hearth foreman; assistant superintendent, open hearth dept.; superintendent, open hearth dept.; assistant general superintendent; works manager, East works; manager, Middletown div.; and assistant vice-president, successively. Mr. Reinartz has been active in many technical societies and delivered papers before several. He has been the recipient of the Alumni Award from Carnegie and holds life honorary membership in the AIME National Open Hearth Conference. One of the organizers of the National Open Hearth Conference, Mr. Reinartz was Chairman, Executive Committee (1927 to 1946) and is presently Chairman of its Finance Committee. In October 1951 he was an American Conferee at the First World Metallurgical Congress held in Detroit. An AIME member since 1925, Mr. Reinartz has been active on numerous committees of the Institute.

For Vice-Presidents

Augustus B. Kinzel has been nominated as a Vice-President and Director of AIME. Dr. Kinzel graduated from Columbia University in 1919 (A.B.); from Massachusetts Institute of Technology in 1921 (B.S. in general engineering); and in 1922 received a D.Met.Eng. from the University of Nancy where he also received the degree of Doctor of Science. Dr. Kinzel has been associated with various metallurgical units of Union Carbide & Carbon Corp. since 1926 and was chief metallurgist of its laboratories from 1931 until he assumed the presidency of the research laboratories in 1947. He is a member of various government committees and is widely known as a lecturer. He was the AIME Howe Memorial Lecturer for 1952.

A. B. KINZEL

L. E. ELKINS

Lloyd E. Elkins, production research director, Stanolind Oil & Gas Co., has been nominated as a Vice-President and Director, AIME. Born at Golden, Colo. in 1912, he received his degree in petroleum production engineering from the Colorado School of Mines. Following graduation he was employed by the Stanolind Oil & Gas Co. at Wink, Texas, and has risen steadily during his years with the company. In 1948 Mr. Elkins was selected to attend the advanced management program at the Harvard Graduate School of Business Administration. He has been active in the Petroleum Branch of AIME as Chairman, Mid-Continent Section (1945); Vice-Chairman, Petroleum Div. (1947); and Chairman, Petroleum Branch (1949). In addition to being an AIME member, Mr. Elkins belongs to the API, Engineers' Club of Tulsa (president, 1950 to 1951), Petroleum Club of Tulsa, and American Assn. of Petroleum Geologists.

John R. Suman, Chairman of the Nominating Committee, has announced nominations for President-elect, Vice-Presidents, and Directors for 1953. As provided in Art. IX, Sec. 2, of the bylaws, 25 members or associate members may sign and transmit to the Secretary's office prior to Sept. 1 "any complete or partial ticket of nominees," should they wish other candidates to be considered.

In such instance, a letter ballot will be forwarded to all members in good standing in the United States, Canada, and Mexico, tabulating both the official ballot and any supplementary nominations. If no supplementary nominations are thus received, no letter ballot will be printed, and nominees on the official ballot shall be declared duly elected at the meeting of the Board of Directors or the Executive Committee in November.

For Directors

Philip D. Wilson has been nominated Director of AIME for a three year term beginning February 1953. Mr. Wilson has previously served as Chairman of the New York Section (1950) and is also a Council Delegate, New York Section. Mr. Wilson graduated from Princeton University in 1909 (B.S.) and Columbia University School of Mines in 1911 (E.M.). He was employed by various mining companies and in 1914 joined the Calumet & Arizona Mining Co. as chief geologist. He later joined The American Metal Co., Ltd., working in South America, South Africa, Europe, Cuba, Mexico, and New York City. He was also general manager

of the subsidiaries in Chile and South Africa. From 1934 to 1942 Mr. Wilson was vice-president of Pardners Mines Corp. In 1946 he joined Lehman Bros. and Lehman Mining Corp. Presently he is consulting mining engineer for this firm. Mr. Wilson is a member of various technical societies, and of several honorary societies.

P. D. WILSON

H. W. JOHNSON

Hjalmar W. Johnson, vice-president, Inland Steel Co., has been nominated as a Director of AIME for three years. He was a Director in 1950 and 1951 and served as Chairman of the Chicago Section in 1942. Born at Joliet, Ill., Mr. Johnson is a graduate of the University of Illinois (B.S.). He was employed by the Illinois Steel Co. at Joliet and later was blast furnace foreman for U.S. Steel Corp. In 1929 he joined Inland as assistant superintendent of blast furnaces. In 1930 he was promoted to superintendent of blast furnaces, and in 1942 became assistant general superintendent. Mr. Johnson was appointed staff assistant to the president in 1946 and three years later was appointed to his present position. Mr. Johnson received the J. E. Johnson, Jr. (AIME) award in 1933 and the American Iron and Steel Institute Medal in 1941.

E. L. OLIVER

E. H. ISERN

Edwin Letts Oliver, president of Oliver United Filters, Inc., has been nominated to serve as an AIME Director from 1953 to 1956. He is a Life Member of AIME and member of the Legion of Honor (class of 1962). Dr. Oliver was born in San Francisco. He graduated from the University of California in 1900. In 1903 he became surveyor and later metallurgist on the staff of the North Star Mines Co., Grass Valley, Calif. He patented a continuous automatic filter for use in the cyanide process and in 1910 opened an office under the name of Oliver Continuous Filter Co. In 1928 Oliver United Filters, Inc. was formed by consolidation with United Filters Corp. Dr. Oliver was Chairman of the James Douglas Gold Medal Committee in 1944. In 1945 he received the honorary degree of Doctor of Laws from the University of California. He is a member of professional societies both here and abroad, and holds numerous patents in connection with filtration equipment.

Elmer Henry Isern has been nominated as an AIME Director for a term from 1953 to 1956. He is a former member of the Milling Methods Committee, 1950 member of the James Douglas Gold Medal Committee, and is present Chairman, Richards Award Committee. Mr. Isern was born in Ellinwood, Kan., June 4, 1899 and graduated from Kansas University in 1922. After graduation Mr. Isern was a research engineer for Anaconda Copper Mining Co. He joined the Eagle-Picher Mining & Smelting Co. in 1939 as superintendent of milling. In 1944 Mr. Isern was appointed vice-president and director. He was later named president, and director of the Eagle-Picher Co. He is presently vice-president and director, and general manager, mining and smelting div., the Eagle-Picher Co. Mr. Isern is an officer and member of various professional societies.

Philip Kraft, currently Vice-President of AIME and Vice-Chairman of its Executive Committee, has been again nominated Director to serve from 1953 to 1956. He was born in New York City in 1890, received his B.S. degree from Columbia College (1910), E.M. degree from Columbia School of Mines (1912), and went on to the Royal School of Mines, Berlin, for his Doctor of Engineering degree (1914). Mr. Kraft spent three years in Canada as a geologist and mining engineer, and from 1917 to 1925 was engaged in war activities, mining examinations, and consulting work. He is Director in Charge of Oil Activities of Newmont Mining Co., and president of Newmont Oil Co. In addition, he is a director of Cyprus Mines Corp., and a number of other companies engaged in the mining, oil, and gas industries. At one time or another, Mr. Kraft has served on most of the important AIME committees, not the least of which has been the Committee to Administer Endowment Fund X.

Gail Francis Moulton, presently a Director of AIME, has been renominated for a three year term beginning 1953. Born in Chicago in 1898, he graduated from the University of Chicago in 1920. Mr. Moulton has had extensive experience in the petroleum industry, served as assistant professor at University of South Dakota, and headed the petroleum section of the Illinois State Geological

PHILIP KRAFT

G. F. MOULTON

Survey. He was later employed by United Gas Co., Electric Bond & Share Co., and Ralph E. Davis, Inc. Late in 1951, he joined Rockefeller Brothers Inc. as a consultant, with offices at 30 Rockefeller Plaza, New York City. A former Vice-Chairman of the Petroleum Branch, Mr. Moulton is a prolific writer in his field, and has served on AIME committees.

Division Officers Nominated for 1953

Institute of Metals Div.

Chairman, Morris Cohen, Massachusetts Institute of Technology; Senior Vice-Chairman, J. H. Scaff, Bell Telephone Laboratories; Vice-Chairman, J. S. Smart, Jr., American Smelting & Refining Co.; Secretary, Ernest Kirkendall, AIME. Executive Committee (three years): R. D. Chapman, Chrysler Corp.; E. R. Parker, University of California; T. A. Read, Columbia University.

Iron and Steel Div.

Chairman, T. J. McLaughlin, U. S. Steel Co.; Vice-Chairman: L. R. Berner, Inland Steel Co.; G. B. McMeans, Kaiser Steel Corp.; L. A. Lambing, Jones & Laughlin Steel Corp. Executive Committee (three years): T. A. Cleary, Youngstown Sheet & Tube Co.; C. G. Hogberg, U. S. Steel Corp. of Del.; E. H. Rose, U. S. Steel Co.

Extractive Metallurgy Div.

Chairman, R. R. McNaughton, Consolidated Mining & Smelting Co. of Canada, Ltd.; Chairman-Elect, P. T. Stroup, Aluminum Co. of America; Secretary, Ernest Kirkendall, AIME. Executive Committee (three years): P. C. Feddersen, Bunker Hill & Sullivan Mining & Concentrating Co.; P. D. I. Honeyman, Inspiration Consolidated Copper Co.

Mineral Industry Education Div.

Chairman, H. H. Power, University of Texas; Vice-Chairman, J. R. Van Pelt, Montana School of Mines; Past Chairman, Allison Butts, Lehigh University. Executive Committee (three years): J. C. Calhoun, Jr., Pennsylvania State College; D. S. Eppelsheimer, Missouri School of Mines & Metallurgy; O. C. Shepard, Stanford University.

First Metals Branch Meeting in Pacific Northwest

May 8, 9, 10 A Huge Success—EMD, IMD, ISD Participate

THE Pacific Northwest's first Metals Branch and fifth Industrial Minerals Div. meeting in Spokane, Wash., drew 260 members, 72 students, and 30 ladies. Contributions from industry helped to pay the way for students from Montana School of Mines, Idaho University, University of British Columbia, Missouri School of Mines, Stanford University, Washington State College, and University of Washington.

The special appeal to students made by the conference was coupled with an attempt to attract younger technical men from the companies located in the northwestern area. Cominco, at Trail, B. C., was represented by 16, Bunker Hill & Sullivan Mining Co., Kellogg, sent more than 20, and 26 came from Kaiser Aluminum & Chemical. In addition to the eight western states Utah, Wyoming, Montana, Idaho, Oregon, and Washington, and Canada's British Columbia, who contributed heavily to the program, members and visitors from Australia, New York, Tulsa, Denver, Toronto, San Francisco, and Los Angeles came.

Past Chairman of the Metals Branch Carlton Long represented that group, along with R. R. McNaughton, Chairman-Elect EMD, E. O. Kirkendall, New York, and Roy O'Brien, Salt Lake City, gave the meeting the Institute touch.

F. R. Morral, General Chairman of the Metals Branch sessions, arranged and directed the conference. R. G. Vervacke, Chairman of the Industrial Minerals meeting, shared the organizational burden.

Thursday, 133 registrants went to Mead, visiting the Pacific Northwest Alloys plants, where they saw the ferrosilicon furnaces, the calcining of dolomite, and the reduction of magnesium oxide. The Kaiser Aluminum reduction plant was also toured and J. Lindemuth, plant works manager, welcomed visitors.

Extractive Metallurgy

The growth of the nonferrous industry in the Pacific Northwest was dramatically portrayed as the extractive metallurgy session got under way Friday at 9 am. Some 125 conferees assembled for a program ranging from copper melting operations to research problems involving physical chemistry. A. Y. Bethune, assistant superintendent of the Sullivan Mining Co., electrolytic zinc plant, Kellogg, Idaho, presided.

Edward Pesout, superintendent of Kennecott's copper smelter at McGill, Nev., described a method for repairing furnace walls and arches during furnace operation which increased continuous operating time 162 pct over the period before hot-patching was employed.

The planning committee of the Pacific Northwest Conference at Seattle, met on the first day of the three-day session to lay the plans which guided the affair through to a conclusion with a minimum of fuss. They are, from the left, going clockwise, W. S. Peterson, E. Kirkendall, G. H. Waterman, F. R. Morral, R. R. McNaughton, H. P. Sherman, R. E. O'Brien, W. W. Staley, R. G. Vervacke, L. C. Richards, and A. O. Bartell.

W. T. Saylor, assistant superintendent, outlined a method and described the procedure used at Anaconda's International plant at Tooele for profitable recovery of values from a stockpile of reverberatory matte and speiss.

Raymond Thompson, superintendent of the American Smelting & Refining Co. plant at Garfield, gave a general outline of operations at the world's largest copper smelter. This paper is in the May 1952 issue of JOURNAL OF METALS.

The paper of R. Bainbridge on lead blast furnace gas handling and dust collection at Consolidated Mining & Smelting Co., Trail, B. C., was given by Robert Eyre, junior development engineer at Trail. Increased recovery of dust and fume at lower cost with elimination of atmospheric pollution resulted from modernization of the recovery system.

Experimental work at the University of Washington on treating roaster reverberatory flue dust indicated that a chloridizing roast followed by an acid-brine leach yields excellent extraction of copper and lead, according to J. A. Finley, assistant professor of the School of Mineral Engineering.

C. S. Samis and J. Halpern of the University of British Columbia presented the method for studying the kinetics of the reaction when galena is oxidized in an aqueous caustic medium.

R. T. C. Rassmussen, chief of the ferrous metals branch, U. S. Bureau of Mines, Albany, Ore. surprised most of the audience with the variety of equipment available at Albany for electric smelting research.

W. C. Aitkenhead, chief of the mining experiment station, State College of Washington, described the problems posed by electrolysis of manganous sulphate solution in making battery active MnO_2. Techniques for making a low lead product, very active as a depolarizer, were given in detail.

L. H. Banning, metallurgist of the USBM, Albany, Ore. station presented a paper on the recovery of the phosphorous, vanadium, and chromium contents of ferrophosphorous by hydrometallurgical means.

Physical Metallurgy

In the opening paper of the physical metallurgy session attended by 50 physical metallurgists, J. B. Hess, Kaiser Aluminum & Chemical Corp., described the structural changes occurring during diffusionless transformation of a series of colbalt-nickel alloys in a paper co-authored by C. S. Barrett, University of Chicago. Deformation by peening was used to activate the transformation detected by X-ray reflection patterns.

W. M. Fassel, Jr. presenting a paper entitled *Empirical Correlation of Band Properties in Solids* by M. A. Cook, showed that band widths calculated from band theory and from the cohesive energy of a metal agreed closely with the band width determined by the use of soft X-rays for several metals. A useful correlation between the strain ratio and the type of earing produced in various face centered cubic metals was described by K. T. Aust and F. R. Morral, Kaiser Aluminum & Chemical Corp., in a paper entitled *Preferred Orientation and Directional Properties of 2S Aluminum*.

In a paper entitled *Theory of Dendritic Growth in Metals*, by Dan Mc-

W. M. Fassell, Jr. spoke at the Saturday morning session of Physical Metallurgy. Ray Ward presided over the session.

Lachlan, University of Utah and presented by H. E. Flanders, University of Utah, the growth of dendrites was attributed to small thermal gradients between sharp geometrical corners or edges of the crystal and the melt.

L. M. Pidgeon, head of the dept. of metallurgical engineering, University of Toronto, spoke at the Metals Branch Friday luncheon. Some 200 guests heard him discuss *Extractive Metallurgy and the Reactive Metals*. The fundamentals of extractive metallurgy were considered on the basis of free energy vs temperature relationships. The brilliant presentation of the application of principles of physical chemistry in the metallurgy of the reactive metals, such as magnesium and titanium, gained an appreciative reaction.

Following the luncheon, Kaiser Aluminum & Chemical Corp. acted as host to about 180 students and faculty members with a tour through the Trentwood rolling mill, where they were greeted by J. B. Russell. A banquet at the plant cafeteria was held in the evening. Wayne Welcome, public relations director, outlined the future of aluminum and its impact on their professional lives. He introduced D. W. Smith, who talked of the role of research in the aluminum industry, and W. Lawler, technical div. superintendent, who described the methods of metallurgical control used throughout the mill.

Mineral Industries Education

The Mineral Industries Education session was called to order Friday evening by Chairman J. P. Spielman of the Washington State College School of Mines. In attendance were 110 students, professors, and representatives of industry.

R. R. McNaughton, metallurgical manager, Consolidated Mining & Smelting Co., Trail, B. C., gave his *Review of the New York Panel Discussion on Training of Extractive Metallurgists*. He noted the general lack of oral ability in presenting ideas and in writing shown by engineering graduates. He spoke of industry's lackadaisical attitude in encouraging students to enroll in mineral engineering college training, of the industry's summer employment and encouragement for keeping professors abreast of practice.

J. Newton of the University of Idaho gave a comprehensive presentation of *Trends in Undergraduate Curricula* in which he included specialization, the whole-man approach (nontechnical subjects), lowering of total hours requirements, and the 5-year program.

Trends in Graduate Training and Specialization was presented by John R. Lewis of the University of Utah. He spoke of the student's awareness of the values of advanced work, of industry's desires for men with more training and of the impact of the Government's preparedness program.

W. L. Schalliol of the General Electric Co. spoke of *The Phase Transformation—Student to Metallurgist*, which dealt with his company's procurement, initiation, orientation, training and placement program in connection with the Hanford Plutonium Plants.

The Bunker Hill and Its Technical Men was discussed by W. G. Woolf, general superintendent of the Sullivan Mining Co. He developed the theme that the nomadic life of the earlier technical and nontechnical man is largely a thing of the past. Job stability, opportunity for advancement, treatment as human beings and personal dignity accordance had brought about the change.

Friday and Saturday sessions of the Physical Metallurgy group were well attended. Members of the Friday morning panel were from left to right: Ray Ward, J. B. Hess, K. T. Aust, W. M. Fassell, Jr. and E. Flanders.

Physical Metallurgy

Ray Ward of the General Electric Co., Richland, Wash., was Chairman of the physical metallurgy meeting that attracted an audience of about 50 on Saturday.

H. Czyzewski's paper *The Propagation of Slip Lines in Face-Centered Cubic Metals*, covered the influence of various intragranular and transgranular interfaces on the propagation of slip lines. Slip was found to be transmitted through, absorbed within, *reflected* from or divided into branches under appropriate conditions.

The High Pressure Oxidation Rate of Metals, I. Copper in Oxygen, by W. M. McKewan and W. M. Fassell, Jr., showed that the oxidation rates of copper are unchanged by oxygen pressures from 14.7 to 400 psi in the temperature range of 600° to 900°C. In all cases both Cu_2O and CuO are present in the oxide films formed on the copper metal.

W. M. McKewan and W. M. Fassel, Jr. co-authored the last paper on *The Parabolic-Linear Oxidation Rate Transition Theory*. They accounted for the type of oxidation followed by metals upon exposure to an oxidizing atmosphere at elevated temperatures with the hypothesis that if the rate of crystal growth of the oxide coating formed on the surface is greater than the oxidation rate of the metal, the coating will be protective and hence will follow the parabolic equation.

Iron and Steel

In the first paper of the iron and steel session, *Raw Materials for Steel Making in the Western States*, S. G. Sargis of the Geneva Steel Corp., Geneva, Utah, covered the sources and recent methods of exploration of the basic raw materials of the western steel industry. Coking coal and limestones are found in Utah, Colorado, Washington, and New Mexico. Iron ore reserves in the western states are estimated to be 600 million tons. Other vital materials, such as manganese and

fluorspar, can be procured, if not available locally, at greater distances from the steel plants.

The paper on *Basic Electric-Arc Furnace Metal for Casting Production* by J. T. Gow and V. E. Belasko, Electric Steel Foundry Co., Portland, Ore., prepared for the AIME Electric Furnace Steel Conference in 1951, was presented by Mr. Belasko. This paper deals with the advantages gained by changing from acid to basic linings in the electric furnace melting of mild steel, low alloy steel, and high alloy stainless.

In his paper on the *Production and Properties of Aluminized Steel*, J. B. Russell, Kaiser Aluminum & Chemical Corp., briefly reviewed the various methods of cleaning steel prior

J. Murphy, of Kaiser Aluminum's div. of metallurgical research explained some of the various types of finishes administered to aluminum to conferees who toured the plant

to continuous coating by the hot-dip method. A relatively simple continuous coating process was described which is expected to produce aluminized steel at a cost not above that of galvanized steel.

L. W. Heinzinger, Bethlehem Pacific Coast Steel Corp., Seattle, discussed, *Adaptation of Instrumentation to Metallurgical Control Processes*. The author appraised use of instrumentation in open hearth and rolling mill practice, with respect to control of temperature, gas pressures, and liquid pressures. Special immersion and optical pyrometers were described.

H. A. Doerner, USBM, summarized the status of the substandard manganese and chrome ores found in Oregon, Montana, and Wyoming in *Utilization of Domestic Chrome and Manganese Ores*. A small part of the ferromanganese and ferrochrome required by the steel industry is derived from domestic ores even when production is stimulated by inflated prices or government subsidies. Only a few known domestic deposits can be mined at low cost.

Ian Campbell, Chairman, Industrial Minerals Div., addressed the Industrial Minerals luncheon. Meeting Chairman R. G. Vervaeke introduced F. Libby, a Director of the Institute, and G. H. Waterman, the next Chairman of the Industrial Minerals meeting. Professor Campbell briefly explained his activities with the Institute and future plans for the division. The luncheon was attended by 181 persons.

Climax to the conference was the joint dinner on Saturday with 253 in attendance. Commissioner Lawson of Spokane bid farewell to the group and invited all to return. Many persons active in conference and Institute activities were presented by the toastmaster and Chairman of the Columbia Section, Professor Staley.

J. F. Bell, vice-president and director, Portland Gas & Coke Co., Portland, Ore., ably assisted by Mrs. Bell, presented his experiences in 1942 to 1943 in *Quartz and Mica Mining in Brazil*. The human interest story intrigued the group.

The Women's Auxiliary at Spokane had organized a brunch for Saturday, at which a local dancing group gave a series of their selections. Some 70 ladies attended.

The editor wishes to express his appreciation to the following persons for their reporting of the meeting: K. T. Aust, D. Baker, A. Y. Bethune, S. L. Channon, S. H. Keller, F. R. Morral, J. B. Russell, J. F. Williams, Jr., and photographer David Edelman.

IMD Fall Meeting Hotel Quota Filled

Although hotel reservation forms were mailed two months early and the first Housing Committee meeting held June 5 this year, more room requests were received by this time than by August 1 in previous years —more requests than the Adelphia Hotel, headquarters for the October 20 to 22 meeting in Philadelphia, was able to handle. While some rooms at other good Philadelphia hotels were still available, AIME members wishing to attend the IMD fall meeting are urged to make their room requests immediately to the Housing Bureau, Architects Building, 17th and Sansome St., Philadelphia. Satisfactory single rooms closer than Atlantic City cannot be promised. Those whose plans are changed, preventing their attendance at the Metal Congress, please be sure to cancel through the Housing Bureau so that another AIME member can use the room. The technical program with two titanium sessions, promises to be as good as the advance room requests.

Conferees visited Kaiser Aluminum's div. of metallurgical research during one of the field trips which highlighted the meeting. They saw various fatigue tests run in the laboratory

Dues Voting Ballot Mailed

A referendum on dues is currently being conducted by the Institute. A statement of the Board's position in the matter and a ballot for voting was mailed to all paid up AIME members in the United States, Canada, and Mexico on June 16, returnable to the Secretary's office not later than July 15. All members who receive a ballot are urged to vote for a continuance of the present scale of dues, so that present Institute services can be fully main-

Annual Meeting Paper Deadline

Sept. 15, 1952 is the deadline for all Institute of Metals Div. papers for the 1953 Los Angeles Annual Meeting and the deadline for all Iron and Steel Div., and Extractive Metallurgy Div. papers to be prepublished.

RESEARCH IN PROGRESS

Research personnel are reminded of the Institute of Metals Div. Research in Progress session planned for Monday afternoon, Oct. 20, 1952 during the Fall Meeting in Philadelphia. Abstracts of proposed papers not exceeding 200 words in length are to be submitted to Institute headquarters prior to Aug. 15, 1952, for inclusion in the October issue of JOURNAL OF METALS. Abstracts not received in time for publication in the October issue may, nevertheless, be presented if received prior to Sept. 15, 1952, according to J. H. Scaff of the IMD Program Committee.

The Program Committee urges those interested to avail themselves of the opportunity of participation in this program in order that new research information be presented for discussion.

tained, and it is hoped, expanded in the future as interest permits.

B. F. Fairless Awarded 1953 John Fritz Medal

Benjamin F. Fairless, president of the U. S. Steel Corp., has been awarded the John Fritz Medal for 1953. The presentation will be made by the American Society of Civil Engineers, of which he is a member, at the Centennial of Engineering at Chicago in September 1952. The medal is given by the four Founder engineering societies for notable scientific or industrial achievement in any field of pure or applied science. Mr. Fairless is cited as "Champion of the American Free Enterprise System for Notable Industrial Achievement in the Production of Steel."

Connecticut Section Holds Social Meeting

The annual social meeting of the Connecticut Section was held at the Copper Kettle Inn, Wolcott, Conn., on May 16. About 30 members and their ladies enjoyed a rather huge buffet complete with dinner music and danced until the hour grew late. Among the ladies, the AIME Women's Auxiliary was well represented.

Coming Events

June 24-28. Industrial Physics Conference, Royal Technical College, Glasgow, Scotland.

June 30-July 2. Materials Handling Institute, annual meeting, Grand Hotel, Mackinac Island, Mich.

July 1-Sept. 30. Centennial of Engineering, Chicago.

Aug. 25-29. Oak Ridge Summer Symposium, Oak Ridge, Tenn.

Sept. 3-6. AIME, fall meeting, Palmer House, Chicago.

Sept. 3-6. AIME. Industrial Minerals Div., annual fall (regional) meeting, Chicago.

Sept. 3-13. AIME, Chicago Section, Centennial of Engineering, Chicago.

Sept. 5-6. Engineers' Council for Professional Development, annual meeting, Hotel Sherman, Chicago.

Sept. 10-12. Porcelain Enamel Institute, annual shop practice forum, University of Illinois, Palmer House, Chicago.

Sept. 11-13. American Institute of Chemical Engineers, Palmer House, Chicago.

Sept. 22-25. American Mining Congress, Metal and Nonmetallic Mining Convention and Exposition, public auditorium, Denver.

Sept. 24-26. Institution of Mining and Metallurgy, conference on mineral dressing, Royal School of Mines, London.

Sept. 29. AIME, Missouri Sub-section, Longfellow Inn, Moreno, Ariz.

Oct. 2. AIME, Southern Ohio Section, National Open Hearth Steel Committee, Deshler-Wallick Hotel, Columbus, Ohio.

Oct. 10. AIME, Eastern Section, National Open Hearth Steel Committee, Warwick Hotel, Philadelphia.

Oct. 16. AIME, Southwestern Section, National Open Hearth Steel Committee, Peoria, Ill.

Oct. 20-22. AIME, Institute of Metals Div. fall meeting with National Metal Congress, Hotel Adelphia, Philadelphia.

Oct. 28. Assn. of Consulting Chemists and Chemical Engineers, Inc., annual symposium, Hotel Belmont Plaza, New York.

Oct. 30-31. AIME, Fuels Conference. Coal Div., AIME; Fuels Div., ASME, Bellevue-Stratford, Philadelphia.

Nov. 7. AIME, Pittsburgh Section, National Open Hearth Steel Committee, Hotel William Penn, Pittsburgh.

Nov. 18. AIME, Buffalo Section, National Open Hearth Steel Committee, Hotel Statler, Buffalo.

Dec. 1-6. AIME, Electric Furnace Steel Conference, Hotel William Penn, Pittsburgh.

Dec. 7-10. American Institute of Chemical Engineers, annual meeting, Hotels Cleveland and Carter, Cleveland.

Dec. 8. AIME, Arizona Section, all-day meeting, Tucson.

Feb. 16-19, 1953. AIME, annual meeting, Statler Hotel, Los Angeles.

Mar. 16-20. National Assn. of Corrosion Engineers, annual conference and exhibition, Hotel Sherman, Chicago.

Apr. 20-22. AIME, National Open Hearth and Blast Furnace, Coke Oven and Raw Materials Conference, Hotel Statler, Buffalo.

X-ray Diffraction is an indispensable instrument in any study involving crystal structure. It is a magnificent industrial tool for determining the course of chemical reactions in the manufacture and use of materials. It is a key aid in our search for better methods and improved products because it provides basic information on component structure that can be obtained in no other known way.

G. L. Clark

● Chief of Analytical Research for Johns-Manville

Serving Science and Industry

At the great Johns-Manville Research Center at Manville, N. J., Norelco X-ray Diffraction equipment shows what happens when building materials are exposed to heat, cold, wear.

It plays a star role in development of new products and improvement of the old. It's the "trouble-shooter" for manufacturing and sales departments. It identifies materials, reveals flaws, serves as the court of last appeal for Johns-Manville scientists.

It helps to maintain the leadership of Johns-Manville in providing new and better building materials for its nation-wide and world-wide market.

Innumerable Applications

Norelco X-ray Diffraction equipment shows us the atomic world we live in . . . paves the way to better food, clothing, shelter, and medical care . . . indicates ways to conserve our resources and broaden our sciences. It permits non-destructive analysis which is impossible for chemistry.

The North American Philips Company welcomes your questions about possible diffraction uses in your company. Also write for free 60-page catalog. *Applications now being accepted for fall term of the Philips Diffraction School (October). Enroll now or write for details.*

A Norelco PRODUCT OF NORTH AMERICAN PHILIPS COMPANY, INC.

Dept. IG-7 · 100 East 42nd St., New York 17, N. Y.

In Canada: Philips Electronics Ltd., 11-19 Brentcliffe Road, Leaside, Toronto 17, Ontario

DOUGLAS H. POLONIS

Douglas H. Polonis is now employed by the Steel Co. of Canada Ltd., Hamilton works, as assistant metallurgist.

L. F. Reinartz, vice-president, Armco Steel Corp., Middletown, Ohio, was awarded the Regional Technical Meeting Award of the American Iron & Steel Institute. Mr. Reinartz is President-Elect for 1953, AIME.

John H. Gorman was appointed field electrochemist for the Hanson-Van Winkle-Munning Co. in the Michigan-Ohio territory.

Richard V. D. Strong, formerly Chicago district manager, F. J. Stokes Machine Co., has been appointed chief engineer.

Henry W. Kruschwitz, Jr., research chemist with Metal Hydrides, Inc., has been transferred to the sales dept. as sales engineer. **Robert D. Gray** has been appointed superintendent of the chemical hydrides div.

Thomas D. Cartledge has been appointed president of Linde Air Products Co. He had been senior vice-president and a director and vice-president of Dominion Oxygen Co., Ltd.

Peter V. Schneider has joined the Ford Motor Co., as technical advisor in the powdered metal div., Dearborn general manufacturing. He had been chief metallurgist for the Powdered Metal Products Corp. of America.

Emanuel Gordon has joined the engineering dept. of Metal Hydrides, Inc., Beverly, Mass.

Albert G. Guy has been appointed associate professor of metallurgical engineering, Purdue University, Lafayette, Ind. He had worked for the General Electric Co., Office of Ordnance Research, and was associate professor of metallurgy at North Carolina State College.

L. D. Woodworth has been named assistant general superintendent, U. S. Steel Co., Youngstown, Ohio.

Walter S. Tower, retired president of the American Iron & Steel Institute was awarded the Gary Memorial Medal. This medal is for outstanding achievement in the industry. Mr. Tower was president of the Institute for 12 years and executive secretary for nearly seven years previously.

Gustav Laub has been elected a director of Vanadium Corp. of America. Mr. Laub has been associated with the company for 37 years, and has been vice-president in charge of sales for four years.

POL DUWEZ

Pol Duwez has been promoted to professor of mechanical engineering, California Institute of Technology, Pasadena.

Richard K. Wuerfel has accepted a position with the Westinghouse Electric Corp., Baltimore. He had been with the National Induction Heating Co.

Don O. Noel is now vice-president, General Metals Powder Co., Akron. He formerly had been associated with the Wah Chang Smelting & Refining Co., Glen Cove, N. Y.

George E. Atwood, former refinery superintendent, Duval Sulphur & Potash Co., Carlsbad, N. Mex., has been promoted to assistant resident manager and refinery superintendent.

Joseph Billy has accepted a position with the Borg-Warner Corp., Marvel-Schebler products div., Decatur, Ill.

George H. Eichelman, Jr. has resigned from the Westinghouse Electric Corp., Pittsburgh, to accept a position with the American Brass Co., metallurgical research laboratory, Waterbury, Conn.

Arthur A. Krieger is presently employed by the Columbia Steel Co., Pittsburg, Calif.

Leonard O. Fines has become smelter superintendent for the Andes Copper Co., Potrerillos, Chile.

Joseph J. Brugman is now employed by North American Aviation, Inc., Downey, Calif. in the materials research group as metallurgical consultant to designers, research, and development engineer.

Franklyn G. Ragan is now special engineer, sheet, tin, and strip mill, Bethlehem Steel Co., Sparrows Point.

Benton W. Norton has been appointed general superintendent of blast furnace, Shenango Furnace Co. and Shenango-Penn Mold Co.

Robert J. Aitchison was elected chairman of the board, Fansteel Metallurgical Corp. and its subsidiary, Vascoloy-Ramet Corp.

Frank H. Driggs was elected president, Fansteel Metallurgical Corp. and its subsidiary, Weigger Weed & Co. **R. Winchester** was named director of technical div. and **Glen Ramsey** was elected vice-president. **Herbert B. Clark** was elected president of Vascoloy-Ramet Corp. and **Harry W. Highriter** was elected vice-president.

Ralph S. Sherwin, Jr., Reynolds Metals Co., is now located in Corpus Christi, Texas. He had been at Sheffield, Ala.

John S. Marsh, research engineer of the Bethlehem Steel Co., Bethlehem, Pa. was recently awarded the American Iron & Steel Institute Medal.

JOHN S. MARSH

HANS F. FISCHER

Hans F. Fischer, president of Fischer & Associates, has opened offices in Cleveland. Mr. Fischer was senior engineer for Joy Mfg. Co. before forming Fischer & Associates.

Carl F. Henzelman has been made superintendent of the No. 2 open hearth dept., Granite City Steel Co., Granite City, Ill.

Ernest H. Klein, manager, metal div., N. J. Zinc Sales Co., New York, was elected president of the Metal Powder Assn. **Thomas L. Robinson,** president of the Wel-Met Co., Kent, Ohio, was elected chairman of the board. **Thomas Moore,** sales manager, Antara Chemicals div., General Dyestuff Corp., New York has been elected vice-president and **George Roberts,** Vanadium-Alloys Steel Co., Latrobe, was elected to the board of directors.

S. E. Flenner, Jr. has recently been named sales manager of Alloy Precision Castings Co., Cleveland.

John G. McMullin is now associated with the General Electric Research Laboratory, Schenectady.

Walter C. Rueckel is now with Kaiser Engineers, div. Henry J. Kaiser Co., Oakland, Calif. He formerly was with the Koppers Co., Inc., New York.

Herman C. Autderhaar, Electro Metallurgical Co., div. Union Carbide & Carbon Corp., was recently transferred from Chicago to New York.

Obituaries

Frank F. Colcord (Member 1905) died on March 21. Born at Boston in 1877, Mr. Colcord attended Massachusetts Institute of Technology. After graduation he joined the Chicago & Aurora Smelting & Refining Co., as assistant to the superintendent. In 1900 Mr. Colcord went to Cripple Creek, Colo. and for three years was chief assayer for Guggenheim & Co. In 1904 Mr. Colcord became associated with the American Smelting & Refining Co., Maurer, N. Y. Several years later he was made chemist for the U. S. Metal Refining Co. In 1920 he was vice-president of U. S. S. Lead Refinery, Inc., New York. Mr. Colcord became vice-president and manager of metals sales for U. S. Smelting, Refining & Mining Co., New York, in 1938. At the time of his death he was residing at San Marino, Calif.

E. A. Collins (Member 1935), retired from the International Nickel Co. of Canada, Ltd., died on February 6. Mr. Collins was born in Smithfield, Ont. on Jan. 19, 1879. After graduation from the Queens University with the degree of B.Sc., he accepted a position with the Osceola Lead & Zinc Co., Webb City, Mo. For three years he was engaged in reporting on deposits in Ontario for various companies. In 1913 he was inspector of mines for the Province of Ontario. Mr. Collins joined the International Nickel Co. in 1918 as safety engineer and in 1920 was promoted to assistant to the general manager.

Charles Ellison MacQuigg (Member 1928), dean of Ohio State University's engineering college for 15 years, died on April 24. Born at Ironton, Ohio, Dr. MacQuigg was associated with the Sante Fe Railroad and the Anaconda Copper Co., after graduation from Ohio State. He was head of the metallurgy dept. of Pennsylvania State College for five years before joining the Army Ordnance Dept. during World War I. Dr. MacQuigg was regional coordinator for the Government's engineering, science, and management war training program during the second world war. He was a member of the National Research Council and held several patents on metallurgical inventions and was the author of numerous technical papers.

Eugene L. Messler (Member 1897) has died. Born in 1873, Dr. Messler graduated from Yale Sheffield Science School with the degree of Ph.B. He was assistant to the president, Peter Conlay Mfg. Co. and in 1915 became president of the Eureka Fire Brick Works, Mount Braddock, Pa. He was also vice-president and general manager of the Wittenau Steel Co.

NECROLOGY

Date Elected	Name	Date of Death
1929	William P. Alderson	February 1951
1911	E. J. Carlyle	Apr. 27, 1952
1911	J. E. S. Clark	Apr. 23, 1952
1950	James A. Creighton	Unknown
1948	Irvan Earl Curtis	Oct. 12, 1951
1913	Theodore F. Fost	Unknown
1941	Samuel Edwin Guthrey	May 13, 1952
1916	Robert L. Hallett	May 16, 1952
1913	John H. Hastings	Unknown
1919	Leslie D. Hawkridge	Apr. 21, 1952
1925	Dudley A. Hoover	Apr. 3, 1952
1936	Russell C. Johnson	Dec. 3, 1951
1921	C. McDermid	May 7, 1952
1919	Andrew C. McLaughlin	January 1952
1909	Joseph H. Rodger	Apr. 23, 1952
1906	Percifer G. Salisbury	May 3, 1952
1914	George B. Waterhouse	May 10, 1952
1944	Clark White	Unknown
1938	Fred Wise	May 1, 1952
1944	C. William Witt	Unknown

Proposed for Membership
— Metals Branch AIME —

Total AIME membership on May 31, 1952 was 17,172, in addition 2412 Student Associates were enrolled.

ADMISSIONS COMMITTEE

T. D. Jones, Chairman; Thomas G. Mason, Vice-Chairman; Harold S. Bell, F. W. Hanson, R. H. Chadwick, T. W. Nelson, J. H. Smith, John F. Alsentzer, A. C. Bunker, John Green, C. A. B. Lavelle, G. P. Luthen, E. A. Pierson, and C. Leslie Rice, Jr.

The Institute desires to extend its privileges to every person to whom it can be of service, but does not desire as members persons who are unqualified. Institute members are urged to review this list as soon as practical and confidentially to inform the Secretary's office if names of people are found who are known to be unqualified for AIME membership.

In the following list C/S means change of status; R, reinstatement; M, Member; J, Junior Member; A, Associate Member; S, Student Associate.

Arizona

Bullhook—Ferguson, William F. (R, C.S.—S-A-J)

California

Beverly Hills—Walker, Frederick (M)
Los Angeles—Houston, Edward F. (J)

Colorado

Canon City—Fargo, Frank B. (A)

Connecticut

New London—Steeves, Arthur F. (J) (R, C.S.—S-J)

Illinois

Chicago—Rasmussen, Adolph P. (J) (R, C.S.—S-J)

Indiana

Gary—Walls, Jr., John M. (M)
Michigan City—Carrie, Wilfred G. (M)

Iowa

Montpelier—Fischer, Robert L. (J)

Maryland

Takoma Park—Blue, Delwin D. (M)

Massachusetts

Cambridge—Dardel, Yves F. (M)

Minnesota

Duluth—Butterworth, Allen C. (M)

New York

Bronx—Frank, Louis (J) (R, C.S.—S-J)
Bronx—Sorrer, Saul Z. (J) (R, C.S.—S-J)
New York—Fiske, Rodney G. (A)
New York—Williams, Clifford D. (A)
Woodhaven—Heyman, Moses D. (M)

Ohio

Bellaire—Felmet, John W., Jr. (J) (R, C.S.—S-J)
Columbus—Kura, John G. (M)
East Liverpool—Moore, Lester W. (M) (C.S.—A-M)
Lyndhurst—Lyman, W. Stuart (J) (R, C.S.—S-J)
Tiltonsville—Conklin, Robert J. (M)

Oregon

Portland—Sherrett, Chester K. (M)

Pennsylvania

Allentown—Rambosek, August F. (M) (R, C.S.—A-M)
Pittsburgh—Christ, Joseph G. (M) (R, M)
Wyomissing—Purdy, Samuel M. (J)

Rhode Island

Wakefield—Matthew, William P. (M)

Wisconsin

Beloit—Jones, Thomas M. (J)

Japan

Kyoto—Matsumura, Gentaro (J)

Mexico

Coahuila—Engle, Lester F., Jr. (M) (C.S.—J-M)

. . . and another

Lectromelt

Smelter is on its way

Lectromelt self-baking electrodes offer these typical advantages:

1. The complete structure is supported on two I-beams just above the furnace roof, resulting in lower and lighter building construction above.
2. No movable parts required at clamp level such as bolts, nuts, springs, etc., which can be damaged by flame.
3. Remote-control clamping device allowing for quick and simple electrode adjustment and easy replacement of clamp shoes.
4. Pressure ring exerts uniform pressure and holds electrode circular.
5. Four cable supports providing minimum distortion of casing at clamp.

For a further listing of advantages of Lectromelt self-baking electrodes and more data on the above, write Pittsburgh Lectromelt Furnace Corporation, 326 32nd St., Pittsburgh 30, Pa.

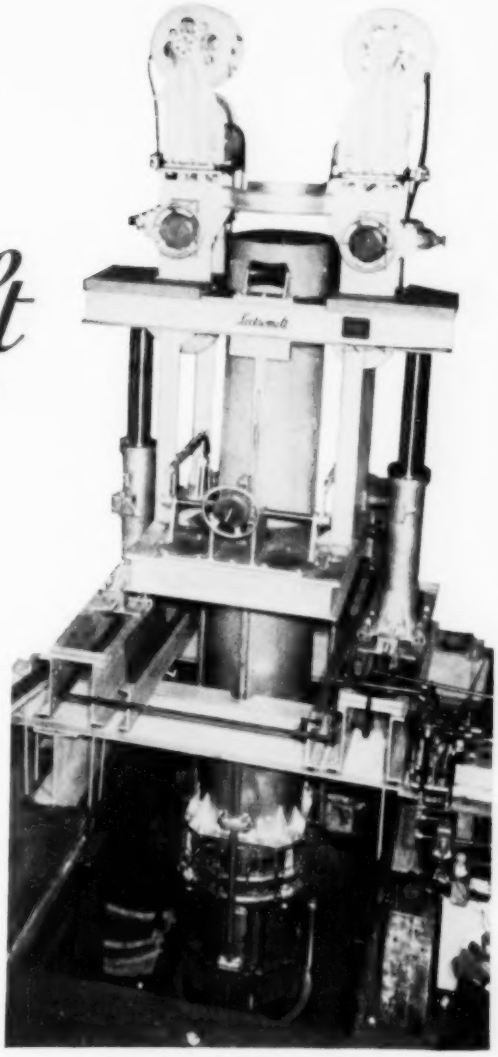

One of three self-baking electrodes for a ferromanganese smelting furnace on Lectromelt's erection floor; testing is completed and ready for shipment.

Manufactured in . . . CANADA: Lectromelt Furnaces of Canada, Ltd., Toronto 2 . . . ENGLAND: Birlec, Ltd., Birmingham . . . AUSTRALIA: Birlec, Ltd., Sydney . . . FRANCE: Stein et Roubaix, Paris . . . BELGIUM: S. A. Belge Stein et Roubaix, Bressoux-Liege . . . SPAIN: General Electrica Espanola, Bilbao . . . ITALY: Forni Stein, Genoa.

WHEN YOU MELT...

MOORE RAPID

*Lectromelt**

Kiln plant No. 4 as it nears completion. This photograph, taken April 29, 1952, shows kilns in position, finished product buildings under construction (at left) and stacks going up (at right).

Erecting steel sections of stacks that exhaust hot gases from kilns. The stacks, 215 feet tall, will tower 95 feet above the raw storage silo.

D-day for dead-burning

SOON after you read this, dead-burned dolomite will be pouring from these new kilns at our Maple Grove works. Favored by weather and well coordinated schedules, concrete work and installation of kilns and accessory equipment have gone forward with unusual speed.

Kiln plant No. 4 will increase very substantially our capacity for producing dead-burned dolomite. Here we will make Magnefer and Syndolag to the same rigid specifications, by the same controlled procedures that have enabled these fettling refractories to win their reputation for high quality and dependable performance.

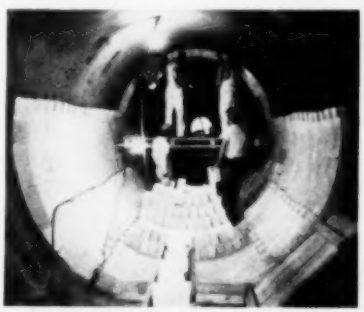

Installing high alumina brick in kiln. Burned basic brick are used in the hot zone in which temperatures above 3000 F are required.

Railroad tracks will soon cross this fill of a quarter million tons to facilitate shipment of dead-burned dolomite and other refractory products.

Basic Refractories Incorporated

845 HANNA BUILDING, CLEVELAND 15, OHIO

Exclusive Agents in Canada: REFRACTORIES ENGINEERING AND SUPPLIES, LTD., Hamilton and Montreal